



Norwegian University of Life Sciences
Faculty of Environmental Sciences
and Natural Resource Management

Philosophiae Doctor (PhD)
Thesis 2023:40

Impact of low dose rate ionising radiation - studies in mice evaluating immediate and long-term molecular responses and transgenerational genomic instability

Virkningen av lav doserate ioniserende
stråling - studier av molekylære responser
og transgenerasjonell genomisk ustabilitet
gjort i mus

Hildegunn Dahl

Impact of low dose rate ionising radiation
Studies in mice evaluating immediate and long-term
molecular responses and
transgenerational genomic instability

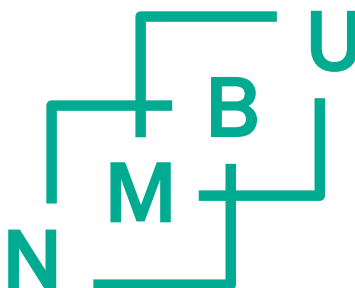
Virkningen av lav doserate ioniserende stråling
Studier av molekylære responser og transgenerasjonell genomisk
ustabilitet gjort i mus

Philosophiae Doctor (PhD) Thesis

Hildegunn Dahl

Norwegian University of Life Sciences
Faculty of Environmental Sciences and Natural Resource Management

Ås 2023



Thesis number 2023:40
ISSN: 1894-6402
ISBN: 978-82-575-2068-7

“Vision without execution is hallucination”

Thomas Edison (1841 -1931)

Supervisors

Professor **Deborah H. Oughton**, PhD

Centre for Environmental Radioactivity (CERAD) CoE

Faculty of Environmental Science and Natural Resource Management (MINA)

Norwegian University of Life Science (NMBU)

E-mail: deborah.oughton@nmbu.no

Research Professor **Ann Karin Olsen**, PhD

Centre for Environmental Radioactivity (CERAD) CoE

Department of Chemical Toxicology

Division of Climate and Environmental Health

Norwegian Institute of Public Health (NIPH)

E-mail: ann-karinhardie.olsen@fhi.no

Research Professor **Nur Duale**, PhD

Centre for Environmental Radioactivity (CERAD) CoE

Department of Chemical Toxicology

Division of Climate and Environmental Health

Norwegian Institute of Public Health (NIPH)

E-mail: nur.duale@fhi.no

Professor **Dag Anders Brede**, PhD

Centre for Environmental Radioactivity (CERAD) CoE

Faculty of Environmental Science and Natural Resource Management (MINA)

Norwegian University of Life Science (NMBU)

E-mail: dag.anders.brede@nmbu.no

Specialist Director **Christine Instanes**, PhD

Department of Chemical Toxicology

Division of Climate and Environmental Health

Norwegian Institute of Public Health (NIPH)

E-mail: Christine.instances@fhi.no

Evaluation Committee

Professor **Andrzej Wojcik**

Centre for Radiation Research,
Stockholm University, Sweden
E-mail: andrzej.wojcik@su.se

Dr **Rhona Anderson**

Centre for Health Effects of Radiological and Chemical Agents,
Brunel University, London
E-mail: Rhona.Anderson@brunel.ac.uk

Associate Professor **Hans-Christian Teien**

Centre for Environmental Radioactivity (CERAD) CoE
Faculty of Environmental Science and Natural Resource Management,
Norwegian University of Life Science (NMBU)
E-mail: Hans-christian.teien@nmbu.no

Acknowledgements

First, I need to give a heartfelt shout-out to my amazing, Stian, for his love and sacrifices, and for giving me the freedom to pursue my academic dream. I remember when you said, “Do it! It’s only three years” – and now, ten years later, we realise that we had forgotten an important factor in that equation, namely life itself. Indeed - life came our way, but you never stopped cheering me on. In moments of self-doubt, you reminded me of my capabilities and encouraged me to keep pushing forward. Thank you for embracing the chaos and being a superhero for me and our wonderful kids.

I sincerely appreciate my esteemed supervisors, Anka, Nur, Christine, Dag A. and Deborah, for their invaluable guidance, mentorship, and expertise throughout my doctoral journey. Thanks to Dag Markus for making the days extra interesting, and to all the co-authors of the papers. The present PhD project was financially supported by the Norwegian Institute of Public Health (NIPH) and by the Research Council of Norway through its Centre of Excellence (CoE) “Centre of Environmental Radioactivity” funding scheme (CERAD, project no. 223268/F50).

To my friends - Camilla, Elisabeth, Monica, Yevgeniya and Johanna – the best support group ever!! You have given me a much-needed sense of normality in the chaos of academic life. Whether it was lending an ear to listen, providing valuable feedback, or offering words of encouragement. Camilla, there is not enough words, so I will just say - Thank you!!!

I would also like to acknowledge and thank all my colleagues and friends at Folkehelse and CERAD – it has been so many years, so many people and memories. Many of you inspired me on this path back in the day, and you all have made the time at the office or in the lab hilarious over the years. Even on Teams during the pandemic lockdowns. Not to forget somebody, I will not mention any names. But you know how you are.

A huge thanks to my family, mamma, pappa, Jim Andre, Kristian, Sandra, Cecilie, Julie and Gommo – for always being there when needed. But a special thanks to my mamma – for all the times you have been here helping us! Finally, the lights in my life. My kids, Emrik and Hennie, my greatest motivation and source of joy. Your boundless energy, infectious laughter and warm hugs have been the perfect antidote to long nights of studying and writing.

Table of Contents

Summary.....	1
Sammendrag	4
Abbreviations and acronyms	7
List of papers.....	9
1 Introduction.....	10
1.1 Ionising radiation (IR)	10
1.1.1 Sources of exposure.....	12
1.1.2 Health effects	14
1.1.3 The concept of (low) dose rate.....	15
1.1.4 Low dose rate effects	16
1.1.5 Cellular and molecular processes	23
1.1.6 DNA damage and oxidative stress	25
1.1.7 Hereditary and transgenerational effects	28
1.2 The epigenome	30
1.2.1 The chromatin.....	30
1.2.2 Transcription and genomic regulatory elements	32
1.2.3 Epigenetic marks	33
1.3 Objectives of the study.....	35
2 Methods and methodological considerations	36
2.1 Experimental design.....	36
2.1.1 Experiment A – Paper III	36
2.1.2 Experiment B – Paper I and II.....	38
2.2 Irradiation and dosimetry.....	39
2.2.1 Experiment A – Paper III	40
2.2.1.1 F ₀ low dose rate gamma irradiation	41
2.2.1.2 F ₂ X-ray challenge dose.....	41
2.2.2 Experiment B – Paper I and II.....	42
2.2.3 General considerations of the dosimetry	43
2.3 Mouse models	44
2.3.1 C57BL/6.....	44
2.3.2 CBA/CaOla (CBA).....	45
2.4 Biological samples	46
2.4.1 Liver	46
2.4.2 Blood.....	47

2.5	Genotoxicity analysis	48
2.5.1	The comet assay	48
2.5.2	Flow-based micronucleus (MN) test in reticulocytes (RETs)	50
2.6	Omics analysis	51
2.6.1	Gene expression analysis (transcriptomics)	52
2.6.2	Chromatin profiling (epigenomics)	54
2.6.2.1	Assay for Transposase-Accessible Chromatin using DNA sequencing (ATAC-seq)	55
2.6.3	Bioinformatic analysis	57
2.6.4	Functional analysis	59
2.6.5	Statistical analysis	60
3	Results – summary of papers	61
3.1	Paper I	61
3.2	Paper II	62
3.3	Paper III	63
4	Discussion	64
4.1	Impact of dose rate	65
4.1.1	Low dose rate	65
4.1.2	Low dose rate compared to high dose rate	68
4.1.3	Transgenerational effects	71
4.2	Methodological considerations	72
5	Conclusions	78
6	Future perspectives	80
7	References	82
8	Papers	105
I	Perturbed transcriptional profiles after chronic low dose rate radiation in mice	105
II	Dose rate dependent reduction in chromatin accessibility at transcriptional start sites long time after exposure to gamma radiation	105
III	Genomic instability in F ₂ male progeny from low dose rate gamma irradiated F ₀ mice	105

Summary

Most of our epidemiological knowledge about radiation-induced health effects originates from atomic bomb survivors. However, the exposure from the atomic bombs was received over a short period and at high dose rates. An increasing number of studies suggest that low dose rate irradiation induces biological effects that differ from responses observed after acute high dose/high dose rate exposures. The modulation of gene expression constitutes an essential part of radiation-induced biological responses, while epigenetic changes have the ability to cause long-term changes in transcriptional programs. In most studies, responses are analysed shortly after exposure. Hence, there is a need to employ longer post-radiation timelines to investigate how (and if) perturbations in gene expression persist post-exposure.

The objectives of this PhD project have been to address research gaps concerning the impact of dose rate using mice models. The experiments were designed to gain information about the impact of low dose rate at three different post-irradiation timepoints; early- (one day), long-term (>100 days (three months)), and across generations. The design was strengthened by including high dose rate exposure groups to compare gene expression profiles and chromatin accessibility in directly exposed mice when all dose rate groups received the same total dose. Two mouse experiments were conducted using different dose rates of gamma radiation from a ⁶⁰Co source. These spanned from low to high dose rates: 1.5 mGy/h to 1.5 Gy (**Experiment A**), and 2.5, 10 and 100 mGy/h to 3 Gy (**Experiment B**). The induced responses were evaluated by profiling the transcriptional activity and chromatin accessibility, in liver tissue using RNA-sequencing and the Assay for Transposase Accessible Chromatin (ATAC)-sequencing in directly exposed mice at the two post-radiation timepoints; early (one day) and later (three months). Effects manifested across generations were evaluated using DNA- and cytogenetic damage to assess

transgenerational inherited genomic instability through the paternal germline. The comet assay and a highly sensitive MN-assay were used for this purpose.

One day post-radiation, the expression of genes and the accessibility to the chromatin were perturbed in a dose rate-specific manner when irradiated to a total dose of 3 Gy. The enrichment of functional pathways indicated that the affected genes were linked to lipid metabolism and inflammation, in addition to cancer, for all dose rate exposures. The overall results suggest a dose-rate-specific response and that prolonged exposure to low dose rates could be assumed to introduce lower level of cellular stress per time inflicting other mechanisms than high dose rate exposures. Furthermore, as the design included the use of two strains of mice, the results displayed that the choice of mouse strain is highly relevant for the molecular outcomes.

Differentially expressed genes were present three months after both low and high dose rate, although to a lesser extent when compared to one day post-radiation. Concerning the long-term (three months after exposure) epigenomic profile, there was no evidence that low dose rate irradiation introduced epigenetic changes affecting the chromatin accessibility. This indicate that the differentially changed chromatin regions present one day after low dose rate irradiation were reverted to a profile comparable with controls. The impact of a high dose rate on the epigenome long-term was clearly different to that seen following low dose rate. Here, the accessibility of the chromatin was almost exclusively reduced, occurring in transcriptional start sites (promoter regions) adjacent to genes relevant for radiation-induced damage, like the repair of DNA double-strand breaks and activation of p53-related responses. In addition, accessibility was also reduced in promoter regions to genes linked to transcriptional regulation.

Paternal transgenerational (F_2) genomic instability was used to investigate inheritance across generations, where F_2 represents the first unexposed generation. The low dose rate irradiated (1,5 mGy/h) F_0 generation was exposed for 45 days to a cumulative total dose of 1.5 Gy. Genomic instability was assessed in the blood samples from male F_2 mice before and after a challenging dose of X-ray. Changes in the rate of repair of induced DNA lesions were also evaluated. The results did display

statistically significant increased endogenously occurring DNA lesions. However, due to a low effect size, it is challenging to conclude whether the results represent a true biological finding or that it relates to methodological aspects. There was further no evidence that F₀ low dose rate irradiation affected the level of DNA damage directly after X-ray, the rate of repair of the DNA lesions, or the formation of micronuclei in reticulocytes.

The overall findings of this PhD project suggest that low dose rate should be considered a significant dose-effect modulating irradiation factor after direct exposure. Concerning transgenerational inheritance, given the experimental conditions a conclusion is elusive. The significance of these results upon the risk for human health needs to be addressed in appropriate epidemiological studies.

Sammendrag

Mye av det vi vet om risiko for helseeffekter etter å ha blitt usatt for ioniserende stråling er kunnskap lært fra de som overlevde atombombene i Hiroshima og Nagasaki. Imidlertid er denne kunnskapen basert på effekter etter høye strålingsnivåer som skjedde over kort tid. Nyere forskningen viser i økende grad at lavere konsentrasjon av stråling (lav doserate), hvor eksponeringen skjer over lengre tid, påvirker cellene våre på andre måter enn stråling med høy konsentrasjon, slik som stråling fra en atombombe. Forandringene som skjer i genene, er antatt å være en viktig bidragsyter til responsene som oppstår ved lav doserate bestråling. Man antar at endringer i såkalte epigenetiske markører kan føre til langvarige forandringer av genuttrykket. De fleste som har studert dette har i all hovedsak undersøkt responsene kort tid etter bestrålingen. Det er derfor et behov for studier som undersøker om endringene er målbare også lenge etter bestrålingen. Dersom langvarige endringer i genuttrykket oppstår, er det videre viktig med kunnskap om hvilke mekanismer som har bidratt til dette.

Formålet med dette doktorgradsprosjektet har derfor vært å bidra med å tette kunnskapshullene knyttet til betydningen av bestrålingsfaktoren «doserate», som beskriver hvor mye man bestråles per tidsenhet. Dette er blitt gjort ved å studere effektene i musmodeller. To strålingsstudier ble gjennomført i FIGARO kilden som driftes av NMBU. Studiene hadde ulike doserater, (1,5 mGy/t til 1,5 Gy (**Eksperiment A**), og 2,5, 10 og 100 mGy/t til 3 Gy (**Eksperiment B**)) gitt med gamma stråling fra en kobolt-60 (^{60}Co) kilde. Et viktig aspekt med prosjektet var å studere betydningen av lav doserate stråling som gis over lengre tid ved å undersøke responsene på tre ulike tidspunkter etter bestråling; kort (én dag), lang (>100 dager (3 måneder)), og over to generasjoner. I musene som ble direkte bestrålt (F_0) fokuserte vi på å undersøke endringer i genprofilene. I tillegg ble det undersøkt om tilgjengeligheten til DNAet, hvor genene er kodet, som blant annet endres av epigenetisk markører (epigenomet), også endret seg etter bestrålingen. For å studere om effekter også var målbare to generasjoner etter mus-bestefar (F_2) var blitt bestrålt, ble det brukt metoder som

måler DNA-skader som kan føre til mutasjoner, og skader som oppstår i kromosomene når cellene deler seg (dannelse av mikrokjerner). Disse metodene ble benyttet for å finne ut om noe hadde endret seg i muse-barnebarna (F_2) som kunne fører til ustabilitet i prosesser som omhandler genomet. For at prosjektet skulle kunne måle dette ble det etablert en meget sensitiv metode for å undersøke effekter på blodceller med mikrokjerner, i tillegg til å optimalisere metoden som måler DNA-skader i hvite blodceller («komet metoden») slik at tellingen av celler ble automatisert.

Resultatene én dag etter bestrålingen viste store endringer i både genuttrykket og i tilgjengeligheten av DNAet. Endringene var større jo høyere doseraten var, selv om alle hadde fått samme totale dose, altså så vi en doserate-spesifikk respons. Det viste seg også at genene var knyttet til biologiske signalveier koblet til kreft, fettmetabolisme og inflammasjon, for alle de målte doseratene. På de ulike tidspunktene var det stor forskjell på genekspressjon og DNA tilgjengelighet mellom lav og høy doserate. Vi brukte to ulike muselinjer i studien og det var store forskjeller mellom disse muselinjene, noe som viser at hvilken muselinje som benyttes har en stor effekt på de molekylære responsene man undersøker.

Selv tre måneder etter bestråling ble det funnet endret genuttrykk, men antall endrede gener var betraktelig færre sammenlignet med én dag etter bestråling. Det er vanskelig å vite den biologiske betydningen av at disse få genene var endret. Når det gjelder tilgjengeligheten til DNAet fant vi ingen endringer tre måneder etter lav doserate bestråling. Derimot, viste det seg at etter bestråling med akutt høy doserate ble det funnet reduserte tilgjengeligheten til gener, viktige for strålingsinduserte effekter, som blant annet har funksjoner i reparasjon av DNA-skader.

I muse-barnebarna av bestrålte muse-bestefedre undersøkte vi genomisk ustabilitet som er mål på nedarvede effekter. Det var ønskelig å studere effekter i muse-barnebarna da disse musene var de første som ble fertilisert av sædceller som ikke hadde vært påvirket av bestrålingen. I tillegg utsatte vi å avle neste generasjon av musene en periode slik at vi kunne være sikre på at sædcellene hadde oppstått fra en bestrålt stamcelle, og ikke blitt bestrålt selv. I blodprøver fra muse-barnebarna målte

vi hvor mye DNA- og kromosom-skader som oppsto av seg selv, hvor mye skade som oppsto rett etter en akutt dose røntgenstråler (betydelig høyere dose enn de vi får ved medisinsk undersøkelse), og i tillegg hvor fort noen typer DNA-skader ble reparert. Resultatene viste at musene som hadde en bestrålt bestefar hadde høyere endogent nivå av DNA-skader (DNA-skade som oppstår «av seg selv»). Denne økningen var veldig lav, og det er vanskelig å konkludere om dette er et biologisk funn eller om det skyldes metodologiske aspekter. Det ble ikke funnet noen holdepunkter for endringer i genomisk ustabilitet etter en akutt dose med røntgenstråler, ei heller på evnen til å reparere DNA-skade.

Hovedfunnene fra dette doktorgradsprosjektet er at doserate har modulerende virkning på type og grad av effekt etter bestråling, og at doserate burde bli tatt med i betraktningen når man vurderer strålingseffekter. Når det gjelder overføring av effektene over generasjoner (transgenerasjonell arvelighet) er det vanskelig å konkludere, gitt de eksperimentelle forholdene, om resultatene skyldes reelle biologiske effekter eller metodologiske aspekter. Resultatene må derfor verifiseres i andre studier.

Abbreviations and acronyms

ALS	Alkali-labile site
AML	Acute myeloid leukaemia
AP	Apurinic/aprimidinic
ATAC-seq	Assay for transposase accessible chromatin using sequencing
BER	Base excision repair
Bp	Base pair
Bq	Becquerel
B6	C57BL/6NHsd mouse strain
CBA	CBA/CaOlaHsd mouse strain
cDNA	Complementary DNA
CERAD	The Centre of Environmental Radioactivity
CT	Computed tomography
DDREF	Dose and dose rate effectiveness factor
DDR	DNA damaging response
DEG	Differential expressed gene
DNA	Deoxyribonucleic acid
DNase-seq	DNase I hypersensitive sites sequencing
DSB	Double-strand breaks
FAIRE-seq	Formaldehyde-assisted isolation of regulatory elements
FDR	False discovery rate
FPG	Formamidopyrimidine-DNA glycosylase
Gy	Gray
HSC	Hematopoietic stem cell
HDR	High dose rate
HNBR	High natural background radiation
HRR	Homologous recombination repair
ICRP	The International Commission on Radiological Protection
IES	Institute for Environmental Sciences
IR	Ionising radiation
J/Kg	Joule per kilogram
keV	Kiloelectronvolt
LDR	Low dose rate
LET	Linear energy transfer

LNT	Linear no-threshold
LSS	Life Span Study
MELODI	Multidisciplinary European Low Dose Initiative
MDR	Mid dose rate
miRNA	microRNA
MN	Micronucleus
MNase-seq	Micrococcal nuclease digestion with deep sequencing
MN-RET	Micronucleated reticulocyte
mRNA	Messenger RNA
5mC	5-Methylcytosine
NCE	Normochromatic erythrocyte
ncRNA	Non-coding RNA
NHEJ	Non-homologous end joining
NIPH	Norwegian Institute of Public Health
NRPA	Norwegian Radiation Protection Authority
nt	Nucleotide
ORA	Over-representation analysis
PTM	Post-translational modification
RBC	Red blood cell
RET	Reticulocyte
RNA	Ribonucleic acid
ROS	Reactive oxygen species
RNS	Reactive nitrogen species
RT-qPCR	Real-time quantitative polymerase chain reaction
Sec	Seconds
sncRNA	Small non-coding RNA
SSB	Single-strand breaks
Sv	Sievert
TB	Topological based
TF	Transcription factor
TLD	Thermoluminescent dosimeters
TSS	Transcriptional start site
UNSCEAR	The United Nations Scientific Committee on the Effects of Atomic Radiation
WBC	White blood cell
w/v	Weight per volume

List of papers

This thesis is based upon the following papers, which are referenced in the text by Roman numerals:

Paper I

H. DAHL, D. M. EIDE, T. TENGS, N. DUALE, J. H. KAMSTRA, D. H. OUGHTON, & A.-K. OLSEN. Perturbed transcriptional profiles after chronic low dose rate radiation in mice. *PLoS One*. 2021 Aug 24;16(8); e0256667. doi: 10.1371/journal.pone.0256667. PMID: 34428250; PMCID: PMC8384182.

Paper II

H. DAHL, J. BALLANGBY, T. TENGS, M.W. WOJEWODZIC, D.M. EIDE, D.A. BREDE, A. GRAUPNER, N. DUALE, & A.-K. OLSEN. Dose rate dependent reduction in chromatin accessibility at transcriptional start sites long time after exposure to gamma radiation. *Epigenetics*. 2023 Dec;18(1):2193936. doi: 10.1080/15592294.2023.2193936. PMID: 36972203; PMCID: PMC10054331.

Paper III

H. DAHL, R. WHITE, D.A. BREDE, C. INSTANES, D.M. EIDE, G. BRUNBORG, & A.-K. OLSEN. Genomic instability in F₂ male progeny from low dose rate gamma irradiated F₀ mice. Manuscript in preparation.

1 Introduction

We are constantly surrounded by ionising radiation, an energy that can ionise and excite the molecules in our body and thereby introduce harmful effects. However, a life without exposure to ionising radiation is not possible. Today, radioactivity also substantially benefits mankind through various applications in industry and medicine. To safely exploit the beneficial properties of ionising radiation, it is necessary to understand the full spectrum of the damaging potential, how cells respond upon different exposures and how this is connected to the manifestation of adverse health effects years after exposure. Despite 100 years of research and first-hand experience with nuclear disasters from industry and military force, there are still knowledge gaps. The effects of chronic radiation (and the irradiation factor "dose rate" (the amount of radiation per time unit)) on human health and the associated risks for hereditary effects for future generations still need to be addressed.

The work presented in this PhD thesis aims to investigating the impact of dose rate upon the effects of dose using global gene expression (transcription) and chromatin accessibility (epigenomic responses) in directly exposed mice both shortly and after a longer post-radiation period. The project has also addressed the inheritance of radiation-induced genomic instability in the first unexposed progeny (F₂) after chronically low dose rate irradiated paternal germline.

1.1 Ionising radiation (IR)

IR, in general terms, is radiation with high enough energy to knock electrons out from atoms and molecules, creating ions (atoms with an electric charge) – in contrast to non-IR (like radio waves, microwaves, infrared light and visible light). IR is released during the decay of radioactive elements (radionuclides). Decay is measured in becquerel [Bq, 1 decay/seconds (sec)], and during decay, electromagnetic photons (gamma rays) or particles (alfa, beta, and neutrons (uncharged particles)) escape from the radionuclide core. X-ray is another type of electromagnetic photons.

However, X-rays are not a result of radioactive decay (IARC, 2000). Photon radiation has higher energy than particle-based radiation and can penetrate matter over longer distances than particle-based types.

The types of IR are further classified based on how their energy is transferred to matter. This energy transfer rate per unit is called “linear energy transfer” (LET, kiloelectronvolt (keV)/mm). Alfa particles (^4He nucleus) and neutrons are defined as high-LET radiation and have a high rate of energy transfer per unit distance (keV/mm), causing more energy to be absorbed in a smaller volume of matter (many ionisations in a smaller area), which generates higher levels of damage upon interaction with macromolecules such as the DNA (deoxyribonucleic acid) (Harley, 2010). Low-LET radiation, which includes beta particles (high-speed electrons), gamma radiation and X-rays, deposits its energy more dispersed but homogeneously along the radiation track, leaving three times fewer ionisations than high-LET radiation (UNSCEAR, 2000). The type of radiation is thus relevant for the damaging potential of IR.

The harmful potential of IR (hazard and excessive risk) for adverse health outcomes is generally considered to depend on the amount of deposited energy, i.e., the amount of energy absorbed by the tissue (the total dose). The absorbed dose to tissue is expressed in Gray (Gy) and is quantified as deposited energy per unit mass (joule per kilogram (J/Kg)). However, other factors of exposure are also involved in modifying the potential of risk, like the radiation type and the type of tissue exposed, as tissues have different sensitivity to IR (ICRP, 2007). Therefore, *weighting factors* are used in radiobiological protection to convert the absorbed dose to weighted dose quantities expressed in Sievert (Sv) when estimating the additional risk related to the exposure. The equivalent dose is the calculated dose for organs, and the effective dose is the calculated dose for the whole body (ICRP, 2010). These factors are essential in radiation protection to ensure that the radiation-induced occurrence of *stochastic effects* is low and *tissue reactions* is avoided (ICRP, 2007). In addition, how the radiation interacts with the body (internal or external) and the duration of exposure can modify the dose-response relationship between effect and exposure. However,

both *if* and *how* these can change the potential risk for health effects compared to that of total absorbed dose are still questions discussed by experts (Haley et al., 2015; Lowe et al., 2022; Paunesku et al., 2021; Rühm et al., 2016; Rühm et al., 2015; Shore et al., 2017; Tanaka, 2022; Tran and Little, 2017; UNSCEAR, 2022). The source of irradiation is therefore relevant for considering potential consequences of exposure.

1.1.1 Sources of exposure

Humans are exposed to IR through a variety of sources:

1. Natural sources – cosmic radiation, naturally occurring radionuclides in soil, including radon
2. Medical procedures – like radiation therapy, computed tomography (CT) and X-ray imaging, and nuclear medicine
3. Occupational exposure – e.g., nuclear power plant workers, radiology workers like cardiologists, and aeroplane crew
4. Nuclear warfare, accidents, and contamination – e.g., the atomic bombings of Hiroshima and Nagasaki (1945), the Chernobyl (1986) and Fukushima (2011) power plant accidents, Techa River dumping and nuclear test sites

Approximately 80% of the exposure to IR comes from natural sources (UNSCEAR, 2016). Globally, the averaged populations-weighted effective dose from natural sources of IR is ~2.4 mSv/year. Due to variations in soil composition and altitude (cosmic radiation), populations can be exposed to an annual effective dose of up to 10 mSv/year, corresponding to a dose rate of ~1 µSv/h (UNSCEAR, 2000). Areas with exceptionally high radiation are known as high natural background radiation (HNBR) areas, and people living in such areas are chronically exposed (Hendry et al., 2009). In contrast, other regions suffer from high radiation levels due to anthropogenic contamination, like the Techa River in the Southern Urals (Kossenko et al., 2005).

The Techa River was contaminated by the dumping of liquid radioactive waste following the activities of the Soviet Union's nuclear bomb project at the Mayak nuclear facility. Residents in downstream villages were exposed to a mixture of

radionuclides (largely strontium-90 and cesium-137). They probably reached annual mean doses of 125 mGy and a maximum individual value of 2700 mGy, corresponding to dose rates of 0.014 mGy/h and 0.34 mGy/h in 1951 (Krestinina et al., 2013; Preston et al., 2017). The workers at the Mayak facility were also subjected to protracted exposure from gamma radiation and plutonium by inhalation. Today the residents along the river (Techa River Cohort) (Kossenko et al., 2005) and the Mayak workers (Mayak worker cohort) (Koshurnikova et al., 1999) are important cohorts for investigating long-term health effects associated with chronic low dose rate external and internal exposure. Other human activities have also led to release of radionuclides into the environment, like the nuclear weapons test sites (Bouville, 2020; Lukashenko et al., 2020) and nuclear power plant accidents (Salbu et al., 1994), such as the Chernobyl accident in 1986 (WHO, 2006) and the Fukushima accident in 2011 (WHO, 2013).

The remaining 20% of human IR exposure is attributed to artificial sources. Medical examinations and treatments are the most significant contributors and use is growing. In 2008, 3.6 billion radiation procedures were performed (UNSCEAR, 2008a). CT scanning provides radiation dose estimated to 15 (in adults)–30 (neonatal) mSv (organ dose), compared with 0.01–0.15 mSv from X-ray imaging (Brenner and Hall, 2007). The total annual collective effective dose from medical and diagnostic radiology (including nuclear medicine) from 1997 - 2007 was 4,200,000 manSv, resulting in a per person effective dose of 0.66 mSv (UNSCEAR, 2008a).

Occupation and lifestyle are also relevant for the total burden of exposure, mainly occupation, like aeroplane crew, nuclear workers, astronauts, and medical personnel (UNSCEAR, 2008b). Exposure due to occupational activities is to be monitored and regulated by national legislation, to ensure that safety measures are taken and that the annual absorbed dose is as low as possible. The International Commission on Radiological Protection (ICRP) is an international organisation composed of experts, providing scientifically based recommendations for all aspects of radiological protection (www.ICRP.org). ICRP recommend that occupational exposure should not exceed an effective dose of 20 mSv/year, averaged over five years (100 mSv in 5

years) and not >50 mSv in a single year (ICRP, 1991; ICRP, 2007). Many countries have adopted this recommendation resulting from the knowledge concerning the risk for long-term radiation-induced health effects such as cancer (solid tumours and leukaemia).

Although accidents and nuclear disasters can cause irradiation at high dose rates and doses, most IR exposures are at low levels (<6 mGy/h) and yield low total doses (<100 mGy) (Lowe et al., 2022). There is therefore a need to close knowledge gaps related to low levels of exposures to enable scientifically sound assessments of low dose rate/dose risks, better information concerning potential outcomes of low level IR, and validated recommendations concerning optimal radiation protection and handling in response to possible future nuclear accidents and disasters.

1.1.2 Health effects

In general, health effects from radiation are classified into two categories: *tissue reactions* (also known as deterministic effects) and *stochastic effects* (Clement et al., 2012). Tissue reactions are characterised by cell death when the absorbed dose exceeds a certain threshold, and the severity increases with the dose. The ICRP has established threshold doses based on morbidity and mortality observations in epidemiological cohorts, such as atomic bomb survivors and medically exposed individuals (ICRP, 2007). Shortly after irradiation (days/weeks) depression of the hematopoiesis (~0.5 Gy), skin reddening and burns (>3 Gy), loss of hair (~4 Gy), sterility (temporary (male: ~0.1 Gy) and permanent (3 Gy (female) 6 Gy (male))) (McBride and Schae, 2020) are examples of tissue reactions. Late-onset tissue reactions can occur years after irradiation, like cataracts (>20 years after exposure, ~0.5 Gy) and circulatory and cerebrovascular disorders (>10 years after exposure, ~0.5 Gy) (Kamiya et al., 2015).

The concept of a threshold dose contrasts with the effects classified as *stochastic effects*, which follow the linear no-threshold (LNT) model. According to the LNT model there are no safe levels of radiation exposure, as radiation can cause DNA damage leading to stochastic effects (cancer and hereditary effects), by chance, in the

exposed population years after exposure. The probability (the risk) of a stochastic outcome increases with the dose, but the severity of the effect is independent of the dose (ICRP, 2007). Therefore, after low levels of IR, cancer and hereditary effects are considered the leading health hazards upon IR exposure. Hereditary effects are radiation-induced health effects in a descendant of the exposed person, result from DNA damage in gametes giving rise to mutations in the human germline (UNSCEAR, 2006b).

Our knowledge about radiation-induced cancer risk is mainly obtained from the follow-up studies of atomic bomb survivors (UNSCEAR, 2006a). The atomic bomb survivors and the long-term follow-up studies (the A-bomb Life Span Study; LSS) are essential sources of information building the basis of radiobiological understanding of IR-induced health effects (Ozasa et al., 2019; UNSCEAR, 2006a). Leukaemia (Folley et al., 1952) and a range of solid cancer types (Ozasa et al., 2012; Preston et al., 2007; Preston et al., 2003) have been observed in this cohort. Cardiovascular (Shimizu et al., 2010) and metabolic disorders (Akahoshi et al., 2003), as well as cataract (Minamoto et al., 2004), have also been observed.

The LSS cohort is recognised to be reliable due to the size of the cohort, exposures of both genders at all ages, and a broad spectrum of individually assessed doses (Ozasa et al., 2019). However, the fact that the irradiation in the LSS cohort was given over a short time and at high dose rates resulting in acute total doses over 100 mGy, the cancer risk at lower doses were extrapolated from high levels of exposure (Ozasa et al., 2019). Notably, experimental studies performed in 1927 by the Nobel prize winner to H. J. Muller, later supported by others, led to the conclusion that the mutation rate is directly proportional to the dose with no threshold level (NobelPrize.org, 2023). The practice of extrapolating the cancer risk from the LSS is supported for radiation protection purposes (ICRP, 2007).

1.1.3 The concept of (low) dose rate

The biological effects from chronic and prolonged exposure to low dose rate IR are still associated with knowledge gaps. In the field of radiation protection, a *dose and*

dose rate effectiveness factor (DDREF) can be applied to account for the temporal variation in dose delivery calculated from epidemiological studies. However, both the use and the numeric value has been debated among international organisations (e.g., UNSCEAR, ICRP, NRC (BEIR VII), SSK and WHO)¹ particular around 2006 when the BEIR VII(NAS, 2006) report were published (Rühm et al., 2015) . Also, the cellular mechanisms involved at different dose rate levels are not well characterised.

Low dose rate was for the first time defined by UNSCEAR in 1986 to be lower than 3 mGy/h, a definition that was maintained for many years. In 1993 results from animal studies contributed to the formation of the DDREF to reduce the excess cancer risk per unit dose if the dose rate were lower than 6 mGy/h, independent of total dose. Currently, low dose rate is defined by the UNSCEAR (2019) (and adopted by ICRP) as:

0.1 mGy/min for low-LET IR when averaged over one hour (~6 mGy/h)

The ICRP (publication 103) recommend using the LNT model concerning stochastic effect (cancer and hereditary effects) when the dose rate exceeds the definition of low dose rate, and that DDREF = 2 (halving the risk) can be applied if the exposure is classified as low dose rate (ICRP, 2007).

1.1.4 Low dose rate effects

Available literature suggests an association between low dose rate IR exposure and human health effects (Little et al., 2009; Tang and Loganovsky, 2018), such as cancer (Hauptmann et al., 2020), circulatory disease (Little et al., 2021), and immune

¹ UNSCEAR, United Nations Scientific Committee on the Effects of Atomic Radiation; ICRP, International Commission on Radiological Protection; NRC (BEIR VII), the US National Research Council's National Academy of Sciences (Biological effects of ionising radiation: Report VII); SSK, Strahlenschutzkommission, the German Commission on Radiological Protection; WHO, World Health Organisation.

adversity (Lumniczky et al., 2021). The impact of dose rate has also been investigated in several animal experiments. Some of these studies are particularly large and have been designed using epidemiological approaches to obtain disease risk estimates, such as the JANUS experiments in mice and dogs (Tran and Little, 2017) and the studies performed at the Institute for Environmental Sciences (IES) in Japan (Braga-Tanaka et al., 2018; Tanaka, 2022). Available murine data have been summarised in several reviews (Lowe et al., 2022; Paunesku et al., 2021; Suzuki et al., 2023a; Suzuki et al., 2023b; Tang et al., 2017). Most of these studies include exposure groups receiving different dose rates over the same exposure period, resulting in total doses that differs between the groups. This makes it challenging to separate the observed effect of dose rate from the effect of total dose.

Some studies have applied different dose rates to a similar total dose, and studies addressing effects on gene expression, epigenetics and genotoxicity have been summarised in Table 1 (note that the table is not a result of a systematic literature search and is thus not necessarily an exhaustive list of eligible studies). All studies in Table 1 are mouse experiments designed to compare the dose rate when the total dose is kept constant. *In vitro* studies and other model organisms are excluded due to the wide variety in experimental conditions and reported responses (Lowe et al., 2022). All studies include one or more low dose rate groups, except for Barnard et al., which only uses high dose rates (defined as >0.05 Gy/min (3000 mGy/h) by UNSCEAR in 1986 (§24 (UNSCEAR, 1986))).

Table 1. Overview of studies in mice where the impact of dose rate when the total dose is constant, and exposure is given continuously is examined. The table is sorted on the endpoints: gene expression, epigenetics, and genotoxicity outcomes. Low dose rate (LDR) exposure is highlighted in bold.

Reference	Strain Age Gender	Irradiation Dose rate (total dose) Duration	Tissue Sampling time	Endpoint (method)	Findings
(Fujikawa et al., 2022)	B6C3F1 8 weeks M/F	γ -rays (^{137}Cs) 0.83 mGy/h (2, 4, 6, 8 Gy) 16.7 mGy/h (2 Gy) Duration: 100, 200, 300, 400 days	Liver Immediately + 95 days MDR to 2 Gy	Gene expression (microarray)	Dose rate effects were addressed for 2 Gy using gene expression. The results show dose rate specific gene responses, especially for p53-related functions. Few genes were identified 95 days after IR.
(Dahl et al., 2021) (Paper I)	C57BL/ 6NHsd CBA/Ca01a 8-9 weeks M	γ -rays (^{60}Co) 2.5 mGy/h (3 Gy) 10 mGy/h (3 Gy) 100 mGy/h (3Gy) Duration: 1200 h, 300 h, 30 h	Liver 19-26 h (early) B6: 106-221 days (late) CBA: 108-178 days (late)	Gene expression (RNA-seq)	Dose rate specific transcriptional profiles were identified, along with mouse strain specific responses. Few differentially expressed genes identified >100 days post-IR, compared to ~1 day after exposure stop.

Reference	Strain Age Gender	Irradiation Dose rate (total dose) Duration	Tissue Sampling time	Endpoint (method)	Findings
(Sunirmal et al., 2015)	C57BL/6 7 weeks M	X-ray No LDR 185 mGy/h (1.1, 2.2, 4.4 Gy) 62x10 ³ mGy/h (1.1, 2.2, 4.4 Gy)	Whole blood 24 h	Gene expression (microarray)	Dose rate is highly relevant for the gene profile at each respective dose, although common and different gene profiles were identified.
(Olipitz et al., 2012)	C57BL/6 8-9 weeks M/F	Flood phantoms under cage (¹²⁵ I) 0.102 mGy/h (0.01 Gy) 4.2x10 ³ mGy/h (0.01 Gy) Duration: LDR: 5 weeks HDR: 1.4 min	WBC Before and immediately after	Gene expression (RT-qPCR)	Dose rate related transcriptional responses. LDR: No sig. changed genes. HDR: Genes related to DNA damage response were significant increased.
(Nakajima et al., 2017)	C57BL/6j 10 weeks (4 Gy) 24 weeks (8 Gy) M	X-ray (acute) γ-rays (¹³⁷ Cs) (chronic LDR) 0.83 mGy/h (8 Gy) 43.2x10 ³ mGy/h (8 or 4 Gy) 33x10 ³ mGy/h (8 or 4 Gy) Duration: 400 days	Liver Acute: 6 days (8 Gy) and 3 months (4 Gy) Chronic: Immediately and 3 months	Protein expression (Antibody microarray)	Chronic (apoptosis) and acute (defence and inflammation) exposure show different protein expressions.

Reference	Strain Age Gender	Irradiation Dose rate (total dose) Duration	Tissue Sampling time	Endpoint (method)	Findings
(Dahl et al., 2023) (Paper II)	CBA/CaOla 8-9 weeks M	γ -rays (^{60}Co) 2.5 mGy/h (3 Gy) 10 mGy/h (3 Gy) 100 mGy/h (3Gy) 1200 h, 300 h and, 30 h.	Liver 19-26 h 108-178 days	Chromatin accessibility (ATAC-seq)	Dose rate specific modulation of chromatin accessibility ~1 day post-IR. LDR do not induce long-term changes in accessible chromatin, while HDR reduce accessibility at TSS of genes related to DNA damage.
(Dahl et al., 2021) (Paper I)	CBA/CaOla 8-9 weeks M	γ -rays (^{60}Co) 2.5 mGy/h (3 Gy) 10 mGy/h (3 Gy) 100 mGy/h (3Gy) Duration: 1200 h, 300 h and, 30 h.	Liver 19-26 h (early) CBA: 108-178 days (late)	DNA methylation (LC-MS/MS)	Changes in global levels of 5mC and 5hmC were not seen.
(D'Auria Vieira de Godoy et al., 2021)	C57BL6/ 6NCrl 4-6 weeks F	γ -rays (^{137}Cs) 1.4 mGy/h (0.1, 0.2, 0.5 and 1 Gy) $\sim 2.2 \times 10^4$ mGy/h (0.1, 0.2, 0.5 and 1 Gy)	Bone marrow 3h and 3 weeks post-IR	Micronuclei formation (CBMN)	Effects of 200 mGy on MN-induction are transient. After 500 and 1000 mGy (both HDR and LDR) lead to increased levels of MN up to 3 weeks after the exposure.

Reference	Strain Age Gender	Irradiation Dose rate (total dose) Duration	Tissue Sampling time	Endpoint (method)	Findings
(Olipitz et al., 2012)	C57BL/6 8-9 weeks M/F	Flood phantoms under cage (¹²⁵ I) 0.102 mGy/h (0.01 Gy) 4.2x10 ³ mGy/h (0.01 Gy) Duration: LDR – 5 weeks HDR – 1.4 min	Bone marrow Immediately 24h after	Micronuclei formation (<i>in vivo</i> MN-RETs)	LDR: No changes were observed HDR: Significantly increase in MN-RETs were seen
(Barnard et al., 2019)	C57BL/6J01aHsd 10 weeks F	γ -rays (⁶⁰ Co) <i>No LDR included in study</i> 18x10 ³ mGy/h (0.5 Gy, 1.0 Gy, 2.0 Gy) 3.78x10 ³ mGy/h (0.5 Gy, 1.0 Gy, 2.0 Gy) 840 mGy/h (0.5 Gy (39 min)) Duration: max 39 min	Isolated PBL 24 h post-exposure LECs 4 and 24 h post-exposure	DNA damage (53BP1 foci)	PBL: DNA damage is dependent on dose and dose rate. Lesser damage is seen with reduced dose rate within each dose. LECs: damage dependent on dose and an inverse dose rate effect is seen
(Olipitz et al., 2012)	C57BL/6 8-9 weeks M/F	¹²⁵ I (Flood phantoms under cage) 0.102 mGy/h (0.01 Gy) 4.2x10 ³ mGy/h (0.01 Gy) Duration: LDR – 5 weeks HDR – 1.4 min	Spleen Immediately	DNA damage (Base lesions) (LC-MS/MS)	Chronic LDR nor acute HDR radiation to 0.01 Gy (10 mGy) changed the levels of base lesions.

Abbreviations: ATAC-seq, Assay for Transposase-Accessible Chromatin using sequencing; F, female; HDR, high dose rate; IR, ionising radiation; LC-MS/MS, Liquid Chromatography with tandem mass spectrometry; LDR, low dose rate; LECs, eye lens epithelial cells; M, male; MDR, mid dose rate; MN, micronucleus; MN-RFTs, micronucleated reticulocytes; PBL, peripheral blood lymphocytes; RETs, reticulocytes; RT-qPCR, real-time quantitative polymerase chain reaction; WBC, white blood cells

1.1.5 Cellular and molecular processes

Through the ability to ionise biological matter, IR can disrupt chemical bonds when “passing” through the cell via two mechanisms for deposition of energy: *directly* and *indirectly* (Goodhead, 2010) (Figure 1). Since damage to the DNA can lead to stochastic effects, which can occur after any exposure with no safe level, the detrimental potential of IR is attributed damage to the DNA. This rationale is based on “the target theory”, also known as the “conventional paradigm of radiobiology”, - where damage to the DNA is proportional to the dose of exposure without a threshold (Belli and Tabocchini, 2020). Depending on the cell type, the insults of IR may result in carcinogenesis in somatic cells, developmental defects upon *in utero* exposure, and hereditary effects in the germ line (Figure 1). Also, cell types with high mitotic activity (like the erythroblasts) are suggested to be more sensitive to the manifestation of damaging insults (UNSCEAR, 2006b).

The current target paradigm and the practice of using the LNT model is debated due to observations of changes in epigenetic markers, gene expressions and alterations to the chromosome organisation particularly in response to low dose/low dose rate exposure (Belli and Tabocchini, 2020). It is suggested that these responses can be related to effects not only in the directly hit nuclei or cells but also in un-hit cells or nuclei. Such effects are termed *non-targeted effects* (Figure 1) (Belli and Indovina, 2020; Desouky et al., 2015; Tharmalingam et al., 2019). Genomic instability and adaptive responses are two types of non-targeted effects (UNSCEAR, 2006b). However, the underlying mechanisms and significance for human health still need to be clarified. UNSCEAR defines genomic instability as “*An all-embracing term to describe the increased rate of acquisition of alterations in the genome. As compared with the direct actions, radiation-induced instability is observed in cells at delayed times after irradiation and manifests in the progeny of exposed cells multiple generations after the initial insult*”. This concept is also adopted to include effects manifested over generations (inter- and transgenerational). Adaptive response is defined as “*the phenomenon by which cells irradiated with a sublethal dose of ionizing radiation*

become less susceptible to subsequent exposure to a higher challenging dose of radiation” (UNSCEAR, 2022).

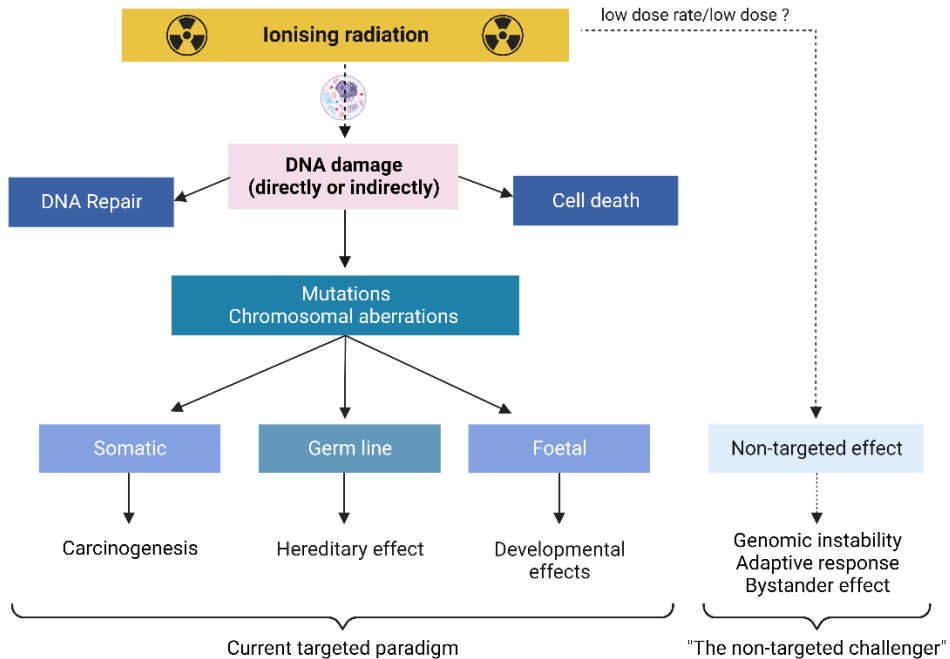


Figure 1. Biological effects of ionising radiation; the current targeted paradigm and the debated non-(DNA)-target effects. Current paradigm: IR deposits its energy in the nucleus and directly and/or indirectly induce DNA damage. The damage may be eliminated through DNA repair, although unrepaired or error-prone processes may cause mutations and chromosomal aberrations (clastogenic effects). Depending on the cell type, various effects may be introduced, including carcinogenesis in somatic cells, hereditary effects in germ cells and developmental effects upon foetal exposure. If the damage is severe enough, cell death may occur. Non-targeted effects: IR-induced cellular effects occur through damage/responses to non-nuclear components or non-irradiated cells/tissue, in principle, resulting from low dose and low dose rate exposures, altering the risk for IR-induced carcinogenesis. The figure is adapted from UNSCEAR 2006, Volume II, Annex C, “Non-targeted and delayed effects of exposure to ionizing radiation” (UNSCEAR, 2006b).

1.1.6 DNA damage and oxidative stress

IR introduces damage to cells and molecules through direct and indirect mechanisms, as illustrated in Figure 2, and further initiates DNA lesions, mutations, chromosomal aberrations, and cell death. Direct damage occurs when IR directly interacts and deposits its energy into the molecules (Figure 2). Indirect damage occurs when IR interacts with water molecules through the chemical process of radiolysis (Figure 2) (Azzam et al., 2012; Harley, 2010).

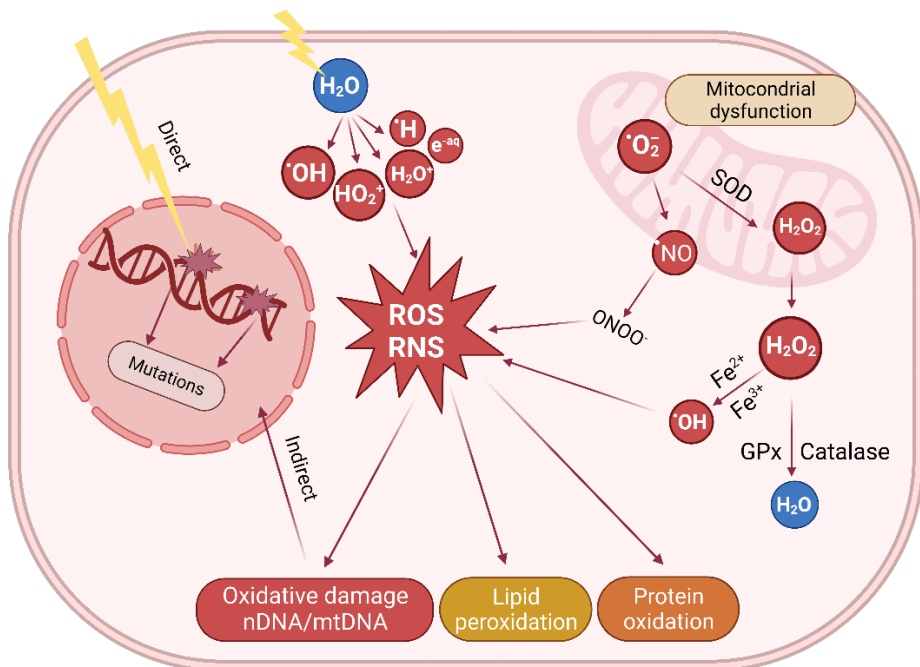


Figure 2. Overview of direct and indirect cellular effects of ionising radiation.

IR cause DNA damage through direct deposition of energy and indirectly via radiolysis of water molecules generating reactive oxygen and nitrogen species (ROS/RNS). Further leading to additional generation of ROS/RNS from endogenous sources. A range of enzymes (like SOD, GPx and catalase) are part of the antioxidant defence fine-tuning the intracellular ROS/RNS levels. By-products from oxidised lipids can interact with the DNA causing additional types of DNA lesions. Oxidised proteins can cause defective DNA damage repair enzymes resulting in impaired DNA damage response and mis-repaired or unrepaired DNA lesions leading to mutation. Thus, depending on the level of

ionisations per time unit (the dose rate), the level of ROS/RNS, and the level of damaged biomolecules, signalling pathways necessary for proper functionality/cellular integrity are induced. High dose rates will cause higher concentrations of ROS/RNS per time unit. Abb: H₂O, water; •OH, hydroxyl radical; H₂O⁺, ionised water; H•, hydrogen radical; e^{-aq}, hydrated electron; HO₂, hydroperoxyl; •O₂⁻, superoxide; •NO, nitric oxide; ONOO⁻, peroxynitrite; Fe²⁺, ferrous; Fe³⁺, ferric; H₂O₂, hydrogen peroxide; ROS, reactive oxygen species; RNS, reactive nitrogen species; SOD, superoxide dismutase; GPx, glutathione peroxidases. Created with www.BioRender.com.

It is assumed that 70% of the deposited energy from low-LET leads to radiolysis, increasing the intracellular oxidative burden (Nikjoo et al., 1998), and the remaining energy (30%) induces DNA damage of different structural and chemical complexity. This is in contrast to high-LET, where 90% of the deposited energy results in clustered DNA damage (Goodhead, 1994). Effects of high-LET are considered outside the scope of this thesis.

The balance between physiological and harmful levels of ROS (redox reactions) is controlled by a range of interconnected enzymatic and non-enzymatic antioxidants (Reisz et al., 2014). When the cellular milieu is unable to balance the redox state and the production of ROS exceed beyond the antioxidant defence response, a state of oxidative stress may occur. This can lead to excessive damage to biomolecules and create e.g., lipid-peroxyl radicals and hydroperoxides, as well as a variety of oxidative DNA lesions and oxidative damage to proteins (Figure 2). Oxidised proteins can undergo conformational modifications causing loss or impairment of their enzymatic activity, and oxidised lipids can change permeability and fluidity of cell membranes and cause cytotoxic by-products upon breakdown (Aranda-Rivera et al., 2022; Klaunig et al., 2011). Further, the redox perturbations can result in mitochondrial dysfunction leading to additional production of mitochondrial ROS (Azzam et al., 2012).

Damage threatening the DNA is of most concern, and include (Baiocco et al., 2022; Ward, 1994) (Pizzino et al., 2017):

1. single-strand breaks (SSBs)
2. double-strand breaks (DSBs) (e.g., >two SSB lesions around 10 base pair (bp) apart)
3. base damage (chemically modified bases and nucleotides, including oxidative lesions (like the 7,8-dihydro-8-oxoguanine (8-oxoG) and DNA adducts (e.g., from malondialdehyde and 4-hydroxy-2-nonenal by-products of lipid peroxidation breakdown))
4. abasic sites (e.g., apurinic/aprimidinic sites (AP-sites))
5. DNA cross-links (e.g., covalent linkage between nucleotides)
6. clustered DNA damage (several damaged lesions in proximity (~25 bp))

Cells have evolved a range of mechanisms to detect and counteract DNA lesions and aberrant DNA structures (e.g., stalled transcription and chromatin perturbations), to ensure genomic stability and integrity, and the initial responses is known as the DNA damaging response (DDR) (Jackson and Bartek, 2009). The DDR include a range of sensor proteins recruited upon damage that activate downstream responses to promote repair of insults by changing the chromatin, stalling the cell cycle via checkpoint activation, modulation of transcription, and induction of programmed cell death (apoptosis) (UNSCEAR, 2022). The recruitment of the DNA repair response corresponds to the type of DNA damage, and can be mediated through specific post-translational modifications (PTMs) of certain proteins, and the efficiency depends upon chromatin structure (Nair et al., 2017).

The main DNA repair pathways related to IR-induced damage include (Jeggo and Löbrich, 2006; Lomax et al., 2013):

1. Base excision repair (BER) - removes damaged bases (error free)
2. Homologous recombination repair (HRR) - repairs DSBs using a homologous DNA template (error-free)
3. Non-homologous end joining (NHEJ) - repairs DSBs without a corresponding template (error-prone)

BER operates throughout the cell cycle and is initiated by DNA glycosylases, which recognize and remove damaged bases, forming AP sites (abasic sites). These are then cleaved by an AP-endonuclease creating a SSB that is further restored by nuclease, DNA polymerase, and DNA ligase (Kubota et al., 1996). The DSBs are repaired in principle by HRR and NHEJ. In general, the main difference between these pathways is that HRR occurs in late synthesis (S phase) and G2 phase (before mitosis) of the cell cycle and depends on an undamaged DNA template for error-free repair. NHEJ can repair DSBs throughout the cell cycle, except during mitosis, as no undamaged template copy is required. The occurrence of DSB is assumed to be approximately 40 DSBs/cell/Gy from low-LET and assumed relatively rare at doses below a few mGy and only present in a fraction of the irradiated cells (UNSCEAR, 2022).

The complexity of the DNA damage insults involve clustered damage sites that depend on the type of damage, number of lesions, and a distribution of lesions dependent on the ionising track and the spatial distribution of the deposited energy (Baiocco et al., 2022). Clustered DNA damage is divided into non-DSB clusters; consisting of SSB, base damage, and abasic sites, and DSB clusters, which have multiple damage sites near the DSB (Lomax et al., 2013; Mavragani et al., 2017; Nikjoo et al., 2001; Ward, 1994). DSB and clustered damage are considered the most potent DNA insult, as these are more challenging to restore (Goodhead, 1994; Iliakis et al., 2019; Kaplan et al., 1997). If the damage is severe enough, the cell may undergo apoptosis or other forms of cell death (like necrosis, autophagy and ferroptosis) (Jiao et al., 2022). Un-repaired or mis-repaired lesions can lead to mutations and chromosome damage that increase the risk for hereditary effects (germ cells) or cancer (Hanahan and Weinberg, 2000).

1.1.7 Hereditary and transgenerational effects

According to the target theory of IR-induced damage to germline cells can be expected to increase the risk for heritable genetic effects in children of irradiated parents (Figure 1) (UNSCEAR, 2001). Despite this, there is no evidence for radiation-induced changes in disease burden and risk of death in children of exposed parents (Gardner et al., 1990). A higher risk of leukaemia has been reported in children of Sellafield

nuclear plant workers (Grant et al., 2015; Izumi et al., 2003; Little et al., 2013), although this has been proposed to be due to other confounding factors such as migration (COMARE, 2016). Studies investigating molecular markers such as the levels of germline mutations have reported increased rates in children of parents exposed in relation to the Chernobyl accident (Dubrova et al., 1996; Dubrova et al., 1997; Weinberg et al., 2001), Techa River (Dubrova et al., 2006), Semipalatinsk nuclear test site (Dubrova et al., 2002) and the accident in Goiania, Brazil (Costa et al., 2018). In contrast, other studies do not support these findings and indicate no evidence for changes in mutations rates in children of atomic bomb survivors (Kodaira et al., 2010; Kodaira et al., 1995), British nuclear test veterans (Moorhouse et al., 2022), occupational exposure at the Sellafield nuclear facility (Tawn et al., 2015), and the Chernobyl accident (Yeager et al., 2021). Even if the risk of heritable effects is considered scientifically plausible, uncertainties related to this topic is acknowledged due to the lack of evidence (ICRP, 2007; NAS, 2006; UNSCEAR, 2001). Currently, ICRP has estimated the risk for heritable genetic effects in offspring from directly exposed parents to be 0.5% Sv⁻¹ (0.2% Gy⁻¹) (ICRP, 2007). Since epidemiological studies have not provided clear evidence of heritable effects in humans, the ICPR estimate the genetic risk based on measured germline mutation frequencies in mice (ICRP, 2007).

Inherited effects across generations that cannot be ascribed to effects of direct exposure is termed transgenerational inheritance (Skinner, 2008). Transgenerational inheritance of radiation-induced effects is still a controversial phenomenon, as the total burden of epidemiological evidence in humans renders inconclusive evidence. For some species, like plants and nematodes, environmental adaptations through several generations are common and possibly necessary for survival (Heard and Martienssen, 2014). In 2018 a systematic literature review also performing evidence mapping of transgenerational effects in both human and animal studies was performed (Walker et al., 2018). This systematic review concluded that risk of bias, few studies, and wide heterogeneity in both exposures and endpoints limits the body of evidence, albeit that radiation exposure was found to be one of the most studied (although still few) environmental exposures in this context (Walker et al., 2018).

Given this, robust experimental studies, and bias-free reporting of both negative and positive results are important to fill the knowledge gaps within this field of research.

Irradiation is suggested to cause transgenerational effects through the mechanism of non-targeted genomic instability (Figure 1) (Barber and Dubrova, 2006). Genomic instability can be measured as chromosomal alterations, changes in ploidy, formation of micronuclei, gene mutations and amplifications and mini- and microsatellite (short tandem repeat) instabilities (UNSCEAR, 2006b). However, the mechanisms behind the transmission of transgenerational genomic instability are unclear, though it is hypothesised that epigenetic mechanisms (section 1.2.3) are involved (Belli and Tabocchini, 2020; Dubrova and Sarapultseva, 2020; Hei et al., 2011; Merrifield and Kovalchuk, 2013; Vaiserman et al., 2017).

1.2 The epigenome

The genome, both human (Venter et al., 2001) and mouse (Waterston et al., 2002; Yue et al., 2014), have been mapped and annotated (ENCODE, 2004). The genome consists of a range of genes and multiple regulatory elements, packed into the chromatin which represents a global collection of all the alterations affecting the accessibility to the DNA sequence and ultimately regulating and controlling the expression of genes (Bernstein et al., 2007; Klemm et al., 2019). The epigenome may therefore be viewed as the chromatin structure and the processes regulating its accessibility (Figure 3) (Klemm et al., 2019).

1.2.1 The chromatin

In eukaryotes, the DNA is organised in a 3D chromatin structure, where the DNA is wrapped around nucleosomes (Figure 3) (Kornberg, 1974; Maeshima et al., 2021; Stevens et al., 2017). The nucleosomes are dynamically unpacked at actively transcribed and regulatory regions. This is a critical aspect of gene regulation, where cis-regulatory elements (CREs) are brought in proximity to their target promoter by forming chromatin loops and recruiting transcription factors (Figure 3) (Hansen et al., 2017) (Maeshima et al., 2021).

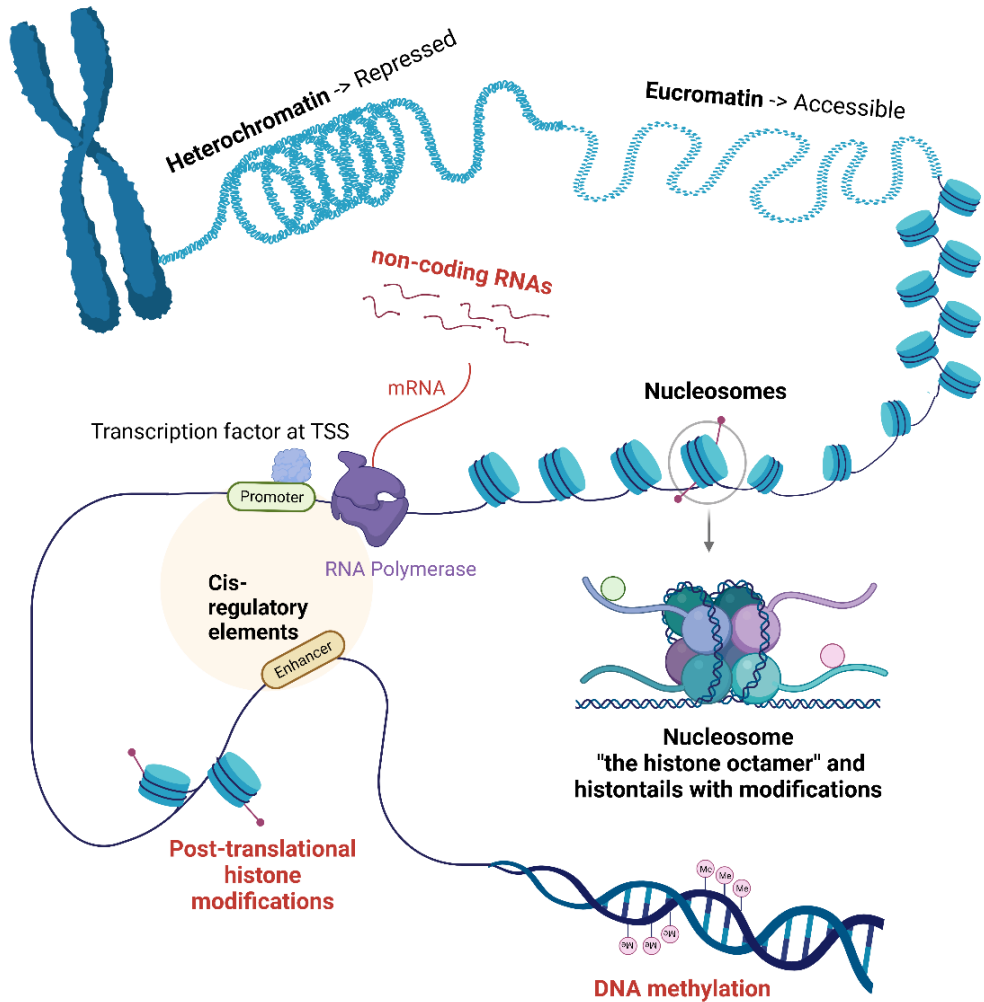


Figure 3. The Epigenome. The sum of factors regulating gene expression without changing the DNA sequence. The DNA is packed into heterochromatin and euchromatin depending on transcriptional activity, where the heterochromatin is densely packed and generally considered transcriptional inactive. The euchromatin is less condensed and constitutes transcriptional active regions (Maeshima et al., 2021). The chromatin sub-units are the nucleosomes composed of two copies of four histones with 147 bp DNA wrapped around (the octamer) (Lee et al., 2004; Thurman et al., 2012). Each histone has extended tail domains critical for the signalling between nucleosome and chromatin through PTMs (one of the epigenetic mechanisms) (Bannister and Kouzarides, 2011).

The epigenetic mechanisms are highlighted using red fonts in figure, mechanisms all associated with regulating of gene transcription. The epigenetic mechanisms are highlighted using red fonts in the figure, which are all associated with regulating gene transcription. Abb: TSS, transcriptional start site; mRNA, messenger RNA. The figure is adapted from the figure "Regulation of Transcription in Eukaryotic Cells", BioRender (2020) retrieved at <https://app.biorender.com/biorender-templates>.

The organisation of the chromatin varies from tightly packed and transcriptional inactive (heterochromatin) to less densely packed parts called euchromatin (Figure 3) (Maeshima et al., 2021). The euchromatin is characterised as "open chromatin" and comprises transcriptional active regions like the gene bodies and regulatory regions, like promoters and enhancers (Figure 4) (Lee et al., 2004; Thurman et al., 2012). The lack of nucleosome binding generally characterises active regulatory regions, and the chromatin accessibilities are often used as a proxy to identify active regulatory elements (Jiang and Pugh, 2009).

1.2.2 Transcription and genomic regulatory elements

The expression of genes, the transcription, is the process of ribonucleic acid (RNA) synthesis from sequence information to generate a gene product. In general, this process requires access to the genetic code and the transfer of this information to a functional molecule with specific functions (coding or non-coding RNAs (ncRNAs)).

Transcription is initiated by the binding of transcription factors (TFs) and the assembly of the transcription initiation complex to the promoter regions, a regulatory sequence generally found upstream of the gene body which contains coding (exon) and non-coding (intron) sequence elements (Figure 4). Regulatory elements (like promoters and enhancers) consist of DNA regions located on the same chromosome as the gene they regulate (termed *cis*-regulatory elements), and regions located on different chromosomes than the gene they regulate (termed *trans*-regulatory elements). A specific feature in eukaryotic genomes is that enhancer regions far from transcriptional start sites (TSS) can sequester TFs to upregulate the rate of transcription and/or bind to the initiation complexes (Riethoven, 2010). Dependent

on the activity of the enhancers, the enhancers adopt a chromatin conformation with specific functional states termed: active, primed, poised or repressed (Barral and Déjardin, 2023).

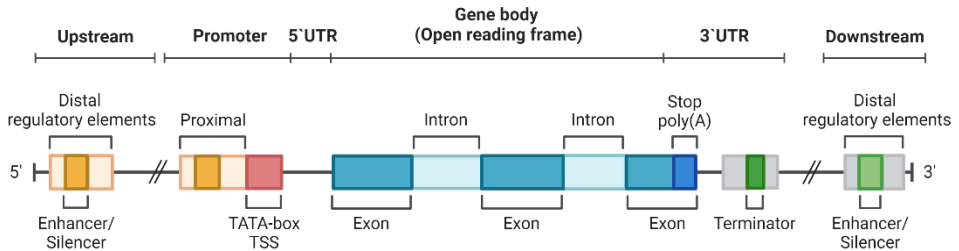


Figure 4. Schematic overview of the gene structure and genomic regulatory elements (relevant for Paper II). Abb: UTR, un-translated region; TSS, transcriptional start site. Adapted from “Eukaryotic Gene Structure”, BioRender (2022) retrieved at <https://app.biorender.com/biorender-templates>.

The regulatory regions can be found up- and downstream of the TSS, within exons and introns, in the 5' and 3' untranslated (UTR) regions, and as far as 100,000 bp in humans and mice from the gene body (Birney et al., 2007). The trans-acting factors can be proteins (like TF, activators or repressors) as well as regulatory ncRNA transcripts (Panigrahi and O'Malley, 2021). The exact mechanisms for how enhancers influence transcriptional activity are still unclear. However, the complexity is extensive, and defined by local and global interaction between promoters and regulatory elements that operates in tight agreement with the chromatin structure and epigenetic control to enable efficient transcriptional control (Panigrahi and O'Malley, 2021).

1.2.3 Epigenetic marks

The concept of epigenetics considers the transduction of heritable patterns of gene expression without changing the DNA sequence through the adaptation of the chromatin (Allis and Jenuwein, 2016; Bird, 2007). These are chemical modifications known as epigenetic marks and include DNA methylation (Jones, 2012; Merrifield and

Kovalchuk, 2013; Razin and Cedar, 1984) and ncRNAs (Holoch and Moazed, 2015), in addition to PTMs to the histone amino acid residuals (Figure 3) (Allfrey et al., 1964).

DNA methylation refers to the addition of a methyl group to bases, predominantly on regions of DNA where a cytosine nucleotide is followed by a guanine nucleotide (CpG dinucleotides) (Jones, 2012). The most abundant methylation modification is the 5-methylcytosine (5mC) (Bird, 2002), representing ~2-5% of all cytosine in the genome (Jones, 2012; Razin and Cedar, 1984) constituting gene silencing like X-chromosome inactivation imprinting and regulate gene transcription (Jones, 2012; Suzuki and Bird, 2008). Around 90% of the 5mCs are found in transposable repeated elements like the Long Interspersed Element-1 (LINE-1) and the Short Interspersed Nuclear Elements (SINE), where the methylation have an essential role in repressing the elements to maintain genomic stability (Miousse et al., 2015). ncRNAs are RNA molecules that are actively transcribed but contain no protein-coding information and are thus not translated (Eddy, 2001). The messenger RNA (mRNA) for protein synthesis is well known, whereas many different types of ncRNAs have been identified. These ncRNA molecules are very heterogeneous in both conformation and length (Esteller, 2011) and are categorised into small ncRNA (sncRNA) (<50 nucleotide (nt)), intermediate ncRNAs (50–500 nt) and long ncRNAs (>500 nt) (Sun and Chen, 2020). ncRNA can arise from, among other processes, transcription of intergenic (between genes) and intronic (within genes) regions, antisense transcription and splicing, and they participate in multiple biological processes such as post-transcriptional regulation of chromatin structure and targeted gene expression (Cech and Steitz, 2014; Holoch and Moazed, 2015).

PTMs of histone proteins are essential for the compactness of chromatin (Ruthenburg et al., 2007). Many PTMs have been identified over the years at different amino acid residuals on the histone tails ranging from the addition of small functional groups like methyl, acetyl, and phosphate, to the addition of larger molecules like ubiquitin (Bannister and Kouzarides, 2011). Specific combinations of core histone PTMs have been identified for active euchromatin, such as the trimethylation (me3) of lysine (K) in position 4 (H3K4me3) and the acetylation (ac) of lysine (K) in position 27

(H3K27ac) (Tsompana and Buck, 2014). In contrast, transcriptionally repressed regions in “closed” chromatin domains are marked by other histone modifications (like H3K27me3 and H3K9me3) (Bannister and Kouzarides, 2011). Promoters (and enhancers) have also been identified to be bivalent (also termed primed or poised depending on cell type and gene function), bearing both activating (H3K4me3) and repressing (H3K27me3) modifications simultaneously preparing essential genes to be rapidly switched-on during differentiation (Bahrami and Drabløs, 2016; Barral and Déjardin, 2023; Bernstein et al., 2006).

1.3 Objectives of the study

The focus for this PhD project has been to investigate the impact of dose rate at three different post-radiation timepoints; early (one day), late (>100 days), and across generations. The following objective were established:

- 1) To identify responses of low dose rate ionising radiation, sub-divided into:
 - a) transcriptional and epigenomic changes at early and late timepoints post-radiation (**Paper I and II**)
 - b) transgenerational genomic instability before and after a challenging dose (**Paper III**)

- 2) To identify difference in response between low dose rate and high dose rate, focusing on
 - a) transcriptional and epigenomic responses at early and late timepoints post-radiation (**Paper I and II**)

2 Methods and methodological considerations

Experimental design, exposure groups, and methods are described in more details in each respective paper. An overview of the experimental design and a brief introduction to the methods and some considerations are presented herein as background for the general discussion of the main results.

2.1 Experimental design

The results presented in this thesis originate from two separate experiments (**A** and **B**), outlined in Figure 5. The analyses were performed in liver (**Paper I** and **II**) and blood (**Paper III**). Both experiments included gamma irradiation at low dose rates following the UNSCEAR definition of low dose rate (UNSCEAR, 2010). Specifically, the low dose rate used in this work was 1.4 mGy/h (**Experiment A**, presented in **Paper III**) and 2.5 mGy/h (**Experiment B**, presented in **Paper I** and **II**).

2.1.1 Experiment A – Paper III

Experiment A (Figure 5) addresses transgenerational radiation-induced genomic instability in blood cells of male F_2 progeny originating from continuously (45 days) low dose rate-exposed F_0 males (1.4 mGy/h, total dose 1.5 Gy). The breeding of F_1 males was postponed for 34 days to ensure that the fertilising spermatozoa was unexposed but originated from an exposed spermatogonia (spermatogonial stem cell). The spermatogenic cells, harbouring the seminiferous tube in the testis (where meiosis occur), exhibit different levels of radiosensitivity (Rube et al., 2011). Differentiation spermatogonia are suggested to be the most radiosensitive (van der Meer et al., 1992a; van der Meer et al., 1992b) and rapidly induces apoptosis upon stress (Rube et al., 2011). Doses as low as 10 mGy is shown to halt the spermatogenesis, primarily related to the induction of apoptosis of spermatogonia (Grewenig et al., 2015).

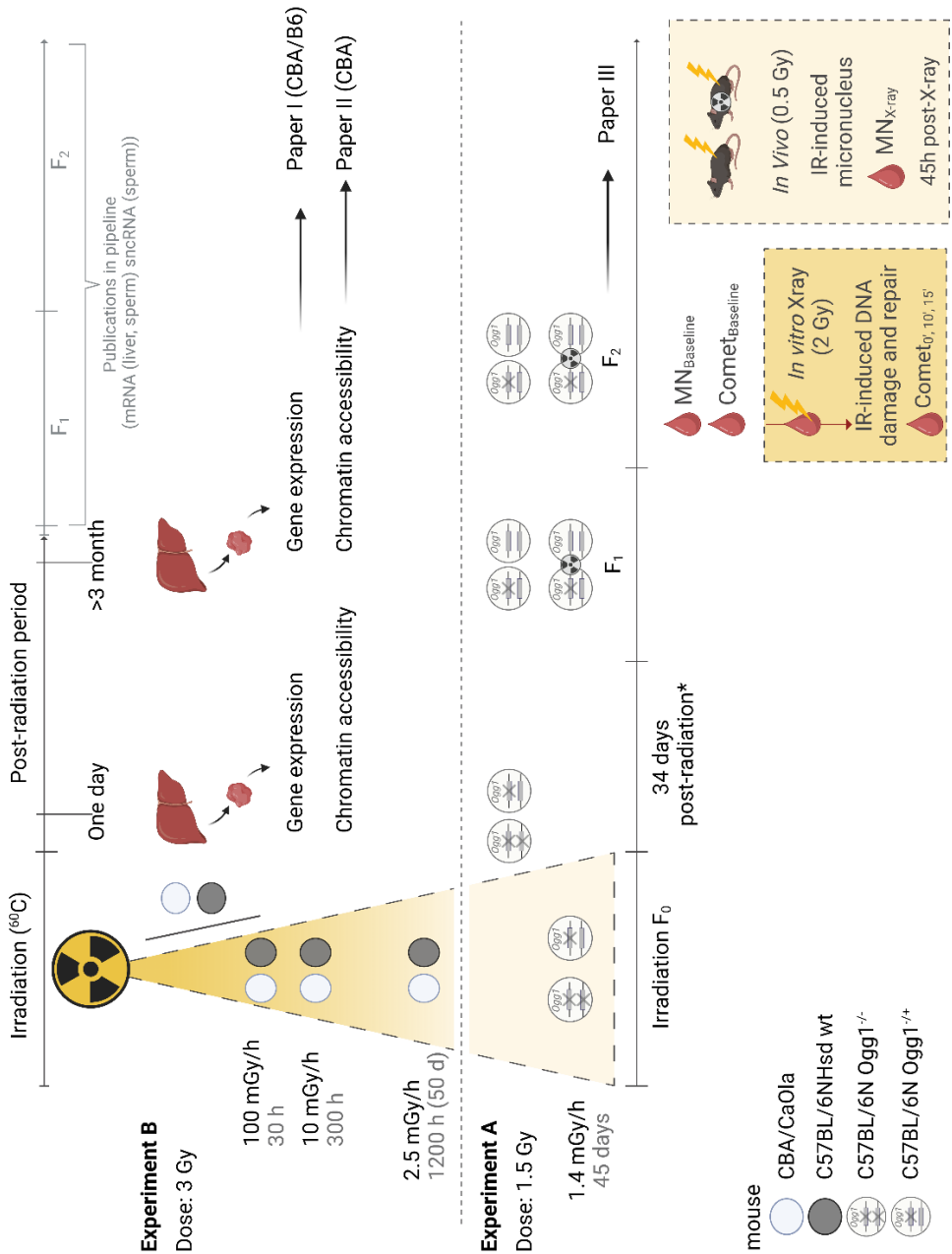


Figure 5. The experimental design. The mouse experiments (A and B) are visualised together to display common features with respect to exposure regimes and endpoints and how each publication is linked to the design. **Experiment B** [two strains: B6 (black

circles) and CBA (white circles)] involve global transcription and epigenomics at two time points post-radiation in directly irradiated mice. Tissue for analyses (relevant to this project) was collected from the liver. **Experiment A** [one strain: B6, two *Ogg1*-genotypes (indicated with open circles)] addresses paternal transgenerational genomic instability, analysed in blood cells following both *in vitro* (2 Gy) and whole-body (0.5 Gy) challenging doses of X-ray. In **Experiment B**, optimisation of a method to isolate *sncRNA* from sperm cells collected from frozen cauda and vas deference was also achieved (not part of this thesis). Sperm were extracted from F_0 and the two filial lines, F_1 and F_2 , where one line was bred from directly irradiated sperm cells and the second line was bred from sperm originating from irradiated spermatogonia. Abb: Gy, gray; h, hour/hours; IR, ionising radiation; m, milli. This figure is created using BioRender.com.

The F_2 male mice were further given an *in vivo* and *in vitro* challenge dose using X-ray to evaluate DNA lesions and cytogenic damage as markers for genomic instability. The dose used for the challenging dose was chosen based on a pilot study measuring the dose-response to micronuclei formation in RETs at different doses; 0, 0.2, 0.5 and 1 Gy. Measurements performed on the directly exposed F_0 males has been reported in a previous PhD thesis (Graupner, 2015; Graupner et al., 2016). A biobank of tissues and cells were assembled from both F_1 and F_2 generations, from the first litter until at least 50 mice were collected of all four hereditary lines.

2.1.2 Experiment B – Paper I and II

Experiment B (Figure 5) (**Paper I and II**) addresses gene expression and chromatin accessibility after chronic low dose rate (LDR) (2.5 mGy/h) and higher dose rates (10 (mid dose rate (MDR)) and 100 (high dose rate (HDR)) mGy/h) gamma irradiation. A split-plot design were employed using two strains (CBA and B6) for mixed-strain housing (two strains share each experimental unit) to improve robustness of the result, increase statistical power, and to reduce the total number of mice according to the principle of the 3 Rs in animal research (Replace, Reduce and Refine) (Altman and Krzywinski, 2015; Festing and Nevalainen, 2014).

All groups were exposed to an equal total dose of 3 Gy. The liver samples were collected at two post-radiation time points; one day and three months.

In **Paper I** results from both mice strains were used. However, due to significant strain differences in gene expression, the split-plot design could not be employed in the desired manner, as each strain required separate analyses. In **Paper II**, we proceed with the Assay for Transposase Accessible Chromatin using sequencing (ATAC-seq) using only the CBA due to lower RNA-seq intra-individual variability of the control group (Figure 6).

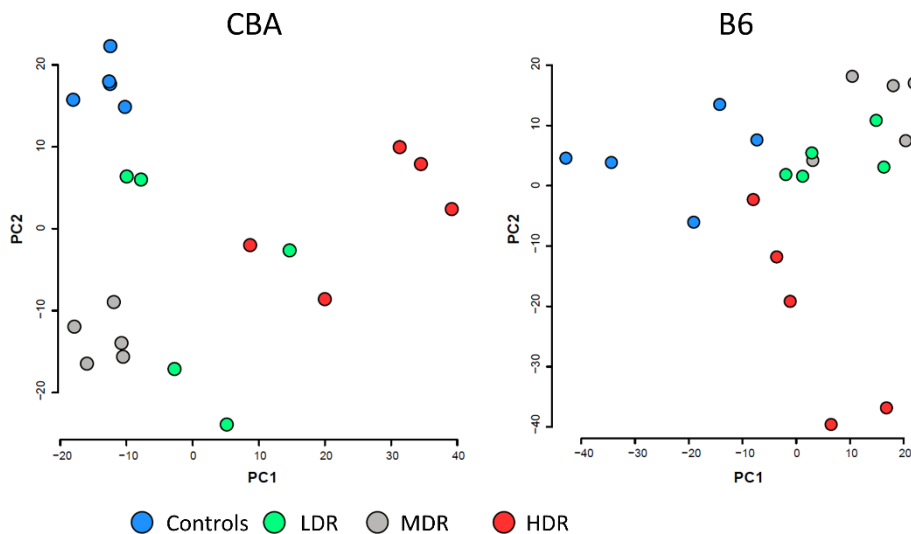


Figure 6. Principal components from RNA-seq data (Paper I) for CBA (left) and B6 (right). Circle-dots represent the individual mice. Abb: LDR, low dose rate; MDR, mid dose rate; HDR, high dose rate; PC, principal component.

2.2 Irradiation and dosimetry

The gamma irradiation in **Experiment A** and **B** (Figure 5) was carried out at the FIGARO Experimental Radiation Facility managed by the Centre of Environmental Radioactivity (CERAD CoE, Norwegian University of Life Sciences, Ås, Norway) (Graupner et al., 2016; Lind et al., 2018). This facility is authorised for irradiating a range of species, including genetically engineered (GMO) strains (used in

Experiment A). The dosimetry is performed by experts from the Norwegian Radiation Protection Authority (NRPA) and radiobiologist affiliated with CERAD.

The FIGARO facility houses a ^{60}Co -source which provides a range of dose rates from 3 Gy/h (inside the collimator at maximum load (400 GBq) down to 0.4 mGy/h at the end of the experimental hall (20.5 m). A near cone-shaped radiation field disperses through the experimental hall and enables exposure of multiple dose rates simultaneously. The dose rates along the axis of the beam and the according distance from the source have been calibrated by the NRPA (Bjerke, 2014).

The experimental hall contains ventilated racks (Scantainers, Scanbur Technology) for housing the mouse cages connected to a climate system. Upon planning the exposure, the position of the racks needed to be positioned to ensure uniformity of the radiation field, and to avoid blockage of the radiation field between racks. The mice were placed in macrolon (polycarbonate) cages, and the climate system controlled the temperature (20-24 °C), humidity (55 ± 10%), and air exchange. The light in the experimental hall is also regulated to give a 12 h light/dark cycle. To ensure uniform radiation conditions, the mice cages were circulated daily by moving each cage one position within the rack. Due to this and general daily animal care, irradiation was interrupted daily for 30 min up to 2 h.

2.2.1 Experiment A – Paper III

Experiment A was the first mouse experiment performed in FIGARO and played an essential role in establishing infrastructure and protocols according to legislation enforced by the national regulatory authorities in Norway (Graupner et al., 2016). The experimental design and the irradiation of F_0 were part of a previously PhD-project (Graupner, 2015) while breeding, handling, and irradiation of the F_2 generation has been as part of this thesis. As the F_0 irradiation laid the foundation for the transgenerational study, the exposure regime used for F_0 is described below.

2.2.1.1 F₀ low dose rate gamma irradiation

The F₀ male mice were irradiated for 45 days at 1.41 mGy/h (0.99 – 1.73 mGy/h), giving a total absorbed dose to water of 1.48 Gy (1.04 – 1.82 Gy). The uncertainties in the dose estimates were 10% (95% confidence level) (Graupner et al., 2016). The control mice were housed inside the experimental hall outside the cone-shaped radiation field. However, the lead shielding had not been installed in the facility at the time of the experiment. Due to scattered radiation in the room, the control mice were estimated to be exposed to a dose rate of 0.002 mGy/h, giving a total dose of 0.00189 Gy (1.89 mGy).

The dose and dose rate ranges were estimated using a phantom mouse and by considering the different places of the mice inside the cage. The phantom mice were 50 ml tubes filled with 10% (w/v) gelatine. The total doses and dose rate at the different positions in the cage were controlled using two dosimetry methods: thermoluminescent dosimeters (TLD) (SCK-CEN, Mol, Belgium) and alanine dosimeters (National Physical Laboratory, Teddington, UK) (Graupner, 2015; Graupner et al., 2016).

2.2.1.2 F₂ X-ray challenge dose

An acute X-ray challenge was given *in vitro* to blood samples collected in Eppendorf tubes on ice from all the F₂ progeny minimum one week before all F₂ mice were given a whole-body challenging dose (Figure 7) using the PIX X-RAD 160C/225C radiation system (Precision X-ray Inc, North Branford, Connecticut, USA) situated at the Norwegian Institute of Public Health (NIPH, Oslo, Norway).

Dosimetry of the X-ray machine was performed by The NRPA (NRPA, Østerås, Oslo) (Hansen EL, 2015). A NE2571 Farmer-type ionisation chamber in conjunction with a PMMA-enclosed (PMMA: polymethyl methacrylate) water phantom was used to measure the absorbed dose at a reference depth of 2.0 g/cm² of water. The size of the water phantom was 11.5 (H) x 21 (L) x 21 (W) cm, and it was placed on the central field axis. The dose rate was calculated from the mean measured accumulated charge

and the true exposure time, also considering the backscatter from the substrate the mice are resting on.

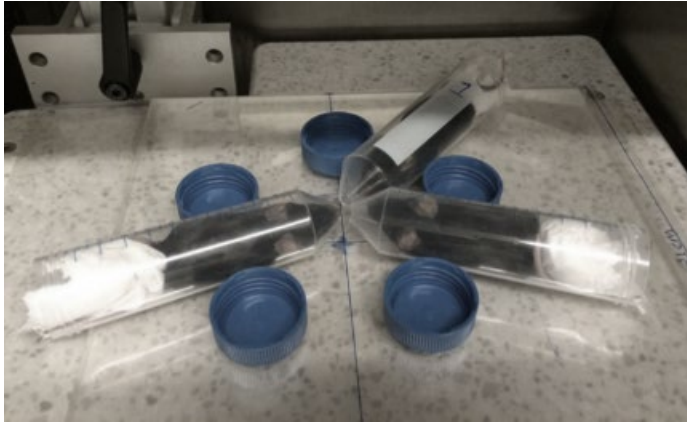


Figure 7. Immobilisation of mice during X-ray. The mice were placed in plastic tubes (50 mL with a breathing hole on the conic end) for irradiation. Three tubes were arranged in a circular pattern covering the field size with the conic ends facing the central field axis. The control mice were similarly placed in tubes and the radiation chamber to simulate the stress during X-ray exposure.

The acute X-ray irradiation was given using a similar exposure regime for both *in vivo* and the *in vitro* exposure: 0.463 ± 0.009 Gy/min absorbed dose rate to water. To receive the estimated total absorbed dose of 0.5 Gy (whole-body) and 2 Gy (*in vitro*), the following X-ray settings were used; 225 kV, 4 mA, 0.5 mm Cu-filter (for beam-hardening). The mice were placed on a platform 50 cm from the source. The duration of exposure was 268 sec for the blood samples and 66 sec whole-body.

2.2.2 Experiment B – Paper I and II

To address the effect of dose rate this study design included three dose rates groups (2.5, 10 and 100 mGy/h) given to a high total dose (3 Gy), compared to the single low dose rate given in **Experiment A**. The increase in total dose were done to ensure more robust data processing through increased genotoxic effect size, compared to the DNA damage levels measured in **Experiment A**, which received 1.5 Gy (Graupner et al.,

2016) (not part of this PhD-thesis). Due to limited space in the radiation field, the irradiation was performed in two rounds: 2.5 and 10 mGy/h were exposed simultaneously, and the 100 mGy/h group were exposed separately as the high dose rate rack would block the irradiation field. To not block the backward radiation field holding cages were used for the MDR mice as the rack could not be connected to the ventilation systems due to physical restrictions. The type of holding cage had lids to ensure appropriate air exchange when not connected to a ventilation system, additionally the covers were opened every day. The duration of the exposure was 1200, 300 and 30 h, respectively.

The control mice were housed in similar ventilated racks in the experimental hall outside the cone-shaped radiation field behind lead shielding. The air kerma rate due to scattered radiation behind the lead shielding was $<7 \mu\text{Gy/h}$ (Lind et al., 2018).

Dosimetry was performed using optically stimulated luminescent dosimeters (nanoDots) (Duale et al., 2020). The obtained air kerma rates considered the source time-dependent activity and cage rotation. The numeric value of the air kerma to whole body absorbed dose conversion coefficient for the chronic exposures was 0.932 ± 0.008 , resulting in an entire body absorbed dose for the 2.5-group of $2.60 \pm 0.19 \text{ Gy}$, the 10-group of $2.67 \pm 0.16 \text{ Gy}$ and for the 100-group of $2.65 \pm 0.13 \text{ Gy}$, all denoted as 3 Gy in the project (Duale et al., 2020; Ellender et al., 2011; Graupner et al., 2017).

2.2.3 General considerations of the dosimetry

In **Experiment A**, the dosimetry was performed using TLD and alanine dosimeters (Bjerke, 2014; Graupner et al., 2016), while in **Experiment B**, the dosimetry was performed using nanoDots (Duale et al., 2020; E. Lindbo Hansen, 2017). NRPA also performed dosimetry on the X-ray machine (Hansen EL, 2015) used for the transgenerational challenging dose. Dosimetry performed by experts warrants reliable dose and dose rate estimates. TLD and alanine tend to have lower sensitivity for lower levels of irradiation than nanoDots. This is reflected in **Experiment A**, where the dose rate levels in the control area (which lacked lead shielding) were

measured to be 0.002 mGy/h. In **Experiment B**, using nanoDots, the scattering radiation was measured to be <0.007 mGy/h behind lead shielding. However, in **Experiment A**, the lack of lead shielding the ventilation racks were placed in front of the control mice, to reduce scattered radiation. The total absorbed dose in controls in both experiments was estimated to be ≤ 8 mGy, approximately 1.5-fold higher than the averaged background level for humans in Norway at 5 mSv/year.

2.3 Mouse models

Strain-specific responses following IR exposure is a known issue in radiobiology, and has been discussed by several researchers (Kadhim, 2003; Rivina et al., 2016; Williams et al., 2010) and endpoints addressed include survival time (Roderick, 1963), chromosomal instability (Darakhshan et al., 2006; Hamasaki et al., 2007; Ponnaiya et al., 1997), expression profiles (genes/proteins) (Jafer et al., 2020; Sproull et al., 2019) and apoptosis (Kadhim, 2003; Mothersill et al., 1999).

This project utilized two inbred mice strains:

- CBA/CaOlaHsd (CBA) (wildtype) (**Paper I and II**)
- C57BL/6N (B6):
 - C57BL/6NHsd (wildtype) (**Paper I**)
 - C57BL/6N (genotype: *Ogg1*^{+/-} and *Ogg1*^{+/+}) (**Paper III**)

2.3.1 C57BL/6

C57BL/6 mice are the most widely used inbred laboratory strain due to their well-characterised genome and low incidence of spontaneous tumours (Inotiv, 2023a). Over the years this strain has been maintained in different laboratories leading to different B6 sub-strains (Mekada et al., 2009). The sub-strain C57BL/6N (termed B6 throughout the paper) is increasingly used due to the initiatives made by The International Mouse Phenotyping Consortium (www.mousephenotype.org), which intends to identify the function of every protein-coding gene in the mouse genome. In relation to radiobiology research, the C57BL/6 strain is identified to exert a phenotype that is thought to be more radioresistant than other mice strains (Kadhim, 2003; Williams et al., 2010), by longer survival time (Roderick, 1963), fewer

chromosomal aberrations (Hamasaki et al., 2007; Ponnaiya et al., 1997), and higher induction of apoptosis (Kadhim, 2003; Mothersill et al., 1999)

In **Experiment A** (Figure 5), the B6 mice is crossed with *Ogg1*-deficient mice (*Ogg1*, 8-Oxoguanine glycosylase 1), enabling in-house breeding of knockout, heterozygote, and wildtype *Ogg1*-mice. Both irradiated and control F₀ mice were stratified according to the *Ogg1* genotype; homozygote *Ogg1*^{-/-} null mice (knockouts) and heterozygote *Ogg1*^{+/-} mice. The *Ogg1*-gene codes for a DNA glycosylase that recognise and removes the oxidative DNA base lesions including 7,8-dihydro-8-oxoguanine, also known as 8-oxoG, and thus catalyse the first step of the BER pathway (Klungland and Lindahl, 1997; Klungland et al., 1999; Kubota et al., 1996). A previous study demonstrated that human testicular cells had limited repair capacity of oxidative DNA lesions, suggesting that a *Ogg1*-deficient mice could simulate more realistic testicular human conditions (Olsen et al., 2003). Studies performed in mice testicular cells in our lab have demonstrated that oxidised purines in *Ogg1*^{+/-} and *Ogg1*^{+/+} mice were repaired at similar rates in testicular cells (ongoing research). The *Ogg1*^{+/-} mice were therefore considered to be functional wildtypes of *Ogg1*^{+/+}.

The breeding from F₀ to F₂ were performed using naïve females (*Ogg1* wildtypes), generating a F₂ generation consisting of only *Ogg1* functional wildtypes (both heterozygote and wildtype) (Figure 5). This was done to create as many biological replicates as possible.

2.3.2 CBA/CaOla (CBA)

The CBA inbred strain was generated around 1920 by crossing a Brag Albino and DBA male. This CBA strain was selected based on its low spontaneous mammary tumours incidence phenotype (Inotiv, 2023b). The CBA mouse strain is one of the primary models for studying leukemogenesis, as it has not been genetically modified and show low spontaneous formation of acute myeloid leukaemia (AML). When AML is induced, the morphology resembles human radiation-induced AML (Major and Mole, 1978; Rithidech et al., 1999; Rivina et al., 2016). Compared to the AML resistant strain B6,

CBA display higher frequency of chromosome aberrations (particularly chr2 and 4, AML related chromosomes) (Darakhshan et al., 2006).

2.4 Biological samples

2.4.1 Liver

In **Paper I** and **II**, liver tissue was used for analysis (Figure 5).

The liver is a multi-functional organ that supports the whole body (Kalra A, 2023). It is an active metabolic organ that monitors and responds to systemic metabolism, detoxification, and homeostasis. The liver contains multiple types of cells, such as hepatocytes, bile duct epithelial cells, Kupffer cells, sinusoid endothelial cells and hepatic stellate cells (Aizarani et al., 2019). The liver stores fat-soluble vitamins, handles cholesterol homeostasis, stores iron and copper, and metabolises reproduction hormone. The liver is essential for functional haematology via haemolysis, coagulation and blood protein synthesis (Kalra A, 2023). The liver performs important immunological function, regulating tolerance and the crosstalk between innate and adaptive immune responses (Bogdanos et al., 2013). It produces acute-phase proteins, cytokines, chemokines and complement components and houses around 90% of the fixed macrophages in the body, namely the Kupffer cells (Nemeth et al., 2009; Robinson et al., 2016). Thereby, the liver endures and is modulated according to lifestyle and environmental risk factors, including IR.

Even though the liver contains multiple cell types, the hepatocytes constitute ~80% of the total cell population in the liver (Blouin et al., 1977), making it suitable for bulk tissue analysis, like RNA-seq (**Paper I**) and ATAC-seq (**Paper II**). The sequenced reads are averaged over the population of cells, making the hepatocyte gene profile the predominant output. This was also confirmed in the data analysis using a cell type transcriptional atlas which identified that the identified transcriptional profiles comprised >98% hepatocytes (**Paper I**).

It has been suggested that whole-body irradiation is inappropriate when studying liver-specific effects due to radiation-induced systemic reactions occurring elsewhere in the organism triggering the liver to respond (Kim and Jung, 2017). However, the aim of this PhD project were not liver-specific responses *per se* but rather to assess the overall systemic impact of chronic low dose rate radiation. In this perspective, the livers' ability to respond to changes in systemic homeostasis was considered beneficial.

2.4.2 Blood

In **Paper III** blood was analysed (Figure 5).

The immature erythrocytes (reticulocytes (RETs)) were analysed using the MN-assay for chromosomal aberrations (section 2.5.2), and nucleated blood cells were studied using the comet assay (section 2.5.1) for pre-mutagenic lesions. The process of haematopoiesis occurs at a high proliferative rate, making these cells highly susceptible to the genotoxic potential of IR.

The hematopoietic system generates and maintains a stable number of all types of blood cells and immune homeostasis via the differentiation of hematopoietic stem cells (HSCs), mainly occurring in the red bone marrow in adults. This system self-renews through asymmetric division of the HSCs, comprising less than 0.1% of adult bone marrow. Further cell division and differentiation lead to specific cell lineages (myeloid or lymphoid). Through the myeloid or lymphoid differentiation lineage, red blood cells (erythrocytes, RBC), white blood cells (leukocytes, WBC) and platelets (thrombocytes) (Orkin and Zon, 2008) are produced.

Out of these circulating blood cells, only the WBC (granulocytes, monocytes, and lymphocytes) contain DNA. During the final stages of erythropoiesis, the erythroblast expels its nucleus to become an immature erythrocyte (RET). The RET then enters the circulating bloodstream, still containing ribosomal RNA. After 2-4 days in circulation, the RNA is degraded (Savill et al., 2009), and the RETs develop into mature normochromatic erythrocytes (NCE, "the ordinary RBC"). In mice, RBC

remain in circulation for 12 days. After 12 days, the spleen will remove the cells with a reducing rate of ~2%/day until about 60 days, where all the cells are removed (Saxena et al., 2012).

2.5 Genotoxicity analysis

Our laboratory at the Department of Chemical Toxicology (NIPH, Oslo) has established an in-house methodology platform for genotoxicity research addressing exposure to both chemicals and IR.

The current project has substantially contributed by enhancing the in-house methodology toolbox. To accomplish **Paper III**, the flow-based micronucleus (MN) assay in RETs was established, along with the establishment of an automated scoring system for fully automated counting of comets. The comet scoring system was optimised to be compatible with the already established in-house high-throughput comet assay (Gutzkow et al., 2013). In **Paper II**, the ATAC-seq laboratory protocol and a bioinformatics pipeline for analysing the data were established.

2.5.1 The comet assay

The comet assay, alkaline single-cell gel electrophoresis, is a sensitive method to detect clastogenic and mutagenic genotoxic insults in agarose-embedded cells, e.g., peripheral blood lymphocytes, cultured cells, and disaggregated tissue. The technique was first reported in 1984 using neutral pH conditions as a method to detect radiation-induced DNA breaks (Ostling and Johanson, 1984) but adapted to alkaline conditions (pH >13 on the electrophoresis solution) (Singh et al., 1988). Under alkaline conditions, the DNA strand will unwind, and by using gel electrophoresis, broken ends within the DNA supercoil will migrate towards the anode (DNA is negatively charged). When DNA is intact, it lacks broken ends and is too large to migrate in the gel. In this way, the generated tail represents the level of DNA breaks in an individual cell.

Alkaline comet assay detects SSBs, DSBs, alkali-labile sites (ALs), i.e., AP-sites and baseless sugars (Collins et al., 2023). However, the spectrum of DNA lesions can be

increased by introducing an enzymatic step following lysis (Asare et al., 2016; Duale et al., 2010; Gutzkow et al., 2016; Hansen et al., 2010; Olsen et al., 2003). Several lesion-specific endonucleases exist (Muruzabal et al., 2021). Dependent on the enzyme used, specific DNA lesions could be detected, and the excised damaged base leave an AP site which is converted to a SSBs under alkaline conditions.

IR is known to introduce oxidative cellular damage (section 1.1.5), and oxidised DNA lesions can be measured by the comet assay when using the *E. coli* formamidopyrimidine-DNA glycosylase (Fpg) (Boiteux and Huisman, 1989)). This enzyme detects a wide range of oxidized lesions, but primarily oxidised purines such as 8-oxoG (Boiteux and Huisman, 1989) and formamidopyrimidines (Fapy, ring-opened purine) (Collins, 2009; Collins, 2014).

The standard method (not including enzyme-detection of specific DNA lesions) is widely used for genotoxicity testing both in *in vitro* and *in vivo* models (OECD, 2016b). Over the years, the assay has been optimised to improve efficiency by utilising multiple gels instead of the standard one or two gels per glass-slide, making it suitable for more extensive experiments. Our laboratory has developed a high-throughput comet assay using GelBond films (Brunborg et al., 2014; Gutzkow et al., 2013) including an automatic scoring system (IMSTAR).

In **Paper III** the high-throughput comet assay, including the *E. coli* Fpg-enzyme (made in-house (Boiteux and Huisman, 1989; Duale et al., 2010)) for oxidised lesions, were applied. The protocol consists of six main steps:

1. Isolation, exposure and embedding of the cells in agarose on the GelBond film (96-minigel format)
2. Cell lysis (overnight) to release the nucleoid
 - a. Enzymatic treatment using Fpg
3. Unwinding and denaturation under alkaline conditions
4. Electrophoresis under controlled electric conditions (0.8 V/cm) with circulating cold electrophoresis solution (four films can be run simultaneously i.e., 384 gels in each tank (reduced inter-gel/film variability))

5. Neutralisation of gels and fixation by dehydration in ethanol
6. DNA-staining (SYBR Gold) and imaging analysis for scoring of DNA damage levels using a fully automated scoring (Pathfinder analysing software using IMSTAR).

2.5.2 Flow-based micronucleus (MN) test in reticulocytes (RETs)

In **Paper III**, addressing radiation-induced transgenerational genomic instability, we assessed *in vivo* MN formation in RETs obtained from peripheral blood cells drawn from the F₂ male mice, measuring both baseline levels and levels induced by the challenging dose of X-rays.

The MN assay can be used to identify substances that cause cytogenetic damage resulting in micronuclei formation (OECD, 2016a). The MN assay detects both clastogenic and aneugenic potential. Clastogenic substances cause structural chromosomal aberrations through breaks in DNA, whereas aneugenic substances induce numerical chromosomal aberrations by the interaction of other targets than DNA (e.g., proteins) (EFSA Scientific Committee, 2021).

Using the *in vivo* MN-assay, MN formation is measured in RETs (also referred to as immature erythrocytes or polychromatic erythrocytes) obtained either from the bone marrow or peripheral blood cells (OECD, 2016a). Unlike mature erythrocytes, RETs contain RNA and certain surface proteins (e.g., transferrin receptor (CD71)) and can be differentially stained based on these features. An increase in the frequency of micronucleated reticulocytes (MN-RETs) indicates acute genotoxicity associated with recent cell divisions. In mice, an increase in the frequency of micronuclei in mature erythrocytes can also indicate accumulated DNA damage associated with a sub-chronic or chronic exposure (Graupner et al., 2016).

In **Paper III**, we applied an automated scoring system using flow cytometry to analyse the MN frequency in both RETs and NCEs (Dertinger et al., 2011; Dertinger et al., 1996; Torous et al., 2000; Torous et al., 2003), to score substantially more samples and particularly more cells (analysing >10⁶ erythrocytes) in less time (time-

effectiveness) compared to manual scoring. This reduce the potential for scoring bias, and issues with manually scoring (e.g., if scoring is not blinded) (Dertinger et al., 2011). The MN-assay in RETs has also proven valuable on radiation exposed samples (Dertinger et al., 2009; Dertinger et al., 2007; Graupner et al., 2016; Sun et al., 2011).

2.6 Omics analysis

The term «omics» describe the range of technologies used to study the diversity of biological molecules; from individual loci *typing* to whole-genome *profiles*. Either as a collection of specific molecules, e.g., mRNAs, or the total pool of biomolecules involved in the biological processes at a given state or time (Dai and Shen, 2022). Depending on dose and dose rate, IR induces multiple cellular processes in all the “omics-layers”, triggering networks of signalling cascades to coordinate the response, from DNA damage to inflammatory responses (Amundson, 2022). Utilising the omics-platform in radiation research can contribute to unravel the holistic/total ensemble of molecular mechanisms underlying the biological effects of radiation exposure in both normal and cancerous tissues. These technologies enable investigation of critical questions such as individual sensitivity, risk assessment, and biomarker discovery (Mortimer et al., 2022). Today, approximately 14% of the published studies in radiation biology address one or more of the “omni-layers” (Subedi et al., 2022).

Since the development of the first high-throughput methodology in the 1990s, the DNA microarray, omics technology has evolved rapidly and developed genome-scale state-of-the-art methods to identify DNA, RNA, and proteins faster and to a lower cost than earlier. The technologies mainly include sequencing and mass spectrophotometric-based approaches to understand the “central dogma” of molecular biology, genomics, transcriptomics, proteomics, and metabolomics. During later years it has expanded to include epi-omics (Callinan and Feinberg, 2006) (epigenomics, epi-transcriptomics and epi-proteomics) and interactomics (the interaction of the molecules) (Dai and Shen, 2022). By systematic analysis of these "omics" we can gain an overall understanding of how structure and interactions of molecules leads to specific function and responses to external stimuli within an organism (Mortimer et al., 2022).

This PhD-project has utilised both transcriptomic (section 2.6.1) (**Paper I**) and epigenomic (section 2.6.2) (**Paper II**) methodology to address radiation-induced molecular perturbations.

2.6.1 Gene expression analysis (transcriptomics)

Transcriptomics studies the expression of genes at the level of RNA. It provides a comprehensive understanding of the transcriptional activity of genes within a biological sample and offers insights into gene regulation, cellular processes, and disease mechanisms. It also enables the discovery of novel genes and the characterisation of ncRNAs that play important regulatory roles (Wang et al., 2009).

The most widely used methods to study gene expression is real-time quantitative polymerase chain reaction (RT-qPCR), microarray and next-generation sequencing. RT-qPCR have been considered the “gold standard” of gene quantification due to its dynamic range and high sensitivity (Wong and Medrano, 2005). RT-qPCR is based on the correlation between the concentration of a PCR product and its fluorescence intensity, as the PCR cycles are monitored in real-time to detect amplification of the target gene (Heid et al., 1996; Higuchi et al., 1993). However, RT-qPCR is limited to measure few gene transcripts, and with the introduction of microarray technology, the gene expression methodology evolved to be high-throughput.

Microarray-based technology hybridises fluorescently labelled complementary DNA (cDNA) to gene-probed arrays (Schena et al., 1995). This method revolutionised the field of molecular biology. However, the technique is restricted by dynamic range, high background noise, and cross-reactions. Both RT-qPCR and microarrays depend on existing knowledge of the genome sequence (preventing detection of novel transcripts). These limitations are currently addressed by the new high-throughput transcriptomic deep-sequencing technology; Next-Generation RNA sequencing (RNA-seq). Compared to microarray, RNA-seq is highly sensitive (detects rare transcripts), have higher resolution (more accurate distinguishing of bases) and is not dependent on known reference sequences (enables detection of novel genes). It can provide information about alternative splicing, allele-specific expression, ncRNA,

and single-nucleotide polymorphisms (Wang et al., 2009). RNA-seq has become the dominant technology for transcriptional analyses and has gradually taken over for the use of microarray, also in the field of radiation biology (Amundson, 2022).

RNA-seq were applied in **Paper I**. RNA-seq has no standard pipeline as both experimental design and research question will depend upon choices for analysis procedures – however, a general RNA-seq workflow have the following steps (Kukurba and Montgomery, 2015):

1. Isolation of RNA from samples
2. Library preparation (vary with interest of RNA type, strand specificity, read type and sequencing depth)
 - a. Description: RNA (total or fractionated such as polyA+) is converted to a library of cDNA fragments with adapters (synthetic oligonucleotides) attached to one or both ends. Adapter-ligated cDNA fragments are then amplified before sequencing
3. Sequencing
 - a. to identify the RNA sequence (a read), each isolated molecule is sequenced in a high-throughput manner to millions of short reads from one end (single-end sequencing) or both ends (pair-end sequencing).
4. Data analysis (highly dependent on research aims) (section 2.6.3 and Figure 9)

In **Paper I**, the total hepatic RNA was isolated from liver tissue samples. From this, RNA was paired-end sequenced (2 x 150 bp) in five biological samples (five mice/experimental group) per group. A paired-end sequencing using a reading frame of 150 bp was selected to reduce the number of unmapped reads during alignment to the mouse reference genome. The sequencing of our samples was performed at Novogene Co., Ltd (Cambridge, UK). However, RNA isolation and quality control were performed in-house. The experimental samples representing “early_response” and “late_response” was sequenced in two separate laboratory setups (**Paper I**), along

with their representative timepoint control group. As this increases the risk for batch effects (variation due to technical arrangement and not biological factors), contrasts were not made across sampling time points.

RNA sequencing was utilised to analyse the genome-wide gene expression profile and to identify differences in gene expression levels after low dose rate, mid dose rate and high dose rate gamma irradiation by linking differential expressed genes (DEGs) to functional signalling pathways (**Paper I**). The transcriptional profiles identified in **Paper I** were integrated with the epigenomic data collected using ATAC-seq (**Paper II**) (section 2.3.2.1.). In **Paper I**, a selection of 18 differentially expressed genes and 11 reference genes were validated by RT-qPCR. The reference genes were selected based on their stability in both controls and exposed samples.

2.6.2 Chromatin profiling (epigenomics)

Epigenomics refers to the “omics” that include genome-wide *profiling* and analysis of epigenetic modifications across the genome. The epigenetic mechanisms (section 1.2.3) modify genomic activity without changing the underlying DNA sequence – and is, therefore, a determinant factor for cellular phenotype through regulating gene expression (Allis and Jenuwein, 2016).

A range of methods to study *loci*-specific epigenetic modifications exists. However, advancements in technology related to the overall omics platform (Callinan and Feinberg, 2006) have led to promoting methods developed to detect, quantify, and visualize chromatin state dynamics. Many of these laboratory approaches have been developed from experiments using endonucleases for locus-specific foot-printing and combined with next-generation methods, like high-throughput sequencing, microarray, and high-quality antibody-based techniques (Klein and Hainer, 2020; Li, 2021), to be able to assess genome-wide chromatin accessibility and to locate DNA-bound proteins within the chromatin. These genome-wide methods often display a proportion of the chromatin with epigenetic modifications compared to the total chromatin. In addition, they serve as a functional channelling of the epigenome

defined by the repertoire of regulatory actions across the genome (Klemm et al., 2019).

2.6.2.1 Assay for Transposase-Accessible Chromatin using DNA sequencing (ATAC-seq)

The ATAC-seq uses a hyperactive Tn5 transposase enzyme with the ability to cut and ligate sequencing adapters to DNA fragments cleaved in open chromatin regions (Buenrostro et al., 2013). This method can identify multiple nucleosome regions using approximately ten times fewer nuclei and obtains a higher signal-to-noise ratio than alternative methods like DNase, MNase and FAIRE methods (Table 2)(Chawla et al., 2021; Klein and Hainer, 2020; Tsompana and Buck, 2014).

Several optimisations of the original ATAC-seq protocol exist, like the FAST-ATAC for blood cells (Corces et al., 2016) and the Omni-ATAC for frozen tissue (Corces et al., 2017), mainly differing by the reagents used. The original ATAC protocol relies on the insertion of DNA and not digestion, making it prone to contamination of mitochondrial DNA. However, this was addressed in Omni-ATAC-seq, where improvement was made to the use of detergents to remove mitochondrial DNA from the transposition reaction and the extra post-lysis washing to remove mitochondrial DNA further. These improvements increased the signal-to-noise background resulting in more information per sequencing read through improved data quality (higher proportion of mapped reads and higher significance using the same sequencing depth) compared to standard ATAC-seq, FAST-ATAC, but also DNase-seq.

ATAC-seq is performed by the following steps (Figure 8):

1. Lysis of cells
2. Tagmentation using Tn5
3. DNA purification and PCR amplification
4. DNA sequencing

A successfully prepared ATAC library is identified through a periodic pattern every 200 bp corresponding with the DNA wrapped around nucleosomes (~147 bp per nucleosome) (Figure 2, **Paper II**) (Buenrostro et al., 2015; Corces et al., 2017). Longer

length suggests fragments protected by the integer of multiple nucleosomes, a quality measure for adequate tagmentation (and not over-tagmented).

Table 2. Overview of the most used genome-wide chromatin profiling methods

Method	Principle	Pros	Cons	Lab time	Genomic target
DNase-seq (Boyle et al., 2008)	DNase I cleave DNA in accessible chromatin	-Widely used -High signal-to-noise ratio -Efficient maps regions proximal to genes	-Cleavage bias (unreliable TF footprints) -High cell input (>1M) -Lab intensive	2-3 days	-Open chromatin ^a -Footprinting ^b
MNase-seq (Albert et al., 2007)	MNase cleave and eliminate accessible DNA	-High resolution -Superior in nucleosome and TF binding information	-High cell input (>1M) -careful enzymatic titrations -AT-cleavage specificity -Indirect detection of accessible regions	2-3 days	-Nucleosome position -Protein-binding sites
FAIRE-seq (Giresi et al., 2007; Nagy et al., 2003)	Crosslinks DNA/protein using formaldehyde	-Isolate both crosslinked DNA and accessible regions -No sequence-specific endonuclease bias	-Low signal-to-noise ratio -Low resolution at promoters of highly expressed genes -Depends on adequate fixation efficiency	3-4 days	-Open chromatin -CORE location
ATAC-seq (Buenrostro et al., 2013; Buenrostro et al., 2015; Corces et al., 2017)	Transposase (Tn5) tagmentate (cleave and ligate adaptors) accessible DNA	-Fast and easy protocol -Low cell input (≤50 000) -Native conditions -Optimised for frozen tissue and mtDNA removal -very high signal-to-noise ratio -detects nucleosome-bound and accessible regions	-Need high seq. coverage for accurate mapping -Tn5 bias towards TF footprints, needs bioinf. corrections	2-3 h	-Open chromatin -Footprinting -Nucleosome occupancy

^a Peak Calling , ^b Cis-regulatory elements. Aberrations: CORE, Cluster of Open Regulatory Element; DNase-seq, DNase I hypersensitive sites sequencing; MNase-seq, Micrococcal Nuclease digestion with deep sequencing; FAIRE-seq, Formaldehyde-assisted isolation of regulatory elements; ATAC-seq, Assay for Transposase-Accessible Chromatin with sequencing; TF, transcription factor; Tn5, Transposase; mtDNA, mitochondrial DNA; AT, adenine-thymine.

In **Paper II**, the Omni-ATAC-seq were utilised for hepatic chromatin accessibility (Corces et al., 2017) (ref). The method was selected for its many benefits in the lab (Table 2), its optimisation for frozen tissue, and its robust output. DNA library

preparations were performed in-house, but DNA sequencing (Illumina NovaSeq6000) was outsourced to Novogene Co (Cambridge, UK).

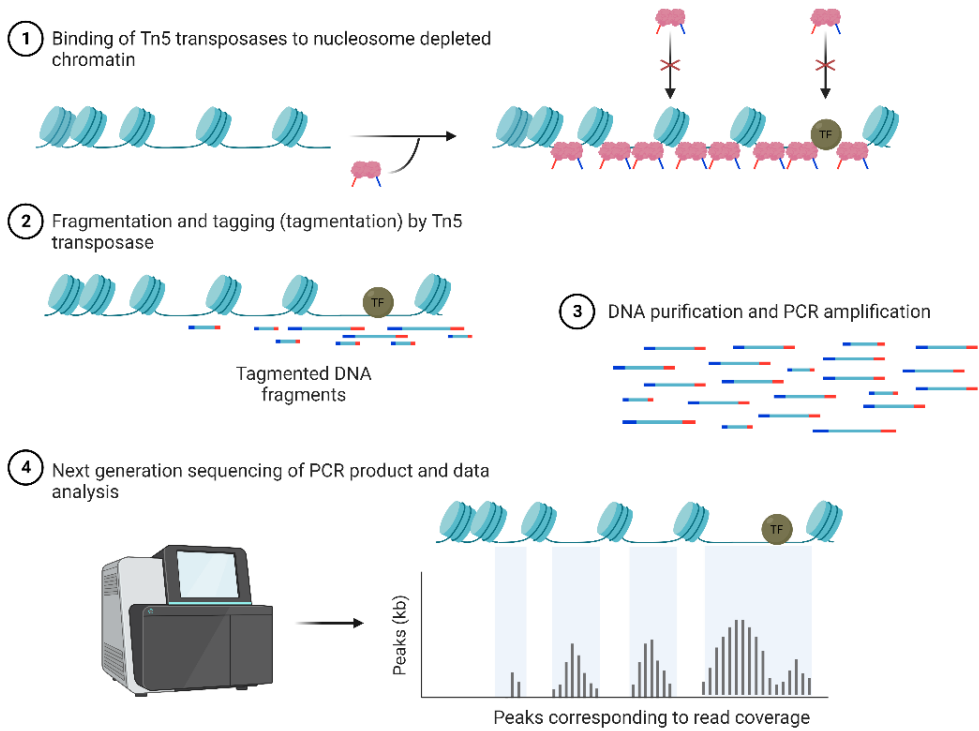


Figure 8. Principal workflow for ATAC-Seq and show a general peak-calling output. Aberrations: Tn5, transposase. Adapted from “ATAC Sequencing”, by BioRender.com (2021). Retrieved from <https://app.biorender.com/biorender-templates>

2.6.3 Bioinformatic analysis

With the growing use of high-throughput sequencing platforms, bioinformatic expertise and computational resources are essential to prepare the data output generated in the sequencing procedure. A common goal with transcriptional data is the search for differentially expressed traits, e.g., genes with differential expression (DEGs), when comparing conditions (treatment vs controls). However, the roadmap from sequencing raw data output to functional analysis and interpretation of the results is complex. The process needs to handle challenges inherent to the next-

generation sequencing technical procedures, such as not uniform read coverage across the genome, mapping bias due to the length of genes, unequal sequencing depth and library size between samples, and a vast difference in expression levels between genes (Conesa et al., 2016). A wide range of computing infrastructures and software have been made to address the sequencing difficulties and to rescale the read counts to generate equal library sizes for all samples – procedures that require complex filtering (removal of inappropriate reads) and normalisation. Figure 9 summarises the main steps in the bioinformatic workflow for both RNA-seq (Wang et al., 2009) and the ATAC-seq data output (Minnoye et al., 2021).

Bioinformatic expertise was used in both **Paper I** and **II** for pre-analysis, alignment, and quantifications. The procedure is described in detail in each respective paper.

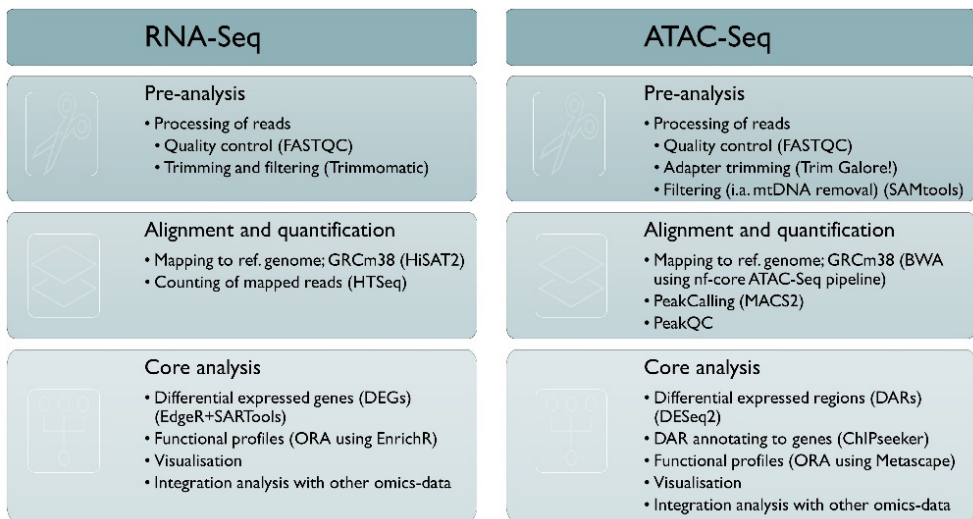


Figure 9. Outline of the bioinformatic analysis of RNA-seq and ATAC-seq data.

The major steps are listed as pre-analysis, alignment and quantification, and core-analysis, addressing the raw reads output the sequencing (Fastq files) down to the core analysis composed of the different functional analysis utilised in this project.

Aberrations: ATAC-Seq, Assay for Transposase-Accessible Chromatin with sequencing; **CORE**, Cluster of Open Regulatory Element; HTSeq, high-throughput sequencing; mtDNA, mitochondrial DNA; ORA, over-representative analysis; RNA-Seq, ribonucleic acid sequencing.

2.6.4 Functional analysis

To identify differentially expressed genes (DEGs) in treatment groups compared to controls, a false discovery rate (FDR) ≤ 0.05 were used in **Paper I**. Log₂-fold change (log₂FC) was used to evaluate the level and direction of the expression, log₂FC cut-offs were not used as filters. Previously, many used gene expression FC cut-offs of 1.5 or 2 to define differential expressions (known from qPCR strategies). However, the FDR already consider the fold change (and variation within groups) since the FDR is quantified based on contrasting two groups. Also, when performing enrichment analysis, FDR is preferable as a small FC in gene expression might affect the whole pathway. In **Paper II**, addressing differentially accessible chromatin regions, FDR < 0.1 were applied.

Functional pathway analysis was performed to identify the biological mechanisms differing between contrasting groups. Today, over 70 methods exist, categorised as topological-based (TB) or non-TB (Nguyen et al., 2019). Non-TB is also known as over-representation analysis (ORA) and do not consider the direction or type of signal transmitted from one gene to another within a given pathway. This strategy was used in **Paper I** and **II**. When using this approach, lists of DEGs are mapped/enriched to functional pathways based on a statistical assessment to which the genes are over- or under-represented in a pathway based on all possible genes (Nguyen et al., 2019).

In **Paper I**, the identified DEGs lists were enriched to the gene set in the database EnrichR using ORA. EnrichR containing curated gene sets from over 100 libraries (Chen et al., 2013; Kuleshov et al., 2016; Xie et al., 2021). In **Paper II**, ORA was performed using MetaScape, a web-based tool to analyse overlapping traits across multiple input gene lists. Both EnrichR and MetaScape use the hypergeometric test to identify relevant functional pathways.

2.6.5 Statistical analysis

In **Paper III**, multivariable regression models were used to estimate the impact of F_0 experimental parameters, like the irradiation and genotype, on F_2 radiation-induced genomic instability both before (baseline) and after a challenging dose. In both genotoxicity tests applied (comet and MN), we included repeated measurements, either from the same blood sample (comet assay) or repeated blood sampling of the same mice (MN), resulting in dependency within samples. Hence, statistical methods assuming a non-dependent relationship between measurements could not be used, like Analysis of Variance and the following *post hoc* tests. However, dependency is not an issue using regression models, and essentially, the modelling assumptions were not violated (cf. normal distribution of measurements, residuals were also independent and normally distributed with homogeneous variance) (Grafen, 2010).

3 Results – summary of papers

3.1 Paper I

Perturbed transcriptional profiles after chronic low dose rate radiation in mice (Dahl et al., 2021)

In **Paper I**, we investigated the hepatic transcriptional response following whole-body exposure to low dose rate and high dose rate. Dose rate-specific perturbed functional pathways, strain-specific responses, and the impact of dose rate on methylation status were analysed.

Early (one day post-radiation) and late (>100 days) hepatic genome-wide transcriptional profiles were assessed in male mice of two strains (CBA/CaOlaHsd and C57BL/6NHsd). The mice were exposed chronically to a low dose rate (2.5 mGy/h; 1200h, LDR), a medium dose rate (10 mGy/h; 300h, MDR) and acutely to a high dose rate (100 mGy/h; 30h, HDR) of gamma irradiation (^{60}Co), given to an equivalent total dose of 3 Gy.

Dose rate and strain-specific transcriptional responses were identified. The transcriptional responses were modulated differently in each dose rate group and were corroborated by the representation of functional biological pathways. Evidence of changed epigenetic regulation by global DNA methylation was not detected. A period of recovery markedly reduced the number of differentially expressed genes. Using enrichment analysis to identify the functional significance of the modulated genes, perturbed signalling pathways associated with both cancer and non-cancer effects were observed, such as lipid metabolism and inflammation. These pathways were seen after chronic low dose rate and were hence not restricted to the acute high dose rate exposure. The transcriptional responses induced by chronic low dose rate IR suggest initiation of molecular processes involved in non-cancerous conditions.

3.2 Paper II

Dose rate dependent reduction in chromatin accessibility at transcriptional start sites long time after exposure to gamma radiation (Dahl et al., 2023)

In **Paper II**, we studied the impact of dose rate, chronic and acute, on the accessibility of the chromatin assessed by whole-genome ATAC-seq.

CBA/CaOlaHsd mice were whole-body exposed to either chronic low dose rate (2.5 mGy/h for 54 days) or the higher dose rates (10 mGy/h for 14 days and 100 mGy/h for 30 h) of gamma radiation (^{60}Co , total dose: 3 Gy). Chromatin accessibility was analysed in liver tissue samples using ATAC-seq after both one day and a three-month post-radiation period (>100 days).

The results show that the dose rate contribute to radiation-induced epigenomic changes in the liver at both sampling timepoints. Interestingly, chronic low dose rate exposure compared to a high total dose (3 Gy) did not inflict long-term changes to the epigenome. In contrast, the acute high dose rate given to the same total dose induced reduced accessibility exclusively at transcriptional start sites (TSS) in genes relevant for the DNA damage response and transcriptional activity.

3.3 Paper III

Genomic instability in F₂ male progeny from low dose rate gamma irradiated F₀ mice (Dahl et al, in prep)

In **Paper III**, we investigated changes in genomic instability and genetic susceptibility in F₂ offspring. F₀ male C57BL/6N were chronically exposed to LDR gamma radiation (1.41 mGy/h for 45 days) to a total dose of 1.5 Gy and mated with naïve females for two generations. Male F₂ offspring were given a challenge dose of X-rays (0.5 Gy, 0.457 Gy/min). Blood samples were collected from F₂ mice prior to exposure to establish baseline levels and 45 h following the challenge dose.

Genotoxicity was assessed by the flow-based assay of MN in RETs and alkaline high-throughput comet assay in nucleated blood cells. Since pre-mutagenic lesions induced would have been repaired at 45 h following 0.5 Gy *in vivo* exposure, whole blood was challenged *in vitro* with 2 Gy of X-rays before assessing induced levels of DNA damage in the comet assay. Repair of pre-mutagenic lesions were also measured in the comet assay at 0, 10 and 15 min after exposure.

The acute challenge dose (0.5 Gy) increased the levels of MN-RETs and reduced the population of RETs compared to baseline measurements. There was no evidence that the irradiation or genotype of F₀ affected the outcome in F₂. Immediately after *in vitro* exposure to 2 Gy, the levels of DNA SSBs/ALSs were statistically significantly increased from baseline, and the repair of SSB/ALS was evident by a statistically significant reduction in lesions at both 10 min and 15 min after X-ray. At baseline, F₂ mice originating from irradiated F₀ mice displayed a higher level of pre-mutagenic lesions than F₂ mice of non-exposed F₀ mice. However, given the low effect size it is challenging to conclude if the findings are true biological differences or related to methodological aspects.

4 Discussion

This PhD project focused on investigating the impact of the irradiation factor “dose rate” on molecular markers, including transcription, epigenetics, chromatin accessibility, and transgenerational radiation-induced genomic instability. Figure 10 presents an overview of what was measured at which time and at which dose rate, along with indications of the findings. In addition, the experimental design (Figure 5) in **Paper I** and **II**, where the total dose was kept constant for all exposure groups, renders the possibility to address the relationship of dose rate.

	Endpoints	One day	Late	Transgenerational
LDR	Genes	yes	no	n.a.
	Chromatin	yes	no	n.a.
	RIGI	n.a.	n.a.	no*
HDR	Genes	yes	no	n.a.
	Chromatin	yes	yes	n.a.

Objective 1) Responses of chronic low dose rate ionising radiation

Findings

- a) Early, low dose rate ionising radiation modulates transcription (**Paper I**) and epigenomic profile (**Paper II**), but not late after exposure.
- b) There was no evidence for transgenerational (F₂) genomic instability from paternal F₀ low dose rate irradiated after a challenging X-ray dose. An increase in endogenously formed DNA lesions was seen, although low effect size drawing conclusive findings is challenging (**Paper III**).

Objective 2) Difference in response between low dose rate and high dose rate

Findings

- a) Early, high dose rate change transcription (**Paper I**) and the epigenome (**Paper II**) more severe than low dose rate. Late, HDR represses the epigenomic profile compared to low dose rate where no modulations were evident (**Paper II**).

Figure 10. Summary of project endpoints, objectives, and overall findings linked to the presented papers. The dose rate is indicated using LDR and HDR. Endpoints are indicated with Genes, Chromatin, and RIGI, and post-IR timepoints are indicated by One day, Late and Transgenerational. The “yes” and “no” indicate reported findings in respective publications. *Transgenerational statistical findings were identified, however, due to low effect size, the results were considered of low biological relevance.

Abb: LDR, low dose rate; HDR, high dose rate, RIGI, Radiation-induced genomic instability; n.a., not analysed.

4.1 Impact of dose rate

4.1.1 Low dose rate

Low dose rate-induced molecular changes were assessed by gene expression analyses (**Paper I**) and chromatin accessibility (**Paper II**). Transgenerational (F₂) genomic instability after paternal (F₀) low dose rate exposure was also addressed (**Paper III**), and these results are discussed in section 4.1.3.

The overall results from low dose rate exposure in **Paper I** and **II** show that the low dose rate given to 3 Gy over a period of 50 days perturbs transcriptional activity one day post-irradiation, seen by changes in the expression of genes and by epigenomic modulation of chromatin accessibility. Biological functions related to aspects of lipid and energy metabolism were identified in **Paper I** for both strains and in **Paper II** one day post-radiation. Others have also reported hepatic molecular changes in genes associated with different functional pathways of lipid metabolism, like fatty acid metabolism and obesity (Uehara et al., 2010) and cholesterol biosynthesis (Fujikawa et al., 2022). These findings were supported by the results presented in **Paper I** (cholesterol biosynthesis, fatty acid metabolism and energy metabolism) and **Paper II** (cholesterol remodelling and glycerolipid biosynthesis). Increased body weight (Fujikawa et al., 2022) and increased lipid content in the liver and serum (Nakamura et al., 2010) have also been reported in mice subjected to prolonged exposure to low dose rate IR, where they hypothesised that the weight gain was related to changes in energy metabolism. Even though the exposure regimes used in the above-referenced studies and in **Paper I** and **II** is not directly compatible, the results consistently show that prolonged exposure to low dose rate IR could induce changes in different aspects of metabolic pathways, which further could pose an increased risk in incidence of metabolic-related diseases.

In addition, the B6-strain displayed several pathways linked to inflammation and infections, like the “*Toll-like receptor signalling pathway*”, and gene profiles are seen during “*hepatitis B*” and “*hepatitis C*”. “*TNF signalling pathway*” and “*JAK-STAT signalling pathway*” are also enriched after the low dose rate exposure, and also present after high dose rate irradiation. IR-induced effects are highly linked to inflammatory processes in multiple ways, reflecting the immune system's complexity. Activation of the immune system is strongly linked to the levels of IR-induced cytotoxic effects (like cell death and induction of ROS) (Yahyapour et al., 2018). Furthermore, the level of cellular stress and stress outcomes like apoptosis, necrosis, senescence, and so forth, determine which role the immune system will play (Lumniczky et al., 2021; Mavragani et al., 2016). In addition to pro-inflammatory responses, studies suggest that radiation can also be anti-inflammatory (Ebrahimian et al., 2018; Mathias et al., 2016; Vieira Dias et al., 2018). However, additional immunological parameter measurements are required to specify the role of the immune system in the context of the exposure regime used in this project.

In the latest UNSCEAR report from 2022 (UNSCEAR, 2022), non-mutational routes (like epigenetic marks) for modifying cellular phenotypes and carcinogenesis were in focus (Hanahan, 2022; Hanahan and Weinberg, 2000; Hanahan and Weinberg, 2011). Radiation has the capacity to change gene (and protein) expressions (recognised by UNSCEAR already in 1994), and the 2022 report highlights several radiation-induced non-mutational mechanisms, like the remodelling of chromatin and changes in epigenetic marks (also reviewed in (Belli and Tabocchini, 2020)) to be linked to changes in gene expression (UNSCEAR, 2022). Moreover, despite reports of radiation-induced changes in gene expression altering mechanisms like DNA methylation, UNSCEAR 2022 emphasise that these effects are rarely reported with actual changes in gene expression. UNSCEAR also raises the issue that most of studies do not investigate long-term alteration to gene expression but generally only up to 48 h after radiation (UNSCEAR, 2022).

An important aspect of the experimental design in **Experiment B**, late responses, in addition to responses one day post-radiation, were investigated approximately three

months post-radiation (**Paper I and II**). The molecular profile identified late after low dose rate exposure in **Paper I** displayed few perturbed genes. As these genes could be false positives, caution is taken to conclude. Recent studies also report that IR-induced changed genes are restored and compatible with controls shortly after exposure (Fujikawa et al., 2022; Jafer et al., 2020). Although perturbed gene expression has been reported in the liver up to 10 weeks post-radiation (1 Gy acute X-ray) in BALB mice, the CBA mice in the same study showed no changes in gene expression in the liver 24 h post-IR (Jafer et al., 2020). A study investigating protein expression in livers of B6 mice reports changes up to three months after both chronic low dose rate and acute high dose rate given to 4 Gy, although not the same proteins (Nakajima et al., 2017). Jafer et al. (2020) identified sncRNA as a marker for epigenetic changes up to 24 h after exposure and hypothesised that epigenetic factors like miRNAs could be involved in the delayed IR-induced effects affecting gene expression. The global long-term epigenomic profile after low dose rate exposure, represented by changes in chromatin accessibility, displayed no evidence for changes in the epigenome (**Paper II**). Following that, the changes in the molecular states identified one day after low dose rate irradiation are, at some point post-radiation, reverted a profile again compatible with the unexposed controls.

Collectively, **Paper I and II**, consistently show that the low dose rate irradiation used in this experiment (2.5 mGy/h), given the experimental conditions, seem not to introduce long-term epigenomic marks with the power to modify the chromatin accessibility nor the expression of genes in liver cells (predominantly hepatocytes). Given the fact that the ATAC-seq identifies regions accessible for the transposase, epigenetic changes occurring in inaccessible regions (like the heterochromatin, Figure 3) would not be identified using this method. An interesting aspect of **Paper II** is the fact that low dose rate radiation did not affect chromatin accessibility. This contrasts with previous publications indicating that radiation-induces epigenetic alterations are more significant after low levels of irradiation (Belli and Tabocchini, 2020; Merrifield and Kovalchuk, 2013; Schofield and Kondratowicz, 2018; Vaiserman, 2011). The aspect of low dose rate compared to high dose rate will be discussed further below.

4.1.2 Low dose rate compared to high dose rate

The impact of low dose rate was an essential aspect for this project, and in **Paper I** and **II**, the interpretation of the low dose rate molecular responses was strengthened by comparing with the responses from high dose rate irradiation. The results show that when the low dose rate at 2.5 mGy/h is increased 40 times to a high dose rate at 100 mGy/h, transcriptional profiles clearly differed, suggesting that different cellular responses are influenced, even though the radiation was given to the same total dose. This dose rate-specific response was evident by the difference in perturbed genes and enriched pathways (**Paper I**), and on the associated changes in chromatin accessibility (**Paper II**), both of which substantiate the functional relevance of dose rate. The collective understanding of this "dose rate specific response" in **Paper I** and **II** is that high dose rate exposure induces significantly more stress compared to low dose rate one day post-radiation. When the dose rate is lowered, the cellular integrity seems to be less challenged by the irradiation. This observation is also in line with the findings reported in the publications listed in Table 1 (section 1.1.4).

When assessing the pathways enriched for high dose rate in **Paper I**, "*p53 signalling pathways*" and "*Ferroptosis*" appeared in both strains after high dose rate irradiation, indicating stress responses linked to DDR and cellular death. Ferroptosis is iron-dependent and a non-apoptotic cell death driven by the accumulation of lipid peroxidation products arising from ROS (Dixon et al., 2012), while p53 is a cellular stress response signalling network that can promote a range of responses depending on the stress, like cell cycle arrest, DNA damage repair, senescence, apoptosis and metabolic changes. The enrichment of these pathways suggests that high dose rate irradiation introduces a higher level of deleterious effects, causing molecular processes to eliminate potentially malignant cells (Jiao et al., 2022). This is in line with a range of studies addressing the genotoxic potential of dose rate using different endpoints, where the majority report that when reducing the dose rate, a lower effect of the total dose is seen (Barnard et al., 2019; D'Auria Vieira de Godoy et al., 2021; Graupner et al., 2017; Olipitz et al., 2012; Tanaka et al., 2014; Turner et al., 2015). Induction of DSBs in lymphocytes measured by the post-translational histone modification γ H2AX and the levels of apoptotic cells were reduced after low dose rate

compared to acute doses (Turner et al., 2015), and by measuring 53BP1 foci fewer foci were observed with reducing dose rate in peripheral blood lymphocytes (Barnard et al., 2019). Although, the same study reported of an inverse dose-rate response in epithelial cells in the eye lens (Barnard et al., 2019). Dose rate-effects evaluated using micronuclei induction, a known biodosimetric marker for (acute) IR-induced chromosomal aberrations known to correlate with total dose, indicate that dose rate also impacts the level of MN in circulating blood cells (D'Auria Vieira de Godoy et al., 2021; Graupner et al., 2017; Olipitz et al., 2012; Tanaka et al., 2014; Turner et al., 2015). However, upon chronic exposure regimes, biological factors (like clearance of cells from the circulation) come into play, challenging the interpretation of dose rate effects as the duration of exposure is a relevant factor when considering the MN levels.

The gene expression profiles for low dose rate analysed late (three months) post-radiation in **Paper I**, displayed as only a few genes differentially changed from controls. Furthermore, no pathways were enriched, and the genes did not reveal any obvious links to the exposure. Intriguingly, in **Paper II**, the impact of high dose rate irradiation on the epigenome is clearly distinct to the low dose rate response, as three months after high dose rate irradiation, the chromatin accessibility was reduced in promoter regions of genes relevant for defence mechanism towards IR-induced damage, such as DSBs and activation of p53-related responses, in addition to genes relevant for transcriptional regulation, like the AP-1 complex, transcription repressor complex and binding of the RNA polymerase II (**Paper II**). As we found reduction in promoter accessibility, a general assumption could be that repressed chromatin is associated with reduced gene expression. However, as discussed in **Paper II**, reduced chromatin accessibility could also be related to facilitating a rapid transcriptional recall (Mansidor and Risca, 2022) if the stressor re-emerges, effected via poised/primed promoters. As we did not observe ATAC-genes related to similar pathways as in **Paper I**, it is tempting to speculate that a challenge would be required to detect possible manifested changes in gene expressions.

Given the reported findings implying general sparing effects when the dose rate is lowered, one could speculate on a "dose rate threshold effect", providing a tolerable "stress" situation where most DNA insults are mitigated, and affected cells survive and functions are maintained. While after high dose rate irradiation, the total burden of stress per time unit would induce a range of cellular responses, like cell death, that reduce the risk of malignant cell transformation. However, such a dose rate threshold would depend on several factors, including cell type and mouse model. As repair of DNA damage is not error-free, a long-term challenged cellular milieu could accumulate unrepaired or mis-repaired bases leading to enhanced cancer risk by increasing the probability of the survival of cells with accumulating damage (Amundson et al., 2003). As lowering the irradiation dose rate is assumed to reduce the risk of direct impact between the gamma photon and the nucleus, ROS could pose the most significant threat at lower radiation levels.

ROS has been linked to many diseases like cancer, diabetes, chronic kidney disease, neurodegenerative disease, cardiovascular disease, chronic obstructive pulmonary disease (Liguori et al., 2018) and in the liver, e.g., non-alcoholic fatty liver disease (Chen et al., 2020; Li et al., 2015). However, although often related to adverse effects, ROS is also a crucial modifying agent upon cellular stress signalling (Sies and Jones, 2020). ROS serve many roles, and one could speculate that the level of ROS (per time unit) is relevant for which role ROS undertake; therefore, it is not unreasonable to assume that long-term/chronic low dose rate exposure could increase the risk for oxidative stress-related conditions. However, since ROS is attributed to a signalling system for redox homeostasis, one can hypothesise that the chemical balance is relevant for the postulated "dose rate threshold" possibly cognate with the exposure time. In situations with exposure below this threshold, the antioxidant response and inflammatory reactions could reduce the net radiation-induced burden. The exact levels of oxidative stress in this project are difficult to estimate without analysing ROS/antioxidant markers, and the results in **Paper I** and **II** did not reveal an obvious role. However, based on the several functional pathways identified, ROS constitutes an important part of the total stress burden has been an essential player during exposure. It is plausible that this is linked to the sampling timepoint as transcriptional

stress response activity is known to return to baseline levels shortly after the termination of stimuli, although the time for transcriptional activity depends on several factors (Pascual-Ahuir et al., 2020).

4.1.3 Transgenerational effects

In **Paper III**, transgenerational (F_2) genomic instability following paternal (F_0) low dose rate gamma radiation has been investigated (Figure 10). The overall results indicate that low dose rate irradiation in the given conditions of **Experiment A** exert little evidence for increased transgenerational genomic instability evaluated by genotoxic endpoint (Section 2.5.1 (comet assay) and 2.5.2 (MN-assay)).

Few published studies have addressed the “unexposed” generations (F_2) of mice originating from exposed F_0 parents. The majority focus on F_1 originating from parents given IR acutely, and F_1 is a generation originating from exposed germ cells within the F_0 generation (Skinner, 2016). Thus, this F_2 represents a valuable addition to the transgenerational discussion, although this study did not display evidence for transmission of genomic instability after paternal F_0 chronic low dose rate irradiation. This is in line with data reported by Y. Dubrova’s research group that argues that low dose and chronic low dose rate irradiation does not destabilise the F_1 genome, and suggests a possible acute exposure threshold for inheritance of genomic instability in mice (Dubrova and Sarapultseva, 2020; Mughal et al., 2012).

Testicular toxicity is an established tissue reaction leading to temporal or permanent sterility, depending on the dose. However, the threshold for testicular tissue reactions depends on the exposure regime, and fractionated exposure is shown to lower the threshold compared to a single dose exposure (Meistrich, 2013). A recent study investigating the role of dose rate upon different organs in mice by comparing low dose rate (3.4 mGy/h) with high dose rate given to similar total doses (2, 4 and 8 Gy) (Bae et al., 2021), observed an inverse dose rate effect where chronic low dose rate irradiation caused the most severe testicular toxicity by reducing the population of spermatogonia to a level where it also manifested as reduced testis weight for doses >2 Gy. In **Experiment A** and **B**, testis weights were recorded. Similar reductions in

relative testis weights were seen, for doses of 1.5 Gy (**Experiment A**) and 3 Gy (**Experiment B**) supporting an inverse dose rate effect upon testicular organ toxicity (manuscript in preparation, not part of this PhD project). Duration of exposure and sampling timepoint is likely to play a role for the interpretation of these results.

Given the reported inverse dose rate effect on spermatogenic cells, chronic low dose rate is suggested to introduce a more severe outcome in the directly irradiated generation, and damaged spermatogonial stem cells are reported to be sensitive and may be removed by apoptosis upon low dose rate exposure. One could speculate that this reduces the risks for transmission of effects, supporting the lack of transgenerational genomic instability reported in **Paper III**. Given the epigenomic data in **Paper II**, one could assume that low dose rate doesn't introduce epigenetic alterations also in the testis. The relevance of such a comparison must be interpreted in relation to the major cell/tissue-specific responses to irradiation, and differences in mechanisms for inheritance, like transfer of sperm exposomes containing sncRNA during fertilisation (Chen et al., 2016a; Chen et al., 2016b; Rassoulzadegan et al., 2006; Sharma, 2014; Sharma et al., 2018).

4.2 Methodological considerations

One strength of the results presented herein is that they have been obtained from controlled mouse experiments. Animal care and protocols have been approved and adhere to national legislation. Laboratory analyses have been performed according to good laboratory practice and using acknowledged and established methodologies. However, methodological circumstances and limiting factors important for conclusions should be considered:

a) Dose rate-response

A limitation to **Experiment A** is the lack of several dose rate (and dose) groups. An acute exposure group would have benefited the design as transgenerational inherited effects have been suggested to have a threshold for acute exposures, and that low dose rate exposure may be below this threshold (Dubrova and Sarapultseva, 2020). As the concept of

transgenerational genomic instability is still controversial, transgenerational studies should consider several factors (like exposure window, timing of breeding with respect to spermatogenesis, multi vs transgenerational effects, parents of origin and choice of endpoints).

In **Experiment B**, mice of two strains were housed together in the same cages to facilitate strain comparisons and the study included three dose rates, all given to the same total dose, to evaluate dose rate response. However, analysing the hepatic molecular endpoints in **Paper I** and **II**, the MDR group (10 mGy/h) deviated from an expected dose rate curve, which was also observed when evaluating genotoxic endpoints one day after radiation (manuscript in preparation, not part of this thesis). The MDR mice were housed in holding cages not connected to the ventilation system (section 2.2.2), which could have led to increased ammonia concentrations affecting the hepatic transcriptional profiles (Ferrecchia et al., 2014). However, considerations were made during the exposure period to reduce the potential build-up of ammonia by using cage lids optimised for air exchange, and the lids were opened daily. However, given the deviating MDR hepatic molecular results, the results are embattled with some uncertainties hindering conclusions regarding dose rate response.

b) Age

All mice had the same age at the start of exposure, and due to difference in duration of exposure (and breeding regime), there are age-differences at sampling, particularly for the F₂ generations in **Experiment A** (Figure 11). However, in **Paper III**, age did not significantly impact the outcome (MN and the comet assay) and was excluded as an independent variable in the statistical models. Although age is known to be relevant in the context of MN in circulating erythrocytes, a slight tendency for an increase in MN was seen with age (not statistically significant). However, weight (a confounding variable with age) was significantly associated with the MN outcome, and this variable was included to be corrected for in the relevant regression models.

Since all variables included in a statistical model consume degrees of freedom, variation increase and reduce statistical power. This is a challenge for results with small effect sizes, like the comet assay results in **Paper III**.

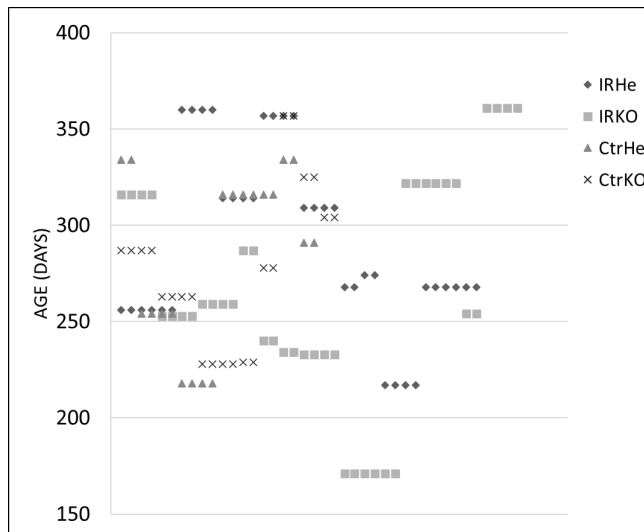


Figure 11. Age distribution in **Experiment A**. F_0 stratified in experimental treatment (IR= low dose rate ionising radiation, Ctr= unexposed) and *Ogg1*-genotype (KO=knockout, He=heterozygote).

c) Detection of oxidative lesions in the comet assay upon X-ray exposure

In **Paper III**, an increase in Fpg-detectable oxidative lesions after exposure to 2 Gy of X-ray was not statistically significantly increased compared to SSB controls. With respect to methodological aspects, several explanations could be envisioned:

- i) impaired Fpg-enzyme activity,
- ii) Our crude Fpg-enzyme preparation is not sensitive (or is used at sub-optimal concentrations) for the specific X-ray induced oxidised DNA lesions,
- iii) the Fpg-enzyme is hindered from binding and excising 8-oxoG lesions due to sequestering to other more severe lesions or hindered enzymatic activity due to proximity of DNA lesions.

Thus, our comet assay experiment would have benefitted from inclusion of cells exposed to a positive control, like potassium bromide or the phototoxic Ro-compound, to confirm enzymatic activity (Møller et al., 2017) to address i) and ii). Point i) is addressed since our Fpg-enzyme preparations are routinely calibrated using cells exposed to increasing concentrations of the phototoxic Ro-compound, so enzyme activity is confirmed. Calibration of the DNA damage dose-response curve using X-ray-treated mammalian cells such as human lymphocytes is acknowledged in the comet community (Brunborg et al., 2023). However, several laboratories using X-ray to calibrate have experienced detection of few Fpg-sensitive purines in addition when applying Fpg. After approximately 30 min post X-ray, SSB are repaired and most of the lesions are Fpg-sensitive. It is hypothesised that this phenomenon can be ascribed to the tendency of X-rays to induce clustered DNA lesions composed of SSB and oxidised bases in proximity, where SSBs need to be repaired before the oxidised lesions are processed (Collins et al., 2008; David-Cordonnier et al., 2001; Olsen et al., 2003), which is consistent with point iii). However, this hypothesis has yet to be addressed using systematic experimental approaches.

d) ATAC-seq

The ATAC-seq is a technology that has evolved rapidly and is considered relatively “easy to use” and robust. However, the development of bioinformatics tools explicitly developed for ATAC-seq is still lagging. A limitation of using genome-wide epigenomic methods is the lack of a general recommendation of an optimal number of replicates required to achieve reproducible and accurate results. This is because the numbers of replicates depend on the signal-to-noise ratio, which differ with the assay used, assay conditions, and the cell/tissue used. In addition, the number of replicates also depends on technical variance, which again is experiment-specific (Tsompana and Buck, 2014). Due to this, we decided to increase the number of biological replicates in our ATAC-seq experiment, causing two separate

sequencing runs in **Paper II**. However, this did not cause any sequencing batch effects.

e) Performing rodent experiments in radiobiology

Experiments A and B were designed to facilitate assessment of genotoxic and reproductive toxicological endpoints, including assessment of breeding efficiency after exposure (not part of this thesis). However, **Paper I-III** reflects a challenge addressing multiple outcomes while meeting ethical, statistical, and biological requirements and practical restrictions. This is not a particular limitation of our studies but more a general challenge in performing rodent studies evaluating radiation-induced effects. Recently, a Multidisciplinary European Low Dose Initiative (MELODI) working group (Lowe et al., 2022) presented some recommendations concerning low dose rate (and low dose) studies in animals. They highlight the importance of including multiple strains, both genders and a range of ages for reliability and repeatability going forward with dose rate studies. They also include experimental irradiation factors that pose outcome modulation properties, like the radiation type, duration, dose rate, and total dose of radiation. All these factors should be addressed in addition to the demands for robust statistical analysis and biologically relevant effect sizes, making rodent experiments very demanding.

Given the limitations, it is equally important to acknowledge the strength of the studies. This study is one of few studies designed to address the dose rate effects and not conflicted by different total doses. In addition, the study includes comparable strains housed within the same cages, additional groups for long-term post-radiation sampling, bringing forward information on the impact of dose rate upon manifesting long-term IR-induced changes. This is an aspect also stressed by the latest UNSCEAR report (UNSCEAR, 2022). Concerning transgenerational inheritance, the mice were bred through two generations to obtain a true transgenerational population. The experiments have been carried out to be controlled and randomised.

Further, the methodologies used throughout this PhD project have been high-throughput assays, increasing the sensitivity of the outcomes studied. Resources often force the use of pooled samples for omics-technique. In this study, we have been fortunate to have the possibility to benefit from individual biological replicates generating information regarding inter-individual variation for both RNA-seq and the ATAC-seq in combination with deep sequencing ($\sim 84 \times 10^6$ and $\sim 50 \times 10^6$ reads/library, respectively). With respect to genotoxicity assays we benefitted from using a flow-based MN-assay, which is a very sensitive method, allowing interrogation of several millions of RBCs per sample, leading to reliable MN-RET quantifications.

5 Conclusions

The focus for this PhD project has been to investigate the impact of dose rate at three different post-radiation timepoints; early (one day), late (>100 days), and across generations. Genome-wide gene expression and chromatin accessibility were evaluated early (one day) and late (>100 days) in the directly exposed mice as markers for changes to the epigenome (**Paper I and II**). The project also focused on the inheritance of radiation-induced genomic instability via low dose rate irradiated paternal germline to the first unexposed progeny (F₂) to address effects across generations (**Paper III**). The objectives (section 1.3, Figure 10) and the respective findings were as follows:

1a) Responses of chronic low dose rate ionising radiation assessing transcriptional and epigenomic changes at early and late timepoints post-radiation

The transcriptional profiles one day post-radiation from liver suggests that exposure to low dose rate IR perturbed genes involved in functional mechanisms linked to lipid metabolism, inflammation, and cancer. However, the impact of the exposure seen by the number of molecular perturbations differs between the two mouse strains. The epigenomic profile one day post-radiation identified modulations in the chromatin accessibility in genomic regions containing genes also linked to aspects of lipid metabolism. However, when evaluating the long-term damage potential of low dose rate, accumulated to a high total dose, for changes in gene transcription and chromatin accessibility, this study did not reveal significant effects late (three months) post low dose rate exposure.

1b) Responses of low dose rate ionising radiation upon transgenerational genomic instability before and after a challenging dose

There was no evidence that the F₀ low dose rate irradiation or genotype introduced genomic instability in F₂ evaluating radiation-induced cytogenetic damage, DNA damage immediately after the challenging X-ray dose and the repair of induced ssb/als. Statistically significant results were found as increased endogenously formed DNA lesions (ssb/als) in F₂ originating from low dose rate irradiated F₀, suggesting stem cell derived radiation-induced transgenerational genomic instability. However, drawing conclusive findings is challenging due to the low effect size observed. Further investigations with larger sample sizes or more sensitive analytical methods are warranted to elucidate the true impact of the results.

2a) Difference in response between chronic low dose rate and acute high dose rate, focusing on transcriptional and epigenomic responses early and late time post-radiation

Differences in transcriptional and epigenomic response have been compared after low dose rate and high dose rate when the IR exposure is given to the same total dose. The data presented in this work show that reducing the dose rate has effect-modulating properties. Both transcriptional and epigenomic profiles indicate that a high dose rate impacts the cellular environment more extensively by dysregulation of several functional pathways compared to a low dose rate. Highly interesting, high dose rate were found to have the potential to introduce long-term changes in chromatin accessibility in genes relevant to the repair of DNA double-strand breaks and transcriptional regulation, in contrast to low dose rate, which did not show any impact at the late timepoint.

The results of this project consistently show that dose rate is a significant effect-modifying factor and that the dose rate must be interpreted in relation to the total dose. However, how dose rate impact genotoxic endpoints in directly exposed mice, and the biological function and relevance of epigenomic changes, need to be addressed in future studies.

6 Future perspectives

Throughout the course of this PhD project, I have read a vast number of reviews on health effects of IR exposure. However, the reviews fail to report how the included studies were identified and the relevance of the studies based on the methodological quality. Going forward, it will be essential to use systematic methodology, like the OHAT handbook (Handbook for Conducting Systematic Reviews for Health Effects Evaluations from the National Toxicology Program) (OHAT, 2019) when summarising the evidence of the impact of dose rate versus total dose. In addition to performing a systematic literature search, it is essential that the research question and eligibility criteria (criteria for which studies should be included in the review) are predefined and made available for the readers. Also, critical appraisal of the included studies is crucial, as methodological factors could have major impact on study outcomes, as the review conclusions should be drawn from the best available evidence.

Furthermore, it is important to understand the transcriptional dynamics of genes throughout the whole exposure period. This project has displayed that both dose rate and the genetic background of the mouse model have significant effects upon the radiation response. Knowledge about the dynamics of different genes could provide an understanding for the reasons why different responses are measured after radiation. Differences in the temporal responses could be an essential factor in understanding inconsistencies between strains when sampling time points are fixed. This information could also prove relevant in the pursuit for molecular biomarkers for exposure. An interesting thought is the concept of delayed onset time of tissue reactions when the dose rate is lowered. Why should we assume that this only applies for detrimental dose levels? It would be very interesting to investigate whether the effects on the epigenome after a high dose rate would be introduced also in the low dose rate groups if the post-radiation sampling time were further delayed.

Further, as regulation of transcription is tightly linked to epigenetic mechanisms and the epigenome, it will be essential to understand the relevance of changes in epigenetic markers upon transcriptional regulations and gene perturbations, and how these again could be linked to progression of adverse biological effects. However, this will only be achieved with efficient tools for analysing, integrating, and interpreting comprehensive data sets. Finally, despite the advances in computational methods, there will still be a need to test hypotheses using laboratory approaches. Particularly with respect to epigenetic and transgenerational effects.

7 References

- Aizarani N, Saviano A, Sagar, Maily L, Durand S, Herman JS, et al. A human liver cell atlas reveals heterogeneity and epithelial progenitors. *Nature* 2019; 572: 199-204, doi:10.1038/s41586-019-1373-2
- Akahoshi M, Amasaki Y, Soda M, Hida A, Imaizumi M, Nakashima E, et al. Effects of radiation on fatty liver and metabolic coronary risk factors among atomic bomb survivors in Nagasaki. *Hypertens Res* 2003; 26: 965-70, doi:10.1291/hypres.26.965
- Albert I, Mavrich TN, Tomsho LP, Qi J, Zanton SJ, Schuster SC, et al. Translational and rotational settings of H2A.Z nucleosomes across the *Saccharomyces cerevisiae* genome. *Nature* 2007; 446: 572-6, doi:10.1038/nature05632
- Allfrey VG, Faulkner R, Mirsky AE. ACETYLATION AND METHYLATION OF HISTONES AND THEIR POSSIBLE ROLE IN THE REGULATION OF RNA SYNTHESIS. *Proc Natl Acad Sci U S A* 1964; 51: 786-94, doi:10.1073/pnas.51.5.786
- Allis CD, Jenuwein T. The molecular hallmarks of epigenetic control. *Nature Reviews Genetics* 2016; 17: 487-500, doi:10.1038/nrg.2016.59
- Altman N, Krzywinski M. Split plot design. *Nature Methods* 2015; 12: 165-166, doi:10.1038/nmeth.3293
- Amundson SA. The transcriptomic revolution and radiation biology. *International Journal of Radiation Biology* 2022; 98: 428-438, doi:10.1080/09553002.2021.1987562
- Amundson SA, Lee RA, Koch-Paiz CA, Bittner ML, Meltzer P, Trent JM, et al. Differential responses of stress genes to low dose-rate gamma irradiation. *Mol Cancer Res* 2003; 1: 445-52,
- Aranda-Rivera AK, Cruz-Gregorio A, Arancibia-Hernández YL, Hernández-Cruz EY, Pedraza-Chaverri J. RONS and Oxidative Stress: An Overview of Basic Concepts. *Oxygen* 2022; 2: 437-478,
- Asare N, Duale N, Slagsvold HH, Lindeman B, Olsen AK, Gromadzka-Ostrowska J, et al. Genotoxicity and gene expression modulation of silver and titanium dioxide nanoparticles in mice. *Nanotoxicology* 2016; 10: 312-21, doi:10.3109/17435390.2015.1071443
- Azzam EI, Jay-Gerin JP, Pain D. Ionizing radiation-induced metabolic oxidative stress and prolonged cell injury. *Cancer Lett* 2012; 327: 48-60, doi:10.1016/j.canlet.2011.12.012
- Bae MJ, Kang MK, Kye YU, Baek J-H, Sim Y-J, Lee H-J, et al. Differential Effects of Low and High Radiation Dose Rates on Mouse Spermatogenesis. *International Journal of Molecular Sciences* 2021; 22, doi:10.3390/ijms222312834

- Bahrami S, Drabløs F. Gene regulation in the immediate-early response process. *Advances in Biological Regulation* 2016; 62: 37-49, doi:<https://doi.org/10.1016/j.jbior.2016.05.001>
- Baiocco G, Bartzsch S, Conte V, Friedrich T, Jakob B, Tartas A, et al. A matter of space: how the spatial heterogeneity in energy deposition determines the biological outcome of radiation exposure. *Radiation and Environmental Biophysics* 2022; 61: 545-559, doi:10.1007/s00411-022-00989-z
- Bannister AJ, Kouzarides T. Regulation of chromatin by histone modifications. *Cell Research* 2011; 21: 381-395, doi:10.1038/cr.2011.22
- Barber RC, Dubrova YE. The offspring of irradiated parents, are they stable? *Mutat Res* 2006; 598: 50-60, doi:10.1016/j.mrfmmm.2006.01.009
- Barnard SGR, McCarron R, Moquet J, Quinlan R, Ainsbury E. Inverse dose-rate effect of ionising radiation on residual 53BP1 foci in the eye lens. *Scientific Reports* 2019; 9: 10418, doi:10.1038/s41598-019-46893-3
- Barral A, Déjardin J. The chromatin signatures of enhancers and their dynamic regulation. *Nucleus* 2023; 14: 2160551, doi:10.1080/19491034.2022.2160551
- Belli M, Indovina L. The Response of Living Organisms to Low Radiation Environment and Its Implications in Radiation Protection. *Front Public Health* 2020; 8: 601711,
- Belli M, Tabocchini MA. Ionizing Radiation-Induced Epigenetic Modifications and Their Relevance to Radiation Protection. *Int J Mol Sci* 2020; 21, doi:10.3390/ijms21175993
- Bernstein BE, Meissner A, Lander ES. The mammalian epigenome. *Cell* 2007; 128: 669-81, doi:10.1016/j.cell.2007.01.033
- Bernstein BE, Mikkelsen TS, Xie X, Kamal M, Huebert DJ, Cuff J, et al. A bivalent chromatin structure marks key developmental genes in embryonic stem cells. *Cell* 2006; 125: 315-26, doi:10.1016/j.cell.2006.02.041
- Bird A. DNA methylation patterns and epigenetic memory. *Genes Dev* 2002; 16: 6-21, doi:10.1101/gad.947102
- Bird A. Perceptions of epigenetics. *Nature* 2007; 447: 396-398, doi:10.1038/nature05913
- Birney E, Stamatoyannopoulos JA, Dutta A, Guigó R, Gingeras TR, Margulies EH, et al. Identification and analysis of functional elements in 1% of the human genome by the ENCODE pilot project. *Nature* 2007; 447: 799-816, doi:10.1038/nature05874

- Bjerke HH, P. O. . The gamma irradiation facility FIGARO – Report on the measurements of dose rate in the cobalt-60 irradiation field. NRPA Technical document no. 2, Norwegian Radiation Protection Authority, Østerås, 2014,
- Blouin A, Bolender RP, Weibel ER. Distribution of organelles and membranes between hepatocytes and nonhepatocytes in the rat liver parenchyma. A stereological study. *J Cell Biol* 1977; 72: 441-55, doi:10.1083/jcb.72.2.441
- Bogdanos DP, Gao B, Gershwin ME. Liver immunology. *Compr Physiol* 2013; 3: 567-98, doi:10.1002/cphy.c120011
- Boiteux S, Huisman O. Isolation of a formamidopyrimidine-DNA glycosylase (fpg) mutant of *Escherichia coli* K12. *Mol Gen Genet* 1989; 215: 300-5,
- Bouville A. Fallout from Nuclear Weapons Tests: Environmental, Health, Political, and Sociological Considerations. *Health Phys* 2020; 118: 360-381, doi:10.1097/hp.0000000000001237
- Boyle AP, Davis S, Shulha HP, Meltzer P, Margulies EH, Weng Z, et al. High-resolution mapping and characterization of open chromatin across the genome. *Cell* 2008; 132: 311-22, doi:10.1016/j.cell.2007.12.014
- Braga-Tanaka I, 3rd, Tanaka S, Kohda A, Takai D, Nakamura S, Ono T, et al. Experimental studies on the biological effects of chronic low dose-rate radiation exposure in mice: overview of the studies at the Institute for Environmental Sciences. *Int J Radiat Biol* 2018; 94: 423-433, doi:10.1080/09553002.2018.1451048
- Brenner DJ, Hall EJ. Computed tomography--an increasing source of radiation exposure. *N Engl J Med* 2007; 357: 2277-84, doi:10.1056/NEJMra072149
- Brunborg G, Eide DM, Graupner A, Gutzkow K, Shaposhnikov S, Kruszewski M, et al. Calibration of the comet assay using ionising radiation. *Mutation Research/Genetic Toxicology and Environmental Mutagenesis* 2023; 885: 503560, doi:<https://doi.org/10.1016/j.mrgentox.2022.503560>
- Brunborg G, Jackson P, Shaposhnikov S, Dahl H, Azqueta A, Collins AR, et al. High throughput sample processing and automated scoring. *Front Genet* 2014; 5: 373, doi:10.3389/fgene.2014.00373
- Buenrostro JD, Giresi PG, Zaba LC, Chang HY, Greenleaf WJ. Transposition of native chromatin for fast and sensitive epigenomic profiling of open chromatin, DNA-binding proteins and nucleosome position. *Nat Methods* 2013; 10: 1213-8, doi:10.1038/nmeth.2688
- Buenrostro JD, Wu B, Chang HY, Greenleaf WJ. ATAC-seq: A Method for Assaying Chromatin Accessibility Genome-Wide. *Curr Protoc Mol Biol* 2015; 109: 21.29.1-21.29.9, doi:10.1002/0471142727.mb2129s109

- Callinan PA, Feinberg AP. The emerging science of epigenomics. *Hum Mol Genet* 2006; 15 Spec No 1: R95-101, doi:10.1093/hmg/ddl095
- Cech TR, Steitz JA. The noncoding RNA revolution-trashing old rules to forge new ones. *Cell* 2014; 157: 77-94, doi:10.1016/j.cell.2014.03.008
- Chawla A, Nagy C, Turecki G. Chromatin Profiling Techniques: Exploring the Chromatin Environment and Its Contributions to Complex Traits. *International journal of molecular sciences* 2021; 22: 7612, doi:10.3390/ijms22147612
- Chen EY, Tan CM, Kou Y, Duan Q, Wang Z, Meirelles GV, et al. Enrichr: interactive and collaborative HTML5 gene list enrichment analysis tool. *BMC Bioinformatics* 2013; 14: 128, doi:10.1186/1471-2105-14-128
- Chen Q, Yan M, Cao Z, Li X, Zhang Y, Shi J, et al. Sperm tsRNAs contribute to intergenerational inheritance of an acquired metabolic disorder. *Science* 2016a; 351: 397-400, doi:10.1126/science.aad7977
- Chen Q, Yan W, Duan E. Epigenetic inheritance of acquired traits through sperm RNAs and sperm RNA modifications. *Nat Rev Genet* 2016b; 17: 733-743, doi:10.1038/nrg.2016.106
- Chen Z, Tian R, She Z, Cai J, Li H. Role of oxidative stress in the pathogenesis of nonalcoholic fatty liver disease. *Free Radic Biol Med* 2020; 152: 116-141, doi:10.1016/j.freeradbiomed.2020.02.025
- Clement CH, Stewart FA, Akleyev AV, Hauer-Jensen M, Hendry JH, Kleiman NJ, et al. ICRP PUBLICATION 118: ICRP Statement on Tissue Reactions and Early and Late Effects of Radiation in Normal Tissues and Organs — Threshold Doses for Tissue Reactions in a Radiation Protection Context. *Annals of the ICRP* 2012; 41: 1-322, doi:10.1016/j.icrp.2012.02.001
- Collins A, Møller P, Gajski G, Vodenková S, Abdulwahed A, Anderson D, et al. Measuring DNA modifications with the comet assay: a compendium of protocols. *Nat Protoc* 2023, doi:10.1038/s41596-022-00754-y
- Collins AR. Investigating oxidative DNA damage and its repair using the comet assay. *Mutat Res* 2009; 681: 24-32, doi:10.1016/j.mrrev.2007.10.002
- Collins AR. Measuring oxidative damage to DNA and its repair with the comet assay. *Biochim Biophys Acta* 2014; 1840: 794-800, doi:10.1016/j.bbagen.2013.04.022
- Collins AR, Oscoz AA, Brunborg G, Gaivao I, Giovannelli L, Kruszewski M, et al. The comet assay: topical issues. *Mutagenesis* 2008; 23: 143-51, doi:10.1093/mutage/gem051
- COMARE. Further consideration of the incidence of cancers around the nuclear installations at Sellafield and Dounreay, 17th report by the Committee on Medical Aspects of Radiation in the Environment Public Health England, Crown, 2016,

- Conesa A, Madrigal P, Tarazona S, Gomez-Cabrero D, Cervera A, McPherson A, et al. A survey of best practices for RNA-seq data analysis. *Genome Biol* 2016; 17: 13, doi:10.1186/s13059-016-0881-8
- Corces MR, Buenrostro JD, Wu B, Greenside PG, Chan SM, Koenig JL, et al. Lineage-specific and single-cell chromatin accessibility charts human hematopoiesis and leukemia evolution. *Nat Genet* 2016; 48: 1193-203, doi:10.1038/ng.3646
- Corces MR, Trevino AE, Hamilton EG, Greenside PG, Sinnott-Armstrong NA, Vesuna S, et al. An improved ATAC-seq protocol reduces background and enables interrogation of frozen tissues. *Nature Methods* 2017; 14: 959-962, doi:10.1038/nmeth.4396
- Costa EOA, Pinto IP, Gonçalves MW, da Silva JF, Oliveira LG, da Cruz AS, et al. Small de novo CNVs as biomarkers of parental exposure to low doses of ionizing radiation of caesium-137. *Scientific Reports* 2018; 8: 5914, doi:10.1038/s41598-018-23813-5
- D'Auria Vieira de Godoy PR, Nakamura A, Khavari AP, Sangsuwan T, Haghdoost S. Effect of dose and dose rate of gamma irradiation on the formation of micronuclei in bone marrow cells isolated from whole-body-irradiated mice. *Environ Mol Mutagen* 2021; 62: 422-427, doi:10.1002/em.22453
- Dahl H, Ballangby J, Tengs T, Wojewodzic MW, Eide DM, Brede DA, et al. Dose rate dependent reduction in chromatin accessibility at transcriptional start sites long time after exposure to gamma radiation. *Epigenetics* 2023; 18: 2193936, doi:10.1080/15592294.2023.2193936
- Dahl H, Eide DM, Tengs T, Duale N, Kamstra JH, Oughton DH, et al. Perturbed transcriptional profiles after chronic low dose rate radiation in mice. *PLOS ONE* 2021; 16: e0256667, doi:10.1371/journal.pone.0256667
- Dai X, Shen L. Advances and Trends in Omics Technology Development. *Front Med (Lausanne)* 2022; 9: 911861, doi:10.3389/fmed.2022.911861
- Darakhshan F, Badie C, Moody J, Coster M, Finnon R, Finnon P, et al. Evidence for complex multigenic inheritance of radiation AML susceptibility in mice revealed using a surrogate phenotypic assay. *Carcinogenesis* 2006; 27: 311-318, doi:10.1093/carcin/bgi207
- David-Cordonnier MH, Laval J, O'Neill P. Recognition and kinetics for excision of a base lesion within clustered DNA damage by the *Escherichia coli* proteins Fpg and Nth. *Biochemistry* 2001; 40: 5738-46, doi:10.1021/bi002605d
- Dertinger SD, Bemis JC, Phonethepswath S, Tsai Y, Nowak I, Hyrien O, et al. Reticulocyte and micronucleated reticulocyte responses to gamma irradiation: effect of age. *Mutat Res* 2009; 675: 77-80, doi:10.1016/j.mrgentox.2009.02.002

- Dertinger SD, Torous DK, Hayashi M, MacGregor JT. Flow cytometric scoring of micronucleated erythrocytes: an efficient platform for assessing in vivo cytogenetic damage. *Mutagenesis* 2011; 26: 139-45, doi:10.1093/mutage/geq055
- Dertinger SD, Torous DK, Tometsko KR. Simple and reliable enumeration of micronucleated reticulocytes with a single-laser flow cytometer. *Mutat Res* 1996; 371: 283-92, doi:10.1016/s0165-1218(96)90117-2
- Dertinger SD, Tsai Y, Nowak I, Hyrien O, Sun H, Bemis JC, et al. Reticulocyte and micronucleated reticulocyte responses to gamma irradiation: dose-response and time-course profiles measured by flow cytometry. *Mutat Res* 2007; 634: 119-25, doi:10.1016/j.mrgentox.2007.06.010
- Desouky O, Ding N, Zhou G. Targeted and non-targeted effects of ionizing radiation. *Journal of Radiation Research and Applied Sciences* 2015; 8: 247-254, doi:<https://doi.org/10.1016/j.jrras.2015.03.003>
- Dixon SJ, Lemberg KM, Lamprecht MR, Skouta R, Zaitsev EM, Gleason CE, et al. Ferroptosis: an iron-dependent form of nonapoptotic cell death. *Cell* 2012; 149: 1060-72, doi:10.1016/j.cell.2012.03.042
- Duale N, Eide DM, Amberger ML, Graupner A, Brede DA, Olsen AK. Using prediction models to identify miRNA-based markers of low dose rate chronic stress. *Sci Total Environ* 2020; 717: 137068, doi:10.1016/j.scitotenv.2020.137068
- Duale N, Olsen AK, Christensen T, Butt ST, Brunborg G. Octyl methoxycinnamate modulates gene expression and prevents cyclobutane pyrimidine dimer formation but not oxidative DNA damage in UV-exposed human cell lines. *Toxicol Sci* 2010; 114: 272-84, doi:10.1093/toxsci/kfq005
- Dubrova YE, Bersimbaev RI, Djansugurova LB, Tankimanova MK, Mamyrbayeva Z, Mustonen R, et al. Nuclear weapons tests and human germline mutation rate. *Science* 2002; 295: 1037, doi:10.1126/science.1068102
- Dubrova YE, Nesterov VN, Krouchinsky NG, Ostapenko VA, Neumann R, Neil DL, et al. Human minisatellite mutation rate after the Chernobyl accident. *Nature* 1996; 380: 683-686, doi:10.1038/380683a0
- Dubrova YE, Nesterov VN, Krouchinsky NG, Ostapenko VA, Vergnaud G, Giraudeau F, et al. Further evidence for elevated human minisatellite mutation rate in Belarus eight years after the Chernobyl accident. *Mutat Res* 1997; 381: 267-78, doi:10.1016/s0027-5107(97)00212-1
- Dubrova YE, Ploshchanskaya OG, Kozionova OS, Akleyev AV. Minisatellite germline mutation rate in the Techa River population. *Mutat Res* 2006; 602: 74-82, doi:10.1016/j.mrfmmm.2006.08.001

- Dubrova YE, Sarapultseva EI. Radiation-induced transgenerational effects in animals. *Int J Radiat Biol* 2020; 1-7, doi:10.1080/09553002.2020.1793027
- E. Lindbo Hansen POH. Air kerma measurements with Landauer nanoDots in Cs-137 and Co-60 beams. Part I - SSDL exposures free in air. Technical document no. 8. NRPA, Norwegian Radiation Protection Authority, Østerås, Oslo, 2017,
- Ebrahimian TG, Beugnies L, Surette J, Priest N, Gueguen Y, Gloaguen C, et al. Chronic Exposure to External Low-Dose Gamma Radiation Induces an Increase in Anti-inflammatory and Anti-oxidative Parameters Resulting in Atherosclerotic Plaque Size Reduction in ApoE(-/-) Mice. *Radiat Res* 2018; 189: 187-196, doi:10.1667/rr14823.1
- Eddy SR. Non-coding RNA genes and the modern RNA world. *Nat Rev Genet* 2001; 2: 919-29, doi:10.1038/35103511
- EFSA Scientific Committee MS, Bampidis V, Bragard C, Halldorsson TI, Hernandez-Jerez AF, Hougaard Bennekou S, Koutsoumanis K, Lambre C, Machera K, Naegeli H, Nielsen S S, Schlatter J, Schrenk D, Turck D, Younes M, Aquilina G, Bignami M, Bolognesi C, Crebelli R, Gurtler R, Marcon F, Nielsen E, Vleminckx C, Carfi M, Martino C, Maurici D, Parra Morte J, Rossi A, Benford D. Scientific Opinion on the guidance on a neogenecity assessment. 9(8):6770, EFSA, 2021, doi:<https://doi.org/10.2903/j.efsa.2021.6770>
- Ellender M, Harrison JD, Meijne E, Huiskamp R, Kozlowski RE, Haines JW, et al. Intestinal tumours induced in Apc(Min/+) mice by X-rays and neutrons. *Int J Radiat Biol* 2011; 87: 385-99, doi:10.3109/09553002.2011.542542
- ENCODE. The ENCODE (ENCyclopedia Of DNA Elements) Project. *Science* 2004; 306: 636-40, doi:10.1126/science.1105136
- Esteller M. Non-coding RNAs in human disease. *Nat Rev Genet* 2011; 12: 861-74, doi:10.1038/nrg3074
- Ferrecchia CE, Jensen K, Van Andel R. Intracage ammonia levels in static and individually ventilated cages housing C57BL/6 mice on 4 bedding substrates. *J Am Assoc Lab Anim Sci* 2014; 53: 146-51,
- Festing MFW, Nevalainen T. The Design and Statistical Analysis of Animal Experiments: Introduction to this Issue. *ILAR Journal* 2014; 55: 379-382, doi:10.1093/ilar/ilu046
- Folley JH, Borges W, Yamawaki T. Incidence of leukemia in survivors of the atomic bomb in Hiroshima and Nagasaki, Japan. *Am J Med* 1952; 13: 311-21, doi:10.1016/0002-9343(52)90285-4

- Fujikawa K, Sugihara T, Tanaka S, Tanaka I, Nakamura S, Nakamura-Murano M, et al. LOW DOSE-RATE RADIATION-SPECIFIC ALTERATIONS FOUND IN A GENOME-WIDE GENE EXPRESSION ANALYSIS OF THE MOUSE LIVER. *Radiat Prot Dosimetry* 2022; 198: 1165-1169, doi:10.1093/rpd/ncac088
- Gardner MJ, Snee MP, Hall AJ, Powell CA, Downes S, Terrell JD. Results of case-control study of leukaemia and lymphoma among young people near Sellafield nuclear plant in West Cumbria. *Bmj* 1990; 300: 423-9, doi:10.1136/bmj.300.6722.423
- Giresi PG, Kim J, McDaniell RM, Iyer VR, Lieb JD. FAIRE (Formaldehyde-Assisted Isolation of Regulatory Elements) isolates active regulatory elements from human chromatin. *Genome Res* 2007; 17: 877-85, doi:10.1101/gr.5533506
- Goodhead DT. Initial events in the cellular effects of ionizing radiations: clustered damage in DNA. *Int J Radiat Biol* 1994; 65: 7-17, doi:10.1080/09553009414550021
- Goodhead DT. New radiobiological, radiation risk and radiation protection paradigms. *Mutat Res* 2010; 687: 13-16, doi:10.1016/j.mrfmmm.2010.01.006
- Grafen AH, R. *Modern Statistics for the Life Sciences*. New York: Oxford University Press, 2010.
- Grant EJ, Furukawa K, Sakata R, Sugiyama H, Sadakane A, Takahashi I, et al. Risk of death among children of atomic bomb survivors after 62 years of follow-up: a cohort study. *Lancet Oncol* 2015; 16: 1316-23, doi:10.1016/s1470-2045(15)00209-0
- Graupner A. Genotoxic effects of continuous chronic low dose rate gamma irradiation and selenium deficiency. Faculty of Medicine. PhD. University of Oslo, University of Oslo, 2015, pp. 80,
- Graupner A, Eide DM, Brede DA, Ellender M, Lindbo Hansen E, Oughton DH, et al. Genotoxic effects of high dose rate X-ray and low dose rate gamma radiation in *Apc(Min/+)* mice. *Environ Mol Mutagen* 2017; 58: 560-569, doi:10.1002/em.22121
- Graupner A, Eide DM, Instanes C, Andersen JM, Brede DA, Dertinger SD, et al. Gamma radiation at a human relevant low dose rate is genotoxic in mice. *Sci Rep* 2016; 6: 32977, doi:10.1038/srep32977
- Grewenig A, Schuler N, Rube CE. Persistent DNA Damage in Spermatogonial Stem Cells After Fractionated Low-Dose Irradiation of Testicular Tissue. *Int J Radiat Oncol Biol Phys* 2015; 92: 1123-31, doi:10.1016/j.ijrobp.2015.04.033
- Gutzkow KB, Duale N, Danielsen T, von Stedingk H, Shahzadi S, Instanes C, et al. Enhanced susceptibility of obese mice to glycidamide-induced sperm chromatin damage without increased oxidative stress. *Andrology* 2016; 4: 1102-1114, doi:10.1111/andr.12233

- Gutzkow KB, Langleite TM, Meier S, Graupner A, Collins AR, Brunborg G. High-throughput comet assay using 96 minigels. *Mutagenesis* 2013; 28: 333-40, doi:10.1093/mutage/get012
- Haley BM, Paunesku T, Grdina DJ, Woloschak GE. The Increase in Animal Mortality Risk following Exposure to Sparsely Ionizing Radiation Is Not Linear Quadratic with Dose. *PLoS One* 2015; 10: e0140989, doi:10.1371/journal.pone.0140989
- Hamasaki K, Imai K, Hayashi T, Nakachi K, Kusunoki Y. Radiation sensitivity and genomic instability in the hematopoietic system: Frequencies of micronucleated reticulocytes in whole-body X-irradiated BALB/c and C57BL/6 mice. *Cancer Sci* 2007; 98: 1840-4, doi:10.1111/j.1349-7006.2007.00641.x
- Hanahan D. Hallmarks of Cancer: New Dimensions. *Cancer Discov* 2022; 12: 31-46, doi:10.1158/2159-8290.Cd-21-1059
- Hanahan D, Weinberg RA. The hallmarks of cancer. *Cell* 2000; 100: 57-70, doi:10.1016/s0092-8674(00)81683-9
- Hanahan D, Weinberg RA. Hallmarks of cancer: the next generation. *Cell* 2011; 144: 646-74, doi:10.1016/j.cell.2011.02.013
- Hansen AS, Pustova I, Cattoglio C, Tjian R, Darzacq X. CTCF and cohesin regulate chromatin loop stability with distinct dynamics. *Elife* 2017; 6, doi:10.7554/eLife.25776
- Hansen EL RHI, Hetland PO, Bjerke H. Absorbed doses to water for x-ray dosimetry on a PXI X-RAD 225, Part I - Measurements. NRPA Technical Document Series 7. NRPA, 2015,
- Hansen SH, Olsen AK, S oderlund EJ, Brunborg G. In vitro investigations of glycidamide-induced DNA lesions in mouse male germ cells and in mouse and human lymphocytes. *Mutat Res* 2010; 696: 55-61, doi:10.1016/j.mrgentox.2009.12.012
- Harley NH. Chapter 25. Toxic Effects of Radiation and Radioactive Materials. In: Klaassen CD, Watkins JB, editors. *Casarett & Doull's Essentials of Toxicology*, 2e. The McGraw-Hill Companies, New York, NY, 2010.
- Hauptmann M, Daniels RD, Cardis E, Cullings HM, Kendall G, Laurier D, et al. Epidemiological Studies of Low-Dose Ionizing Radiation and Cancer: Summary Bias Assessment and Meta-Analysis. *JNCI Monographs* 2020; 2020: 188-200, doi:10.1093/jncimonographs/lgaa010
- Heard E, Martienssen RA. Transgenerational epigenetic inheritance: myths and mechanisms. *Cell* 2014; 157: 95-109, doi:10.1016/j.cell.2014.02.045
- Hei TK, Zhou H, Chai Y, Ponnaiya B, Ivanov VN. Radiation induced non-targeted response: mechanism and potential clinical implications. *Curr Mol Pharmacol* 2011; 4: 96-105,

- Heid CA, Stevens J, Livak KJ, Williams PM. Real time quantitative PCR. *Genome Res* 1996; 6: 986-94, doi:10.1101/gr.6.10.986
- Hendry JH, Simon SL, Wojcik A, Sohrabi M, Burkart W, Cardis E, et al. Human exposure to high natural background radiation: what can it teach us about radiation risks? *J Radiol Prot* 2009; 29: A29-42, doi:10.1088/0952-4746/29/2a/s03
- Higuchi R, Fockler C, Dollinger G, Watson R. Kinetic PCR Analysis: Real-time Monitoring of DNA Amplification Reactions. *Bio/Technology* 1993; 11: 1026-1030, doi:10.1038/nbt0993-1026
- Holoch D, Moazed D. RNA-mediated epigenetic regulation of gene expression. *Nature Reviews Genetics* 2015; 16: 71-84, doi:10.1038/nrg3863
- IARC. ICRP Working Group on the Evaluation of Carcinogenic Risks to Humans; Ionizing Radiation, Part 1: X- and Gamma (γ)-Radiation, and Neutrons. Lyon (FR): International Agency for Research on Cancer; 2000. (IARC Monographs on the Evaluation of Carcinogenic Risks to Humans, No. 75.) X-radiation and γ -radiation, 2000,
- ICRP. ICRP Publication 60; The 1990 Recommendations of the International Commission on Radiological Protection. 1991; *Ann. ICRP* 21 (1-3),
- ICRP. ICRP publication 103; The 2007 Recommendations of the International Commission on Radiological Protection *Ann ICRP*. 37, 2007, pp. 1-332, doi:10.1016/j.icrp.2007.10.003
- ICRP. Conversion Coefficients for Radiological Protection Quantities for External Radiation Exposures, ICRP Publication 116. *Ann ICRP* 2010; 40: 2-5,
- Iliakis G, Mladenov E, Mladenova V. Necessities in the Processing of DNA Double Strand Breaks and Their Effects on Genomic Instability and Cancer. *Cancers (Basel)* 2019; 11, doi:10.3390/cancers11111671
- Inotiv. C57BL/6 inbred mice. 2023. Inotivco, www.inotivco.com, 2023a,
- Inotiv. CBA/Ca inbred mice. 2023. Inotiv, Inotivco, 2023b,
- Izumi S, Koyama K, Soda M, Suyama A. Cancer incidence in children and young adults did not increase relative to parental exposure to atomic bombs. *Br J Cancer* 2003; 89: 1709-13, doi:10.1038/sj.bjc.6601322
- Jackson SP, Bartek J. The DNA-damage response in human biology and disease. *Nature* 2009; 461: 1071-1078, doi:10.1038/nature08467
- Jafer A, Sylvius N, Adewoye AB, Dubrova YE. The long-term effects of exposure to ionising radiation on gene expression in mice. *Mutat Res* 2020; 821: 111723, doi:10.1016/j.mrfmmm.2020.111723
- Jeggio P, Löbrich M. Radiation-induced DNA damage responses. *Radiat Prot Dosimetry* 2006; 122: 124-7, doi:10.1093/rpd/ncl495
- Jiang C, Pugh BF. Nucleosome positioning and gene regulation: advances through genomics. *Nat Rev Genet* 2009; 10: 161-72, doi:10.1038/nrg2522

- Jiao Y, Cao F, Liu H. Radiation-induced Cell Death and Its Mechanisms. *Health Phys* 2022; 123: 376-386, doi:10.1097/hp.0000000000001601
- Jones PA. Functions of DNA methylation: islands, start sites, gene bodies and beyond. *Nature Reviews Genetics* 2012; 13: 484-492, doi:10.1038/nrg3230
- Kadhim MA. Role of genetic background in induced instability. *Oncogene* 2003; 22: 6994-9, doi:10.1038/sj.onc.1206883
- Kalra A YE, Wehrle CJ, et al. *Physiology, Liver*. Treasure Island (FL): StatPearls Publishing, 2023.
- Kamiya K, Ozasa K, Akiba S, Niwa O, Kodama K, Takamura N, et al. Long-term effects of radiation exposure on health. *Lancet* 2015; 386: 469-78, doi:10.1016/s0140-6736(15)61167-9
- Kaplan MI, Limoli CL, Morgan WF. Perpetuating radiation-induced chromosomal instability. *Radiat Oncol Investig* 1997; 5: 124-8, doi:10.1002/(sici)1520-6823(1997)5:3<124::aid-roi8>3.0.co;2-#
- Kim J, Jung Y. Radiation-induced liver disease: current understanding and future perspectives. *Exp Mol Med* 2017; 49: e359, doi:10.1038/emm.2017.85
- Klaunig JE, Wang Z, Pu X, Zhou S. Oxidative stress and oxidative damage in chemical carcinogenesis. *Toxicol Appl Pharmacol* 2011; 254: 86-99, doi:10.1016/j.taap.2009.11.028
- Klein DC, Hainer SJ. Genomic methods in profiling DNA accessibility and factor localization. *Chromosome Res* 2020; 28: 69-85, doi:10.1007/s10577-019-09619-9
- Klemm SL, Shipony Z, Greenleaf WJ. Chromatin accessibility and the regulatory epigenome. *Nature Reviews Genetics* 2019; 20: 207-220, doi:10.1038/s41576-018-0089-8
- Klungland A, Lindahl T. Second pathway for completion of human DNA base excision-repair: reconstitution with purified proteins and requirement for DNase IV (FEN1). *Embo j* 1997; 16: 3341-8, doi:10.1093/emboj/16.11.3341
- Klungland A, Rosewell I, Hollenbach S, Larsen E, Daly G, Epe B, et al. Accumulation of premutagenic DNA lesions in mice defective in removal of oxidative base damage. *Proc Natl Acad Sci U S A* 1999; 96: 13300-5,
- Kodaira M, Ryo H, Kamada N, Furukawa K, Takahashi N, Nakajima H, et al. No evidence of increased mutation rates at microsatellite loci in offspring of A-bomb survivors. *Radiat Res* 2010; 173: 205-13, doi:10.1667/rr1991.1
- Kodaira M, Satoh C, Hiyama K, Toyama K. Lack of effects of atomic bomb radiation on genetic instability of tandem-repetitive elements in human germ cells. *Am J Hum Genet* 1995; 57: 1275-83,

- Kornberg RD. Chromatin structure: a repeating unit of histones and DNA. *Science* 1974; 184: 868-71, doi:10.1126/science.184.4139.868
- Koshurnikova NA, Shilnikova NS, Okatenko PV, Kreslov VV, Bolotnikova MG, Sokolnikov ME, et al. Characteristics of the cohort of workers at the Mayak nuclear complex. *Radiat Res* 1999; 152: 352-63,
- Kossenko MM, Thomas TL, Akleyev AV, Krestinina LY, Startsev NV, Vyushkova OV, et al. The Techa River Cohort: study design and follow-up methods. *Radiat Res* 2005; 164: 591-601, doi:10.1667/rr3451.1
- Krestinina LY, Davis FG, Schonfeld S, Preston DL, Degteva M, Epifanova S, et al. Leukaemia incidence in the Techa River Cohort: 1953-2007. *Br J Cancer* 2013; 109: 2886-93, doi:10.1038/bjc.2013.614
- Kubota Y, Nash RA, Klungland A, Schär P, Barnes DE, Lindahl T. Reconstitution of DNA base excision-repair with purified human proteins: interaction between DNA polymerase beta and the XRCC1 protein. *Embo j* 1996; 15: 6662-70,
- Kukurba KR, Montgomery SB. RNA Sequencing and Analysis. *Cold Spring Harb Protoc* 2015; 2015: 951-69, doi:10.1101/pdb.top084970
- Kuleshov MV, Jones MR, Rouillard AD, Fernandez NF, Duan Q, Wang Z, et al. Enrichr: a comprehensive gene set enrichment analysis web server 2016 update. *Nucleic Acids Res* 2016; 44: W90-7, doi:10.1093/nar/gkw377
- Lee CK, Shibata Y, Rao B, Strahl BD, Lieb JD. Evidence for nucleosome depletion at active regulatory regions genome-wide. *Nat Genet* 2004; 36: 900-5, doi:10.1038/ng1400
- Li S, Tan HY, Wang N, Zhang ZJ, Lao L, Wong CW, et al. The Role of Oxidative Stress and Antioxidants in Liver Diseases. *Int J Mol Sci* 2015; 16: 26087-124, doi:10.3390/ijms161125942
- Li Y. Modern epigenetics methods in biological research. *Methods* 2021; 187: 104-113, doi:10.1016/j.ymeth.2020.06.022
- Liguori I, Russo G, Curcio F, Bulli G, Aran L, Della-Morte D, et al. Oxidative stress, aging, and diseases. *Clin Interv Aging* 2018; 13: 757-772, doi:10.2147/cia.S158513
- Lind OC, Helen Oughton D, Salbu B. The NMBU FIGARO low dose irradiation facility. *Int J Radiat Biol* 2018: 1-6, doi:10.1080/09553002.2018.1516906
- Little MP, Azizova TV, Hamada N. Low- and moderate-dose non-cancer effects of ionizing radiation in directly exposed individuals, especially circulatory and ocular diseases: a review of the epidemiology. *Int J Radiat Biol* 2021: 1-49, doi:10.1080/09553002.2021.1876955

- Little MP, Goodhead DT, Bridges BA, Bouffler SD. Evidence relevant to untargeted and transgenerational effects in the offspring of irradiated parents. *Mutat Res* 2013; 753: 50-67, doi:10.1016/j.mrrev.2013.04.001
- Little MP, Wakeford R, Tawn EJ, Bouffler SD, Berrington de Gonzalez A. Risks associated with low doses and low dose rates of ionizing radiation: why linearity may be (almost) the best we can do. *Radiology* 2009; 251: 6-12, doi:10.1148/radiol.2511081686
- Lomax ME, Folkes LK, O'Neill P. Biological Consequences of Radiation-induced DNA Damage: Relevance to Radiotherapy. *Clinical Oncology* 2013; 25: 578-585, doi:<https://doi.org/10.1016/j.clon.2013.06.007>
- Lowe D, Roy L, Tabocchini MA, Rühm W, Wakeford R, Woloschak GE, et al. Radiation dose rate effects: what is new and what is needed? *Radiation and Environmental Biophysics* 2022; 61: 507-543, doi:10.1007/s00411-022-00996-0
- Lukashenko S, Kabdyrakova A, Lind OC, Gorlachev I, Kunduzbayeva A, Kvochkina T, et al. Radioactive particles released from different sources in the Semipalatinsk Test Site. *Journal of Environmental Radioactivity* 2020; 216: 106160, doi:<https://doi.org/10.1016/j.jenvrad.2020.106160>
- Lumniczky K, Impens N, Armengol G, Candéias S, Georgakilas AG, Hornhardt S, et al. Low dose ionizing radiation effects on the immune system. *Environ Int* 2021; 149: 106212, doi:10.1016/j.envint.2020.106212
- Maeshima K, Iida S, Tamura S. Physical Nature of Chromatin in the Nucleus. *Cold Spring Harb Perspect Biol* 2021; 13,
- Major IR, Mole RH. Myeloid leukaemia in x-ray irradiated CBA mice. *Nature* 1978; 272: 455-6, doi:10.1038/272455a0
- Mansidor AR, Risca VI. Chromatin accessibility: methods, mechanisms, and biological insights. *Nucleus* 2022; 13: 236-276, doi:10.1080/19491034.2022.2143106
- Mathias D, Mitchel RE, Barclay M, Wyatt H, Bugden M, Priest ND, et al. Correction: Low-Dose Irradiation Affects Expression of Inflammatory Markers in the Heart of ApoE -/- Mice. *PLoS One* 2016; 11: e0157616, doi:10.1371/journal.pone.0157616
- Mavragani IV, Laskaratou DA, Frey B, Candéias SM, Gaipf US, Lumniczky K, et al. Key mechanisms involved in ionizing radiation-induced systemic effects. A current review. *Toxicol Res (Camb)* 2016; 5: 12-33, doi:10.1039/c5tx00222b
- Mavragani IV, Nikitaki Z, Souli MP, Aziz A, Newsheer S, Aziz K, et al. Complex DNA Damage: A Route to Radiation-Induced Genomic Instability and Carcinogenesis. *Cancers (Basel)* 2017; 9, doi:10.3390/cancers9070091

- McBride WH, Schae D. Radiation-induced tissue damage and response. *J Pathol* 2020; 250: 647-655, doi:10.1002/path.5389
- Meistrich ML. Effects of chemotherapy and radiotherapy on spermatogenesis in humans. *Fertil Steril* 2013; 100: 1180-6, doi:10.1016/j.fertnstert.2013.08.010
- Mekada K, Abe K, Murakami A, Nakamura S, Nakata H, Moriwaki K, et al. Genetic differences among C57BL/6 substrains. *Exp Anim* 2009; 58: 141-9,
- Merrifield M, Kovalchuk O. Epigenetics in radiation biology: a new research frontier. *Front Genet* 2013; 4: 40, doi:10.3389/fgene.2013.00040
- Minamoto A, Taniguchi H, Yoshitani N, Mukai S, Yokoyama T, Kumagami T, et al. Cataract in atomic bomb survivors. *Int J Radiat Biol* 2004; 80: 339-45, doi:10.1080/09553000410001680332
- Minnoye L, Marinov GK, Krausgruber T, Pan L, Marand AP, Secchia S, et al. Chromatin accessibility profiling methods. *Nature Reviews Methods Primers* 2021; 1: 10, doi:10.1038/s43586-020-00008-9
- Miousse IR, Chalbot MC, Lumen A, Ferguson A, Kavouras IG, Koturbash I. Response of transposable elements to environmental stressors. *Mutat Res Rev Mutat Res* 2015; 765: 19-39,
- Moorhouse AJ, Scholze M, Sylvius N, Gillham C, Rake C, Peto J, et al. No evidence of increased mutations in the germline of a group of British nuclear test veterans. *Scientific Reports* 2022; 12: 10830, doi:10.1038/s41598-022-14999-w
- Mortimer M, Fang W, Zhou X, Vodovnik M, Guo L-H. Omics Approaches in Toxicological Studies. In: Guo L-H, Mortimer M, editors. *Advances in Toxicology and Risk Assessment of Nanomaterials and Emerging Contaminants*. Springer Singapore, Singapore, 2022, pp. 61-94.
- Mothersill CE, O'Malley KJ, Murphy DM, Seymour CB, Lorimore SA, Wright EG. Identification and characterization of three subtypes of radiation response in normal human urothelial cultures exposed to ionizing radiation. *Carcinogenesis* 1999; 20: 2273-2278, doi:10.1093/carcin/20.12.2273
- Mughal SK, Myazin AE, Zhavoronkov LP, Rubanovich AV, Dubrova YE. The dose and dose-rate effects of paternal irradiation on transgenerational instability in mice: a radiotherapy connection. *PLoS One* 2012; 7: e41300, doi:10.1371/journal.pone.0041300
- Muruzabal D, Collins A, Azqueta A. The enzyme-modified comet assay: Past, present and future. *Food and Chemical Toxicology* 2021; 147: 111865, doi:<https://doi.org/10.1016/j.fct.2020.111865>
- Møller P, Jantzen K, Løhr M, Andersen MH, Jensen DM, Roursgaard M, et al. Searching for assay controls for the Fpg- and hOGG1-modified comet assay. *Mutagenesis* 2017; 33: 9-19, doi:10.1093/mutage/gex015

- Nagy PL, Cleary ML, Brown PO, Lieb JD. Genomewide demarcation of RNA polymerase II transcription units revealed by physical fractionation of chromatin. *Proc Natl Acad Sci U S A* 2003; 100: 6364-9, doi:10.1073/pnas.1131966100
- Nair N, Shoaib M, Sørensen CS. Chromatin Dynamics in Genome Stability: Roles in Suppressing Endogenous DNA Damage and Facilitating DNA Repair. *International Journal of Molecular Sciences* 2017; 18: 1486,
- Nakajima T, Wang B, Ono T, Uehara Y, Nakamura S, Ichinohe K, et al. Differences in sustained alterations in protein expression between livers of mice exposed to high-dose-rate and low-dose-rate radiation. *J Radiat Res* 2017; 58: 421-429, doi:10.1093/jrr/rrw133
- Nakamura S, Tanaka IB, 3rd, Tanaka S, Nakaya K, Sakata N, Oghiso Y. Adiposity in female B6C3F1 mice continuously irradiated with low-dose-rate gamma rays. *Radiat Res* 2010; 173: 333-41, doi:10.1667/rr1962.1
- NAS. Health Risks from Exposure to Low Levels of Ionizing Radiation; BEIR VII. Washington, DC: The National Academies Press, 2006.
- Nemeth E, Baird AW, O'Farrelly C. Microanatomy of the liver immune system. *Semin Immunopathol* 2009; 31: 333-43, doi:10.1007/s00281-009-0173-4
- Nguyen TM, Shafi A, Nguyen T, Draghici S. Identifying significantly impacted pathways: a comprehensive review and assessment. *Genome Biol* 2019; 20: 203, doi:10.1186/s13059-019-1790-4
- Nikjoo H, O'Neill P, Wilson WE, Goodhead DT. Computational approach for determining the spectrum of DNA damage induced by ionizing radiation. *Radiat Res* 2001; 156: 577-83, doi:10.1667/0033-7587(2001)156[0577:cafdts]2.0.co;2
- Nikjoo H, Uehara S, Wilson WE, Hoshi M, Goodhead DT. Track structure in radiation biology: theory and applications. *Int J Radiat Biol* 1998; 73: 355-64, doi:10.1080/095530098142176
- NobelPrize.org. Hermann J. Muller – Nobel Lecture December 12,1946. . 2023. Nobel Prize Outreach AB 2023, 2023,
- OECD. Test No. 474: Mammalian Erythrocyte Micronucleus Test, 2016a.
- OECD. Test No. 489: In Vivo Mammalian Alkaline Comet Assay, 2016b.
- OHAT. Handbook for Conducting a Literature-Based Health Assessment Using OHAT Approach for Systematic Review and Evidence Integration in: D. o. t. N. T. P. Office of Health Assessment and Translation (OHAT), National Institute of Environmental Health Sciences (Ed.). 2019,

- Olipitz W, Wiktor-Brown D, Shuga J, Pang B, McFaline J, Lonkar P, et al. Integrated molecular analysis indicates undetectable change in DNA damage in mice after continuous irradiation at ~ 400-fold natural background radiation. *Environmental health perspectives* 2012; 120: 1130-1136, doi:10.1289/ehp.1104294
- Olsen AK, Duale N, Bjoras M, Larsen CT, Wiger R, Holme JA, et al. Limited repair of 8-hydroxy-7,8-dihydroguanine residues in human testicular cells. *Nucleic Acids Res* 2003; 31: 1351-63,
- Orkin SH, Zon LI. Hematopoiesis: an evolving paradigm for stem cell biology. *Cell* 2008; 132: 631-44, doi:10.1016/j.cell.2008.01.025
- Ostling O, Johanson KJ. Microelectrophoretic study of radiation-induced DNA damages in individual mammalian cells. *Biochem Biophys Res Commun* 1984; 123: 291-8, doi:10.1016/0006-291x(84)90411-x
- Ozasa K, Cullings HM, Ohishi W, Hida A, Grant EJ. Epidemiological studies of atomic bomb radiation at the Radiation Effects Research Foundation. *International Journal of Radiation Biology* 2019; 95: 879-891, doi:10.1080/09553002.2019.1569778
- Ozasa K, Shimizu Y, Suyama A, Kasagi F, Soda M, Grant EJ, et al. Studies of the mortality of atomic bomb survivors, Report 14, 1950-2003: an overview of cancer and noncancer diseases. *Radiat Res* 2012; 177: 229-43, doi:10.1667/rr2629.1
- Panigrahi A, O'Malley BW. Mechanisms of enhancer action: the known and the unknown. *Genome Biology* 2021; 22: 108, doi:10.1186/s13059-021-02322-1
- Pascual-Ahuir A, Fita-Torró J, Proft M. Capturing and Understanding the Dynamics and Heterogeneity of Gene Expression in the Living Cell. *Int J Mol Sci* 2020; 21, doi:10.3390/ijms21218278
- Paunesku T, Stevanović A, Popović J, Woloschak GE. Effects of low dose and low dose rate low linear energy transfer radiation on animals - review of recent studies relevant for carcinogenesis. *Int J Radiat Biol* 2021; 97: 757-768, doi:10.1080/09553002.2020.1859155
- Pizzino G, Irrera N, Cucinotta M, Pallio G, Mannino F, Arcoraci V, et al. Oxidative Stress: Harms and Benefits for Human Health. *Oxid Med Cell Longev* 2017; 2017: 8416763, doi:10.1155/2017/8416763
- Ponnaiya B, Cornforth MN, Ullrich RL. Radiation-induced chromosomal instability in BALB/c and C57BL/6 mice: the difference is as clear as black and white. *Radiat Res* 1997; 147: 121-5,
- Preston DL, Ron E, Tokuoka S, Funamoto S, Nishi N, Soda M, et al. Solid cancer incidence in atomic bomb survivors: 1958-1998. *Radiat Res* 2007; 168: 1-64, doi:10.1667/rr0763.1

- Preston DL, Shimizu Y, Pierce DA, Suyama A, Mabuchi K. Studies of mortality of atomic bomb survivors. Report 13: Solid cancer and noncancer disease mortality: 1950-1997. *Radiat Res* 2003; 160: 381-407, doi:10.1667/rr3049
- Preston DL, Sokolnikov ME, Krestinina LY, Stram DO. Estimates of Radiation Effects on Cancer Risks in the Mayak Worker, Techa River and Atomic Bomb Survivor Studies. *Radiation Protection Dosimetry* 2017; 173: 26-31, doi:10.1093/rpd/ncw316
- Rassoulzadegan M, Grandjean V, Gounon P, Vincent S, Gillot I, Cuzin F. RNA-mediated non-mendelian inheritance of an epigenetic change in the mouse. *Nature* 2006; 441: 469-74, doi:10.1038/nature04674
- Razin A, Cedar H. DNA Methylation in Eukaryotic Cells. In: Bourne GH, Danielli JF, Jeon KW, editors. *International Review of Cytology*. 92. Academic Press, 1984, pp. 159-185.
- Reisz JA, Bansal N, Qian J, Zhao W, Furdui CM. Effects of ionizing radiation on biological molecules--mechanisms of damage and emerging methods of detection. *Antioxidants & redox signaling* 2014; 21: 260-292, doi:10.1089/ars.2013.5489
- Riethoven J-JM. Regulatory Regions in DNA: Promoters, Enhancers, Silencers, and Insulators. In: Ladunga I, editor. *Computational Biology of Transcription Factor Binding*. Humana Press, Totowa, NJ, 2010, pp. 33-42.
- Rithidech KN, Cronkite EP, Bond VP. Advantages of the CBA mouse in leukemogenesis research. *Blood Cells Mol Dis* 1999; 25: 38-45, doi:10.1006/bcmd.1999.0225
- Rivina L, Davoren MJ, Schiestl RH. Mouse models for radiation-induced cancers. *Mutagenesis* 2016; 31: 491-509, doi:10.1093/mutage/gew019
- Robinson MW, Harmon C, O'Farrelly C. Liver immunology and its role in inflammation and homeostasis. *Cell Mol Immunol* 2016; 13: 267-76, doi:10.1038/cmi.2016.3
- Roderick TH. THE RESPONSE OF TWENTY-SEVEN INBRED STRAINS OF MICE TO DAILY DOSES OF WHOLE-BODY X-IRRADIATION. *Radiat Res* 1963; 20: 631-9,
- Rube CE, Zhang S, Miebach N, Fricke A, Rube C. Protecting the heritable genome: DNA damage response mechanisms in spermatogonial stem cells. *DNA Repair (Amst)* 2011; 10: 159-68, doi:10.1016/j.dnarep.2010.10.007
- Ruthenburg AJ, Li H, Patel DJ, David Allis C. Multivalent engagement of chromatin modifications by linked binding modules. *Nature Reviews Molecular Cell Biology* 2007; 8: 983-994, doi:10.1038/nrm2298

- Rühm W, Azizova TV, Bouffler SD, Little MP, Shore RE, Walsh L, et al. Dose-rate effects in radiation biology and radiation protection. *Annals of the ICRP* 2016; 45: 262-279, doi:10.1177/0146645316629336
- Rühm W, Woloschak GE, Shore RE, Azizova TV, Grosche B, Niwa O, et al. Dose and dose-rate effects of ionizing radiation: a discussion in the light of radiological protection. *Radiat Environ Biophys* 2015; 54: 379-401, doi:10.1007/s00411-015-0613-6
- Salbu B, Krekling T, Oughton DH, Østby G, Kashparov VA, Brand TL, et al. Hot particles in accidental releases from Chernobyl and Windscale nuclear installations. *Analyst* 1994; 119: 125-130, doi:10.1039/AN9941900125
- Savill NJ, Chadwick W, Reece SE. Quantitative analysis of mechanisms that govern red blood cell age structure and dynamics during anaemia. *PLoS Comput Biol* 2009; 5: e1000416, doi:10.1371/journal.pcbi.1000416
- Saxena RK, Bhardwaj N, Sachar S, Puri N, Khandelwal S. A Double in vivo Biotinylation Technique for Objective Assessment of Aging and Clearance of Mouse Erythrocytes in Blood Circulation. *Transfus Med Hemother* 2012; 39: 335-41, doi:10.1159/000342524
- Schena M, Shalon D, Davis RW, Brown PO. Quantitative monitoring of gene expression patterns with a complementary DNA microarray. *Science* 1995; 270: 467-70, doi:10.1126/science.270.5235.467
- Schofield PN, Kondratowicz M. Evolving paradigms for the biological response to low dose ionizing radiation; the role of epigenetics. *Int J Radiat Biol* 2018; 94: 769-781,
- Sharma A. Novel transcriptome data analysis implicates circulating microRNAs in epigenetic inheritance in mammals. *Gene* 2014; 538: 366-72, doi:10.1016/j.gene.2014.01.051
- Sharma U, Sun F, Conine CC, Reichholz B, Kukreja S, Herzog VA, et al. Small RNAs Are Trafficked from the Epididymis to Developing Mammalian Sperm. *Dev Cell* 2018; 46: 481-494.e6, doi:10.1016/j.devcel.2018.06.023
- Shimizu Y, Kodama K, Nishi N, Kasagi F, Suyama A, Soda M, et al. Radiation exposure and circulatory disease risk: Hiroshima and Nagasaki atomic bomb survivor data, 1950-2003. *Bmj* 2010; 340: b5349, doi:10.1136/bmj.b5349
- Shore R, Walsh L, Azizova T, Rühm W. Risk of solid cancer in low dose-rate radiation epidemiological studies and the dose-rate effectiveness factor. *Int J Radiat Biol* 2017; 93: 1064-1078, doi:10.1080/09553002.2017.1319090
- Sies H, Jones DP. Reactive oxygen species (ROS) as pleiotropic physiological signalling agents. *Nat Rev Mol Cell Biol* 2020; 21: 363-383, doi:10.1038/s41580-020-0230-3

- Singh NP, McCoy MT, Tice RR, Schneider EL. A simple technique for quantitation of low levels of DNA damage in individual cells. *Experimental Cell Research* 1988; 175: 184-191, doi:[https://doi.org/10.1016/0014-4827\(88\)90265-0](https://doi.org/10.1016/0014-4827(88)90265-0)
- Skinner MK. What is an epigenetic transgenerational phenotype? F3 or F2. *Reprod Toxicol* 2008; 25: 2-6, doi:10.1016/j.reprotox.2007.09.001
- Skinner MK. Endocrine disruptors in 2015: Epigenetic transgenerational inheritance. *Nat Rev Endocrinol* 2016; 12: 68-70, doi:10.1038/nrendo.2015.206
- Sproull M, Shankavaram U, Camphausen K. Comparison of Proteomic Biodosimetry Biomarkers Across Five Different Murine Strains. *Radiat Res* 2019; 192: 640-648, doi:10.1667/rr15442.1
- Stevens TJ, Lando D, Basu S, Atkinson LP, Cao Y, Lee SF, et al. 3D structures of individual mammalian genomes studied by single-cell Hi-C. *Nature* 2017; 544: 59-64, doi:10.1038/nature21429
- Subedi P, Moertl S, Azimzadeh O. Omics in Radiation Biology: Surprised but Not Disappointed. *Radiation* 2022; 2: 124-129,
- Sun H, Tsai Y, Nowak I, Dertinger SD, Wu JH, Chen Y. Response kinetics of radiation-induced micronucleated reticulocytes in human bone marrow culture. *Mutat Res* 2011; 718: 38-43, doi:10.1016/j.mrgentox.2010.10.007
- Sun Y-M, Chen Y-Q. Principles and innovative technologies for decrypting noncoding RNAs: from discovery and functional prediction to clinical application. *Journal of Hematology & Oncology* 2020; 13: 109, doi:10.1186/s13045-020-00945-8
- Sunirmal P, Lubomir BS, Carl DE, Sally AA. Radiation Dose-Rate Effects on Gene Expression in a Mouse Biodosimetry Model. *Radiation Research* 2015; 184: 24-32, doi:10.1667/RR14044.1
- Suzuki K, Imaoka T, Tomita M, Sasatani M, Doi K, Tanaka S, et al. Molecular and cellular basis of the dose-rate-dependent adverse effects of radiation exposure in animal models. Part I: Mammary gland and digestive tract. *Journal of Radiation Research* 2023a; 64: 210-227, doi:10.1093/jrr/rrad002
- Suzuki K, Imaoka T, Tomita M, Sasatani M, Doi K, Tanaka S, et al. Molecular and cellular basis of the dose-rate-dependent adverse effects of radiation exposure in animal models. Part II: Hematopoietic system, lung and liver. *Journal of Radiation Research* 2023b; 64: 228-249, doi:10.1093/jrr/rrad003
- Suzuki MM, Bird A. DNA methylation landscapes: provocative insights from epigenomics. *Nature Reviews Genetics* 2008; 9: 465-476, doi:10.1038/nrg2341

- Tanaka IB. EXPERIMENTAL STUDIES AT THE IES ON THE BIOLOGICAL EFFECTS OF CHRONIC LOW DOSE-RATE RADIATION EXPOSURE IN MICE. *Radiat Prot Dosimetry* 2022; 198: 985-989, doi:10.1093/rpd/ncac025
- Tanaka K, Satoh K, Kohda A. Dose and dose-rate response of lymphocyte chromosome aberrations in mice chronically irradiated within a low-dose-rate range after age adjustment. *Radiat Prot Dosimetry* 2014; 159: 38-45, doi:10.1093/rpd/ncu173
- Tang FR, Loganovsky K. Low dose or low dose rate ionizing radiation-induced health effect in the human. *J Environ Radioact* 2018; 192: 32-47, doi:10.1016/j.jenvrad.2018.05.018
- Tang FR, Loke WK, Khoo BC. Low-dose or low-dose-rate ionizing radiation-induced bioeffects in animal models. *J Radiat Res* 2017; 58: 165-182, doi:10.1093/jrr/rrw120
- Tawn EJ, Curwen GB, Rees GS, Jonas P. Germline minisatellite mutations in workers occupationally exposed to radiation at the Sellafield nuclear facility. *J Radiol Prot* 2015; 35: 21-36, doi:10.1088/0952-4746/35/1/21
- Tharmalingam S, Sreetharan S, Brooks AL, Boreham DR. Re-evaluation of the linear no-threshold (LNT) model using new paradigms and modern molecular studies. *Chemico-Biological Interactions* 2019; 301: 54-67, doi:10.1016/j.cbi.2018.11.013
- Thurman RE, Rynes E, Humbert R, Vierstra J, Maurano MT, Haugen E, et al. The accessible chromatin landscape of the human genome. *Nature* 2012; 489: 75-82, doi:10.1038/nature11232
- Torous DK, Dertinger SD, Hall NE, Tometsko CR. Enumeration of micronucleated reticulocytes in rat peripheral blood: a flow cytometric study. *Mutat Res* 2000; 465: 91-9, doi:10.1016/s1383-5718(99)00216-8
- Torous DK, Hall NE, Murante FG, Gleason SE, Tometsko CR, Dertinger SD. Comparative scoring of micronucleated reticulocytes in rat peripheral blood by flow cytometry and microscopy. *Toxicol Sci* 2003; 74: 309-14, doi:10.1093/toxsci/kfg143
- Tran V, Little MP. Dose and dose rate extrapolation factors for malignant and non-malignant health endpoints after exposure to gamma and neutron radiation. *Radiat Environ Biophys* 2017; 56: 299-328, doi:10.1007/s00411-017-0707-4
- Tsompana M, Buck MJ. Chromatin accessibility: a window into the genome. *Epigenetics & Chromatin* 2014; 7: 33, doi:10.1186/1756-8935-7-33
- Turner HC, Shuryak I, Taveras M, Bertucci A, Perrier JR, Chen C, et al. Effect of Dose Rate on Residual gamma-H2AX Levels and Frequency of Micronuclei in X-Irradiated Mouse Lymphocytes. *Radiat Res* 2015; 183: 315-24, doi:10.1667/rr13860.1

- Uehara Y, Ito Y, Taki K, Neno M, Ichinohe K, Nakamura S, et al. Gene expression profiles in mouse liver after long-term low-dose-rate irradiation with gamma rays. *Radiat Res* 2010; 174: 611-7, doi:10.1667/rr2195.1
- UNSCEAR. Report to the General Assembly with Scientific Annexes (1986): Genetic and somatic effects of ionizing radiation. United Nations, New York, 1986,
- UNSCEAR. UNSCEAR 2000 Report Volume II: "Effects of ionizing radiation". Annex F: DNA repair and mutagenesis. In: 2 UR, editor, 2000,
- UNSCEAR. Hereditary effects of radiation. United Nations, New York, 2001,
- UNSCEAR. UNSCEAR 2006, "Effect of Ionizing Radiation" Volume I, Annex A "Epidemiological studies of radiation and cancer" 2006a,
- UNSCEAR. UNSCEAR 2006, "Effects of Ionizing radiation" Volume II, Annex C "Non-targeted and delayed effects of exposure to ionizing radiation" UN, New York, 2006b,
- UNSCEAR. UNSCEAR 2008 Report Volume I: "Sources and effects of ionizing radiation", Annex A: Medical radiation exposures, 2008a,
- UNSCEAR. UNSCEAR 2008 Report Volume I: "Sources and effects of ionizing radiation", Annex B: Exposures of the public and workers from various sources of radiation, 2008b,
- UNSCEAR. Report of the United Nations Scientific Committee on the Effects of Atomic Radiation 2010; Summary of low-dose radiation effects on health. United Nations, United Nations publications, 2010, pp. 106
- UNSCEAR. RADIATION: EFFECTS AND SOURCES: UNEP, 2016.
- UNSCEAR. UNSCEAR 2020/2021 Report Volume III scientific annex C: Biological mechanisms relevant for the inference of cancer risks from low-dose and low-dose-rate radiation, 2022,
- Vaiserman AM. Hormesis and epigenetics: is there a link? *Ageing Res Rev* 2011; 10: 413-21, doi:10.1016/j.arr.2011.01.004
- Vaiserman AM, Koliada AK, Jirtle RL. Non-genomic transmission of longevity between generations: potential mechanisms and evidence across species. *Epigenetics Chromatin* 2017; 10: 38, doi:10.1186/s13072-017-0145-1
- van der Meer Y, Huiskamp R, Davids JA, van der Tweel I, de Rooij DG. The sensitivity of quiescent and proliferating mouse spermatogonial stem cells to X irradiation. *Radiat Res* 1992a; 130: 289-95,
- van der Meer Y, Huiskamp R, Davids JA, van der Tweel I, de Rooij DG. The sensitivity to X rays of mouse spermatogonia that are committed to differentiate and of differentiating spermatogonia. *Radiat Res* 1992b; 130: 296-302,

- Venter JC, Adams MD, Myers EW, Li PW, Mural RJ, Sutton GG, et al. The sequence of the human genome. *Science* 2001; 291: 1304-51, doi:10.1126/science.1058040
- Vieira Dias J, Gloaguen C, Kereselidze D, Manens L, Tack K, Ebrahimian TG. Gamma Low-Dose-Rate Ionizing Radiation Stimulates Adaptive Functional and Molecular Response in Human Aortic Endothelial Cells in a Threshold-, Dose-, and Dose Rate-Dependent Manner. *Dose Response* 2018; 16: 1559325818755238, doi:10.1177/1559325818755238
- Walker VR, Boyles AL, Pelch KE, Holmgren SD, Shapiro AJ, Blystone CR, et al. Human and animal evidence of potential transgenerational inheritance of health effects: An evidence map and state-of-the-science evaluation. *Environ Int* 2018; 115: 48-69, doi:10.1016/j.envint.2017.12.032
- Wang Z, Gerstein M, Snyder M. RNA-Seq: a revolutionary tool for transcriptomics. *Nature Reviews Genetics* 2009; 10: 57-63, doi:10.1038/nrg2484
- Ward JF. The complexity of DNA damage: relevance to biological consequences. *Int J Radiat Biol* 1994; 66: 427-32, doi:10.1080/09553009414551401
- Waterston RH, Lindblad-Toh K, Birney E, Rogers J, Abril JF, Agarwal P, et al. Initial sequencing and comparative analysis of the mouse genome. *Nature* 2002; 420: 520-62, doi:10.1038/nature01262
- Weinberg HS, Korol AB, Kirzhner VM, Avivi A, Fahima T, Nevo E, et al. Very high mutation rate in offspring of Chernobyl accident liquidators. *Proc Biol Sci* 2001; 268: 1001-5, doi:10.1098/rspb.2001.1650
- WHO. Health Effects of the Chernobyl Accidents and Special Health Care Programmes; Report of the UN Chernobyl Forum Expert Group "Health", WHO Press, 2006, pp. 182,
- WHO. Health risk assessment from the nuclear accident after the 2011 Great East Japan earthquake and tsunami, based on a preliminary dose estimation, 2013, pp. 172,
- Williams JP, Brown SL, Georges GE, Hauer-Jensen M, Hill RP, Huser AK, et al. Animal models for medical countermeasures to radiation exposure. *Radiat Res* 2010; 173: 557-78, doi:10.1667/rr1880.1
- Wong ML, Medrano JF. Real-time PCR for mRNA quantitation. *BioTechniques* 2005; 39: 75-85, doi:10.2144/05391rv01
- Xie Z, Bailey A, Kuleshov MV, Clarke DJB, Evangelista JE, Jenkins SL, et al. Gene Set Knowledge Discovery with Enrichr. *Curr Protoc* 2021; 1: e90, doi:10.1002/cpz1.90
- Yahyapour R, Amini P, Rezapour S, Cheki M, Rezaeyan A, Farhood B, et al. Radiation-induced inflammation and autoimmune diseases. *Military Medical Research* 2018; 5: 9, doi:10.1186/s40779-018-0156-7

- Yeager M, Machiela MJ, Kothiyal P, Dean M, Bodelon C, Suman S, et al. Lack of transgenerational effects of ionizing radiation exposure from the Chernobyl accident. *Science* 2021; 372: 725-729, doi:10.1126/science.abg2365
- Yue F, Cheng Y, Breschi A, Vierstra J, Wu W, Ryba T, et al. A comparative encyclopedia of DNA elements in the mouse genome. *Nature* 2014; 515: 355-64, doi:10.1038/nature13992

8 Papers

- I Perturbed transcriptional profiles after chronic low dose rate radiation in mice**

- II Dose rate dependent reduction in chromatin accessibility at transcriptional start sites long time after exposure to gamma radiation**

- III Genomic instability in F₂ male progeny from low dose rate gamma irradiated F₀ mice**

Paper I

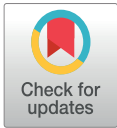
RESEARCH ARTICLE

Perturbed transcriptional profiles after chronic low dose rate radiation in mice

Hildegunn Dahl^{1,2*}, Dag M. Eide^{1,2}, Torstein Tengs^{1,2}, Nur Duale^{1,2}, Jorke H. Kamstra^{2,3}, Deborah H. Oughton², Ann-Karin Olsen^{1,2}

1 Department of Infection Control and Environmental Health, Norwegian Institute of Public Health, Oslo, Norway, **2** Centre for Environmental Radiation (CERAD), Norwegian University of Life Sciences (NMBU), Ås, Norway, **3** Faculty of Veterinary Medicine, Department of Population Health Sciences, Institute for Risk Assessment Sciences, Utrecht University, Utrecht, The Netherlands

* hildegunn.dahl@fhi.no



OPEN ACCESS

Citation: Dahl H, Eide DM, Tengs T, Duale N, Kamstra JH, Oughton DH, et al. (2021) Perturbed transcriptional profiles after chronic low dose rate radiation in mice. PLoS ONE 16(8): e0256667. <https://doi.org/10.1371/journal.pone.0256667>

Editor: Tim A. Mousseau, University of South Carolina, UNITED STATES

Received: May 27, 2021

Accepted: August 11, 2021

Published: August 24, 2021

Peer Review History: PLOS recognizes the benefits of transparency in the peer review process; therefore, we enable the publication of all of the content of peer review and author responses alongside final, published articles. The editorial history of this article is available here: <https://doi.org/10.1371/journal.pone.0256667>

Copyright: © 2021 Dahl et al. This is an open access article distributed under the terms of the [Creative Commons Attribution License](https://creativecommons.org/licenses/by/4.0/), which permits unrestricted use, distribution, and reproduction in any medium, provided the original author and source are credited.

Data Availability Statement: The raw counts underlying the results presented in the study are available from the NCBI Sequence Read Archive (SRA) (<https://www.ncbi.nlm.nih.gov/sra>) (accession no. PRJNA747753).

Abstract

Adverse health outcomes of ionizing radiation given chronically at low dose rates are highly debated, a controversy also relevant for other stressors. Increased knowledge is needed for a more comprehensive understanding of the damaging potential of ionizing radiation from all dose rates and doses. There is a lack of relevant low dose rate data that is partly ascribed to the rarity of exposure facilities allowing chronic low dose rate exposures. Using the FIG-ARO facility, we assessed early (one day post-radiation) and late (recovery time of 100–200 days) hepatic genome-wide transcriptional profiles in male mice of two strains (CBA/CaO-laHsd and C57BL/6NHsd) exposed chronically to a low dose rate (2.5 mGy/h; 1200h, LDR), a mid-dose rate (10 mGy/h; 300h, MDR) and acutely to a high dose rate (100 mGy/h; 30h, HDR) of gamma irradiation, given to an equivalent total dose of 3 Gy. Dose-rate and strain-specific transcriptional responses were identified. Differently modulated transcriptional responses across all dose rate exposure groups were evident by the representation of functional biological pathways. Evidence of changed epigenetic regulation (global DNA methylation) was not detected. A period of recovery markedly reduced the number of differentially expressed genes. Using enrichment analysis to identify the functional significance of the modulated genes, perturbed signaling pathways associated with both cancer and non-cancer effects were observed, such as lipid metabolism and inflammation. These pathways were seen after chronic low dose rate and were not restricted to the acute high dose rate exposure. The transcriptional response induced by chronic low dose rate ionizing radiation suggests contribution to conditions such as cardiovascular diseases. We contribute with novel genome wide transcriptional data highlighting dose-rate-specific radiation responses and emphasize the importance of considering both dose rate, duration of exposure, and variability in susceptibility when assessing risks from ionizing radiation.

Introduction

Ionizing radiation (IR), both natural (i.e., radon, cosmic, soil, and food) and human-made (i.e., medical, nuclear industry, and power plant accidents), are recognized as hazardous for

Funding: DO received fundings from the Research Council of Norway through its Centres of Excellence funding scheme, project number 223268/F50 CERAD. AKO received fundings from CERAD. AKO had a role in study design, decision to publish, and preparation of the manuscript. DO had a role in the preparation of the manuscript. <https://www.forskningssradet.no/en/>. <https://www.nmbu.no/en/services/centers/cerad> The funders had no role in study design, data collection, and analysis, decision to publish, or preparation of the manuscript.

Competing interests: The authors have declared that no competing interests exist.

human health and the environment [1]. Some of the most important studies, building the basis for the biological understanding of radiation-induced health effects, involve high doses and high dose rates with a short duration of exposure. These studies include the long-term follow-up of the atomic (A)-bomb survivors (Life Span Study; LSS) [2–4]. The LSS is recognized as a reliable source of epidemiological data due to cohort size, exposures of both genders at all ages, and a wide spectrum of individually assessed doses, although given over a short time and at high dose rates.

The epidemiological evidence for increased cancer risks with radiation dose from studies of the A-bomb survivors [5–7] largely supported the Linear No-Threshold (LNT) risk assessment model [4]. This model assumes that cancer risks after low doses of ionizing radiation (<100 mGy) can be extrapolated linearly from acute high dose data as a no-threshold exponent. The use of this model in the low dose area is highly debated [8,9]. Accumulating evidence indicates that disease progression following low total dose or low dose rates (<6 mGyh⁻¹) [10–14] may be different from high dose and high dose rate exposures.

Besides cancer, high levels of radiation exposure also lead to a range of non-cancer effects [15–17], like circulatory (cardiovascular and stroke) [18,19] and metabolic diseases. Concerning the liver, observations of the Hiroshima and Nagasaki A-bomb survivors showed increased incidences of both cancer and fatty livers [7,20]. Increased incidences of non-cancer effects are also identified after low levels of radiation [21–23]. Several of these effects emerge late after exposure, but inconsistencies and confounding factors make associations difficult [15].

A dose of radiation given over a short period is more effective in producing certain kinds of biological damage, such as double-strand breaks (DSB) than when the same dose is delivered over a more extended period [24–27]. Radiation brings about cellular damage directly, indirectly, and non-targeted [28,29]. The *direct* hit of the radioactive photon can lead to a broad spectrum of damage and alterations to both DNA and other cellular molecules. *Indirect effects* arise from hydrolysis, generating highly reactive oxygen species (ROS) capable of reacting with every molecule in the cell. ROS is a well-known radiation-induced mechanism of toxicity. If the antioxidant capacity is overwhelmed, cellular oxidative stress may result in oxidation of cellular components, initiating response cascades to restore cellular integrity. *Non-targeted effects* are seen in cells not directly exposed to the radiation and are characterized as genomic instability and bystander effects [30]. It is suggested that indirect and non-targeted effects may play a more critical role after exposure to low total doses and low dose rates [31] and that the cellular implications from the direct effects might be negligible. However, the significance of disease manifestation from radiation-induced indirect and non-targeted effects is still debated.

Radiation exposure activates and inhibits numerous transcriptional pathways in response to different exposure regimes (low or high dose; acute, chronic, or protracted exposure). Knowledge regarding the molecular events mediating responses is critical to understand radiation toxicity. There is great emphasis on genetic mutations and chromosomal aberrations following radiation-induced DNA damage as the main mechanism contributing to increased cancer incidence and genetic instability. However, modulators may exist that could change the levels of disease risk [32]. DNA methylation has been proposed as a modulator, affecting gene transcription via silencing gene expression directly. Evidence indicates that these mechanisms are widely involved in ionizing radiation response [33]. Various exposure regimes are shown to induce different patterns of gene expression after high and low dose and dose rates [34]. A comprehensive understanding of these radiation-induced molecular events is essential as the transcriptional response may play a role in health outcomes [32] and could act as biomarkers of exposure and response [35].

We expect hepatic signaling pathways to be modulated by high dose rate ionizing radiation at the transcriptional level and that this could be identified through genome-wide

transcriptional profiling. We hypothesize that the transcriptional profile is modulated differently after chronic low dose rate ionizing radiation when given the same total dose as the high dose rate, thus impacting other biological signaling pathways. Our study is designed to address this hypothesis by a) investigating the hepatic transcriptional response following whole-body exposure to low and high dose rate γ -irradiation given to the same high total dose (3 Gy), b) identifying dose rate-specific perturbed functional pathways, c) detecting strain-specific dose and dose rate radiation responses; and d) evaluating the impact of dose rate on the DNA methylation status.

Materials and methods

Animals and housing

Specific Pathogen Free CBA/CaOlaHsd and C57BL/6NHsd male mice (called CBA and B6 throughout the article), purchased from Envigo (Horst, The Netherlands), were used (3–8 weeks old at arrival). The mice were acclimatized for a minimum of four days after delivery and randomly housed in groups of five. Mice from each line were mixed in the cages (2–3 per mouse strain). They were housed in individually ventilated disposable PET plastic cages (IVC racks) (Innovive, San Diego, USA) under controlled temperature and light conditions ($21 \pm 2^\circ\text{C}$, $45 \pm 15\%$ relative humidity, 50 air changes h^{-1} and 12h light phase) with *ad libitum* access to tap water in PET bottles and SDS RM1 feed (Special Diet Services, Essex, UK). Due to space limitations in the radiation field, the mid dose rate (MDR) groups were housed in disposable PET cages like the other groups but using transport lids outside the IVC rack during the radiation exposure. Aspen tree bedding (Nestpack, Datesand Ltd., Manchester, UK) was used in all cages. At termination, the mice were administered anesthesia using ZRF-cocktail (Zolazepam, Tiletamine, Xylazine, and Fentanyl) followed by heart puncture and collection of blood (EDTA coated S-Monovette[®], Sarstedt, Germany) before cervical dislocation and collection of tissues. The tissues were snap-frozen in liquid nitrogen and stored at -80°C until use. Care of animals and experimental protocols were in adherence to the national legislation for animal experimentation and approved by the Norwegian Food Safety Authority (NFSA, Approval no. 8803). No mice died or showed clinical signs due to the exposure.

Experimental design

The chronic gamma radiation exposure was performed at the FIGARO low dose gamma irradiation facility (Norwegian University of Life Sciences, Ås, Norway) managed by the CoE Centre of Environmental Radioactivity (CERAD CoE). The mice were moved and acclimatized at the radiation facility before radiation started. This study includes two segments to obtain specific information regarding early (one day post-radiation) and late effects (>100 days post-radiation) of ionizing radiation given by different dose rates (Fig 1).

A total of 70 mice (35 CBA and 35 B6 mice) were used for the experimental setup. Groups of five mice (8–9 weeks at radiation start) were divided into 14 experimental study groups; control (early and late); low dose rate (LDR) (early and late); mid dose rate (MDR) (early), and high dose rate (HDR) (early and late). Each experimental exposure group included five mice. The same day as radiation ended, the mice were transported to the Norwegian Institute of Public Health (NIPH, Oslo, Norway) to terminate the early effect groups, housing of the recovery groups, and breeding inter- and trans-generational study groups. The early effect mice were terminated (age: 9–16 weeks, Fig 2) the day after irradiation ended (19–26 hours). The late effects mice were terminated 106–221 days post-radiation (106–221 days for B6 and 108–178 days for CBA; age range at termination 17–41 weeks). Age range and termination time-points is reflected by the breeding regimes.

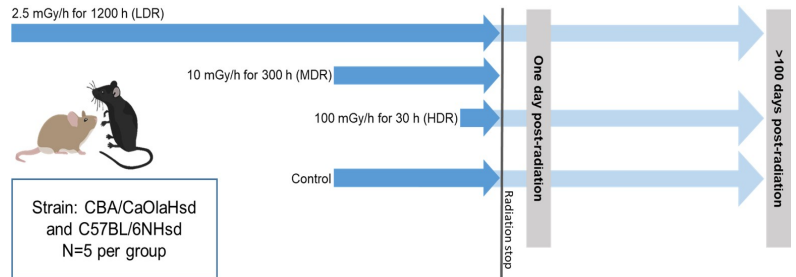


Fig 1. Schematic overview of the experimental study design. The study includes studying the effects of γ -radiation (^{60}Co) at two time points after exposure: One day post-radiation and >100 days post-radiation (Late effect). Gamma radiation was given at three different dose rates (DR): Low (LDR 2.5 mGy/h), Mid (MDR 10 mGy/h), and High (HDR 100 mGy/h). All dose rate groups received a cumulative dose of 3 Gy; exposure duration for each exposure group in hours is stated in the figure. One day post-radiation, all three dose rate groups were profiled. For the Late effects, only LDR and HDR were included. The figure is modified from previously published material [36].

<https://doi.org/10.1371/journal.pone.0256667.g001>

Radiation and dosimetry

All exposure groups received a pre-calculated total dose of 3 Gy gamma radiation (^{60}Co -source), given at different dose rates; 2.5 (LDR), 10 (MDR), and 100 (HDR) mGy/h. The pre-calculated exposure duration was 1200, 300, and 30 h, respectively. The dosimetry was performed using nanoDots [25,37]. The numeric value of air kerma to whole-body absorbed dose conversion coefficient for chronic exposures was 0.932 ± 0.008 , resulting in a total whole-body absorbed dose of 2.60 ± 0.19 Gy for the 2.5 mGy/h-group, 2.67 ± 0.16 Gy for the 10 mGy/h-group and 2.65 ± 0.13 for the 100 mGy/h-group, all denoted as 3 Gy throughout the article. Irradiation was interrupted daily for 30–120 min for animal care. The beam-on time was adjusted correspondingly to achieve the pre-calculated exposure duration and hence total dose of 3 Gy. All cages were rotated daily to assure uniform exposure. Unexposed control mice were housed behind lead shielding outside the radiation field but within the exposure room.

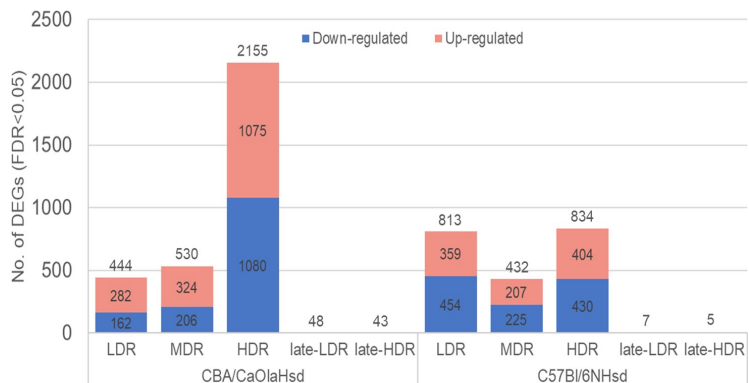


Fig 2. Numbers of differentially expressed genes. Total numbers of statistically significant ($FDR < 0.05$) differentially expressed genes (DEGs) one day post-radiation (LDR, MDR, and HDR) and following recovery of >100 days post-radiation (late-LDR and late-HDR). The stacked bar plot indicates the numbers of significant DEGs (compared to control) for each dose rate and mouse strain (total number DEGs are seen over the bar; upper section (red): Number of up-regulated DEGs; lower section (blue): Numbers of down-regulated DEGs). For late-LDR and late-HDR, only total numbers of DEGs are given.

<https://doi.org/10.1371/journal.pone.0256667.g002>

Global DNA methylation

DNA was isolated from CBA liver using the QIAamp DNA Mini kit (Cat.no. 51304). Integrity and concentrations were assessed in 2–4 technical parallels. Global levels of 5-methylcytosine (5mC) and 5-hydroxymethylcytosine (5hmC) were quantified using liquid chromatography-mass spectrometry/mass spectrometry (LC-MS/MS) as described in detail [38].

In brief, DNA is enzymatically digested to nucleosides, after which a mixture of internal standards was added. Pilot experiments were performed to establish a suitable mouse liver standard curve range at 0–5% for 5mC and 0–0.08% for 5hmC, all relative to guanine (G). A volume of 5 μ L was injected on an Agilent 1200 μ HPLC coupled with a triple quadrupole (QQQ) MS (6490, Agilent). The conditions for the LC/MS-MS analysis, calculation of sample concentrations, and quality control were as described [38]. A quality control sample composed of pooled DNA from human peripheral blood was included in every run to ensure that inter-run accuracy was within acceptable limits. 5mC and 5hmC are given as % of total cytosine (C) (represented by levels of the complementary G), and ratio 5mC:5hmC was calculated.

RNA isolation

Total RNA was isolated from liver tissue using the miRNeasy mini kit (Qiagen, Hilden, Germany, cat. #217004) according to the manufacturer's instructions. Lysis buffer was added to the frozen liver tissue and homogenized as previously described [36].

RNA quality and quantity were assessed using Agilent 2100 Bioanalyzer (Agilent Technologies, Santa Clara, California, USA), Qubit 2.0 with RNA-BR (Broad range) assay kit (Thermo Fisher Scientific, Massachusetts, USA), and a NanoDrop Spectrophotometer (Thermo Fisher Scientific, Massachusetts, USA).

RNA sequencing

Library preparations (TruSeq Stranded mRNA kit (v2, Illumina) (insert length 250~300)) and paired-end sequencing (2 X 150 bp) were performed by Novogen Co., Ltd (Cambridge, UK). The early and late samples were sequenced in two separated laboratory setups.

Quantitative real-time PCR

Quantitative real-time PCR (qPCR) was used to validate some selected statistically significantly differential expressed genes (DEGs) identified by RNA-Seq analysis, i.e., 29 genes (18 target genes (listed in S2 Fig) and 11 reference genes (*Araf*, *Cfl2*, *Coa5*, *Gapdh*, *Hprt*, *Mapk1*, *Pgk1*, *Rpl13a*, *Tbp*, *Vps54* and *Ywhaz*)). The reverse transcription reaction and qPCR analyses were carried out as previously described [39–41]. In brief, total RNA (1.0 μ g) from each sample was reverse transcribed to cDNA using the High Capacity cDNA Reverse Transcription Kit (Thermo Fisher Scientific, Massachusetts, USA) according to the manufacturer's protocol. The resulting reverse transcription reaction product was stored at -20°C for further analysis.

Gene specific qPCR analysis was carried out in 384-well plates using QuantiTect SYBR Green PCR kit (Qiagen, Hilden, Germany) according to the manufacturer's protocol, on a CFX384 Touch Real-Time PCR Detection System (Bio-Rad, Hercules, California, USA). cDNA (1:40 dilution) from each sample was run for each gene. All samples were analyzed on the same 384-plate to reduce run-by-run variations. A melting curve analysis and non-template controls (NTC) were included in each run. The quantification cycle (Cq) values were recorded with CFX Manager™ Software (Bio-Rad, Hercules, California, USA). One target gene was excluded from downstream analysis due to primer mismatch. The raw Cq values were analyzed by the comparative Cq-method [42,43] as previously described [39,40]. Target genes

were normalized by the average of eleven reference genes by calculating ΔCq ; where ΔCq (sample) = Cq (target gene) – Cq (mean of reference genes). The eleven reference genes were selected from RNAseq data based on their stability in both control and irradiated groups (CV % < 3%).

Bioinformatic pipeline and functional gene enrichment

Raw reads (fastq files) were trimmed and filtered using Trimmomatic (version 0.39) using recommended settings (<http://www.usadellab.org/cms/?page=trimmomatic>). Trimmed reads were mapped to the mouse genome (version GRCm38; NCBI annotation) using HISAT2 (version 2.2.0.) [44] with default settings. Counting of mapped reads was done using the HTSeq-count program [45] (HTSeq package version 0.11.1.). Approximately 84×10^6 reads were generated per library, and the average mapping rate was >95%. The counting of mapped reads with acceptable coverage generated more than 12,000 genes per sample. Raw count files have been made available via the NCBI Sequence Read Archive (SRA) (Accession: PRJNA747753).

Statistical analysis

Differentially expressed genes (DEGs) were identified using the R (v. 4.0.1) wrapper SARTools [46] (v. 1.7.3) and EdgeR [47,48] (v. 3.86.1.) with default parameters (TMM normalization, cpm cutoff = 1). The false discovery rate (FDR) was set to 0.05 to identify the significant DEGs compared to controls. The log₂-ratio (log₂-FoldChange) was used to evaluate the level and direction of the expression.

Statistically significant DEGs, regardless of the log₂-ratio, were compared to KEGG [49] and Gene Ontology (GO) [50,51] Biological gene sets implementing over-representations analysis (ORA) through EnrichR [52,53]. 8918 genes are members of a KEGG gene set, while 11 290 genes are annotated in GO Biological Terms gene sets (2021-04-26). DEGs common for all dose rates groups within strain was evaluated in EnrichR against the database “Transcription Factor (TF) perturbation followed by expression”, experiments mined from the Gene Expression Omnibus [54,55].

The differential gene expression was compared between strains at each dose rate by Pearson's correlation and linear regression using CBA log₂-ratios on B6 log₂-ratios. Linear regression (F-test) were used to validate qPCR ΔCq -values and RNASeq log₂-ratios. Global methylation data were analyzed by one-way ANOVA using dose rate as independent variable and the Dunnett's t-test as post hoc analysis. All statistical analysis has been performed using JMP Pro 15.2.0 (SAS Institute, NC, USA), and additional graphical illustrations were made using Office 360 and the R package *ggplot2* (<https://ggplot2.tidyverse.org/>).

Results

Overall, we identified statistically significant changed hepatic transcriptional profiles, in both CBA and B6, for both the low (2.5 mGy/h), medium (10 mGy/h), and high (100 mGy/h) dose rate exposure groups one day post-radiation, when radiation was given to a similar total dose of 3 Gy. These observed transcriptional modulations included two main findings; I) dose rate specific response, seen by a) different numbers of DEGs, b) low overlap of DEGs, and c) difference in representation of the functional pathways, and II) strain-specific response, identified by differently modulated transcriptional response across dose rates. Evidence of changed epigenetic regulation, assessed by global DNA methylation, was not seen. After a recovery period of >100 days, the number of differentially expressed genes between treatment groups and controls was markedly lower.

Differentially expressed genes in CBA and B6 one day post-radiation

Exposure to chronic LDR induced statistically significant DEGs in both CBA and B6 (Figs 2 and 3). Comparing the numbers of significant DEGs for each dose rate, CBA showed a more pronounced increase in the numbers of DEGs, than B6 which showed comparable numbers of DEGs at LDR and HDR. Regardless of dose rate, CBA expressed 2608 significant DEGs in total compared to control one day after gamma radiation, whereas B6 expressed a total of 1449 significant DEGs. All identified statistically significant DEGs is presented in [S1 Table](#).

The identified DEGs were correlated with previously identified and published miRNAs-markers [36] identified as possible predictors of exposure to γ -radiation. These miRNAs were identified from the same livers as used in this experiment. The correlation analysis was performed using Ingenuity Pathway Analysis (IPA) (Qiagen, Hilden, Germany - www.digitalinsights.qiagen.com), and is presented in [S1 Fig](#). We observed some inverses correlation between six of the predicted miRNAs and a few of the genes in our DEGs list.

From the qPCR validation analysis of the selected DEGs, we observed a good correlation between the Δ Cq-values and the RNA-Seq normalized counts ($R^2 = 0.806$, p-value < 0.001) ([S2 Fig](#)).

Evaluating the overlapping DEGs across dose rate ([Fig 4](#)); CBA LDR and MDR shared 22%, MDR and HDR 11%, and LDR and HDR 7% of the DEGs. Comparing all three CBA dose rate groups, only 3% mutual DEGs were observed ([Fig 4A](#)). B6 showed an overall higher degree of common DEGs across dose rates, with 31% for LDR and MDR, 23% for MDR and HDR, and 21% for LDR and HDR. There were 9% mutual DEGs when all three B6 dose rate groups were compared ([Fig 4B](#)).

Comparing the statistically significant DEGs for each dose rate group across strain ([Fig 5](#)), we observed the following degree of mutual DEGs; LDR_{CBA}LDR_{B6}: 9%, MDR_{CBA}MDR_{B6}: 12%, HDR_{CBA}HDR_{B6}: 8%. Overall, 24 DEGs overlapped across all exposure groups ([Fig 5](#)). Out of these, 19 DEGs were inversely expressed in the two strains, i.e., upregulated in the CBA strain and downregulated in the B6 strain. The 24 common DEGs were evaluated using the database "Transcription factor perturbation followed by gene expression". The over-representation analysis revealed DEGs with highly statistically significant enrichment to the transcription factors *Stat3* (6.882e-9) and *Myc* (1.197-8).

Evaluation of the strain-specific relationship for each dose rate showed a tendency for opposite expression levels in B6 compared to CBA for both LDR and MDR groups (β 's of -0.81 and -0.52, respectively). For HDR, no correlation (regression $\beta = 0$ and R-square = 0) was detected. This independence between DEG levels indicates a strong strain-specific response after the acute high dose rate exposure.

Functional enriched pathways

Biological significance related to the identified DEGs one day post-radiation was evaluated using the gene sets available in the KEGG database. The statistically significantly over-represented pathways (adj. p < 0.05) for each dose rate per strain is presented in [Fig 6](#). Of the identified DEGs, 10% (CBA) and 25% (B6) were annotated to a functional pathway. Even if CBA displayed a higher total number of statistically significant perturbed DEGs than B6, CBA displayed a lower number of statistically over-represented functional pathways compared to B6. For both strains, the number of DEGs associated with functional pathways for the different dose rates was in the order of HDR>LDR>MDR. Nine pathways were common for both strains regardless of dose rate, however not identified for the same dose rate groups across strain ([Fig 6](#), indicated in bold). Overall, functional, and biological significance seen by the identified perturbed pathways is related to cancer, lipid metabolism, and inflammation.

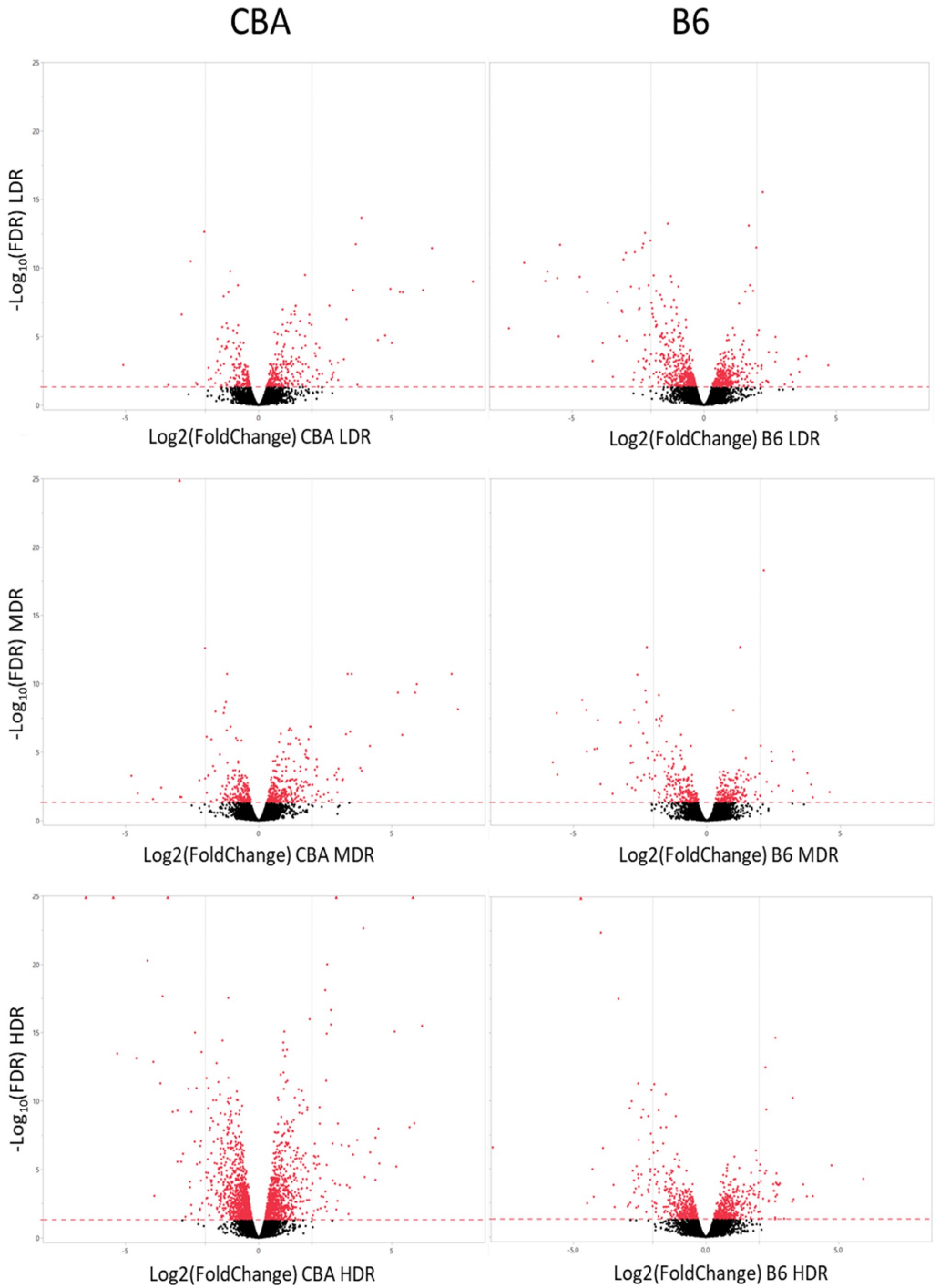


Fig 3. Volcano plots illustrating the radiation induced response on gene expression one day post-radiation in CBA and B6. The statistically significant threshold (FDR = 0.05) are shown by a read dashed line, and the statistically significant DEGs (FDR < 0.05) are shown in red. The vertical line represents log₂-ratio = 2, and dots left and right of this line have log₂-ratios > 2.

<https://doi.org/10.1371/journal.pone.0256667.g003>

CBA one day post-radiation. In CBA (Fig 6), five pathways were enriched for LDR, two for MDR, and fourteen for HDR. Three pathways were specific for LDR, whereas thirteen pathways were modulated only for HDR. The percentage of DEGs represented in a significant KEGG gene set for LDR, MDR and HDR were 9%, 5%, and 10%, respectively. The only pathway common for all dose rates was the “PPAR signaling pathway”. However, increasing the adjusted p-value to < 0.1, the “Biosynthesis of unsaturated fatty acid” appeared for all dose rates (MDR adj. p-value = 0.072 and HDR adj. p-value = 0.086). All DEGs mapping to “PPAR Signaling pathway” and “Biosynthesis of unsaturated fatty acid” were downregulated compared to the control.

For CBA LDR, the significant KEGG Gene Sets seen in Fig 6. indicated a response associated with the biosynthesis of fatty acids and the activation of complement. Due to multiple annotations across several biological processes, identical DEGs are seen for multiple KEGG Gene Sets; different DEGs of the Glutathione s-Transferase family overlap between “Drug metabolism” and “The metabolism of xenobiotics by cytochrome P450”. Most of the CBA LDR DEGs represented to a KEGG Gene Set shown in Fig 6. were suppressed compared to controls, except “Complement and coagulation cascade”, where all represented DEGs were upregulated. Using the GO terms for Biological Processes to generalize the functional representation of the DEGs (GO result output is presented in S2 Table), fatty acid biosynthetic process (GO:0006633), and regulation of complement activation (GO:0030449) confirm the findings in the KEGG database. Significant GO terms were also related to an acute inflammatory response (GO:0002673) and response to endoplasmic reticulum stress (GO:0034976).

A higher number of DEGs were significantly modulated in the CBA HDR exposure group and is reflected by a higher number of over-represented KEGG Gene Sets (Fig 6). Overall, the significantly perturbed functional pathways were mainly related to hepatic lipid metabolism as represented by several KEGG Gene Sets. Pathways associated with the regulation of cell survival and modulation of immune response were also perturbed; Ferroptosis (adj. p-value = 0.019), “p53 signaling pathway” (adj. p-value = 0.027), and “TNF Signaling Pathway”

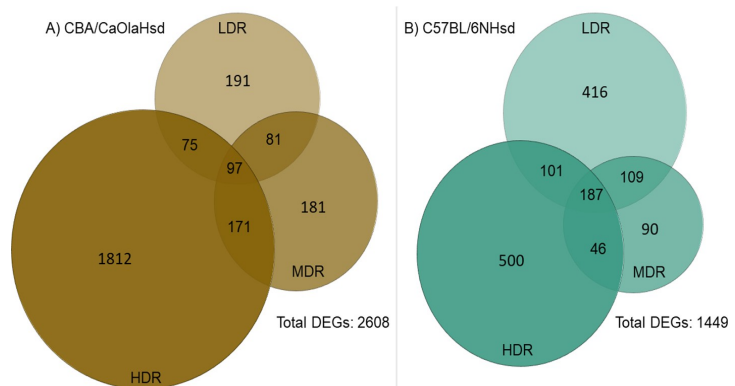


Fig 4. Venn diagrams of the differentially expressed genes. The Venn diagrams illustrate the numbers of statistically significant DEGs specific and overlapping across dose rate for the two strains: A) CBA/CaOlaHsd and B) C57BL/6NHsd.

<https://doi.org/10.1371/journal.pone.0256667.g004>

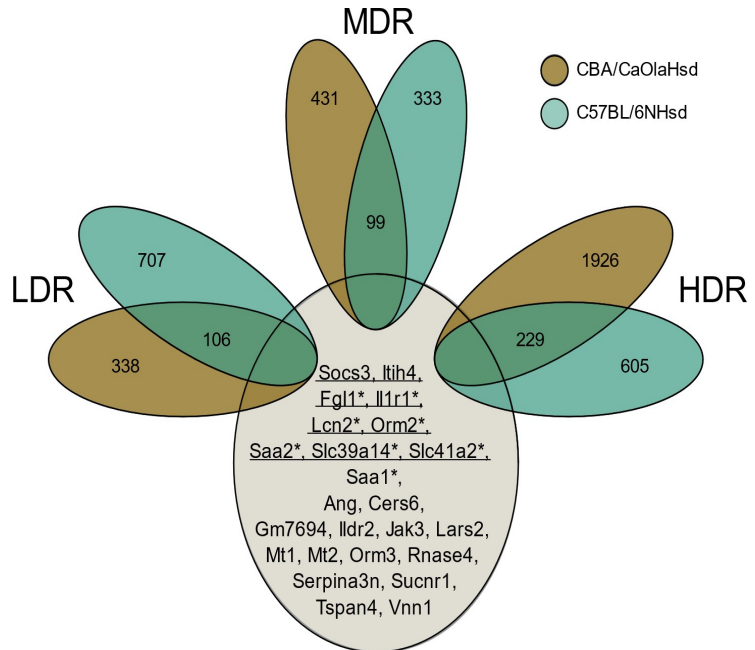


Fig 5. Venn diagram illustrating dose-rate-specific transcriptional features across strain. There were 24 DEGs common for all groups, indicated with gene names. Genes related to the transcription factor *Stat3* (eight genes) are underlined, and genes with a * are related to the transcription factor *Myc* (seven genes).

<https://doi.org/10.1371/journal.pone.0256667.g005>

(adj. p-value = 0.024). The KEGG Gene Set “Fluid shear stress and atherosclerosis” were also significantly (adj. p-value 0.020) perturbed. However, whether the pathways are generally activated or suppressed is not clear based on these molecular patterns. Common DEGs were linked to the cytokine-related pathways “Osteoclast differentiation”, “TNF signaling pathway”, and “Fluid shear stress and atherosclerosis”.

In B6 one day post-radiation. Overall, in B6, fifteen pathways were enriched for LDR, three for MDR and 36 for HDR (Fig 6). Six pathways were specific for LDR, whereas 25 pathways were specific for HDR. The percentage of DEGs represented by a significant KEGG gene set were 14% for LDR, 6% for MDR and 23% for HDR. The KEGG Gene Sets, “TNF Signaling Pathway” and “Complement and coagulation cascade”, was perturbed for all dose rates.

In LDR, the KEGG Gene Sets identified from modulated DEGs after LDR exposure show perturbation in biological processes related to inflammation and cellular lipid metabolism (Fig 6). Some of these pathways are significantly expressed only for B6 LDR; the related inflammatory gene sets: “Toll-like receptor signaling pathway”, “Hepatitis B and C” and “Chagas disease”, and the response of cellular lipids: “sphingolipid metabolism” and “linoleic acid metabolism”. The KEGG gene sets related to “Hepatitis B and C” and “Chagas disease” mainly consisted of DEGs also represented by the toll-like receptor signaling pathway. Represented DEGs in the gene set for “linoleic acid metabolism” overlap with the gene sets for “retinol metabolism” and “steroid hormone biosynthesis”, gene sets commonly represented for both LDR and HDR. Using GO terms for biological processes to generalize the functional representation of the DEGs, GO terms related to both an inflammatory response and response to lipids appeared significant (S2 Table). The GO terms also revealed statistically significant

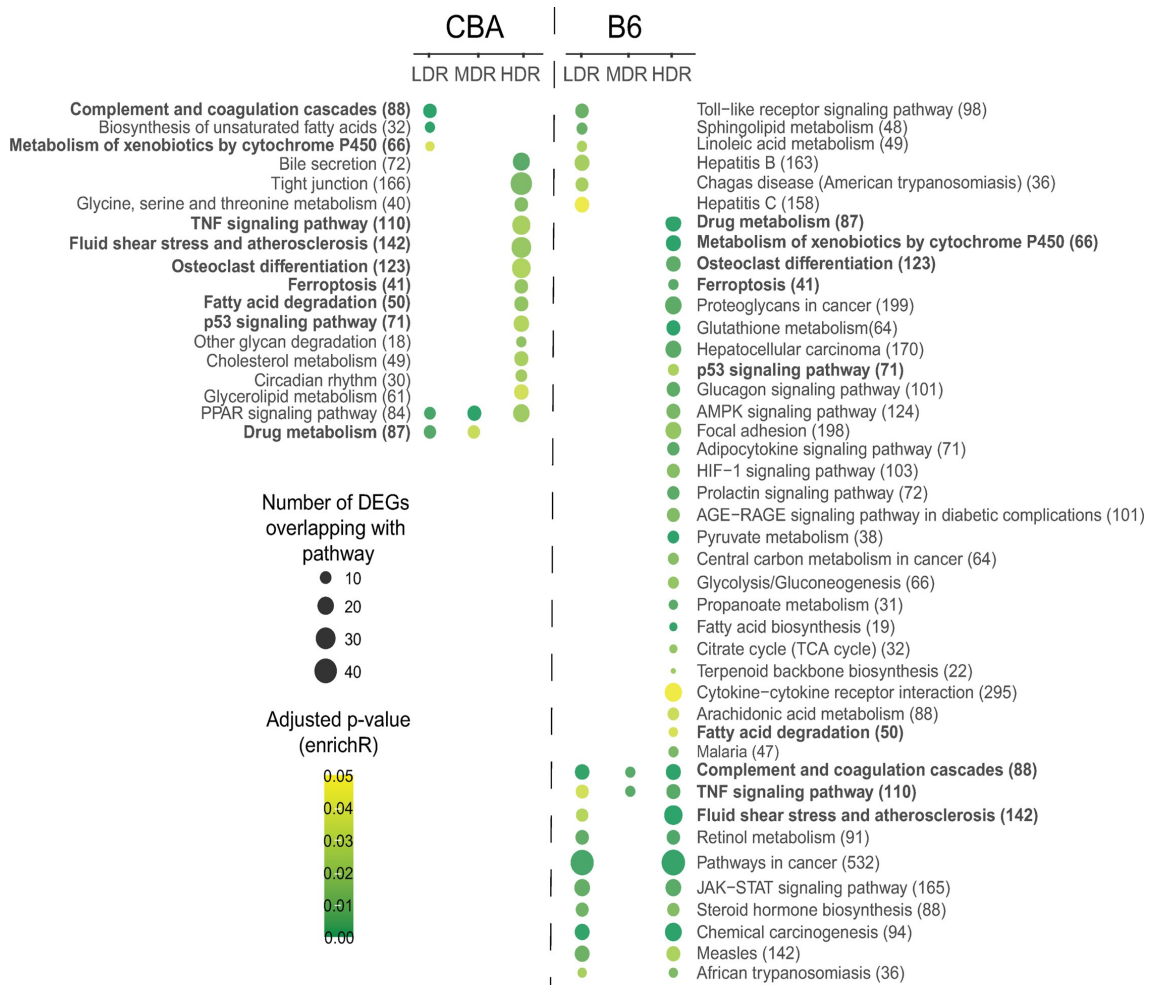


Fig 6. Functional pathway enrichment analysis visualized as a strain-specific dot-plot. The statistically significant (adj. p-value < 0.05) over-represented pathways for all exposure groups are shown. The pathways are sorted within strain by dose rate (LDR-MDR-HDR). Dot color indicates the level of significance, and dot size reflects the number of identified DEGs represented for the pathway. Pathways highlighted in bold are enriched in both strains. The total number of genes annotated to each KEGG gene set is shown in brackets.

<https://doi.org/10.1371/journal.pone.0256667.g006>

representation of DEGs to gene sets downregulating apoptotic signaling (“Negative regulation of extrinsic apoptotic signaling pathway via death domain receptors” (GO:1902042), adj. p-value = 0.4e-3). The DEGs enriched to the regulation of apoptotic signaling was also seen in pathways related to endothelial cells (“Negative regulation of endothelial cell apoptotic signaling pathway” (GO:2000352, adj. p-value = 0.009)).

For HDR, which expressed a comparable number of significant DEGs as LDR (Fig 2), showed a higher number of significant over-represented pathways than LDR. These KEGG gene sets represent signaling pathways relevant for several functional mechanisms, ranging from carcinogenesis, inflammation, lipid metabolism and energy production. Exploring the GO biological process terms, DEGs are represented in gene sets related to the regulation of

steroid biosynthetic processes (GO:0050810, adj. p-value = 3.12e-8), glutathione derivative biosynthetic processes (GO:1901687, adj. p-value = 3.8e-5), acute-phase inflammatory response (GO:0006953, adj. p-value = 7.0e-5) and several significant gene sets related to the regulation of apoptotic response.

B6 and CBA >100 days post-radiation. Transcriptional changes that persist after considerable time for recovery (100–200 days post-radiation) were analyzed in a separate sequencing run than one day post-radiation, only focusing on the LDR and HDR groups. The late response groups showed a considerably lower number of modulated genes compared to control groups, than the early response groups. CBA showed a higher number of DEGs for both LDR and HDR than B6 (Fig 2).

No significant over-representation of functional pathways was seen for the CBA LDR late DEGs. However, the KEGG pathway “Transcriptional misregulation in cancer” were represented with four genes mapping to the pathway (*Bcl6*, *Zbtb16*, *Aff1*, and *Dusp6*), but not significant (adj. p-value = 0.07036). For the CBA HDR late DEGs, no significant over-represented pathways nor identified GO terms were seen. Pathway enrichment was not conducted for the B6 late groups due to the low numbers of significantly modulated DEGs.

Oxidative stress

The KEGG database lacks a predefined pathway specific for genes related to oxidative stress (it only includes “oxidative phosphorylation” consisting of 134 genes). Due to this, and the fact that ionizing radiation is a potent inducer of ROS, we investigated how our significant DEGs overlapped with the Biological Process GO Term “Response to oxidative stress” (GO:0006979) consisting of 408 genes (Mouse Genome Informatics, www.informatics.jax.org, date:11.2.2021). The numbers and the overlapping DEGs are illustrated in Fig 7, and the identified oxidative stress-related genes are listed in the S1 Table.

In CBA, the number of significant DEGs increased with dose rate, and five genes overlapped for all dose rates. The LDR group displayed in total seven genes. Two of these genes were specific for the CBA LDR group, *Aldh3b1* (Aldehyde Dehydrogenase 3 Family Member

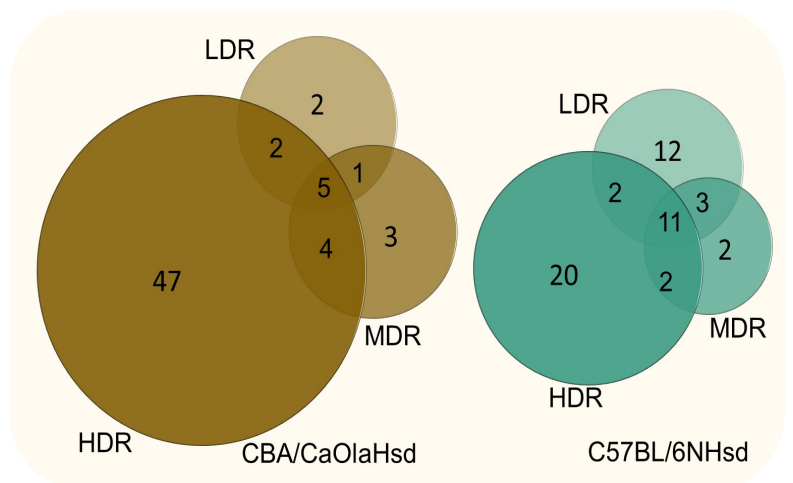


Fig 7. Oxidative stress related DEG. Numbers of DEGs overlapping with the GO Term “Response to Oxidative Stress” (GO:0006979 (408 annotated genes)) visualized with Venn diagrams for the two strains.

<https://doi.org/10.1371/journal.pone.0256667.g007>

B1, adj. p-value = 1.34E-02) and *Cflar* (Casp8 And FadD Like Apoptosis Regulator, adj. p-value = 1.60E-02), both upregulated. In B6, eleven genes were mutual for all dose rates, and twelve genes were specific for LDR.

Functional enrichment analysis (not performed for LDR due to low numbers of genes) of the identified CBA HDR DEGs (58 genes) revealed a highly statistically significant GO term “Response to hydrogen peroxide (GO:0042542)” (adj. p-value = 6.251e-10), a reactive oxygen species known to be induced by ionizing radiation. Among the KEGG Gene Sets “Apoptosis” (adj. p-value = 1.39e-5), “Fluid shear stress and atherosclerosis” (adj. p-value = 1.39e-5), “Ferropoptosis” (adj. p-value = 2.04e-4), “Mitophagy” (adj. p-value = 7.24e-4), and “Protein processing in ER” (adj. p-value = 0.0021) were significantly over-represented. In B6, exploring the specific oxidative stress related LDR DEGs (12 genes) in the KEGG database, several pathways were statistically enriched. The genes *Jun*, *Atf4*, and *Egfr* were annotated to several of these functional pathways. Evaluating all significant DEGs identified for B6 LDR (28 genes), “Apoptosis” is the most significantly enriched pathway (adj. p-value = 4.8e-6). Considering the oxidative stress-related HDR B6 DEGs (35 genes) with the KEGG database, “Fluid shear stress and atherosclerosis” (adj. p-value 1.614e-8), “Apoptosis” (adj. p-value = 1.09e-5) and “Pathways in cancer” (adj. p-value = 1.49e-4) were the three most significantly enriched pathways.

Across the two strains, two DEGs were shared: Vanin-1 (*Vnn1*) and Lipocalin-2 (*Lcn2*). *Vnn1* was suppressed for all exposure groups in both strains, whereas *Lcn2* was upregulated in CBA and downregulated in B6. However, *Lcn2* displayed a high individual variation in expression level.

Global DNA methylation

Gene expression is regulated by epigenetic mechanisms, hence we assessed global DNA methylation levels of both 5mC and 5hmC in CBA livers using HPLC-MS. The levels of 5mC and 5hmC did not change significantly due to the exposure to ionizing radiation at any dose rate level, however the 5mC:5hmC-ratio were borderline significant ($p = 0.043$) for the HDR exposure group using Dunnett’s test (Fig 8). However, applying Tukey’s test with multiple corrections, this significant level disappears.

Discussion

Insights into molecular events initiated by exposure to different dose rates can give valuable contributions to the ongoing debate regarding the relevance of the dose rate upon cellular responses and health outcomes of ionizing radiation [24,32,56]. Our study shows that hepatic transcriptional profiles are modulated **dose-rate-specific** in response to whole-body exposure to an equal total dose gamma irradiation, given at low, medium, and high dose rates, chronic to acute. The study also demonstrates that the transcriptional response is modulated differently for CBA and B6 mice, indicating **strain-specific** irradiation-induced responses.

The chronic low dose rate used in our study (2.5 mGy/h; ~60 mGy/day for 55 days (3 Gy)) initiated transcriptional events in both CBA and B6 livers. Our results for the LDR exposure group are in line with another study using chronic low dose rate exposure, reporting modulation to the B6 hepatic gene expression profile [57]. However, compared to our study, the dose rates were lower (20, 1.0, and 0.05 mGy/day), and the total doses were not directly comparable (8.0, 0.4, and 0.02 Gy). Collectively, the results demonstrate that ionizing radiation given at chronic low dose rates does initiate molecular events, suggesting that such exposures may impact response cascades important for radiation-induced biological outcomes.

The transcriptional profile, one day post-radiation, differed between the two mouse strains (Figs 2–5). Within CBA mice, the group exposed to low dose rate shared only 7% of the DEGs

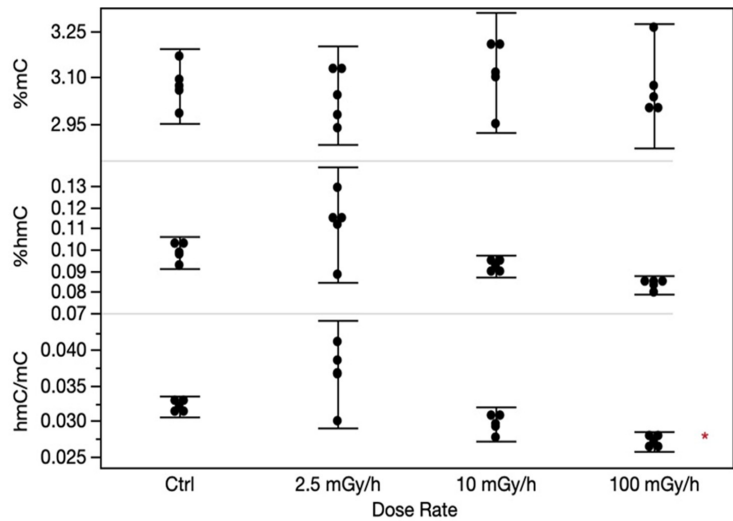


Fig 8. The levels of global methylation in CBA/CaOlaHsd livers analyzed by HPLC-MS/MS. In the panels, %mC (upper panel) and %hmC (mid panel), and the ratio between %hmC and %mC (lower panel) are shown. Each error bar represents the 95% confidence intervals of the means. Asterisk indicate borderline significance ($p = 0.043$) for the HDR hmC:mC-ratio.

<https://doi.org/10.1371/journal.pone.0256667.g008>

with the high dose rate. The corresponding number in B6 mice was markedly higher, 20%. These dissimilarities are reflected in the pathway enrichment analysis that revealed differing results depending on both strain and dose rate (Fig 6). Recently, radiation-induced strain-specific gene expression response was reported after acute irradiation of BALB/c and CBA mice [58]. Strain-specific radiation-induced responses have also been reported from others investigating other endpoints than gene expression [59–61], suggesting C57BL/6 be less susceptible to radiation-induced responses. Together with our results, we conclude that mouse genetic background is important when evaluating low LET radiation-induced genetic instability [30].

In general, the biological significance of the modulated DEGs in each exposure group revealed pathways involved in cancer, lipid metabolism, and inflammation. One day post-radiation, DEGs involved in cancer development and suppression, as well as ROS, were identified after HDR exposure in both strains: i.e., “*p53 signaling pathway*” and “*Ferroptosis*”. Ferroptosis is intriguing in this context. It is an iron-dependent form of programmed cell death induced by accumulation of lipid peroxidation (mainly peroxidation of phospholipids), resulting from an overload of the protective glutathione-dependent antioxidants and characterized by mitochondrial shrinkage [62]. Additionally, in B6, the HDR exhibit “*Pathways for cancer*”, “*Chemical carcinogenesis*”, “*Proteoglycans in cancer*”, and “*Hepatocellular carcinoma*”. Exposure to high dose rates of ionizing radiation to the total dose used herein is acknowledged to increase cancer risk. Gene expression changes indicating carcinogenic effects for the HDR exposure group were anticipated. “*Pathways for cancer*” and “*Chemical carcinogenesis*” were also significantly perturbed for the B6 LDR exposure group, suggesting that exposure chronically to a low dose rate, although given to a high total dose of 3 Gy, do modulate genes involved in cancer development. The majority of the DEGs represented in “*Chemical carcinogenesis*” were up-regulated, while the DEGs represented in “*Pathways for cancer*” were both up- and downregulated. Likewise, others have shown hepatic DEGs grouped to tumorigenesis and chromosomal damage in B6 mice following exposure to a low dose rate of 20 mGy/day to a total dose of 8

Gy. However, these genes were suppressed [57]. Regarding mutation induction, studying heteroplasmy in a mitochondrial gene (*Mtcb*) in B6 and BALB/c exposed to the Chernobyl environment for 30–40 days (~0.04 Gy/day) receiving 1.2–1.6 Gy, showed no significant gene mutation risk [27]. Considering these studies, chronic low dose rate gives rise to molecular changes associated with cancer. The potential of ionizing radiation to impact biological effects appears to depend on both the dose rate and duration of exposure when the cumulative dose is kept constant.

Collections of genes related to lipid metabolism are dysregulated in both LDR and HDR exposure groups one day post-radiation. In CBA, the “PPAR Signaling Pathway” was perturbed for all three dose rates. The PPAR Signaling Pathway is involved in energy homeostasis, including cholesterol and fatty acid metabolism. PPAR α has a central role in lipid (fatty acid oxidation) and glucose metabolism, where it exerts both an anti-inflammatory and an anti-oxidative function [63]. Elaborating on the specific genes represented in this pathway, the LDR group showed enrichment of PPAR α target genes related to fatty acid transport and fatty acid oxidation. The numbers of DEGs enriched to fatty acid transport and oxidation increase in the higher dose rate groups. Whether the mechanisms, as such, are activated or suppressed remains unclear. Transcriptional change in the gene coding for the nuclear receptor PPAR α itself was not observed at our sampling timepoint. In B6, other pathways related to lipid metabolism (i.e., fluid shear stress and atherosclerosis) were enriched for both LDR and HDR. However, not the PPAR signaling pathway. Previous findings of changed expression of genes related to hepatic lipid metabolism following low dose rate radiation are reported in both mice [57] and rats [64]. Together, the results suggest that exposure to low dose rate ionizing radiation perturb molecular signaling pathways related to different aspects of hepatic lipid metabolism, which may have implications for radiation-induced non-cancer effects such as cardiovascular disease and non-alcoholic fatty liver disease. In the B6 LDR group, other sets of genes related to the metabolism of sphingolipid and linoleic acid were significantly enriched. Sphingolipids are highly bioactive membrane lipids controlling cell division and cell death. Due to a high metabolic network among various sphingolipids, transcriptional modulation of genes related to the pathway “sphingolipid metabolism” could result in the progression of several conditions, i.e., diabetes and hepatocellular carcinoma [65].

Pathways related to aspects of inflammation are enriched for both LDR and HDR in both CBA and B6. In B6, perturbed DEGs are seen for the “Toll-like receptor signaling pathway”, which plays a crucial role in the innate immune system. The toll-like receptors initiate inflammation by recognizing damage-associated molecular patterns (DAMPs), molecules released by cell injury/death, and stress [66]. The “Complement and coagulation cascade” is perturbed in the CBA LDR exposure group and in all B6 dose rate groups. The toll-like receptors and the complement system are both players in the innate immune system. The crosstalk between them is related to the pathophysiology of atherosclerosis [67]. It is also known that the complement response is elicited following high acute doses such as those used in cancer therapy [68]. The perturbation of these two pathways by chronic LDR ionizing radiation suggests that inflammatory responses are elicited, which may contribute to the development of cardiovascular disease, including atherosclerosis, where ROS is known to play a central role. It should be kept in mind that the gene expression profiles observed may be an indirect effect of biological response in other tissues due to the whole-body exposure regime. The liver acts as a surveillance and response hub for the whole body by regulating systemic metabolism and maintaining homeostasis after external stimulus, particularly related to inflammatory responses and vascular damage [69,70].

Interestingly, we identified a gene set of 24 DEGs that could be representative of a radiation-specific transcriptional response, regardless of dose rate and genetic background (Fig 5).

Transcription factor over-representation analysis revealed that the 24 genes were significantly associated with the transcription factors *Stat3* and *Myc*. *Stat3* has been shown to be activated by gamma radiation *in vitro* [71]. In addition, upregulation of *Stat3* has been shown to have both anti- and pro-inflammatory roles during the pathogenesis of liver fibrosis [72]. *c-myc* has been linked with both ROS formation and DNA damage [73]. In our study, the *c-myc* transcription level was not differentially expressed in any of the exposure groups. On the other hand, the transcript level of *Stat3* was upregulated in CBA LDR and MDR and downregulated in B6 at all dose rates.

One of the major pathological routes of ionizing radiation toxicity is the generation of ROS [74,75]. We previously demonstrated induction of DNA damage in mice following similar and lower chronic low dose rates given to equal or lower total doses of gamma irradiation [25,76]. However, we do not have explicit evidence that these are indeed oxidative DNA lesions. Oxidative stress is a complex and multifactorial process resulting from an imbalance between ROS production (endogenous and exogenous production) and antioxidant capacity. Disturbance of redox homeostasis is linked to several pathological conditions, such as cardiovascular disease, hepatic damage [77], and tumor development [78]. Among the LDR and HDR enriched KEGG gene sets (Fig 6), no direct response to increased ROS generation or induction of DNA damage response was evident. One explanation could be that the sampling timepoint was sub-optimal regarding the transcriptional biodynamic of the genes in question. Several of the enriched functional pathways, for both LDR and HDR, could be associated with an imbalance in ROS homeostasis, even if it was not directly apparent in the identified transcriptional pathways.

Based on this, we performed pathway enrichment analysis on the genes annotated to the GO biological process “Response to oxidative stress” using the KEGG database. This exercise identified functional signaling pathways enriched with ROS annotated genes. Several of these “ROS-enriched” pathways were also enriched by our identified DEGs for all dose rate groups, regardless of the low representation of the ROS annotated genes. Higher numbers of specific oxidative stress-related DEGs were expressed in the HDR group than in the MDR and the LDR groups (Fig 7). In agreement with our HDR results, rats exposed to acute high dose rates of gamma radiation (1.5–3.5 Gy) once a week for one month expressed significantly changed antioxidant enzyme activities in liver and skeletal muscle tissues one month after radiation, which is indicative of oxidative stress [79]. Whether exposure to chronic low dose rate ionizing radiation in our study has led to an imbalance between the ROS generation and the antioxidant capacity, reaching a state of liver oxidative stress, is unclear. These results, taken together, suggest that exposure to chronic low dose rate ionizing radiation has a lower potential to bring ROS homeostasis to imbalance than higher dose rates, even if the total cumulative dose is equal and high. This is possibly linked to several factors, including the number of generated ROS per time unit of exposure and the cellular antioxidant capacity.

Among the identified ROS-related DEGs, two genes were modified across all groups: Vanin-1 (*Vnn1*) and Lipocalin-2 (*Lcn2*). *Vnn1* is highly expressed in centrilobular hepatocytes, and its function is related to energy production, coenzyme A-, lipid- [80], and xenobiotic metabolism [81]. *Vnn1* is a tissue sensor of oxidative stress [82,83] and participates in stress-related adaptive tissue responses [84]. *Vnn1*-deficient mice exposed to whole-body gamma radiation (6 Gy acute) showed increased resistance to oxidative injury in the thymus compared to wild-type controls. The transient increased thymic expression of *Vnn1* was seen two days post-radiation followed by down-regulation [85]. The observed down-regulation of *Vnn1* in all dose rate groups in CBA and B6 in our study suggests that this gene could be an essential player in response to ionizing radiation, also after chronic low dose rate exposure.

To investigate the long-term effect of radiation, we measured changes in transcriptional responses after a recovery period of 100–200 days (14–28 weeks). The transcriptional response was, as expected, markedly lower in both strains, as the role of the transcriptional change is to rapidly and most often transiently respond to a cellular stress to ensure cellular integrity. The late_DEGs overlapped poorly with the one day post-radiation DEGs. The larger variation in age at sampling in the late effect recovery groups, due to breeding, could have impacted the individual variation in gene expression and hence affected the degree of significant DEGs. A recent report investigating long-term effects following acute exposure to gamma radiation (1 Gy) in CBA and BALB/c mice found alterations of hepatic gene expression profiles in BALB/c up to ten weeks post-radiation, whereas significant changes were identified in CBA/Ca only at four hours post-irradiation but not at later time points (24 h, one week and ten weeks) [58]. This is in line with the transcriptional response being mainly transient and not persist long-term. However, genes may be regulated on a longer time perspective to facilitate a rapid response in case of future exposures.

It has been proposed that exposure to chronic low dose rate radiation is more likely to induce epigenetic changes than acute exposures [86]. In our study, approaching changes in the epigenome at the global level did not reveal significant changes in the overall 5mC level or the 5hmC at the dose regimens tested (Fig 8). Methods investigating epigenetic mechanisms at base resolution level can be used in follow-up experiments to further explore the transcriptional etiology and other epigenetic mechanisms. For example, since epigenetic modulations could affect the transcription through changes in chromatin accessibility, assessing changes in chromatin architecture could reveal relevant epigenetic modulations initiated by ionizing radiation at the different dose rates.

Conclusion

To our knowledge, this is the first study evaluating the impact of dose rate on the hepatic transcriptional profile after exposure to ionizing radiation in two mouse strains, in a chronic low dose rate versus acute high dose rate regimen to a similar total dose. We demonstrate that the transcriptional profile is differently modulated following low dose rate versus high dose rate exposure, illustrating the importance of both the dose rate, duration of exposure and total dose when evaluating radiation-induced molecular responses. As also discussed by others, our data, although at the level of gene expression, support that the cumulative dose alone may be insufficient to predict the associated risk, as both dose rate and duration of exposure seem to play a role. Exposure to chronic low dose rate ionizing radiation affects the maintenance of genomic and cellular integrity differently than acute high dose rate exposures. The marked differences in response between the mouse strains suggest variations in radiation-induced defense mechanism capacities. Our findings contribute to the understanding of radiation-induced carcinogenesis as well as non-cancer effects such as cardiovascular effects.

Supporting information

S1 Fig. Correlation between predicted miRNAs and identified DEGs. The table presents $\log_2(\text{FoldChange})$ values for six miRNAs predicted in Duale et al. (2020) that show correlations with some of our identified mRNAs. Inverse correlations are indicated with $\log_2(\text{FoldChange})$ -values **in bold**. Green upwards arrows indicate upregulations, while red downwards arrows indicate downregulation. Yellow arrows indicate mRNA expression levels less than the chosen $\log_2(\text{FoldChange})$ cutoff at 0.5. (TIF)

S2 Fig. Validation of DEGs using qPCR. Each dot or circle represents the ΔCq -value from the qPCR analysis and the \log_2 [normalized count] from the RNA-Seq analysis of the selected targets analyzed for B6 control (circle) and B6 LDR samples (dot). The selected genes of interest are listed to the right.

(TIF)

S1 Table. Excel file containing all identified statistically significant DEGs. DEGs representing one day post-radiation are found in the sheet: "DEGs_one_day_post_rad", the late response is seen in sheet: "DEGs_>100days_post_rad", and the identified oxidative stress related DEGs can be found in the sheet: "Ox_Stress_DEGs". DEGs are listed by Gene_name, \log_2 (FoldChange), and FDR.

(XLSX)

S2 Table. Excel file containing the total result output using the GO biological process terms.

(XLSX)

Acknowledgments

Thanks to Jill Andersen, Norwegian Institute of Public Health, for excellent technical assistance.

Author Contributions

Conceptualization: Hildegunn Dahl, Dag M. Eide, Nur Duale, Deborah H. Oughton, Ann-Karin Olsen.

Data curation: Torstein Tengs.

Formal analysis: Hildegunn Dahl, Dag M. Eide, Torstein Tengs.

Funding acquisition: Deborah H. Oughton, Ann-Karin Olsen.

Investigation: Hildegunn Dahl, Jorke H. Kamstra.

Methodology: Hildegunn Dahl, Dag M. Eide, Nur Duale, Ann-Karin Olsen.

Project administration: Hildegunn Dahl, Ann-Karin Olsen.

Software: Torstein Tengs.

Supervision: Ann-Karin Olsen.

Visualization: Hildegunn Dahl, Dag M. Eide, Torstein Tengs.

Writing – original draft: Hildegunn Dahl.

Writing – review & editing: Dag M. Eide, Torstein Tengs, Nur Duale, Jorke H. Kamstra, Deborah H. Oughton, Ann-Karin Olsen.

References

1. UNSCEAR. Sources, Effects and Risks of Ionizing Radiation: UNSCEAR 2017 Report to the General Assembly, with Scientific Annexes. United Nations publications: 2017 978-92-1-142322-8.
2. Health Risks from Exposure to Low Levels of Ionizing Radiation: BEIR VII Phase 2. Washington, DC: The National Academies Press; 2006. 422 p.
3. UNSCEAR. Effects of ionizing radiation: UNSCEAR 2006 Report to the General Assembly, with scientific annexes A and B. United Nations publications: 2009 978-92-1-142263-4.

4. ICRP. The 2007 Recommendations of the International Commission on Radiological Protection. ICRP publication 103. 2007 0146–6453 Contract No.: 2–4.
5. Folley JH, Borges W, Yamawaki T. Incidence of leukemia in survivors of the atomic bomb in Hiroshima and Nagasaki, Japan. *Am J Med.* 1952; 13(3):311–21. [https://doi.org/10.1016/0002-9343\(52\)90285-4](https://doi.org/10.1016/0002-9343(52)90285-4) PMID: 12985588
6. Ozasa K, Shimizu Y, Suyama A, Kasagi F, Soda M, Grant EJ, et al. Studies of the mortality of atomic bomb survivors, Report 14, 1950–2003: an overview of cancer and noncancer diseases. *Radiation research.* 2012; 177(3):229–43. <https://doi.org/10.1667/rr2629.1> PMID: 22171960
7. Preston DL, Ron E, Tokuoka S, Funamoto S, Nishi N, Soda M, et al. Solid cancer incidence in atomic bomb survivors: 1958–1998. *Radiation research.* 2007; 168(1):1–64. <https://doi.org/10.1667/RR0763.1> PMID: 17722996
8. Mothersill C, Rusin A, Seymour C. Towards a New Concept of Low Dose. *Health physics.* 2019; 117(3):330–6. <https://doi.org/10.1097/HP.0000000000001074> PMID: 31349357
9. Mullenders L, Atkinson M, Paretzke H, Sabatier L, Bouffler S. Assessing cancer risks of low-dose radiation. *Nature reviews Cancer.* 2009; 9(8):596–604. <https://doi.org/10.1038/nrc2677> PMID: 19629073
10. Tang FR, Loganovsky K. Low dose or low dose rate ionizing radiation-induced health effect in the human. *Journal of environmental radioactivity.* 2018; 192:32–47. <https://doi.org/10.1016/j.jenvrad.2018.05.018> PMID: 29883875
11. Tang FR, Loke WK, Khoo BC. Low-dose or low-dose-rate ionizing radiation-induced bioeffects in animal models. *Journal of radiation research.* 2017; 58(2):165–82. <https://doi.org/10.1093/jrr/rw120> PMID: 28077626
12. Tharmalingam S, Sreetharan S, Brooks AL, Boreham DR. Re-evaluation of the linear no-threshold (LNT) model using new paradigms and modern molecular studies. *Chemico-Biological Interactions.* 2019; 301:54–67. <https://doi.org/10.1016/j.cbi.2018.11.013> PMID: 30763548
13. UNSCEAR. Report of the United Nations Scientific Committee on the Effects of Atomic Radiation 2010; Summary of low-dose radiation effects on health. United Nations publications: United Nations, 2010 2011. Report No.: 978-92-1-642010-9.
14. UNSCEAR. Biological mechanisms of radiation actions at low doses; A white paper to guide the Scientific Committee's future programme of work. United Nations publications 2012. 45 p.
15. Little MP. A review of non-cancer effects, especially circulatory and ocular diseases. *Radiation and environmental biophysics.* 2013; 52(4):435–49. <https://doi.org/10.1007/s00411-013-0484-7> PMID: 23903347
16. Preston DL, Shimizu Y, Pierce DA, Suyama A, Mabuchi K. Studies of mortality of atomic bomb survivors. Report 13: Solid cancer and noncancer disease mortality: 1950–1997. *Radiation research.* 2003; 160(4):381–407. <https://doi.org/10.1667/rr3049> PMID: 12968934
17. Tapio S, Little MP, Kaiser JC, Impens N, Hamada N, Georgakilas AG, et al. Ionizing radiation-induced circulatory and metabolic diseases. *Environment international.* 2021; 146:106235. <https://doi.org/10.1016/j.envint.2020.106235> PMID: 33157375
18. Little MP, Tawn EJ, Tzoulaki I, Wakeford R, Hildebrandt G, Paris F, et al. A Systematic Review of Epidemiological Associations between Low and Moderate Doses of Ionizing Radiation and Late Cardiovascular Effects, and Their Possible Mechanisms. *Radiation research.* 2008; 169(1):99–109, 11. <https://doi.org/10.1667/RR1070.1> PMID: 18159955
19. Shimizu Y, Kodama K, Nishi N, Kasagi F, Suyama A, Soda M, et al. Radiation exposure and circulatory disease risk: Hiroshima and Nagasaki atomic bomb survivor data, 1950–2003. *BMJ (Clinical research ed).* 2010; 340:b5349. <https://doi.org/10.1136/bmj.b5349> PMID: 20075151
20. Akahoshi M, Amasaki Y, Soda M, Hida A, Imaizumi M, Nakashima E, et al. Effects of radiation on fatty liver and metabolic coronary risk factors among atomic bomb survivors in Nagasaki. *Hypertens Res.* 2003; 26(12):965–70. <https://doi.org/10.1291/hyres.26.965> PMID: 14717339
21. Baselet B, Rombouts C, Benotmane AM, Baatout S, Aerts A. Cardiovascular diseases related to ionizing radiation: The risk of low-dose exposure (Review). *Int J Mol Med.* 2016; 38(6):1623–41. <https://doi.org/10.3892/ijmm.2016.2777> PMID: 27748824
22. Little MP. Radiation and circulatory disease. *Mutation Research/Reviews in Mutation Research.* 2016; 770:299–318. <https://doi.org/10.1016/j.mrrev.2016.07.008> PMID: 27919337
23. Little MP, Azizova TV, Bazyka D, Bouffler SD, Cardis E, Chekin S, et al. Systematic review and meta-analysis of circulatory disease from exposure to low-level ionizing radiation and estimates of potential population mortality risks. *Environmental health perspectives.* 2012; 120(11):1503–11. <https://doi.org/10.1289/ehp.1204982> PMID: 22728254
24. Brooks AL. The impact of dose rate on the linear no threshold hypothesis. *Chem Biol Interact.* 2019; 301:68–80. <https://doi.org/10.1016/j.cbi.2018.12.007> PMID: 30763551

25. Graupner A, Eide DM, Brede DA, Ellender M, Lindbo Hansen E, Oughton DH, et al. Genotoxic effects of high dose rate X-ray and low dose rate gamma radiation in Apc(Min/+) mice. *Environmental and molecular mutagenesis*. 2017; 58(8):560–9. <https://doi.org/10.1002/em.22121> PMID: 28856770
26. Oilipitz W, Wiktor-Brown D, Shuga J, Pang B, McFaline J, Lonkar P, et al. Integrated molecular analysis indicates undetectable change in DNA damage in mice after continuous irradiation at ~ 400-fold natural background radiation. *Environmental health perspectives*. 2012; 120(8):1130–6. <https://doi.org/10.1289/ehp.1104294> PMID: 22538203
27. Wickliffe JK, Rodgers BE, Chesser RK, Phillips CJ, Gaschak SP, Baker RJ. Mitochondrial DNA Heteroplasmy in Laboratory Mice Experimentally Enclosed in the Radioactive Chernobyl Environment. *Radiation research*. 2003; 159(4):458–64, 7. [https://doi.org/10.1667/0033-7587\(2003\)159\[0458:mhdmlm\]2.0.co;2](https://doi.org/10.1667/0033-7587(2003)159[0458:mhdmlm]2.0.co;2) PMID: 12643790
28. Mavragani IV, Nikitaki Z, Souli MP, Aziz A, Nowsheen S, Aziz K, et al. Complex DNA Damage: A Route to Radiation-Induced Genomic Instability and Carcinogenesis. *Cancers*. 2017; 9(7). <https://doi.org/10.3390/cancers9070091> PMID: 28718816
29. Merrifield M, Kovalchuk O. Epigenetics in radiation biology: a new research frontier. *Frontiers in genetics*. 2013; 4:40. <https://doi.org/10.3389/fgene.2013.00040> PMID: 23577019
30. Kadhim MA. Role of genetic background in induced instability. *Oncogene*. 2003; 22(45):6994–9. <https://doi.org/10.1038/sj.onc.1206883> PMID: 14557803
31. Mavragani IV, Laskaratou DA, Frey B, Candéias SM, Gaipal US, Lumniczky K, et al. Key mechanisms involved in ionizing radiation-induced systemic effects. A current review. *Toxicol Res (Camb)*. 2016; 5(1):12–33. <https://doi.org/10.1039/c5tx00222b> PMID: 30090323
32. Rühm W, Woloschak GE, Shore RE, Azizova TV, Grosche B, Niwa O, et al. Dose and dose-rate effects of ionizing radiation: a discussion in the light of radiological protection. *Radiation and environmental biophysics*. 2015; 54(4):379–401. <https://doi.org/10.1007/s00411-015-0613-6> PMID: 26343037
33. Belli M, Tabocchini MA. Ionizing Radiation-Induced Epigenetic Modifications and Their Relevance to Radiation Protection. *International journal of molecular sciences*. 2020; 21(17). <https://doi.org/10.3390/ijms21175993> PMID: 32825382
34. Ghandhi SA, Smilenov LB, Elliston CD, Chowdhury M, Amundson SA. Radiation dose-rate effects on gene expression for human biodosimetry. *BMC Med Genomics*. 2015; 8:22. <https://doi.org/10.1186/s12920-015-0097-x> PMID: 25963628
35. Pernet E, Hall J, Baatout S, Benotmane MA, Blanchardon E, Bouffler S, et al. Ionizing radiation biomarkers for potential use in epidemiological studies. *Mutation research*. 2012; 751(2):258–86. <https://doi.org/10.1016/j.mrev.2012.05.003> PMID: 22677531
36. Duale N, Eide DM, Amberger ML, Graupner A, Brede DA, Olsen AK. Using prediction models to identify miRNA-based markers of low dose rate chronic stress. *The Science of the total environment*. 2020; 717:137068. <https://doi.org/10.1016/j.scitotenv.2020.137068> PMID: 32062256
37. E. Lindbo Hansen POH. Air kerma measurements with Landauer nanoDots in Cs-137 and Co-60 beams. Part I—SSDL exposures free in air. Technical document no. 8. Norwegian Radiation Protection Authority, Østerås, Oslo: NRP A, 2017 2017-12-07.
38. Kamstra JH, Sales LB, Aleström P, Legler J. Differential DNA methylation at conserved non-genic elements and evidence for transgenerational inheritance following developmental exposure to mono(2-ethylhexyl) phthalate and 5-azacytidine in zebrafish. *Epigenetics & chromatin*. 2017; 10:20. <https://doi.org/10.1186/s13072-017-0126-4> PMID: 28413451
39. Duale N, Olsen AK, Christensen T, Butt ST, Brunborg G. Octyl methoxycinnamate modulates gene expression and prevents cyclobutane pyrimidine dimer formation but not oxidative DNA damage in UV-exposed human cell lines. *Toxicological sciences: an official journal of the Society of Toxicology*. 2010; 114(2):272–84. <https://doi.org/10.1093/toxsci/kfq005> PMID: 20071424
40. Duale N, Steffensen IL, Andersen J, Brevik A, Brunborg G, Lindeman B. Impaired sperm chromatin integrity in obese mice. *Andrology*. 2014; 2(2):234–43. <https://doi.org/10.1111/j.2047-2927.2013.00178.x> PMID: 24459046
41. Gutzkow KB, Duale N, Danielsen T, von Stedingk H, Shahzadi S, Instanes C, et al. Enhanced susceptibility of obese mice to glycidamide-induced sperm chromatin damage without increased oxidative stress. *Andrology*. 2016; 4(6):1102–14. <https://doi.org/10.1111/andr.12233> PMID: 27575329
42. Livak KJ, Schmittgen TD. Analysis of relative gene expression data using real-time quantitative PCR and the 2(-Delta Delta C(T)) Method. *Methods (San Diego, Calif)*. 2001; 25(4):402–8. <https://doi.org/10.1006/meth.2001.1262> PMID: 11846609
43. Schmittgen TD, Livak KJ. Analyzing real-time PCR data by the comparative C(T) method. *Nature protocols*. 2008; 3(6):1101–8. <https://doi.org/10.1038/nprot.2008.73> PMID: 18546601

44. Kim D, Paggi JM, Park C, Bennett C, Salzberg SL. Graph-based genome alignment and genotyping with HISAT2 and HISAT-genotype. *Nat Biotechnol*. 2019; 37(8):907–15. <https://doi.org/10.1038/s41587-019-0201-4> PMID: 31375807
45. Anders S, Pyl PT, Huber W. HTSeq—a Python framework to work with high-throughput sequencing data. *Bioinformatics*. 2015; 31(2):166–9. <https://doi.org/10.1093/bioinformatics/btu638> PMID: 25260700
46. Varet H, Brillet-Gueguen L, Coppee JY, Dillies MA. SARTools: A DESeq2- and EdgeR-Based R Pipeline for Comprehensive Differential Analysis of RNA-Seq Data. *PLoS one*. 2016; 11(6):e0157022. <https://doi.org/10.1371/journal.pone.0157022> PMID: 27280887
47. McCarthy DJ, Chen Y, Smyth GK. Differential expression analysis of multifactor RNA-Seq experiments with respect to biological variation. *Nucleic acids research*. 2012; 40(10):4288–97. <https://doi.org/10.1093/nar/gks042> PMID: 22287627
48. Robinson MD, McCarthy DJ, Smyth GK. edgeR: a Bioconductor package for differential expression analysis of digital gene expression data. *Bioinformatics*. 2009; 26(1):139–40. <https://doi.org/10.1093/bioinformatics/btp616> PMID: 19910308
49. Ogata H, Goto S, Sato K, Fujibuchi W, Bono H, Kanehisa M. KEGG: Kyoto Encyclopedia of Genes and Genomes. *Nucleic acids research*. 1999; 27(1):29–34. <https://doi.org/10.1093/nar/27.1.29> PMID: 9847135
50. Ashburner M, Ball CA, Blake JA, Botstein D, Butler H, Cherry JM, et al. Gene ontology: tool for the unification of biology. The Gene Ontology Consortium. *Nature genetics*. 2000; 25(1):25–9. <https://doi.org/10.1038/75556> PMID: 10802651
51. GeneOntologyConsortium. The Gene Ontology resource: enriching a GOld mine. *Nucleic acids research*. 2021; 49(D1):D325–d34. <https://doi.org/10.1093/nar/gkaa1113> PMID: 33290552
52. Kuleshov MV, Jones MR, Rouillard AD, Fernandez NF, Duan Q, Wang Z, et al. Enrichr: a comprehensive gene set enrichment analysis web server 2016 update. *Nucleic acids research*. 2016; 44(W1):W90–7. <https://doi.org/10.1093/nar/gkw377> PMID: 27141961
53. Chen EY, Tan CM, Kou Y, Duan Q, Wang Z, Meirelles GV, et al. Enrichr: interactive and collaborative HTML5 gene list enrichment analysis tool. *BMC Bioinformatics*. 2013; 14:128. <https://doi.org/10.1186/1471-2105-14-128> PMID: 23586463
54. Barrett T, Wilhite SE, Ledoux P, Evangelista C, Kim IF, Tomashevsky M, et al. NCBI GEO: archive for functional genomics data sets—update. *Nucleic acids research*. 2013; 41(D1):D991–D5. <https://doi.org/10.1093/nar/gks1193> PMID: 23193258
55. Edgar R, Domrachev M, Lash AE. Gene Expression Omnibus: NCBI gene expression and hybridization array data repository. *Nucleic acids research*. 2002; 30(1):207–10. <https://doi.org/10.1093/nar/30.1.207> PMID: 11752295
56. Leuraud K, Richardson DB, Cardis E, Daniels RD, Gillies M, Haylock R, et al. Risk of cancer associated with low-dose radiation exposure: comparison of results between the INWORKS nuclear workers study and the A-bomb survivors study. *Radiation and environmental biophysics*. 2021; 60(1):23–39. <https://doi.org/10.1007/s00411-020-00890-7> PMID: 33479781
57. Uehara Y, Ito Y, Taki K, Neno M, Ichinohe K, Nakamura S, et al. Gene expression profiles in mouse liver after long-term low-dose-rate irradiation with gamma rays. *Radiation research*. 2010; 174(5):611–7. <https://doi.org/10.1667/RR2195.1> PMID: 20954861
58. Jafer A, Sylvius N, Adewoye AB, Dubrova YE. The long-term effects of exposure to ionising radiation on gene expression in mice. *Mutation research*. 2020; 821:111723. <https://doi.org/10.1016/j.mrfmmm.2020.111723> PMID: 33096319
59. Ponnaiya B, Cornforth MN, Ullrich RL. Radiation-induced chromosomal instability in BALB/c and C57BL/6 mice: the difference is as clear as black and white. *Radiation research*. 1997; 147(2):121–5. PMID: 9008202.
60. Watson GE, Lorimore SA, Clutton SM, Kadhim MA, Wright EG. Genetic factors influencing alpha-particle-induced chromosomal instability. *International journal of radiation biology*. 1997; 71(5):497–503. <https://doi.org/10.1080/095530097143824> PMID: 9191894
61. Yu Y, Okayasu R, Weil MM, Silver A, McCarthy M, Zabriskie R, et al. Elevated breast cancer risk in irradiated BALB/c mice associates with unique functional polymorphism of the Prkdc (DNA-dependent protein kinase catalytic subunit) gene. *Cancer research*. 2001; 61(5):1820–4. PMID: 11280730.
62. Mao L, Zhao T, Song Y, Lin L, Fan X, Cui B, et al. The emerging role of ferroptosis in non-cancer liver diseases: hype or increasing hope? *Cell Death & Disease*. 2020; 11(7):518. <https://doi.org/10.1038/s41419-020-2732-5> PMID: 32647111

63. Wang Y, Nakajima T, Gonzalez FJ, Tanaka N. PPARs as Metabolic Regulators in the Liver: Lessons from Liver-Specific PPAR-Null Mice. *International journal of molecular sciences*. 2020; 21(6). <https://doi.org/10.3390/ijms21062061> PMID: 32192216
64. Ngan Tran K, Choi JI. Gene expression profiling of rat livers after continuous whole-body exposure to low-dose rate of gamma rays. *International journal of radiation biology*. 2018; 94(5):434–42. <https://doi.org/10.1080/09553002.2018.1455009> PMID: 29557699
65. Pralhada Rao R, Vaidyanathan N, Rengasamy M, Mammen Oommen A, Somaiya N, Jagannath MR. Sphingolipid Metabolic Pathway: An Overview of Major Roles Played in Human Diseases. *Journal of Lipids*. 2013; 2013:178910. <https://doi.org/10.1155/2013/178910> PMID: 23984075
66. Alisi A, Carsetti R, Nobili V. Pathogen- or damage-associated molecular patterns during nonalcoholic fatty liver disease development. *Hepatology*. 2011; 54(5):1500–2. <https://doi.org/10.1002/hep.24611> PMID: 22045668
67. Hovland A, Jonasson L, Garred P, Yndestad A, Aukrust P, Lappegård KT, et al. The complement system and toll-like receptors as integrated players in the pathophysiology of atherosclerosis. *Atherosclerosis*. 2015; 241(2):480–94. <https://doi.org/10.1016/j.atherosclerosis.2015.05.038> PMID: 26086357
68. Surace L, Lysenko V, Fontana AO, Cecconi V, Janssen H, Bivic A, et al. Complement is a central mediator of radiotherapy-induced tumor-specific immunity and clinical response. *Immunity*. 2015; 42(4):767–77. <https://doi.org/10.1016/j.immuni.2015.03.009> PMID: 25888260
69. Baselet B, Sonveaux P, Baatout S, Aerts A. Pathological effects of ionizing radiation: endothelial activation and dysfunction. *Cellular and molecular life sciences: CMLS*. 2019; 76(4):699–728. <https://doi.org/10.1007/s00018-018-2956-z> PMID: 30377700
70. Lumniczky K, Impens N, Armengol G, Candéias S, Georgakilas AG, Hornhardt S, et al. Low dose ionizing radiation effects on the immune system. *Environment international*. 2021; 149:106212. <https://doi.org/10.1016/j.envint.2020.106212> PMID: 33293042
71. Gao L, Li FS, Chen XH, Liu QW, Feng JB, Liu QJ, et al. Radiation induces phosphorylation of STAT3 in a dose- and time-dependent manner. *Asian Pacific journal of cancer prevention: APJCP*. 2014; 15(15):6161–4. <https://doi.org/10.7314/apjcp.2014.15.15.6161> PMID: 25124591
72. Zhao J, Qi YF, Yu YR. STAT3: A key regulator in liver fibrosis. *Ann Hepatol*. 2020; 21:100224. <https://doi.org/10.1016/j.aohp.2020.06.010> PMID: 32702499
73. Vafa O, Wade M, Kern S, Beeche M, Pandita TK, Hampton GM, et al. c-Myc can induce DNA damage, increase reactive oxygen species, and mitigate p53 function: a mechanism for oncogene-induced genetic instability. *Mol Cell*. 2002; 9(5):1031–44. [https://doi.org/10.1016/s1097-2765\(02\)00520-8](https://doi.org/10.1016/s1097-2765(02)00520-8) PMID: 12049739
74. Azzam EI, Jay-Gerin JP, Pain D. Ionizing radiation-induced metabolic oxidative stress and prolonged cell injury. *Cancer letters*. 2012; 327(1–2):48–60. <https://doi.org/10.1016/j.canlet.2011.12.012> PMID: 22182453
75. Szumiel I. Ionizing radiation-induced oxidative stress, epigenetic changes and genomic instability: the pivotal role of mitochondria. *International journal of radiation biology*. 2015; 91(1):1–12. <https://doi.org/10.3109/09553002.2014.934929> PMID: 24937368
76. Graupner A, Eide DM, Instanes C, Andersen JM, Brede DA, Dertinger SD, et al. Gamma radiation at a human relevant low dose rate is genotoxic in mice. *Scientific reports*. 2016; 6:32977. <https://doi.org/10.1038/srep32977> PMID: 27596356
77. Li S, Tan HY, Wang N, Zhang ZJ, Lao L, Wong CW, et al. The Role of Oxidative Stress and Antioxidants in Liver Diseases. *International journal of molecular sciences*. 2015; 16(11):26087–124. <https://doi.org/10.3390/ijms161125942> PMID: 26540040
78. Liou G-Y, Storz P. Reactive oxygen species in cancer. *Free radical research*. 2010; 44(5):479–96. <https://doi.org/10.3109/10715761003667554> PMID: 20370557
79. Zakaria. Effect of Gamma Ray on Reactive Oxygen Species at Experimental Animals. *OMICS J Radiol* 2017; 6: 283. <https://doi.org/10.4172/2167-7964.1000283>
80. Rommelaere S, Millet V, Gensollen T, Bourges C, Eeckhoutte J, Hennuyer N, et al. PPARalpha regulates the production of serum Vanin-1 by liver. *FEBS Lett*. 2013; 587(22):3742–8. <https://doi.org/10.1016/j.febslet.2013.09.046> PMID: 24140347
81. Katz NR. Metabolic heterogeneity of hepatocytes across the liver acinus. *J Nutr*. 1992; 122(3 Suppl):843–9. https://doi.org/10.1093/jn/122.suppl_3.843 PMID: 1542056
82. Bartucci R, Salvati A, Olinga P, Boersma YL. Vanin 1: Its Physiological Function and Role in Diseases. *International journal of molecular sciences*. 2019; 20(16):3891. <https://doi.org/10.3390/ijms20163891> PMID: 31404995
83. Chen S, Zhang W, Tang C, Tang X, Liu L, Liu C. Vanin-1 is a key activator for hepatic gluconeogenesis. *Diabetes*. 2014; 63(6):2073–85. <https://doi.org/10.2337/db13-0788> PMID: 24550194

84. Naquet P, Pitari G, Duprè S, Galland F. Role of the Vnn1 pantetheinase in tissue tolerance to stress. *Biochem Soc Trans*. 2014; 42(4):1094–100. <https://doi.org/10.1042/BST20140092> PMID: 25110008
85. Berruyer C, Martin FM, Castellano R, Macone A, Malergue F, Garrido-Urbani S, et al. Vanin-1^{-/-} Mice Exhibit a Glutathione-Mediated Tissue Resistance to Oxidative Stress. *Molecular and Cellular Biology*. 2004; 24(16):7214–24. <https://doi.org/10.1128/MCB.24.16.7214-7224.2004> PMID: 15282320
86. Kovalchuk O, Burke P, Besplug J, Slovack M, Filkowski J, Pogribny I. Methylation changes in muscle and liver tissues of male and female mice exposed to acute and chronic low-dose X-ray-irradiation. *Mutation research*. 2004; 548(1–2):75–84. <https://doi.org/10.1016/j.mrfmmm.2003.12.016> PMID: 15063138

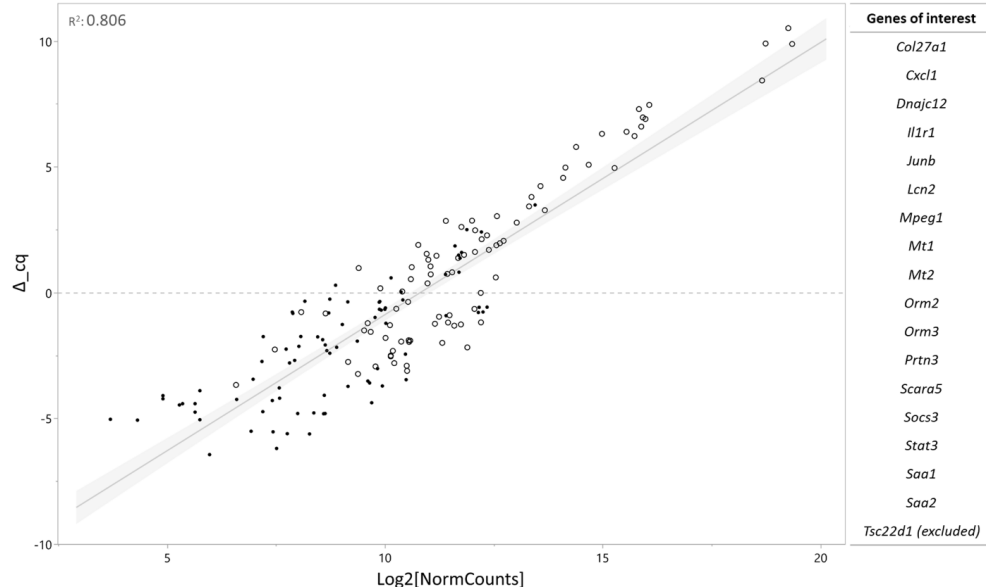
S1 Fig. Correlation between predicted miRNAs and identified DEGs.

The table presents log₂(FoldChange) values for six miRNAs predicted in Duale et al. (2020) that show correlations with some of our identified mRNAs. Inverse correlations are indicated with log₂(FoldChange)-values in bold. Green upwards arrows indicate upregulations, while red downwards arrows indicate downregulation. Yellow arrows indicate mRNA expression levels less than the chosen log₂(FoldChange) cutoff at 0.5.

		CBA/CaOlaHsd						C57BL/6NHsd					
		LDR		MDR		HDR		LDR		MDR		HDR	
miRNAID	Gene Symbol	miRNA	mRNA	miRNA	mRNA	miRNA	mRNA	miRNA	mRNA	miRNA	mRNA	miRNA	mRNA
miR-125b-5p	<i>Il1rn</i>			↑ 1,17	↑ 1,13			↑ 1,64	↓ -2,22	↑ 1,83	↓ -1,52	↑ 1,91	↓ -1,54
miR-125b-5p	<i>Saa2</i>	↑ 1,87	↑ 8,03	↑ 1,17	↑ 7,49	↑ 1,66	↑ 5,17	↑ 1,64	↓ -7,37	↑ 1,83	↓ -5,60	↑ 1,91	↓ -4,48
miR-125b-5p	<i>Usp2</i>					↑ 1,66	↑ 5,79	↑ 1,64	↓ -1,26	↑ 1,83	↓ -0,68	↑ 1,91	↓ -0,52
miR-130a-3p	<i>Cebpe</i>							↑ 1,62	⇒ -0,19	↑ 2,29	⇒ -0,42	↑ 1,84	↓ -0,75
miR-130a-3p	<i>Epha7</i>	↑ 2,58		↑ 1,65	↓ -0,83	↑ 2,30	⇒ -0,25	↑ 1,62	↑ 0,99	↑ 2,29	↑ 0,81	↑ 1,84	↑ 0,90
miR-140-3p	<i>Gngt1</i>	↑ 3,10	↓ -1,21	↑ 2,21	↓ -0,59	↑ 2,86	↓ -1,58	↑ 1,56	↑ 0,77	↑ 1,92	↑ 0,77	↑ 2,00	↑ 0,99
miR-140-3p	<i>Irak3</i>							↑ 1,56	↓ -2,05	↑ 1,92	↓ -1,96	↑ 2,00	↓ -1,85
miR-140-3p	<i>Tifa</i>	↑ 3,10	↑ 1,39	↑ 2,21	↑ 0,60	↑ 2,86	⇒ 0,02	↑ 1,56	↓ -1,95	↑ 1,92	↓ -2,27	↑ 2,00	↓ -2,56
miR-145a-5p	<i>Apcs</i>	↑ 1,90	↑ 1,47	↑ 1,40	↑ 1,57	↑ 1,73	⇒ 0,32	↑ 1,49	↓ -2,43	↑ 2,26	↓ -2,25	↑ 1,86	↓ -2,10
miR-145a-5p	<i>Npr3</i>	↑ 1,90		↑ 1,40		↑ 1,73	⇒ -0,18	↑ 1,49	↑ 0,88	↑ 2,26	↑ 0,65	↑ 1,86	↑ 0,99
miR-145a-5p	<i>Nrg4</i>	↑ 1,90		↑ 1,40		↑ 1,73	↑ 2,08	↑ 1,49	↓ -1,20	↑ 2,26	↓ -0,61	↑ 1,86	⇒ -0,28
miR-145a-5p	<i>Serpine1</i>							↑ 1,49	↓ -1,74	↑ 2,26	↓ -1,77	↑ 1,86	↓ -1,95
miR-145a-5p	<i>Sox9</i>	↑ 1,90	↑ 1,01	↑ 1,40	↓ -0,57	↑ 1,73	↓ -1,51	↑ 1,49	⇒ 0,50	↑ 2,26	⇒ -0,10	↑ 1,86	↓ -0,70
miR-181a-5p	<i>Wnt9a</i>							↑ 1,45	↓ -1,02	↑ 1,90	↓ -0,66	↑ 1,71	↓ -1,15
miR-499-5p	<i>Cxcl10</i>	↑ 2,58	↓ -1,61	↑ 2,46	↓ -0,98	↑ 4,18	↓ -1,45	↑ 1,30	↓ -1,02	↑ 1,42	↓ -0,77	↑ 1,05	↓ -0,97
miR-499-5p	<i>Dnajc12</i>	↑ 2,58	↑ 1,30	↑ 2,46	↑ 1,86	↑ 4,18	⇒ 0,18	↑ 1,30	↓ -2,23	↑ 1,42	↓ -2,25	↑ 1,05	↓ -2,06
miR-499-5p	<i>Gngt1</i>	↑ 2,58	↓ -1,21	↑ 2,46	↓ -0,59	↑ 4,18	↓ -1,58	↑ 1,30	↑ 0,77	↑ 1,42	↑ 0,77	↑ 1,05	↑ 0,99

S2 Fig. Validation of DEGs using qPCR.

Each dot or circle represents the ΔC_q -value from the qPCR analysis and the $\log_2[\text{normalized count}]$ from the RNA-Seq analysis of the selected targets analyzed for B6 control (circle) and B6 LDR samples (dot). The selected genes of interest are listed to the right.



S1 Table. Excel file containing all identified statistically significant DEGs.

DEGs representing one day post-radiation are found in the sheet: "DEGs_one_day_post_rad", the late response is seen in sheet: "DEGs_>100days_post_rad", and the identified oxidative stress related DEGs can be found in the sheet: "Ox_Stress_DEGs". DEGs are listed by Gene_name, $\log_2(\text{FoldChange})$, and FDR.

Available Online <https://doi.org/10.1371/journal.pone.0256667.s003>

S2 Table. Excel file containing the total result output using the GO biological process terms.

Available Online <https://doi.org/10.1371/journal.pone.0256667.s004>

Paper I:

The authors` contributions are in compliance with the Vancouver agreement, and were as follows:



The overall animal experiment was planned by AKO, DE and ND, HD participated in termination in harvest of biological samples. AKO, DE, ND, DHO and HD participated in the conceptualisation of the sub-project in question. Experimental planning and lab work were performed by HD assisted by laboratory personnel, commented by ND and AKO. JHK performed the HPLC methylation analysis and provided advice on mtDNA result handling. TT was responsible for transforming the raw sequencing files (obtained from Novogene) to clean data sets suitable for enrichment - and statistical analyses. HD performed all data and statistics analysis on DEGs and qPCR analysis advised by TT, DME and ND. ND performed the correlations analyses using IPA between miRNA and DEGs. HD made all visualizations in the manuscript in collaboration with TT and DE. HD wrote the first draft of the manuscript, and all authors read and commented. The manuscript was finalized by HD, approved by all authors.

Paper II

RESEARCH ARTICLE



Dose rate dependent reduction in chromatin accessibility at transcriptional start sites long time after exposure to gamma radiation

Hildegunn Dahl ^{a,b}, Jarle Ballangby^{a,b}, Torstein Tengs^{a,b,c}, Marcin W. Wojewodzc ^{a,b,d}, Dag M. Eide^{a,b},
Dag Anders Brede^{b,e}, Anne Graupner^{a,b}, Nur Duale^{a,b}, and Ann-Karin Olsen^{a,b}

^aDivision of Climate and Environmental Health, Department of Chemical Toxicology, Norwegian Institute of Public Health, Oslo, Norway; ^bCentre for Environmental Radiation (CERAD), Norwegian University of Life Sciences (NMBU), Ås, Norway; ^cDivision for Aquaculture, Department of breeding and genetics, Nofima, Ås, Norway; ^dDepartment of Research, Section Molecular Epidemiology and Infections, Cancer Registry of Norway, Oslo, Norway; ^eFaculty of Environmental Sciences and Natural Resource Management (MINA), Norwegian University of Life Sciences (NMBU), Ås, Norway

ABSTRACT

Ionizing radiation (IR) impact cellular and molecular processes that require chromatin remodelling relevant for cellular integrity. However, the cellular implications of ionizing radiation (IR) delivered per time unit (dose rate) are still debated. This study investigates whether the dose rate is relevant for inflicting changes to the epigenome, represented by chromatin accessibility, or whether it is the total dose that is decisive. CBA/CaOlaHsd mice were whole-body exposed to either chronic low dose rate (2.5 mGy/h for 54 d) or the higher dose rates (10 mGy/h for 14 d and 100 mGy/h for 30 h) of gamma radiation (⁶⁰Co, total dose: 3 Gy). Chromatin accessibility was analysed in liver tissue samples using Assay for Transposase-Accessible Chromatin with high-throughput sequencing (ATAC-Seq), both one day after and over three months post-radiation (>100 d). The results show that the dose rate contributes to radiation-induced epigenomic changes in the liver at both sampling timepoints. Interestingly, chronic low dose rate exposure to a high total dose (3 Gy) did not inflict long-term changes to the epigenome. In contrast to the acute high dose rate given to the same total dose, reduced accessibility at transcriptional start sites (TSS) was identified in genes relevant for the DNA damage response and transcriptional activity. Our findings link dose rate to essential biological mechanisms that could be relevant for understanding long-term changes after ionizing radiation exposure. However, future studies are needed to comprehend the biological consequence of these findings.

ARTICLE HISTORY

Received 12 October 2022
Revised 16 February 2023
Accepted 8 March 2023

KEYWORDS



Gamma radiation; chronic exposure; acute exposure; low dose rate; long-term response; chromatin accessibility; ATAC-Seq; CBA mice strain

Introduction

Ionizing radiation (IR) is an environmental carcinogen [1], with natural (radon, cosmic, soil and food) and human-made (medical, nuclear industry and power plant accidents) exposure sources. Exposure to IR occurs through different radiation regimes (low or high doses and dose rates; acutely, chronically, or protracted). Solid cancers [2] and leukaemia [3] are well-known radiation-induced human health effects [4]. However, health effects also extend to other possible conditions, including cardiovascular [5–7], metabolic [8,9] and ocular diseases [10]. The predictions of health effects from exposure to IR are based on populations mainly exposed to high doses and high dose rates (e.g., A-bomb survivors from Hiroshima and Nagasaki (the Life Span Study

[11]). Whether the risk coefficients drawn from these studies are relevant when predicting health risks from nuclear incidents where lower doses and dose rates of IR are more typical, like the Chernobyl [12] and the Fukushima Daiichi nuclear powerplant accidents [13], is still debated [14–16].

Ionizing radiation introduces a range of cellular effects, from direct DNA damage and the induction of reactive oxygen species (ROS) [17,18]. These IR-induced insults further activate events to restore cellular and genetic integrity, like the recognition of DNA damage, cell cycle arrest, damage repair, and cellular death [19–21]. Events dependent upon the dynamic regulation of the chromatin structure [22–25]. Epigenetic changes are also reported after

CONTACT Hildegunn Dahl  hildegunn.dahl@fhi.no  Division of Climate and Environmental Health, Department of Chemical Toxicology, Norwegian Institute of Public Health, Oslo, NO-0213, Norway

 Supplemental data for this article can be accessed online at <https://doi.org/10.1080/15592294.2023.2193936>

© 2023 The Author(s). Published by Informa UK Limited, trading as Taylor & Francis Group.

This is an Open Access article distributed under the terms of the Creative Commons Attribution License (<http://creativecommons.org/licenses/by/4.0/>), which permits unrestricted use, distribution, and reproduction in any medium, provided the original work is properly cited. The terms on which this article has been published allow the posting of the Accepted Manuscript in a repository by the author(s) or with their consent.

radiation exposure [26–28], like DNA methylation of cytosines [29] and post-translational modification of histones [30–32]. These epigenetic mechanisms can adopt chromatin accessibility without changing the DNA sequence. The chromatin can thus be viewed as the functional form of genetic information referred to as the epigenome. Gene expression and transcriptional activity are, therefore, intimately linked to the chromatin structure and the remodelling dynamics [33]. Over the years, studies have addressed altered gene expression as a mechanistic explanation for radiation-induced outcomes [34–37]. However, how these responses progress to disease and how the dose rate is relevant to the outcome is debated [38–42].

There is a growing understanding of the epigenome's relevance for cancer initiation and progression [43]. Therefore, considering the extent of IR-induced responses affecting the epigenome, mapping the radiation-induced changes in chromatin accessibility (how it rearranges upon exposure and how this could be linked to changes in gene expression) could be essential for establishing causality between radiation-induced effects and the progression of adverse health effects. The Assay for Transposase-Accessible Chromatin using DNA sequencing (ATAC-Seq) is an epigenomic method for mapping open chromatin regions (OCRs) using a probing transposase (Tn5) [44,45]. The Tn5 cleaves the DNA at open chromatin regions and simultaneously inserts adapters for high-throughput DNA sequencing (HTS). The Omni-ATAC-Seq [46] reduces the contamination from mitochondrial DNA and is optimized for frozen tissues making it suitable for extensive animal experiments.

In this study, we investigated two hypotheses related to the epigenomic effects of ionizing radiation. We hypothesize that exposure to gamma radiation inflicts significant changes in the epigenomic feature of chromatin accessibility. Furthermore, we hypothesize that radiation-induced changes in chromatin structure persist over time, depending on the dose rate. The hypotheses were addressed by characterizing

whole-genome chromatin accessibility in liver tissue of mice exposed to acute high, intermediate, or chronic low dose rate gamma radiation, all to a total dose of 3 Gy.

Materials and methods

Animals and housing

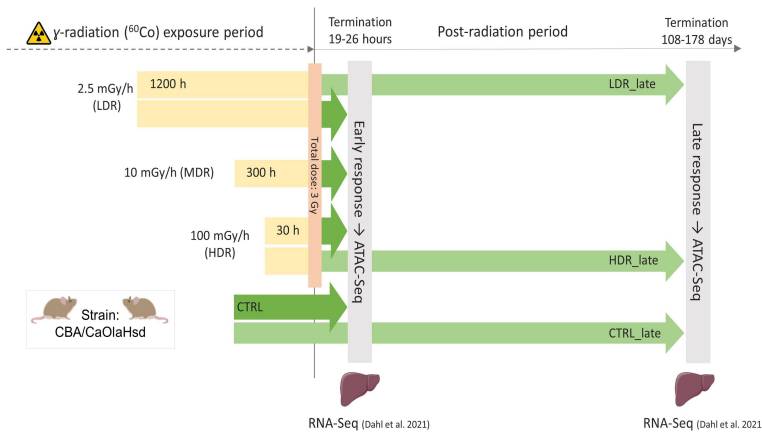
This study follows the previous descriptions of the animal experiment [36,47]. Specific Pathogen Free CBA/CaOlaHsd (3–8 weeks) mice were purchased from Envigo (Horst, The Netherlands). Acclimation took place for a minimum of 4 d. The mice were then randomly housed in groups of two to three in individually ventilated disposable PET plastic cages (IVC racks) (Innovive, San Diego, USA) using Aspen tree bedding (Nestpack, Datesand Ltd., Manchester, UK). Temperature and light conditions were controlled ($21 \pm 2^\circ\text{C}$, $45 \pm 15\%$ relative humidity, 50 air changes h^{-1} and photoperiod 12:12 (L:D). Mice had ad libitum access to tap water in PET bottles and SDS RM1 feed (Special Diet Services, Essex, UK). Due to space limitations in the radiation field, the mid-dose rate (MDR) groups were housed outside the IVC rack during irradiation, but in the same disposable PET cages but using transport lids. At termination, the mice were administered anaesthesia using ZRF-cocktail (Zolazepam, Tiletamine, Xylazine, and Fentanyl) followed by heart puncture before cervical dislocation and collection of tissues. The tissues were snap-frozen in liquid nitrogen and stored at -80°C . We adhered to the national legislation for animal experimentation, and the experimental protocol was approved by the Norwegian Food Safety Authority (NFSA, approval no. 8803). No mice died or showed clinical signs due to the exposure.

Radiation and dosimetry

As previously described [47], all groups received gamma radiation (^{60}Co -source) exposure using different dose rates (DR); 2.5 (low DR (LDR)), 10.0 (mid DR (MDR)) and 100.0 (high DR (HDR)) mGy/h (Table 1, Figure 1). The pre-calculated duration of exposure was 1200 h, 300 h

Table 1. Experimental descriptive details: groups, post-radiation time in days, dose rate, age at termination in days, and number of samples per group used in ATAC-Seq.

Groups		Days post-radiation mean \pm SD	Nominal dose rate (mGy/h)	Whole-body absorbed dose (Gy)	Age at termination (days) mean \pm SD (range)	n samples ATAC-Seq
Early response	CTRL	-	-	-	70 \pm 0	5
	LDR	1 \pm 0	2.5	2.60 \pm 0.19	112 \pm 0	3
	MDR	1 \pm 0	10	2.67 \pm 0.16	70 \pm 0	3
	HDR	1 \pm 0	100	2.65 \pm 0.13	63 \pm 0	3
Late response	CTRL_late	-	-	-	185 \pm 70 (118–245)	4
	LDR_late	108 \pm 0	2.5	2.60 \pm 0.19	216 \pm 0	3
	HDR_late	149 \pm 35	100	2.65 \pm 0.13	248 \pm 34 (216–284)	3

**Figure 1.** Experimental design ATAC-Sequencing was utilised to investigate radiation-induced effects on liver chromatin accessibility at two post-radiation timepoints: early (19–26 hours) and late (108–178 d). Gamma radiation was administered using three dose rates (low (LDR), mid (MDR) and high HDR)) to a total dose of 3 Gy. Liver samples were collected for ATAC-Seq (current study) and transcriptional response both early and late (RNA-Seq) [36].

and 30 h for the respective groups. Dosimetry was performed using nanoDots as described [48,49]. The numeric value of air kerma to whole-body absorbed dose conversion coefficient for chronic exposures was 0.932 ± 0.008 , resulting in a total whole-body absorbed dose of 2.60 ± 0.19 Gy for the 2.5 mGy/h-group, 2.67 ± 0.16 Gy for the 10 mGy/h-group, and 2.65 ± 0.13 Gy for the 100 mGy/h-group, all denoted as 3 Gy throughout the article. The irradiation took place at the FIGARO low dose gamma irradiation facility, managed by the CoE Centre of Environmental Radioactivity (CERAD CoE, Norwegian University of Life Sciences, Ås, Norway) [48,50,51]. For animal care, the irradiation was interrupted daily (30–120 min). Thus, the beam-on time was adjusted according to animal care off-time to achieve the

pre-calculated total dose of 3 Gy. Cage positions were rotated daily to assure uniform exposure. Unexposed control mice were housed behind lead shielding outside the radiation field but inside the exposure room. Further details regarding dosimetry and the current experimental design have been described [36,47].

Experimental design

The mice ($n = 35$) were divided into four experimental exposure groups (controls (CTRL), LDR, MDR and HDR) (Figure 1, Table 1). The CTRL, LDR, and HDR were further divided into two post-radiation termination groups. A total of seven experimental groups were thus generated; four groups were terminated 19–26 hours after

the end of irradiation (Early response groups: CTRL, LDR, MDR and HDR, and three groups were terminated after a post-radiation period of 108–178 d (late response groups, CTRL_late, LDR_late, and HDR_late. CTRL and CTRL_late represent the corresponding control groups for the two termination timepoints, early and late, respectively. The mice were transported to the Norwegian Institute of Public Health (NIPH, Oslo, Norway) for post-radiation housing until termination.

Assay for transposase-accessible chromatin (ATAC-Seq)

Samples ($N = 24$) were processed using an ATAC-Seq protocol for frozen tissues (Omni-ATAC) [46]. Approximately 20 mg of liver tissue was collected from snap-frozen samples stored at -80°C and homogenized in 1 mL OptiPrep solution D in a 7 mL Kimble Dounce tissue grinder set (DWK Life Sciences, Mainz, Germany) as described [46]. All steps were performed on ice unless specified otherwise. The tissue was homogenized using six strokes with pestle A and six with pestle B. The homogenate (400 μL) was diluted 1:1 in OptiPrep solution C (5:1 of OptiPrep solution A and OptiPrep solution B (Sigma-Aldrich® Brand (cat. nr: D1556), Merck KGaA, Darmstadt, Germany)) to a final concentration of 25% iodixanol. A gradient consisting of two layers of iodixanol, 29% (w/v) and 35% (w/v), was used to separate the nuclei ($3000 \times g$, 4°C , 20 minutes). The band of nuclei was extracted (200 μL) and diluted in 800 μL ATAC-RSB, and pelleted at $500 \times g$ for 10 min at 4°C . The nuclei pellet was suspended in ATAC TD-buffer (22 mM Tris – HCl pH 7.4, 10 mM MgCl_2 , 20% Dimethylformamide; pH 7.4) to a final concentration of 50 K – 100 K nuclei/50 μL . The nuclei solutions (50 μL) were incubated at 37°C for 30 min with 2.5 μL Illumina Tagment DNA Enzyme Illumina, San Diego, CA, USA (cat. nr: 20034197) for tagmentation. The fragmented DNA was purified using PCR Purification Kit (QIAGEN, Hilden, Germany) and eluted in 20 μL elution buffer. Amplification of the tagged DNA (20 μL) was performed using 25 μL 2 \times NEBnext High-Fidelity PCR Master Mix (New England BioLabs (cat. nr:

M0541L), Ipswich, MA, USA) and 2.5 μL forward and reverse Nextera DNA CD indexes (Illumina, San Diego, CA, USA). The cycling conditions were: (1) 72°C for 5 min, (2) 98°C for 30 sec, (3) 98°C for 10 sec, (4) 63°C for 30 sec, and (5) 72°C for 30 sec. Steps 3–5 were repeated five times. Based on a tape station trace (4200 TapeStation, Agilent, Santa Clara, USA), the libraries were further amplified with 5–7 cycles (to a total of 10–13 cycles). The libraries were purified and size-selected using AMPure XP beads (Beckman Coulter, Brea, CA, USA) to eliminate fragments <100 nt and >1500 nt and diluted to 5 nM. Paired-end sequencing (PE150) with an average depth of 50 million raw reads was sequenced on Illumina NovaSeq6000 at Novogene Co., Ltd (Cambridge, UK).

Pre-processing of sequencing reads and downstream analysis

Sequencing

The exact parameters of pipelines used for raw-data and differential analysis are presented in Supplementary_1 (S1). The FASTQC files were quality controlled using the FASTQC tool (bioinformatics.babraham.ac.uk/projects/fastqc/). Adapter trimming was performed using Trim Galore! (bioinformatics.babraham.ac.uk/projects/trim_galore/). The reads were aligned to the mouse genome (GRCm38) with BWA [52] using the nf-core ATAC-seq pipeline [53]. Further, the reads from accessible regions (<100 nt) were extracted from the Binary Alignment Map (BAM) files and peak called using MACS2 (v2.2.7) [54]. The quality of peaks were controlled using the ChIPQC (v1.26.0) [55], and non-overlapping consensus peaks in 8 of the 24 biological samples were used for differential analysis. The ATAC-Seq raw reads supporting the findings in this study are made openly available at the public NCBI Sequence Read Archive (SRA) (www.ncbi.nlm.nih.gov/sra), using BioProject accession id: PRJNA832920.

Analysis of differentially accessible regions (DARs)

All downstream analysis was performed using R-statistical environment (R-Core Team (2020)). Differentially accessible peaks were called using

DESeq2 (v1.30.1) [56] and adjusted for the age of animals, as age could potentially introduce changes in chromatin structure [57]. Statistically significant differentially accessible regions (DARs) were identified using a false discovery rate (FDR) <0.1 when comparing exposure groups to the respective control group (early: LDR vs CTRL, MDR vs CTRL, HDR vs CTRL and late: LDR_late vs CTRL_late and HDR_late vs CTRL_late). DAR-associated genes (DAGs) were annotated using ChIPseeker (v1.26.2) [58] with 'org.Mm.eg.db' (3.8.2) [59]. Entrez gene identifiers were used. All the genes in proximity to the DARs (regardless of distance and genomic region) were identified as a DAR-associated gene (DAG) ('nearest approach').

Enrichment analysis of DAR-associated genes (DAGs)

MetaScape (v3.5, used: 23.02.2022), a web-based tool, (<http://metascape.org>) was used for multiple gene-lists enrichment analysis [60]. In short, the default settings for enrichment were used and covered the following ontology sources: KEGG Pathway, GO Biological Processes, GO Cellular Components, GO Molecular Functions, Reactome Gene Sets, CORUM, TRRUST, PaGenBase, WikiPathways and PANTHER Pathway. P-value <0.01 (accumulative hypergeometric distribution), min. overlap of three genes, and an enrichment factor >1.5 were used to identify statistically significant terms. By default, the whole genome is used as background gene list by MetaScape for enrichment analysis. The top 20 statistically significant terms represent each cluster in the cytoscape, surrounded by membership terms with a similarity score >0.3 . Benjamini-Hochberg procedure is used for adjusted p-value (q-value). The complete MetaScape-output is found in Supplementary_2 (S2).

Comparing the ATAC-Seq data with RNA-Seq

The association between differentially expressed genes (DEGs) from our previously reported RNA-Seq data [36] and the DAGs in the current study was performed. Hepatic RNA isolation, mRNA

sequencing and data analysis are described in [36]. The list of differentially expressed genes (DEGs) were found from in Dahl et al. (2021) supplementarytable 1, and cross-analysed with the ATAC-Seq data. The RNA sequencing raw data is available at the NCBI Sequence Read Archive (SRA) (PRJNA747753).

First, the DAGs overlapping a DEGs were visualized using the web-based tool, InteractiVenn [61]. Further, the mRNA expression levels (\log_2FC) were categorized as 'up-regulated' or 'down-regulated' based on the expression level threshold cut-offs of $\log_2(\text{FoldChange}) > \pm 0.3$, respectively. When the mRNA $\log_2(\text{FoldChange})$ fell between the cut-offs, the mRNA expression was classified as 'stable' (unaffected by exposure). If the gene identified as a DAG had no mRNA data, the DAG were classified as 'not expressed.' The DAGs were grouped based on the chromatin accessibility as reduced (negative \log_2 -ratio) or gained (positive \log_2 -ratio), and the two categories presented in a mosaic plot.

Results

To investigate the influence of dose rate (chronic and acute) on chromatin landscape, whole-genome ATAC-Sequencing were performed on tissue collected from mouse livers. The chromatin accessibility was evaluated at two post-radiation timepoints: one day post-radiation (early) and after a longer post-radiation period (late). We will focus on the LDR and HDR exposure groups, both early and late.

Quality control of ATAC-Seq

The quality of the libraries was assessed both to validate the ATAC-Seq protocol and the results according to recommendation [44,46]. The tagmentation procedure showed the expected distribution with abundance of sequenced fragments less than 100 bases and progressively fewer fragments of larger size (Figure 2a). Principal component analysis (PCA) showed no batch effects (Figure 2b). After quality filtering and adaptor removal, the overall rates of aligned reads to mg38 ranged from 93.8% to 98.6% (Supplementary_3 (S3)). A total of 65,981

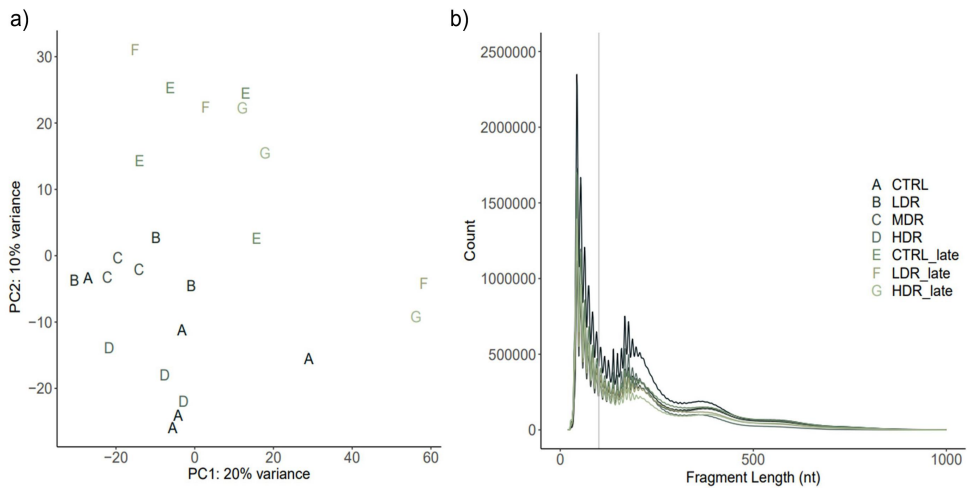


Figure 2. ATAC-Seq quality control by the sequenced fragments length distribution and principal component analysis a) a principal component analysis (PCA) plot illustrates the samples sorted represented by experimental group using upper-case letter and color. b) Transposase tagmentation sequence fragment lengths distribution. Each line represents the mean counts per fragment per experimental group. Fragment lengths up to 100 bp represents the ATAC-Seq fragments corresponding to nucleosome-free regions (NFRs) used for peak calling. The characteristic shape of waves along the x-axis (fragments length) represents fragments spanning nucleosomes; mono- (186–282 bp), di- (ca 400 bp) and tri- (ca 600 bp) nucleosomes. The fragment distribution per sample in Supplementary 4 (S4).

consensus peaks were identified when merging the peak data sets from controls and experimental groups. The identified peaks were associated with 31,121 ENSMUST transcripts, representing 17,164 different genes (Ensembl 102) [62].

Radiation-induced changes in genome-wide chromatin accessibility

To identify changes in the chromatin landscape driven by dose rate at the post-radiation time-points, we contrasted all exposure groups to their respective control group. Statistically significant ($FDR < 0.1$) differentially accessible regions (DARs) were identified for all contrasts except LDR_late vs CTRL_late (Table 2,

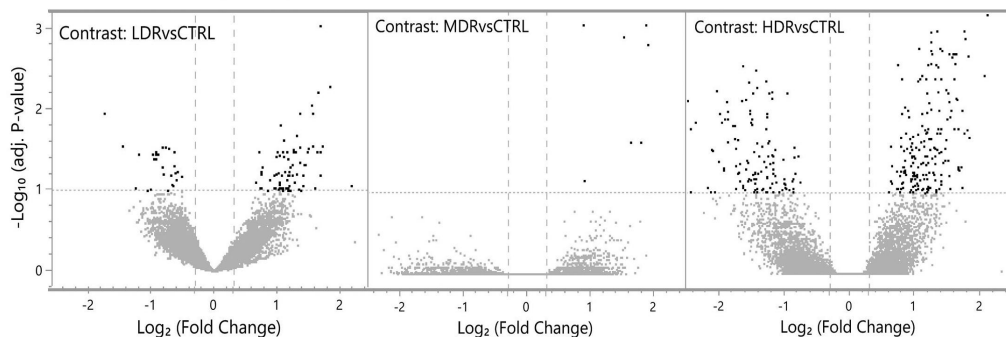
Figure 3). The magnitude of changed chromatin accessibility and the statistical significance is illustrated in volcano plots (Figure 3). Higher numbers of DARs were observed in HDR compared to LDR one day post-radiation (early) (Table 2). By stratifying the early response DARs in gained accessibility (positive \log_2 -ratio) and reduced accessibility (negative \log_2 -ratio) more than 60% of the DARs in all three groups showed gained accessibility compared to control (CTRL). Few DARs were identified for MDR, all of them had gained accessibility.

Following the longer post-radiation period (late), the chromatin accessibility in chronic low dose rate exposed mice (LDR_late) were not different from control mice, while the high

Table 2. Differentially accessible regions (DARs) by dose rate. The DARs ($FDR < 0.1$) are stratified into regions with gained or reduced accessibility contrasted to the respective control group (relative percentage in brackets). The total number of DAR-associated genes (DAGs) is listed with the numbers of DAGs also identified by RNA sequencing in Dahl et al. 2021 in brackets (*mrna).

Group Contrasts		Total DARs	Reduced accessibility	Gained accessibility	DAGs (*mrna)
Early response	LDR vs CTRL	100	26 (26%)	74 (74%)	96 (67)
	MDR vs CTRL	7	0	7 (100%)	7 (6)
	HDR vs CTRL	326	121 (36%)	205 (64%)	295 (161)
Late response	LDR_late vs CTRL_late	0	0	0	0
	HDR_late vs CTRL_late	371	360 (97%)	11 (3%)	364 (331)

a) Early (1 day after exposure)



b) Late (>100 days after exposure)

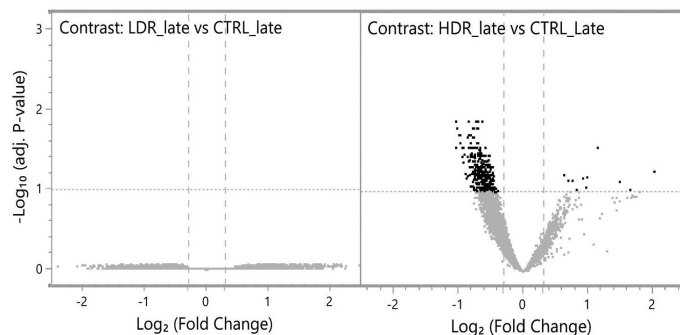


Figure 3. Differentially changed accessible regions (DARs) the statistical significance and the magnitude of the differentially changed accessible regions (DARs, dark spots) are presented as repressed (upper left quadrant) or gained (upper right quadrant) compared to controls, using false discovery rate (FDR) < 0.1, illustrated by the horizontal line at $-\log$.

dose rate exposed mice were markedly different from controls (HDR_late). The DARs identified for HDR_late vs CTRL_late demonstrated almost exclusively reduced accessibility (Table 2).

The overlap between exposure groups was evaluated to identify a radiation dose-specific chromatin DAR peak signatures. The most prominent finding is the large fraction of dose-rate- and time-point-specific responses, as only few of the DARs overlapped between the exposure groups. All the early groups share three DARs, LDR_early and HDR_early shared nine DARs, HDR_late shared four DARs with LDR_early. HDR_late did not share any DARs with HDR_early (Figure 4a).

Functional classification of DARs

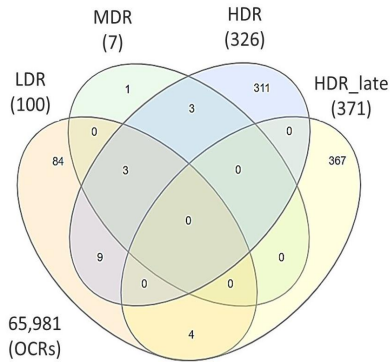
The genomic elements containing the open chromatin regions (OCRs) were identified (Figure 4c,

Table 3). The results showed that the occupancy within genomic elements differed between dose rates and post-radiation timepoints. At DPR1, DARs were mostly present within promoters (≤ 1 kb), distal intergenic and intronic regions. However, the DARs occurrence differed between chronic LDR and the acute HDR exposure one day post-radiation, which demonstrated fewer DARs in promoter regions and more in intergenic and intronic regions (Supplementary Table). The HDR_late DARs were almost exclusively located in promoter (≤ 1 kb) regions (92%). Of these 94% were found at the transcriptional start site (TSS).

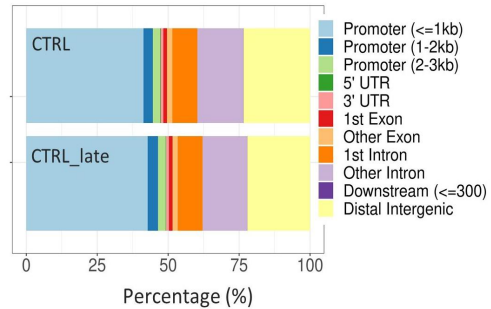
The DAR-associated genes (DAGs)

Only few DARs were localized to the same gene, seen by the lowered numbers of DAGs compared to DARs in Table 2. As for the DARs, most of the DAGs are dose-rate-specific (Figure 4b) and

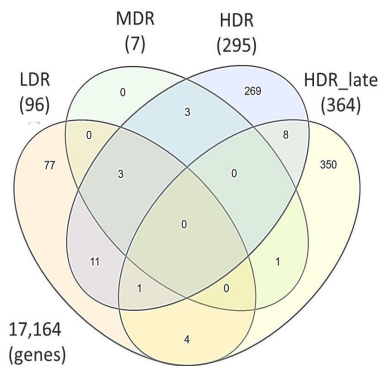
a) Differential Accessible Regions (DARs)



c) Distribution of Open Chromatin Regions (OCRs) to genomic elements



b) DAR-associated genes (DAGs)



d) Distribution of DARs to genomic elements

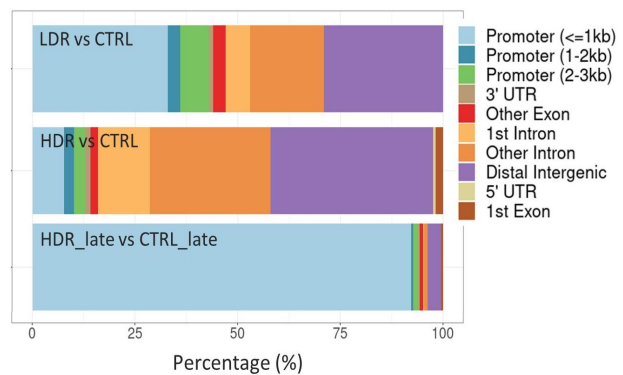


Figure 4. Overlap of Differential Accessible Regions (DARs) and DAR-associated genes (DAGs), and the allocation of open chromatin regions (OCRs) and DARs to genomic elements. Venn diagrams of DARs (a) and DAGs (b) for all experimental groups. The numbers of DARs and DAGs for each group in brackets. Total numbers of identified OCRs (a) and the corresponding genes (b) outside Venn diagram. c) Allocation of OCRs to genomic elements for both controls (CTRL and CTRL_late) after merging the biological replicates. d) Allocation of DARs after contrasting the experimental group to respective controls. MDR and LDR_late are not represented in d) due to few or no DARs identified, respectively. The distribution of the DARs within the genomic elements of the exposure groups were tested by χ^2 -test and found statistically significant different (χ^2 statistics = 472.62, p -value < 0.001).

a slight increase in the number of overlapping DAGs between the dose rate groups were seen. Even if the gene overlap was marginal, the enriched pathways network showed shared biological functions between HDR_early and HDR_late (Figure 5, Supplementary 2).

In general, the network of enriched pathways also supports a specific response for each dose rate, both early and late. Few significantly enriched pathways were identified for LDR_early and for HDR_early DAGs. The numbers of MDR DAGs were too few to impact the overall enrichment analysis (Supplementary 2). The highest number of enriched terms were found for

HDR_late, and they were in majority specific to this group (Figure 5c). Enriched terms found for LDR_early is related to aspects of lipid metabolism (Glycerolipid biosynthesis (adj. p -value 0.009) and HDL remodelling (adj. p -value 0.013)). For HDR_early, the trend was the same, with few enriched pathways, which functions were related to the GO term 'Small-molecule metabolic processes' (adj. p -value 0.0004).

The most enriched pathway for HDR_late included 'Cellular response to DNA damage stimulus' (adj. p -value 0.0001), 'IL-5 signalling pathway' (adj. p -value 0.0001) and 'Transcription factor AP-1 complex' (adj. p -value 0.0031). The

Table 3. Relative portion of open chromatin regions (OCRs) and differential accessible regions (DARs) allocated to genomic elements.

Genomic Element	Open Chromatin Regions (OCRs)						Differential accessible regions (DARs)				
	Early				Late		Early			Late	
	CTRL	LDR	MDR	HDR	CTRL _{late}	LDR _{late}	HDR _{late}	LDR vs CTRL	MDR vs CTRL	HDR vs CTRL	HDR _{late} vs CTRL _{late}
Promoter (<=1kb)	41.3	42.4	43.3	30.9	42.8	49.2	50.8	33.0	28.6	7.7	92.2
Distal Intergenic	23.5	22.5	21.8	26.3	22.1	20.1	19.9	29.0	28.6	39.6	3.2
Other Intron	16.2	15.9	15.5	19.6	15.7	13.8	13.6	18.0	28.6	29.4	0.8
1st Intron	8.8	8.8	9.0	10.7	8.8	7.6	7.3	6.0		12.6	0.3
Promoter (1-2kb)	3.3	3.4	3.6	4.3	3.7	3.3	2.7	3.0		2.5	0.5
Promoter (2-3kb)	2.6	2.6	2.7	3.4	2.7	2.2	1.9	7.0		2.8	1.3
Other Exon	1.9	1.9	1.8	2.0	1.8	1.6	1.6	3.0	14.3	1.8	0.8
1st Exon	1.2	1.3	1.2	1.2	1.2	1.2	1.2			1.8	0.5
3' UTR	1.0	1.0	1.0	1.3	1.1	0.9	0.8	1.0		1.2	0.3
5' UTR	0.2	0.1	0.1	0.1	0.1	0.2	0.1			0.6	
Downstream (<=300)	0.1	0.1	0.1	0.1	0.1	0.1	0.1				
Total (%)	100	100	100	100	100	100	100	100	100	100	100

cluster ‘Cellular response to DNA damage stimulus’ (red nodes in [Figure 5A](#)) also comprises the GO term ‘DNA Repair’ and ‘Double-strand break repair’.

HDR_{late} shared only five terms with HDR_{early}, although only slightly significant for HDR_{early}. Examining genes enriched to several terms, mutual DAGs are shared between ‘Transcription factor binding’, ‘Negative regulation of cell differentiation’ and ‘Haematopoietic or lymphoid organ development’. ‘Circadian rhythm’ and ‘Regulation of fat cell differentiation’ also shared DAGs.

Association between chromatin accessibility and transcription profile

Chromatin structure is relevant for gene expression, and the overlap between the identified DAGs and the differentially expressed genes (DEGs) [36] was explored ([Figure 6](#)). Some overlap between the early DAGs and the DEG was seen. Further on, no overlap was observed late after exposure. However, correlating the DAGs and the RNA-Seq gene transcripts, only very weak correlations were seen between these variables (data not shown). Therefore, the association between the DARs chromatin state (reduced accessibility, gained accessibility, or stable) and the direction of gene expression (down-regulated, up-regulated, stable, or not expressed) are addressed in [Figure 7](#).

Most of the identified DAGs (regardless of chromatin state) had stable RNA transcription

levels, and no clear association were seen between a reduction or increase in the accessibility and the expression level of the cognate gene. A higher portion of the DAGs identified early, compared to late, had no detectable transcripts. Even if the DARs for HDR_{late} showed reduced accessibility, most of the cognate genes showed stable gene expression levels (297), whereas a small fraction of the genes was up-regulated (23), and another fraction was down-regulated (11).

Discussion

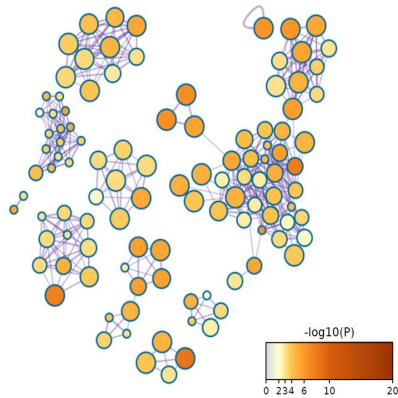
This study explores how chronic low dose rate gamma radiation impacts chromatin accessibility and whether changes in chromatin could persist long time after exposure to ionizing radiation. We demonstrate that modifications to the epigenome, represented by chromatin accessibility, were dose rate dependent, not only one day post-radiation but also after a post-radiation period of more than 3 months. We found that exposure to chronic low dose rate; 1) generated a different chromatin pattern compared to acute high dose rate one day post-radiation, and 2) the chromatin state was restored and comparable to controls over 3 months after irradiation. Long-term chromatin changes were only observed after acute HDR exposure. These changes were evident by the reduction in chromatin accessibility at transcriptional start sites (TSS) of genes related to DNA double-strand breaks and regulation of transcriptional activity.

We have focused on the LDR and HDR-groups, both early and late, since few DARs were identified

a) Clusters of biological terms



- Cellular response to DNA damage stimulus (GO:0006974)
- IL-5 signaling pathway (WP151)
- Regulation of small molecule metabolic process (GO:0062012)
- Transcription factor binding (GO:0008134)
- Transcription factor AP-1 complex (GO:0035976)
- Protein kinase binding (GO:0019901)
- Kinase activity (GO:0016301)
- Circadian rhythm (GO:0007623)
- Macrolide binding (GO:0005527)
- Regulation of myeloid cell differentiation (GO:0045637)
- Glycerolipid biosynthetic process (GO:0045017)
- Transcription repressor complex (GO:0017053)
- Neuronal cell body (GO:0043025)
- Vitellogenesis (GO:0007296)
- HDL remodeling (R-MMU-8964058)
- Hematopoietic or lymphoid organ development (GO:0048534)
- Negative Regulation of cell differentiation (GO:0045596)
- TP53 Regulates Transcription of Cell Cycle Genes (R-MMU-6791312)
- Regulation of fat cell differentiation (GO:0045598)
- Pathways in cancer (mmu05200)

b) p-value ($-\log_{10}$)

c) Dose rate group

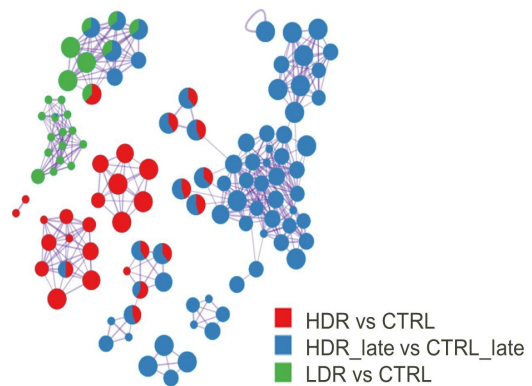


Figure 5. Network of top 20 enriched biological terms of the DAGs. The identical clustering network is presented as: (a) biological terms by colouring. Node size reflects number of input genes. The list of terms is sorted by p-value. b) p-value ($-\log_{10}(\text{p-value})$), and c) coloured according to contrast group, where each pie sector is proportional to the number of hits from the respective input gene list. The MDR exposure group is not represented due to few DAGs.

in the MDR_early group, and no linear dose-rate dependent trend was observed. Similar findings for the MDR group were also observed in our previous RNA-Seq data [36]. One possible explanation for the observed MDR group discrepancy might be related to the space limitations in the radiation exposure field, resulting in housing of the MDR mice in cages outside the IVC rack. However, non-monotonic dose responses are previously observed and discussed by others [28,63,64], alleging that the reduced response for a mid-dose rate could be linked to biological

aspects rather than experimental issues, and should be pursued in future studies.

One day post-radiation, the results support that gamma radiation remodels chromatin accessibility. This remodelling appeared dose-rate-specific, where HDR exposure led to more extensive changes than LDR exposure. These results are coherent with the transcriptomic profiles that also demonstrated gene perturbations to be dose-rate-specific [36]. This pattern was seen for DARs, DAGs and the DAGs functional enrichment analysis. Common traits between LDR and HDR were

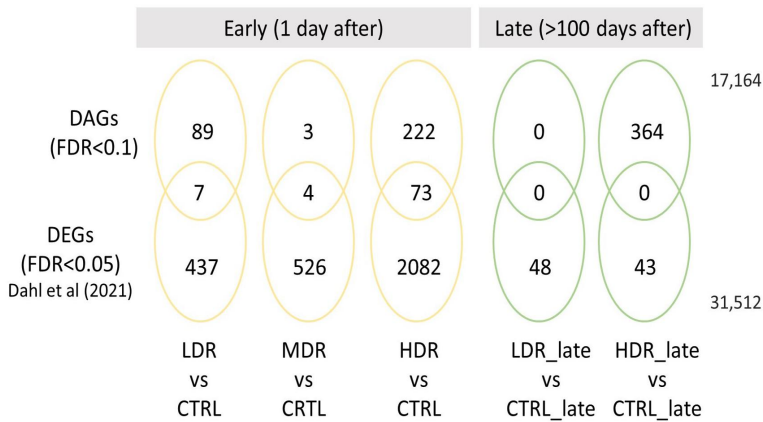


Figure 6. The association between the DAGs and previously reported differentially expressed genes (DEGs) Overlap between statistically significant DAGs (Fdr<0.1) derived from ATAC-Seq and the previously published statistically significantly (Fdr<0.05) differentially expressed genes (DEGs) in Table S1 found in Dahl et al (2021) [36]. Total numbers of genes outside Venn diagram.

seen when the allocation of the DARs to the genomic elements, where the most striking difference was found in intergenic and intronic regions where the number of DARs allocated to the regions increased with dose rate. Except for MDR, which showed few chromatin changes. Intergenic and intronic regions are assumed to possess essential transcriptional regulatory regions like enhancer elements [65]. Most of the identified DARs gained accessibility (>60%) one day post-radiation for both the LDR and HDR exposure, indicative of a possible linkage to the increase in transcriptional activity [36].

The enrichment analysis of both LDR_early and HDR_early DAGs revealed terms related to metabolic processes. Mechanisms previously showed to respond to radiation [66,67]. Further, the enrichment analysis revealed few statistically significant terms for both LDR_early and HDR_early. Since all the DARs were cognate to the nearest proximal gene, this could introduce ‘false genes’ and confound the enrichment analysis. Implying that the DARs harbour distal regulatory properties to other genes than the nearest. The high number of identified DAGs where the mRNA transcript is not expressed [36] could also support this (Figure 7).

As the ATAC-sequencing method is based on the depletion of nucleosomes, it is presumed that the mapped reads should be in regions associated with transcriptional activity. However, comparing

the DARs with the DEGs from the RNA-Seq analysis [36], some overlap is seen one day post-radiation and none later. Studies attempting to correlate gene expression data with ATAC-Seq data are inconsistent. Some studies show correlation between the chromatin state and gene expression [68–72], and others report no correlation [73,74]. Due to this, and the lack of observed correlation between the data sets herein (data not shown), we stratified the DARs and associated them with mRNA stratified on expression direction (Figure 7). This exercise demonstrated that chromatin regions with reduced accessibility were proximal to or within upregulated genes and vice versa. This indicates that changes in chromatin configuration are not strongly associated with mRNA expression in samples collected at the same time points (Figure 7), as also observed by others [68]. We assume that the transcriptional activity observed could represent past events compared to the chromatin status. Hence, differentially expressed genes do not necessarily have differentially changed accessible regions nearby in response to radiation. It should be noted that reduced chromatin accessibility also can be linked to increased transcriptional activity through binding of regulatory proteins [75].

The results one day post-radiation supports a generally accepted presumption that the biological system responds differently to chronic low and

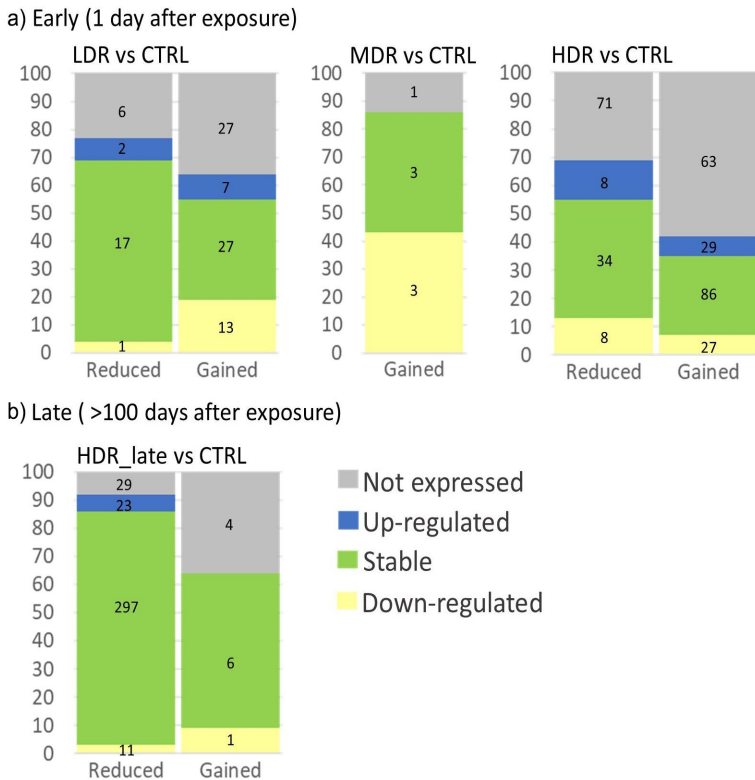


Figure 7. The association between the chromatin accessibility and the gene expression directions for each exposure group a) early (1 day after) and b) late (>100 d after). Each DAR corresponds to the nearest gene (DAGs), and the expression of these DAGs have been extracted using the RNA-Seq data [36]. The DAGs expression level is categorised as “not expressed” (not detected mRNA), “up-regulated” when $\log_2(\text{FoldChange}) > 0.3$, “stable” when $-0.3 \leq \log_2(\text{FoldChange}) \leq 0.3$ and “down-regulated” when $\log_2(\text{FoldChange}) < -0.3$. The mosaic plots represent the percentage of genes in each RNA expression category, and the numbers inside the bar show the number of genes in each category. The mosaic plot for LDR_late is missing as no DARs were identified. .

acute high dose rates when given the same total dose. However, this statement is highly debated due to inconsistent cellular, animal, and human research results [40,76]. The dose rate related response, seen in this study, could be linked to several factors like type and repair of DNA damage [77], as the DNA damage response introduces alterations to the chromatin structure (reviewed in [78]). Changes in the chromatin packaging are also suggested to be an essential factor for DNA damage, as condensed chromatin, due to the nucleosome-binding of DNA [79], is assumed to be more resistant to radiation damage and the attack from ROS [80–82]. Genomic regions depleted of nucleosomes, such as promoters, are thus more susceptible to DNA damage. This could result in restricting the genomic distribution of

possible DNA damage sites. Therefore, we hypothesize that the difference in chromatin accessibility could be due to the difference in the genotoxic susceptibility between the chronic LDR and acute HDR. However, as the open chromatin regions in tissue represent an average accessibility profile generated from heterogeneous cell types and chromatin states, we anticipate that chromatin changes related to DNA damage-sensing and -repair cannot be detected in bulk tissue using ATAC-Seq alone.

The long-term changes in chromatin accessibility demonstrated a clear dose-rate-specific response. Interestingly, only a long-term response after HDR exposure was identified, while no measurable changes were seen after the LDR irradiation. After the HDR exposure, a significant differential

reduction in accessibility was inflicted, primarily confined to transcriptional start sites (TSS). The magnitude of the late DARs was in the same order as HDR_early, but the regions did not overlap. Additionally, only a few DAR-associated genes (DAGs) overlapped between the two HDR time points. Nevertheless, the enrichment analysis revealed common biological pathways at the two time points. Suggesting that different regions could be connected via biological functions, even if the overlap between the DARs and the DAGs were marginal. Taken together, a shift in chromatin conformation in the period between the sampling timepoints is evident, where the chromatin state after the low dose rate is restored whilst the high dose rate induces long-term changes.

The biological terms enriched for HDR_late are related to known radiation-induced effects, such as DNA double-strand breaks. Other interesting pathways included transcription factor binding relevant for RNA polymerase II, the AP-1 complex and the transcription repressor complex, terms sharing the transcription factors *Jun* and *Fos*. These genes are well-characterized as immediate-early response genes (IEGs) [83], radiation-responsive proto-oncogenes [84], and also, they are the two dimers constituting the AP-1 complex [85]. As we report a reduction in accessibility over TSS in genes enriched to these critical processes, we hypothesize that these results could be related to molecular processes hindering the transposase from accessing the DNA [86,87]. Such could include the protein binding to the DNA (e.g., TFs and polymerase II) [33] or changes in epigenetic states. Identifying specific protein-binding motifs within the DARs genomic sequence could enlighten this issue and should be pursued in future studies.

Epigenetic mechanisms involving altered chromatin accessibility have been linked to multiple radiation-induced effects (reviewed in [28,88]) like histone-methylation (H3K27me3 [89]) resulting in gene repression or gene-specific hyper-methylation [90]. Such changes could be a result of exposure-induced poised or primed genes/promoters. Primed/poised genes are transcriptionally silenced genes in the absence of stimulus, but the promoters have both repressive and activating properties for rapid activation upon new stimuli [91]. It is thus interesting to note that we observed reduced accessibility of

enriched terms related to transcriptional activity. A genome-wide mapping study of chromatin states identified repressed TSSs enriched with active chromatin marks and RNA polymerase II. They also showed that repressive and activating properties are strongly associated with IEGs [92]. A repressed chromatin state does not necessarily represent a condensed chromatin state that hinders transcription but, in contrast, represents a regulatory mark for rapid transcriptional activation upon subsequent stimuli [93]. Taken together, poised/primed genes could be a plausible explanation for our results that could represent essential mechanisms in radiation-induced adaptive response. However, this notion must be verified by methods complementary to ATAC-Seq.

Other factors for the observed long-term HDR response could be linked to changes in the cellular composition of the liver due to cell death, differentiation, or senescence. However, the abovementioned liver responses are seen related to the doses and dose rate used [28,94]. The bulk liver tissue also contains multiple cell types, each of which could have distinct epigenomic patterns. Without complementary methods, it is challenging to comprehend the extent of these possible mechanisms and whether they appear to the extent that would affect the overall ATAC-Seq output. However, hepatocytes are the dominant cell type in the liver [95], and when we compared the gene expression profile [36] with single-cell RNA-Seq data from flow cytometry separated mouse liver cells, the gene expression profile was calculated to comprise >98% hepatocytes (data not shown). We, therefore, assume that the hepatocyte epigenome dominates the signal in these datasets. To detect long-term effects after chronic low dose rate exposure may require a larger experiment than this current study. However, the HDR_late results are evident despite inherent experimental factors (like biological replicates and bulk tissue samples), highlighting a critical difference in acute and chronic long-term potential even though the total dose is the same.

Conclusions

To our knowledge, this is the first study to evaluate the impact of ionizing radiation low chronic vs high acute dose rate exposure on chromatin accessibility to identical total dose of 3 Gy. We show that chronic low dose rate exposure to a high total dose of 3 Gy do not

induce permanent changes in chromatin accessibility, in contrast to the acutely given high dose rate of the same total dose where repressed promoter regions in genes relevant for DNA damage and transcriptional regulation were evident. Our results highlight that dose rate and exposure regime are relevant factors for radiation-induced epigenomic changes to mice liver and is important for understanding long-term changes after ionizing radiation exposure. However, as the ATAC-Seq method alone is insufficient to capture the mechanisms leading to the observed results, future studies are needed to fully comprehend the biological consequence of these findings.

Acknowledgments

The authors acknowledge every contribution throughout the mouse experiment, planning and initiation, animal care, dosimetry, and all the support from colleagues during termination and collection of samples, also for challenging and energetic discussions concerning bioinformatics, statistics, and the biological relevance of the results. We thank Y. Kassaye, K. Gulbrandsen and A. Ikhsani for their assistance with animal care and sampling procedures.

Disclosure statement

No potential conflict of interest was reported by the authors.

Funding

was received from the Research Council of Norway through its Centers of Excellence funding scheme, project number 223268/F50 CERAD.

Data availability statement

The data that support the findings of this study are openly available in the Sequence Read Archive (SRA) at <https://www.ncbi.nlm.nih.gov/sra>, with the reference nr: PRJNA832920.

ORCID

Hildegunn Dahl  <http://orcid.org/0000-0003-4783-4582>
Marcin W. Wojewodzic  <http://orcid.org/0000-0003-2501-5201>

References

- [1] ICRP. The 2007 recommendations of the international commission on radiological protection. ICRP Publication. 2007;103:0146–6453. Contract No: 2-4.
- [2] Preston DL, Ron E, Tokuoka S, et al. Solid cancer incidence in atomic bomb survivors: 1958–1998. *Radiat Res.* 2007;168(1):1–64.
- [3] Folley JH, Borges W, Yamawaki T. Incidence of leukemia in survivors of the atomic bomb in Hiroshima and Nagasaki, Japan. *Am j med.* 1952;13(3):311–321.
- [4] NAS. Health risks from exposure to low levels of ionizing radiation; BEIR VII. Washington, DC: The National Academies Press; 2006p. 422.
- [5] Little MP, Tawn EJ, Tzoulaki I, et al. A systematic review of epidemiological associations between low and moderate doses of ionizing radiation and late cardiovascular effects, and their possible mechanisms. *Radiat Res.* 2008;169(1):99–109, 11.
- [6] Shimizu Y, Kodama K, Nishi N, et al. Radiation exposure and circulatory disease risk: hiroshima and Nagasaki atomic bomb survivor data, 1950–2003. *BMJ (Clin Res Ed).* 2010;340:b5349.
- [7] Gillies M, Richardson DB, Cardis E, et al. Mortality from circulatory diseases and other non-cancer outcomes among nuclear workers in France, the United Kingdom and the United States (INWORKS). *Radiat Res.* 2017;188(3):276–290. DOI:10.1667/rr14608.1
- [8] Akahoshi M, Amasaki Y, Soda M, et al. Effects of radiation on fatty liver and metabolic coronary risk factors among atomic bomb survivors in Nagasaki. *Hypertens Res.* 2003;26(12):965–970.
- [9] Tapio S, Little MP, Kaiser JC, et al. Ionizing radiation-induced circulatory and metabolic diseases. *Environ Int.* 2021;146:106235.
- [10] Minamoto A, Taniguchi H, Yoshitani N, et al. Cataract in atomic bomb survivors. *Int J Radiat Biol.* 2004;80(5):339–345. DOI:10.1080/09553000410001680332
- [11] Ozasa K, Cullings HM, Ohishi W, et al. Epidemiological studies of atomic bomb radiation at the radiation effects research foundation. *Int J Radiat Biol.* 2019;95(7):879–891.
- [12] WHO. Health effects of the chernobyl accidents and special health care programmes; report of the UN chernobyl forum expert group “health”. WHO Press. 2006;9241594179.
- [13] WHO. Health risk assessment from the nuclear accident after the 2011 Great East Japan earthquake and tsunami, based on a preliminary dose estimation. 2013 978 92 4 150513 0.
- [14] Rühm W, Azizova TV, Bouffler SD, et al. Dose-rate effects in radiation biology and radiation protection. *Ann ICRP.* 2016;45(1_suppl):262–279. DOI:10.1177/0146645316629336

- [15] Little MP. Evidence for dose and dose rate effects in human and animal radiation studies. *Ann ICRP*. 2018;47(3–4):97–112.
- [16] SSK. Dose- and dose-rate-effectiveness factor (DDREF), recommendation by the German commission on radiological protection with scientific grounds. Bonn, Germany: German Commission on Radiological Protection; 2014.
- [17] UNSCEAR. Biological mechanisms of radiation actions at low doses; a white paper to guide the scientific committee's future programme of work. United Nations Publications. 2012;45.
- [18] Reisz JA, Bansal N, Qian J, et al. Effects of ionizing radiation on biological molecules—mechanisms of damage and emerging methods of detection. *Antioxidants & Redox Signaling*. 2014;21(2):260–292.
- [19] Mavragani IV, Nikitaki Z, Mp S, et al. Complex DNA damage: a route to radiation-induced genomic instability and carcinogenesis. *Cancers (Basel)*. 2017;9(7):91. DOI:10.3390/cancers9070091
- [20] Azzam EI, Jay-Gerin JP, Pain D. Ionizing radiation-induced metabolic oxidative stress and prolonged cell injury. *Cancer Lett*. 2012;327(1–2):48–60.
- [21] Huang R, Zhou P-K. DNA damage repair: historical perspectives, mechanistic pathways and clinical translation for targeted cancer therapy. *Signal Transduct Target Ther*. 2021;6(1):254.
- [22] Aleksandrov R, Hristova R, Stoynov S, et al. The chromatin response to double-strand DNA breaks and their repair. *Cells*. 2020;9(8):1853. PubMed PMID: rayyan-676545108. 10.3390/cells9081853.
- [23] Pandita T, Kumar R, Horikoshi N, et al. Chromatin modifications and the DNA damage response to ionizing radiation. *Front Oncol*. 2013;2. DOI:10.3389/fonc.2012.00214.
- [24] Tsompana M, Buck MJ. Chromatin accessibility: a window into the genome. *Epigenetics & Chromatin*. 2014;7(1):33.
- [25] Stadler J, Richly H. Regulation of DNA repair mechanisms: how the chromatin environment regulates the DNA damage response. *Int J Mol Sci*. 2017;18(8):1715.
- [26] Merrifield M, Kovalchuk O. Epigenetics in radiation biology: a new research frontier. *Front Genet*. 2013;4:40.
- [27] Tharmalingam S, Sreetharan S, Kulesza AV, et al. Low-dose ionizing radiation exposure, oxidative stress and epigenetic programming of health and disease. *Radiat Res*. 2017;188(4.2):525–538.
- [28] Belli M, Tabocchini MA. Ionizing radiation-induced epigenetic modifications and their relevance to radiation protection. *Int J Mol Sci*. 2020;21(17):5993.
- [29] Miousse IR, Kutanzi KR, Koturbash I. Effects of ionizing radiation on DNA methylation: from experimental biology to clinical applications. *Int J Radiat Biol*. 2017;93(5):457–469. PubMed PMID: rayyan-676545029. 10.1080/09553002.2017.1287454.
- [30] Pogribny I, Koturbash I, Tryndyak V, et al. Fractionated low-dose radiation exposure leads to accumulation of DNA damage and profound alterations in DNA and histone methylation in the murine thymus. *Mol Cancer Res*. 2005;3(10):553–561. PubMed PMID: rayyan-676545057.
- [31] Friedl A, Mazurek B, Seiler D. Radiation-induced alterations in histone modification patterns and their potential impact on short-term radiation effects. *Front Oncol*. 2012;2. DOI:10.3389/fonc.2012.00117
- [32] Van HT, Santos MA. Histone modifications and the DNA double-strand break response. *cell cycle (georgetown, tex)*. 2018;17(21–22):2399–2410. DOI:10.1080/15384101.2018.1542899
- [33] Klemm SL, Shipony Z, Greenleaf WJ. Chromatin accessibility and the regulatory epigenome. *Nat Rev Genet*. 2019;20(4):207–220.
- [34] Jafer A, Sylvius N, Adewoye AB, et al. The long-term effects of exposure to ionising radiation on gene expression in mice. *Mutat Res*. 2020;821:111723.
- [35] Jain V, Das B. Global transcriptome profile reveals abundance of DNA damage response and repair genes in individuals from high level natural radiation areas of Kerala coast. *PLoS ONE*. 2017;12(11):e0187274.
- [36] Dahl H, Eide DM, Tengs T, et al. Perturbed transcriptional profiles after chronic low dose rate radiation in mice. *PLoS ONE*. 2021;16(8):e0256667. DOI:10.1371/journal.pone.0256667
- [37] Uehara Y, Ito Y, Taki K, et al. Gene expression profiles in mouse liver after long-term low-dose-rate irradiation with gamma rays. *Radiat Res*. 2010;174(5):611–617. DOI:10.1667/rr2195.1
- [38] Burgio E, Piscitelli P, Migliore L. Ionizing radiation and human health: reviewing models of exposure and mechanisms of cellular damage an epigenetic perspective. *Int J Environ Res Public Health*. 2018;15(9):1971.
- [39] Paunesku T, Stevanović A, Popović J, et al. Effects of low dose and low dose rate low linear energy transfer radiation on animals - review of recent studies relevant for carcinogenesis. *Int J Radiat Biol*. 2021;97(6):757–768.
- [40] Brooks AL, Hoel DG, Preston RJ. The role of dose rate in radiation cancer risk: evaluating the effect of dose rate at the molecular, cellular and tissue levels using key events in critical pathways following exposure to low LET radiation. *Int J Radiat Biol*. 2016;92(8):405–426.
- [41] Bae MJ, Kang MK, Kye YU, et al. Differential effects of low and high radiation dose rates on mouse spermatogenesis. *Int J Mol Sci*. 2021;22(23). DOI:10.3390/ijms222312834
- [42] Tanaka K, Kohda A, Satoh K, et al. Dose-rate effectiveness for unstable-type chromosome aberrations detected in mice after continuous irradiation with low-dose-rate gamma rays. *Radiat Res*. 2009;171(3):290–301.
- [43] Flavahan WA, Gaskell E, Bernstein BE. Epigenetic plasticity and the hallmarks of cancer. *Science*.

- 2017;357(6348): PubMed PMID: rayyan-676545096. DOI:10.1126/science.aal2380
- [44] Buenrostro JD, Wu B, Chang HY, et al. ATAC-seq: a method for assaying chromatin accessibility genome-wide. *Curr Protoc Mol Biol.* 2015;109(1):21.9.1–9.9.
- [45] Buenrostro JD, Giresi PG, Zaba LC, et al. Transposition of native chromatin for fast and sensitive epigenomic profiling of open chromatin, DNA-binding proteins and nucleosome position. *Nat Methods.* 2013;10(12):1213–1218.
- [46] Corces MR, Trevino AE, Hamilton EG, et al. An improved ATAC-seq protocol reduces background and enables interrogation of frozen tissues. *Nat Methods.* 2017;14(10):959–962. DOI:10.1038/nmeth.4396
- [47] Duale N, Eide DM, Amberger ML, et al. Using prediction models to identify miRNA-based markers of low dose rate chronic stress. *Sci Total Environ.* 2020;717:137068.
- [48] Graupner A, Eide DM, Brede DA, et al. Genotoxic effects of high dose rate X-ray and low dose rate gamma radiation in *Apc(Min/+)* mice. *Environ Mol Mutagenesis.* 2017;58(8):560–569.
- [49] E. Lindbo Hansen POH. Air kerma measurements with landauer nanoDots in Cs-137 and Co-60 beams. Part I - SSDL exposures free in air. Technical document no. 8. Norwegian Radiation Protection Authority, Østerås, Oslo: NRPA, 2017-12-07. Report No.: Contract No.: 8.
- [50] Graupner A, Eide DM, Instanes C, et al. Gamma radiation at a human relevant low dose rate is genotoxic in mice. *Sci Rep.* 2016;6(1):32977. DOI:10.1038/srep32977
- [51] Lind OC, Helen Oughton D, Salbu B. The NMBU FIGARO low dose irradiation facility. *Int J Radiat Biol.* 2018;95(1):1–6.
- [52] Li H, Durbin R. Fast and accurate short read alignment with burrows-wheeler transform. *Bioinformatics.* 2009;25(14):1754–1760.
- [53] Ewels PA, Peltzer A, Fillinger S, et al. The nf-core framework for community-curated bioinformatics pipelines. *Nat Biotechnol.* 2020;38(3):276–278.
- [54] Zhang Y, Liu T, Meyer CA, et al. Model-based analysis of ChIP-Seq (MACS). *Genome Bio.* 2008;9(9):R137. DOI:10.1186/gb-2008-9-9-r137
- [55] Carroll TS, Liang Z, Salama R, et al. Impact of artifact removal on ChIP quality metrics in ChIP-seq and ChIP-exo data. *Front Genet.* 2014;5:75.
- [56] Love MI, Huber W, Anders S. Moderated estimation of fold change and dispersion for RNA-seq data with DESeq2. *Genome Bio.* 2014;15(12):550.
- [57] Kane AE, Sinclair DA. Epigenetic changes during aging and their reprogramming potential. Critical reviews in biochemistry and molecular biology. 2019;54(1):61–83. DOI:10.1080/10409238.2019.1570075
- [58] Yu G, Wang LG, He QY. ChIPseeker: an R/Bioconductor package for ChIP peak annotation, comparison and visualization. *Bioinformatics.* 2015;31(14):2382–2383.
- [59] Carlson M. org.Mm.eg.db: Available from. Genome wide annotation for mouse bioconductor2019. Genome wide annotation for mouse, primarily based on mapping using entrez gene identifiers.]. <https://bioconductor.org/packages/release/data/annotation/html/org.Mm.eg.db.html>.
- [60] Zhou Y, Zhou B, Pache L, et al. Metascape provides a biologist-oriented resource for the analysis of systems-level datasets. *Nat Commun.* 2019;10(1):1523. DOI:10.1038/s41467-019-09234-6
- [61] Heberle H, Meirrelles GV, da Silva FR, et al. InteractiVenn: a web-based tool for the analysis of sets through Venn diagrams. *BMC Bioinf.* 2015;16(1):169.
- [62] Yates AD, Achuthan P, Akanni W, et al. Ensembl 2020. *Nucleic Acids Res.* 2020;48(D1):D682–8. DOI:10.1093/nar/gkz966
- [63] Song Y, Xie L, Lee Y, et al. Integrative assessment of low-dose gamma radiation effects on *Daphnia magna* reproduction: toxicity pathway assembly and AOP development. *Sci Total Environ.* 2020;705:135912.
- [64] Vaiserman A, Cuttler JM, Socol Y. Low-dose ionizing radiation as a hormetin: experimental observations and therapeutic perspective for age-related disorders. *Biogerontology.* 2021;22(2):145–164.
- [65] Ray-Jones H, Spivakov M. Transcriptional enhancers and their communication with gene promoters. *Cell Mol Life Sci.* 2021;78(19):6453–6485.
- [66] Lysek-Gladysinska M, Wiczorek A, Walaszczyk A, et al. Long-term effects of low-dose mouse liver irradiation involve ultrastructural and biochemical changes in hepatocytes that depend on lipid metabolism. *Radiat Environ Biophys.* 2018;57(2):123–132. DOI:10.1007/s00411-018-0734-9
- [67] Golla S, Golla JP, Krausz KW, et al. Metabolomic analysis of mice exposed to gamma radiation reveals a systemic understanding of total-body exposure. *Radiat Res.* 2017;187(5):612–629. DOI:10.1667/rr14592.1
- [68] Rajbhandari P, Thomas BJ, Feng AC, et al. IL-10 signaling remodels adipose chromatin architecture to limit thermogenesis and energy expenditure. *Cell.* 2018;172(1–2):218–33.e17.
- [69] Starks RR, Biswas A, Jain A, et al. Combined analysis of dissimilar promoter accessibility and gene expression profiles identifies tissue-specific genes and actively repressed networks. *Epigenetics & Chromatin.* 2019;12(1):16.
- [70] Corces MR, Granja JM, Shams S, et al. The chromatin accessibility landscape of primary human cancers. *Science.* 2018;362(6413).
- [71] Lara-Astiaso D, Weiner A, Lorenzo-Vivas E, et al. Immunogenetics. Chromatin state dynamics during

- blood formation. *Science*. 2014;345(6199):943–949. DOI:10.1126/science.1256271
- [72] Zheng S, Papalexis E, Butler A, et al. Molecular transitions in early progenitors during human cord blood hematopoiesis. *Mol Syst Biol*. 2018;14(3):e8041.
- [73] Li X, Chen Y, Fu C, et al. Characterization of epigenetic and transcriptional landscape in infantile hemangiomas with ATAC-seq and RNA-seq. *Epigenomics*. 2020;12(11):893–905. DOI:10.2217/epi-2020-0060
- [74] de la Torre-Ubieta L, Stein JL, Won H, et al. The dynamic landscape of open chromatin during human cortical neurogenesis. *Cell*. 2018;172(1–2):289–304.e18.
- [75] Minnoye L, Marinov GK, Krausgruber T, et al. Chromatin accessibility profiling methods. *Nat Rev Dis Primers*. 2021;1(1):10. DOI:10.1038/s43586-020-00008-9
- [76] Rühm W, Woloschak GE, Shore RE, et al. Dose and dose-rate effects of ionizing radiation: a discussion in the light of radiological protection. *Radiat Environ Biophys*. 2015;54(4):379–401. DOI:10.1007/s00411-015-0613-6
- [77] Lomax ME, Folkes LK, O'Neill P. Biological consequences of radiation-induced DNA damage: relevance to radiotherapy. *Clin Oncol*. 2013;25(10):578–585.
- [78] Dabin J, Fortuny A, Polo Sophie E. Epigenome maintenance in response to DNA damage. *Molecular Cell*. 2016;62(5):712–727.
- [79] Brambilla F, Garcia-Manteiga JM, Monteleone E, et al. Nucleosomes effectively shield DNA from radiation damage in living cells. *Nucleic Acids Res*. 2020;48(16):8993–9006. PubMed PMID: rayyan-676545021.
- [80] Elia MC, Bradley MO. Influence of chromatin structure on the induction of DNA double strand breaks by ionizing radiation. *Cancer Res*. 1992;52(6): 1580–1586. PubMed PMID: 1540967.
- [81] Falk M, Lukášová E, Kozubek S. Chromatin structure influences the sensitivity of DNA to γ -radiation. *Biochim Biophys Acta, Mol Cell Res*. 2008;1783(12):2398–2414.
- [82] Takata H, Hanafusa T, Mori T, et al. Chromatin compaction protects genomic DNA from radiation damage. *PLoS ONE*. 2013;8(10):e75622. DOI:10.1371/journal.pone.0075622
- [83] Healy S, Khan P, Davie JR. Immediate early response genes and cell transformation. *Pharmacol Ther*. 2013;137(1):64–77.
- [84] Sherman ML, Datta R, Hallahan DE, et al. Ionizing radiation regulates expression of the c-jun protooncogene. *Proc Natl Acad Sci USA*. 1990;87(15):5663–5666.
- [85] Bejjani F, Evanno E, Zibara K, et al. The AP-1 transcriptional complex: local switch or remote command? *Biochim Biophys Acta Rev Cancer*. 2019;1872(1):11–23.
- [86] Atlasi Y, Stunnenberg HG. The interplay of epigenetic marks during stem cell differentiation and development. *Nat Rev Genet*. 2017;18(11):643–658.
- [87] Bernstein BE, Mikkelsen TS, Xie X, et al. A bivalent chromatin structure marks key developmental genes in embryonic stem cells. *Cell*. 2006;125(2):315–326. DOI:10.1016/j.cell.2006.02.041
- [88] Ilnytskyy Y, Kovalchuk O. Non-targeted radiation effects-an epigenetic connection. *Mutat Res*. 2011;714(1–2):113–125.
- [89] Lindeman LC, Kamstra JH, Ballangby J, et al. Gamma radiation induces locus specific changes to histone modification enrichment in zebrafish and Atlantic salmon. *PLoS ONE*. 2019;14(2):e0212123. PubMed PMID: rayyan-676545106.
- [90] Kovalchuk O, Burke P, Besplug J, et al. Methylation changes in muscle and liver tissues of male and female mice exposed to acute and chronic low-dose X-ray-irradiation. *Mutat Res*. 2004;548(1–2):75–84.
- [91] Bahrami S, Drablos F. Gene regulation in the immediate-early response process. *Adv Biol Regul*. 2016;62:37–49.
- [92] Rye M, Sandve GK, Daub CO, et al. Chromatin states reveal functional associations for globally defined transcription start sites in four human cell lines. *BMC Genomics*. 2014;15(1):120. DOI:10.1186/1471-2164-15-120
- [93] Chereji RV, Eriksson PR, Ocampo J, et al. Accessibility of promoter DNA is not the primary determinant of chromatin-mediated gene regulation. *Genome Res*. 2019;29(12):1985–1995.
- [94] Zhu W, Zhang X, Yu M, et al. Radiation-induced liver injury and hepatocyte senescence. *Cell Death Discovery*. 2021;7(1):244.
- [95] Baratta JL, Ngo A, Lopez B, et al. Cellular organization of normal mouse liver: a histological, quantitative immunocytochemical, and fine structural analysis. *Histochem Cell Biol*. 2009;131(6):713–726.

Appendices (as appropriate);

Supplementary 1 (S1)

Details of the bioinformatic pipeline used for data pre-processing (1-3) and downstream analysis (4-5).

Supplementary 1 (S1) Details of the pipeline used for data pre-processing (1-3) and downstream analysis (4-5).

1. nf-core ATAC-seq pipeline

The detailed pipeline command used in the pre-processing analysis can be found under the following GitHub repository: <https://github.com/nf-core/atacseq>

Script name used: main.nf
Workflow container version: nfcore/atacseq:1.2.1
Container engine: Singularity v3.6.4
Nextflow version: version 20.11.0-edge, build 5448 (16-11-2020 08:23 UTC)

Workflow summary of the ATAC-seq pipeline contained following arguments:

```
-profile singularity,  
--genome GRCh38,  
--input design.csv,  
--max_cpus 8.
```

Workflow was run with maximal resources: 31 GB memory, 8 CPU, 10 days per job given.

2. Command for extraction of nucleosome free regions from sorted .bam-files

```
samtools view -h "input" | perl -lane '$! = 0; $F[5] =~ s/(\\d+)[MX=DN]/$!+=$1/eg; print if $! < 100 or /\\^@/' | samtools view -bS - > "output"
```

3. Peak Calling with MACS2 v2.2.7

```
macs2 callpeak -t "input" -f BAMPE --outdir ./ --name "output" -g mm
```

4. Differential analysis with DESeq2 (data post processing)

```
dds <- DESeqDataSetFromMatrix(countData, colData, ~group + age, rowRanges =  
consensusToCount)
```

```
dds <- DESeq(dds)
```

5. Annotation of contrasts with annotatePeak package and TxDb

```
contrastData_annotated <- annotatePeak(contrastData, TxDb =  
TxDb.Mmusculus.UCSC.mm10.knownGene)
```

Supplementary 2 (S2) –

The complete MetaScape-output.

Available online due to size of file <https://www.ncbi.nlm.nih.gov/pmc/articles/PMC10054331/>

Supplementary 4 (S4)

The fragment distribution per sample in S4_QC_library_trace_allsample.zip

Available online <https://www.ncbi.nlm.nih.gov/pmc/articles/PMC10054331/>

Supplementary_3 (S3). ATAC-Seq metadata and mapping statistics.

Group	Sample ID	QC-passed Reads	Mapped (%)	Properly Paired (%)	NFR Reads (<100bp)	NFR Reads (%)	QC-passed Peaks	Reads In Peaks (RIP) (%)
CTRL	R1	126,340,392	99.20	97.46	31,602,553	25.67	84,668	22.90
CTRL	R2	101,390,920	99.24	98.16	16,341,608	16.42	33,834	9.43
CTRL	R3	108,434,882	99.46	96.98	26,904,111	25.58	71,562	17.70
CTRL	R4	119,045,374	99.60	98.57	23,415,170	19.95	61,287	16.50
CTRL	R5	101,809,468	99.24	96.58	27,211,347	27.67	90,235	25.60
LDR	R1	109,019,826	98.98	98.01	18,260,419	17.09	33,511	8.32
LDR	R2	119,542,410	99.19	98.21	23,936,039	20.39	85,433	29.60
LDR	R3	139,725,676	99.33	98.38	27,009,957	19.65	57,127	12.30
MDR	R1	104,344,204	96.91	95.80	19,587,762	19.60	40,734	10.50
MDR	R2	112,859,786	98.91	97.74	19,324,976	17.52	55,206	18.10
MDR	R3	123,694,052	99.49	98.24	21,694,519	17.85	41,636	9.75
HDR	R1	112,942,896	99.54	97.51	30,931,600	28.09	84,327	22.80
HDR	R2	103,929,930	99.45	97.39	27,856,183	27.52	85,469	26.10
HDR	R3	134,222,048	99.36	98.10	29,457,900	22.37	78,373	19.80
CTRL_late	R1	102,700,534	98.51	97.37	19,084,020	19.08	38,504	9.89
CTRL_late	R2	118,384,442	98.82	97.67	20,308,738	17.56	68,267	21.60
CTRL_late	R3	112,638,514	98.58	97.55	21,380,994	19.46	39,718	9.34
CTRL_late	R4	111,220,712	97.65	96.42	32,469,830	30.28	83,292	19.80
LDR_late	R1	105,383,454	98.96	97.94	23,046,990	22.33	26,057	5.07
LDR_late	R2	132,908,782	95.16	93.84	25,580,042	20.51	74,029	20.50
LDR_late	R3	114,117,356	99.06	97.97	24,964,040	22.33	37,179	7.28
HDR_late	R1	107,317,296	98.07	95.54	36,590,080	35.69	20,123	2.44
HDR_late	R2	102,548,600	96.51	95.46	17,975,665	18.36	67,396	23.40
HDR_late	R3	120,073,874	99.13	98.12	21,856,440	18.55	29,440	5.53

Paper II:

The authors` contributions are in compliance with the Vancouver agreement, and were as follows:

The overall animal experiment was planned by AKO, DE and AG, HD participated in termination in harvest of biological samples. HD, AKO, DE and ND participated in the conceptualisation of the ATAC-seq sub-project. AKO and HD performed experimental planning, labwork were performed by JB, supervised by AKO. JB did the bioinformatic coding to transform raw sequencing files (obtained from Novogene) to make clean data sets, supervised by the bioinformatics MWW and the statistician DE, in collaboration/coordinated with HD. HD performed all data and statistical analysis. HD made all visualizations in the manuscript, fig 2 and 4 assisted from JB. HD wrote the first draft of the manuscript, and all authors read and commented. The manuscript was finalized by HD, approved by all authors.

Paper III

1 Genomic instability in F₂ male progeny from low dose rate
2 gamma irradiated F₀ mice

3 **Hildegunn Dahl***^{1,2}, Richard A White⁴, Dag Anders Brede^{1,3}, Christine Instanes^{1,2}, Dag M.
4 Eide^{1,2}, Gunnar Brunborg^{1,2}, Ann-Karin Olsen^{1,2}

5

6 ¹ Division of Climate and Environmental Health, Norwegian Institute of Public Health,
7 Oslo, NO-0213, Norway

8 ² Centre for Environmental Radiation (CERAD), Norwegian University of Life Sciences
9 (NMBU), Ås, NO-1432, Norway

10 ³ Faculty of Environmental Sciences and Natural Resource Management (MINA),
11 Norwegian University of Life Sciences (NMBU), Ås, NO-1432, Norway

12 ⁴ Department of Method Development and Analytics, Norwegian Institute of Public
13 Health, Oslo, NO-0213, Norway

14

15

16

17

18

19

20

21 *Corresponding author

22 Hildegunn Dahl

23 Phone: (+47) 21 07 70 00

24 Email: hildegunn.dahl@fhi.no

25

26

1 **ABSTRACT**

2 The hypothesis of transgenerational genomic instability after paternal exposure to
3 irradiation is still controversial due to inconsistent results and lack of a mechanistic
4 understanding. In this study, we investigated paternal transgenerational radiation-
5 induced genomic instability in F₂ males derived from C57BL/6N Ogg1^{-/-} and Ogg1^{-/+} males
6 chronically exposed to low dose rate (1.41 mGy/h) gamma radiation (⁶⁰Co) for 45 days to
7 a total dose of 1.5 Gy. Breeding was delayed for 34 days post-irradiation to create progeny
8 that originates from sperm derived from irradiated spermatogonia. Genomic instability
9 was evaluated in blood using two complementary genotoxicity assays: the alkaline comet
10 assay for DNA damage in nucleated blood and the flowcytometry-based *in*
11 *vivo* micronuclei (MN) assay for chromosomal aberrations in reticulocytes. The levels of
12 DNA- and cytogenic damage were assessed before and after a challenging X-ray dose,
13 along with changes in the rate of DNA lesion repair. The results did not show evidence of
14 DNA and cytogenic damage or change in the rate of DNA repair in F₂ ascribed to low dose
15 rate irradiation to F₀. A statistically significant increase in baseline DNA lesions (p-value
16 = 0.03, coef. 1.117) was seen in F₂ originating from irradiated F₀, which could imply
17 transgenerational inheritance of genomic instability. However, due to the small effect size,
18 it is challenging to conclude whether the results represent a true biological finding or
19 relate to methodological aspects. The results of this study demonstrate that chronic low
20 dose rate irradiation of F₀ to a total dose of 1.5 Gy did not severely compromise the
21 genome integrity in their F₂ male progeny.

22 **KEYWORDS**

23 Transgenerational, genomic instability, ionising radiation, chronic exposure, low dose
24 rate, comet assay, micronucleus, challenging dose

25

26

27

1 INTRODUCTION

2 Radiation-induced genomic instability (RIGI) is described as a non-targeted phenomena
3 observed in progenies of directly irradiated cells displaying a tendency to increased
4 spontaneous mutation rate and/or other genomic changes, such as chromosomal
5 aberrations (UNSCEAR, 2006). Genomic instability in somatic cells could drive
6 tumorigenesis (Hanahan and Weinberg, 2011; Huang et al., 2003; Shen, 2011), while
7 genomic instability in germ cells could be a source of heritable effects, causing genomic or
8 epigenomic alterations causing disease and disorders in offspring (Russo et al., 2015;
9 UNSCEAR, 2006).

10 Currently, studies addressing radiation-induced adversity in children of exposed parents
11 do not show evidence for heritable transmission of effects (Izumi et al., 2003; Kodaira et
12 al., 2010; Kodaira et al., 1995; Yoshimoto et al., 1990) given the limitations of
13 epidemiological studies. There is yet no evidence for increased cancer incidence among
14 the children of fathers surviving the blasts in Nagasaki and Hiroshima (Yeager et al.,
15 2021). Also, no germline *de novo* mutations (DNMs) were found in children of Chernobyl
16 nuclear accident clean-up workers (Yeager et al., 2021), and no elevated mutation rates
17 in the germline of a group of British nuclear test veterans (Moorhouse et al., 2022).

18 However, results from controlled mouse studies (Barber et al., 2002; Gomes et al., 2015;
19 Koturbash et al., 2006; Paris et al., 2015) have reported radiation-induced changes in F₁
20 progeny. It is suggested that these responses could be linked to epigenetic factors rather
21 than changes in the DNA sequence, like DNA methylation, histone modifications and
22 ncRNA (reviewed in (Bohacek and Mansuy, 2015; Dubrova and Sarapultseva, 2020; Gapp
23 and Bohacek, 2018; Legoff et al., 2019; Marcho et al., 2020; Merrifield and Kovalchuk,
24 2013).

25 The gap in knowledge concerning radiation exposure and the risk of transmitting
26 radiation-induced health effects to progeny is a concern for populations exposed to
27 ionising radiation (Fukunaga et al., 2022; Kamiya et al., 2015). It is therefore necessary to
28 continue to elucidate the potential role of transgenerational effects. Today, there are still
29 controversies concerning RIGI transmitted to descendants. Many factors may influence
30 the risk of such outcomes, including exposure route, exposure window, differences
31 between species/strains and more.

1 The current study investigates changes in genomic instability in the F₂ male progeny
2 origination from F₀ paternal low dose rate gamma irradiated to a total dose of 1.5 Gy. As
3 previous studies of transgenerational inheritance points to spermatogonia as a possible
4 sensitive germ cell stage (Barber et al., 2006; Mughal et al., 2012), the study design
5 focused on litters originating from spermatozoa originating from exposed spermatogonia.
6 Genomic instability was investigated by DNA damage using the high-throughput alkaline
7 comet assay in nucleated blood cells, including enzymatic detection of oxidative DNA
8 lesions, and chromosomal damage in reticulocytes (RETs) assessed using the sensitive
9 flowcytometry-based micronucleus assay.

10 **MATERIALS AND METHODS**

11 **Animals and housing**

12 As previously described (Graupner et al., 2015), BigBlue™ C57Bl/6N was initially
13 purchased from Stratagene (Stratagene, La Jolla, CA, USA) and crossed with *Ogg1* (8-oxoG-
14 DNA-Glycosylase 1) deficient mice (*Ogg1*^{-/-}) on mixed B6/SV129 background (Klungland
15 et al., 1999), generously provided by the University of Oslo, Norway. These mice were
16 backcrossed for nine generations to generate an isogenic *Ogg1*-mouse line on C57BL/6
17 background. From in-house breeding, homozygote (*Ogg1*^{-/-}) and heterozygote (*Ogg1*^{+/-})
18 mice were made, and litter mates were used in this study. Isogenic mice were maintained
19 with continuous in-house backcrossing using *Ogg1*^{+/-} C57BL/6. The *Ogg1*-genotype were
20 determined by PCR (Klungland et al., 1999).

21 The F₀ mice were caged in groups of three. F₁ and F₂ mice were caged in groups of a
22 maximum of five in individually ventilated disposable PET plastic cages (IVC racks)
23 (Innovive, San Diego, USA) using aspen bedding (Nestpack, Datesand Ltd., Manchester,
24 UK). Tap water in PET bottles and SDS RM1 food (Special Diet Services, Essex, UK) were
25 available *ad libitum*. Temperature, humidity, air, and light conditions were controlled
26 (22±2 °C, 55±10 % relative humidity, 50 air changes h⁻¹ and photoperiod 12:12 (L:D)).

27 The Norwegian Food Safety Authority approved the experimental protocols. Approvals
28 were received for the F₀ exposure (no. 6570), X-ray pilot studies (no. 7162), and the F₂ X-
29 ray challenge experiment (no. 6582). No mice died or showed clinical signs associated
30 with radiation.

1 **Radiation and dosimetry**

2 **F₀ generation:** Radiation of the *F₀* generation has been described previously (Graupner
3 et al., 2016). In short, male mice (Ogg1^{-/-} and Ogg1^{+/-} C57BL/6N) were gamma irradiated
4 (⁶⁰Co) using a low dose rate (1.41 mGy/h (0.0235 mGy/min) (0.99–1.73 mGy/h) for 45
5 days to a total dose of 1.48 Gy (1.04–1.82 Gy), at the FIGARO radiation facility (Graupner
6 et al., 2016; Lind et al., 2018). The absorbed dose rate at different source distances along
7 the beam axis is available (Bjerke, 2014). A phantom mouse (50 ml tube filled with 10%
8 (w/v) gelatine) considering all possible positions in the cage was used to estimate the
9 range of dose rate and total dose, and two types of dosimeter systems: TL-dosimeters
10 (SCK•CEN, Mol, Belgium) and alanine (National Physical Laboratory, Teddington, UK)
11 applied to selected cages were used to calculate the total doses. The non-irradiated
12 control mice were housed in separate Scantainers in the irradiation room outside the
13 gamma beam field. Due to scattered radiation in the room, the control mice were exposed
14 to a dose rate of 0.002 mGy/h (total dose: 1.89 mGy).

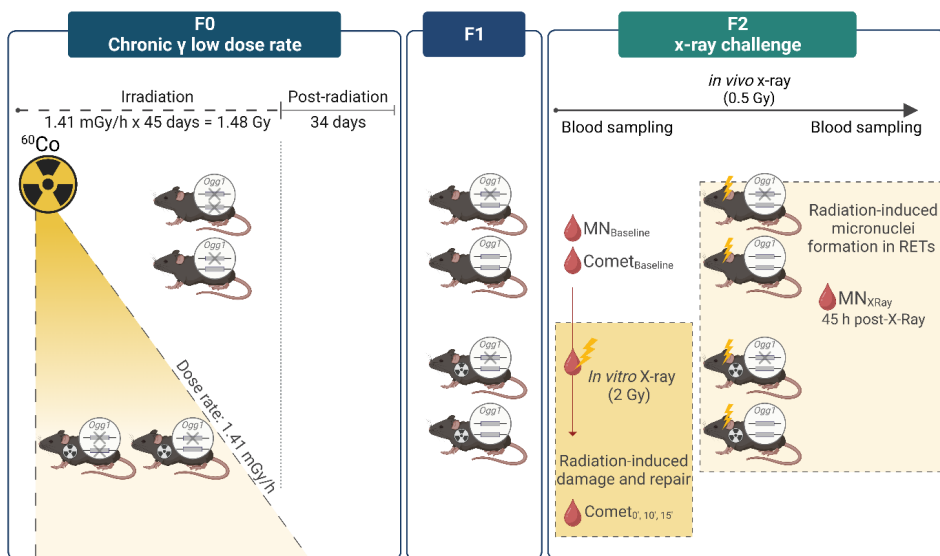
15 **F₂ generation:** The *F₂* *in vivo* challenging dose were given by immobilising the mice in 50
16 ml Falcon tubes inside a PIX X-RAD 160C/225C radiation system (Precision X-ray Inc,
17 North Branford, Connecticut, USA) giving a total dose of 0.5 Gy using dose rate 0.457 ±
18 0.009 Gy/min, using the following instrument settings: voltage: 225 kV, current: 4 mA,
19 filtering: Cu (0.5 mm), platform distance from anode: 50 cm. Dosimetry measurements
20 was performed by The Norwegian Radiation Protection Authority (Hansen EL, 2015)
21 using a water phantom and a NE2571 Farmer-type ionisation chamber, as well as
22 measurements with Gafchromic EBT films. The selection of whole-body challenging dose
23 was based on a pre-liminary study addressing the X-ray (0, 0.2, 0.5 and 1 Gy) and
24 micronucleus relationship. The dose-response curve presented in (supplementary).

25 *In vitro* radiation of blood samples for the comet assay were performed in Eppendorf
26 tubes (1.5 ml) on ice exposed using an equal dose rate of 0.457 Gy/min, and instrumental
27 settings, as the whole-body *in vivo* exposure. Duration of exposure: 268 sec for 2 Gy *in*
28 *vitro* and 66 sec for 0.5 Gy whole-body irradiation.

29 **Experimental design**

30 Exposure duration of 45 days were chosen to expose all stages of spermatogenesis, and
31 the post-radiation period of 34 days ensure that the spermatozoa originated from

1 exposed stem cells, the spermatogonia (Olsen et al., 2010; Olsen et al., 2005; Taft, 2007).
 2 8 irradiated (F₀-IR, *Ogg1*^{-/-} and *Ogg1*^{+/-}) and 8 non-irradiated (F₀-Ctrl, *Ogg1*^{-/-} and *Ogg1*^{+/-})
 3) males were mated with naïve females in pairs for two weeks to generate F₁ offspring
 4 (*Ogg1*^{+/+} and *Ogg1*^{+/-}). Exclusively, F₁ *Ogg1*^{+/-} males were mated further with naïve
 5 females in pairs, to generate the F₂ male offspring (*Ogg1*^{+/+} and *Ogg1*^{+/-}) (Fig. 1). The F₂
 6 study population (N=67) originated from 2-3 F₀ males and 3-4 F₁ males per experimental
 7 group stratified on F₀ irradiation and genotype (Tab. 1). Blood samples to be analysed on
 8 the comet assays were collected one week prior to the *in vivo* whole body 0.5 Gy X-ray
 9 challenge dose. According to protocol requirement (OECD, 2016) blood was collected 45
 10 hours after *in vivo* radiation for the flowcytometry-based micronucleus assays (Fig. 1).
 11



12
 13 **Figure 1. Experimental set-up.** Figure is created using www.BioRender.com. Abb:({*Ogg1*)
 14 *8-oxoG-DNA-Glycosylase 1; MN micronucleus assay*

15 **Blood sampling**

16 Whole blood was collected from *the saphenous vein* using a 25-gauge needle. To ensure
 17 free-flowing blood, mice were pre-warmed under a heating lamp. For the micronucleus
 18 assay, 60 μ l of free-flowing blood was collected using a K₂EDTA-coated capillary tube
 19 (Bilbate Ltd, Daventry, UK) and added to 350 μ l anticoagulant supplied with the Mouse
 20 MicroFlow^{PLUS} kit (Litron Laboratories, US), mixed well, and kept at room temperature

1 (RT) until fixation. For the comet assay, 25 μ l free-flowing whole blood was suspended in
 2 100 μ l heparin anticoagulant and kept on ice until irradiation.

3 **Table 1. Descriptive statistics.** *The total of F₂ males (N = number of mice produced, n=*
 4 *number of samples processed for each respective assay) stratified in groups based on the F₀*
 5 *experimental factors (irradiation: ctrl and IR, Ogg1 genotype: knockout (KO) or*
 6 *heterozygote (He) and the distribution of the F₂ Ogg1-genotype (heterozygote (He) or*
 7 *wildtype (Wt)), along with F₂ age and weight.*

8

F ₀		F ₁	F ₂					
Group	F ₀ sire	F ₁ sire	N (=67)	Age (weeks) Mean \pm SD (Range)	Ogg1 (He/Wt)	Weight (g) Mean \pm SD (Range)	MN (n=59)	Comet (n=23)
Ctrl KO	3	3	12	39.1 \pm 7.7 (28-50)	3/8	34.8 \pm 3.1 (28.1-39.5)	11	5
Ctrl He	2	3	11	40.1 \pm 7.5 (27-48)	5/5	35.9 \pm 4.1 (30.6-41.4)	10	6
IR KO	3	4	22	38.3 \pm 7.8 (24-51)	11/9	35.6 \pm 4.7 (29.6-43.1)	20	7
IR He	2	3	22	41.3 \pm 6.8 (27-51)	11/7	36.9 \pm 3.1 (31.1-41.9)	18	5

9

10 **Micronucleus (MN) assay**

11 The MN analysis was conducted using the Mouse MicroFlow^{PLUS} Kit (Litron Laboratories,
 12 Rochester, NY). The protocol was performed according to the MicroFlow^{PLUS} kit
 13 specifications described in the instruction manual (version: 140217) (Dertinger et al.,
 14 2011; Torous et al., 2003).

15 180 μ l of the blood/anticoagulant suspension were dispensed into 2 ml ultra-cold (-80°C)
 16 pure methanol and stored at -80°C for at least three days until flow cytometric analysis.
 17 Fixed samples were washed and labelled using anti-CD71-FITC (transferrin), anti-CD61-
 18 PE (platelets) and propidium iodide (PI) and analysed using a BD™ LSR II flow cytometer
 19 equipped with a 488-nm laser. CD71-negative cells and malaria-infected red blood cells
 20 supplied with the kit were stained following the test samples, to calibrate the instrument.

21 The data were acquired using the BD FACSDiva™ software CellQuest Pro v5.2 (Becton
 22 Dickinson, San Jose, CA). Four erythrocyte subpopulations were counted: the percentage
 23 of RETs (%RET, as an index for erythropoiesis function) and the percentage of

1 micronucleated RETs (%MN-RET, an index for recent chromosomal damage). The
2 stopping gate was set at 20`000 CD-71 positive RETs counted per sample. The raw
3 MicroFlow data output was processed and calculated as described (Torous et al., 2003),
4 using Microsoft® Excel® for Microsoft 365 MSO (version: 2202). Due to haemorrhage,
5 incorrect X-ray exposure and insufficient blood sampling eight mice with were excluded
6 from the micronucleus analysis.

7 **Comet assay (Single Cell Gel Electrophoresis)**

8 The alkaline comet assay's high throughput version (Gutzkow et al., 2013) was used with
9 minor improvements. The whole blood/anticoagulant suspension (ca. 10⁶ leukocytes/ml;
10 mixed 1:10 with 0.75% low melting point agarose) was moulded in gels to determine the
11 levels of baseline DNA lesions (control sample) prior to *in vitro* irradiation on ice. The
12 samples were incubated at 37 °C after radiation to allow DNA repair. The
13 blood/anticoagulant suspensions were moulded at different time points after X-ray
14 exposure to study repair dynamics; 0' (directly after, 10 and 15 min after X-ray). At each
15 timepoint, four technical replicates pr biological sample (4 x 4 µl) were moulded onto a
16 cold GelBond® film (Lonza, Rockland, ME, USA) in a 96-format. Lysis was performed
17 overnight at 4°C. For analysis of oxidative DNA lesions, GelBond® films were immersed in
18 fresh pre-warmed 37°C enzyme buffer ("Collins buffer": 40 mM Hepes, 0.1 M KCl, 0.5 mM
19 Na₂EDTA, adjusted pH 7.6 using 7 M KOH) with 0.2 mg/ml BSA and 0.5 µg/ml
20 Formamidopyrimidine DNA glycosylase (crude Fpg extract, produced *in house* according
21 to previous publications (Boiteux and Huisman, 1989; Duale et al., 2010; Hansen et al.,
22 2010). The Fpg concentration was optimised based on titration experiments using a
23 photo-activated compound (Ro 12-9786) measuring oxidised DNA bases, as
24 recommended (Asare et al., 2016; Collins et al., 2008; Duale et al., 2010; Gutzkow et al.,
25 2016; Olsen et al., 2003). After 60 min enzyme treatment at 37°C (with and without Fpg),
26 films were transferred to an alkaline electrophoresis solution at 4°C to unwind the DNA
27 for 40 min, followed by 25 min electrophoresis at 8°C, 25 V and 0.8 V/cm in freshly made
28 alkaline electrophoresis solution, using circulation of the solution during electrophoresis.
29 Subsequently, the GelBond® films were submerged in a neutralisation buffer and fixed
30 using ethanol. DNA was stained using SYBR®Gold Nucleic Acid Stain (10`000x units
31 concentrated in DMSO) (Life Technologies™, Carlsbad, CA, USA) 1:1000 diluted in TE-
32 buffer (1 mM Na₂EDTA, 10 mM Tris-HCl, pH 8.0).

1 The level of DNA lesions was measured using a fully automated scoring system, IMSTAR
2 PathFinder™ (Imstar SA, Paris, France). Pathfinder™ Cellscan (Imstar SA, Paris, France)
3 automatically quantifies the amount of DNA damage of fluorescing DNA in the comet tail
4 (% tail-DNA) against the whole comet, corrected for gel background. Exclusion criteria of
5 the IMSTAR scores comprised omitting technical replicates with too dense cells leaving
6 overlapping comets. All countable comets per technical replicate (2-4) were scored
7 (average numbers of scored comets per gel = 1519). Some films were also scored semi-
8 automatically using Perceptives Comet IV (Perceptive Instruments Ltd., Suffolk, UK) and
9 the results were comparable (results not shown). The level of DNA damage is expressed
10 as percent intensity of DNA in the tail relative to the whole comet. The standard alkaline
11 Comet assay reveals DNA single-strand breaks (ssb) plus alkali-labile sites (als), whereas
12 oxidised purines are detected when adding the Fpg-enzyme. Throughout the paper, ssb
13 and als will only be termed ssb from this point. One mouse was excluded from the analyses
14 due to incorrect genotype results.

15 **Statistical analysis**

16 StataSE 17 (StataCorp LLC, Texas, US), JMP Pro 16 (SAS Institute Inc., Cary, NC, US) and
17 Microsoft® Excel® for Microsoft 365 MSO (Version 2202) have been used for descriptive
18 and statistical analysis.

19 13 multivariable regression models were used to investigate if F_0 experimental
20 parameters (i.e., irradiation, genotype, and the interaction of these factors) significantly
21 impacted the F_2 measurements. The 13 multivariable regression models corresponded to
22 one model per outcome (ssb/als: baseline, directly after X-ray, 10 min post-X-ray, 15 min
23 post-X-ray; oxidative lesions: baseline, directly after X-ray, 10 min post-X-ray, 15 min
24 post-X-ray; MN-assay: Baseline (RETs, MN-RETs, MN-NCEs), post-X-ray (RETs, MN-
25 RETs)). The outcome of each regression model is presented in Supplementary. The
26 residuals from the regression models were investigated, and modelling assumptions were
27 not violated. Age and weight did not influence the comet outcomes and were not included
28 in the regression model, while weight was corrected for in the MN regression models.

29 Tukey-Kramer HSD (honestly significant difference) test for multiple comparisons were
30 used to test difference in DNA damage across timepoints (baseline, directly after, 10 min
31 and 15 min).

1 RESULTS

2 To study the impact of paternal F₀ chronic low dose rate gamma irradiation on genomic
3 instability in F₂ male progeny, DNA- and chromosomal damage were investigated in
4 whole blood. Baseline levels and changes in levels of pre-mutagenic DNA lesions and MN
5 formation after a whole-body as well as Dan damage and repair after an *in vitro* given X-
6 ray challenge (MN; *in vivo* 0.5 Gy. Comet Assay; *in vitro* 2 Gy) were measured. The
7 experimental set-up is depicted in Fig. 1.

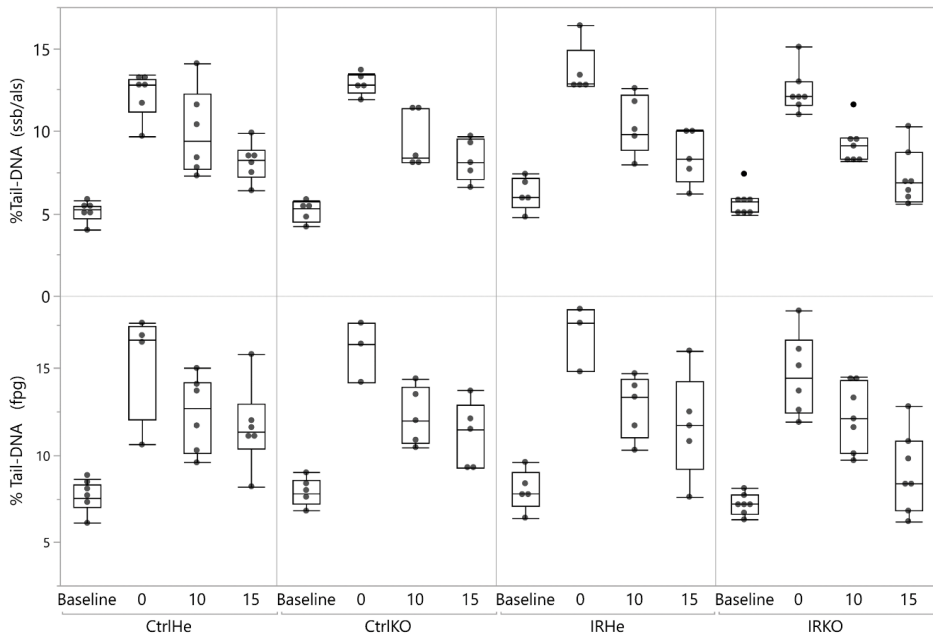
8 DNA damage measured by the Comet Assay – *in vitro* X-ray

9 The mean %tail-DNA of ssb and Fpg-sensitive sites (oxidative lesions) measured in whole
10 blood immediately after *in vitro* 2 Gy of X-ray, and after repair (10 and 15 minutes),
11 compared to the baseline levels, is visualised in Fig. 2.

12 Immediately after the X-ray irradiation, the levels of single-strand DNA breaks and alkali
13 label sites increased significantly from baseline ($p < 0.000$) (Fig. 2). Repair of ssb lesions
14 were also evident by statistically significant reduction in the levels of damaged lesions at
15 both 10 min and 15 min after exposure. The levels for oxidative lesions were not reported
16 as net Fpg-sensitive sites (Fpg-sensitive sites minus the levels of ssb/als) as only a slight
17 increase in the net % tail-DNA mean was observed (Fig. 2, lower panel). When stratifying
18 the F₂ study population into the four F₀ irradiation and genotype groups (Tab. 1, Fig. 2),
19 the DNA levels at 10 min and 15 min were no longer statistically significant when
20 compared with each other, due to intra-group variation.

21 Multiple multivariable regression model was used to evaluate the impact of the F₀
22 experimental variables (i.e., irradiation, genotype, and the interaction of these factors) on
23 the induction of ssb lesions and the repair 10- and 15-min post-X-ray (ssb: Tab. 2,
24 oxidative lesions (ssb not subtracted): Tab. 3) in F₂. Evaluating the impact of F₀
25 experimental variables (i.e., irradiation, genotype, and the interaction of these factors) on
26 the baseline levels of induced ssb, we found that F₂ males originating from irradiated F₀
27 mice had a higher level of DNA damage than F₂ mice originating from non-irradiated F₀
28 mice (coef. 1.117; 95% CI (0.121-2.113; p-value 0.03, Tab. 2). There was no evidence that
29 F₀ mice *Ogg1*^{-/-} or *Ogg1*^{-/+} genotype alone or interaction with F₀ irradiation influenced
30 the F₂ ssb baseline levels (Tab. 2). Further, there was no evidence that the F₀ variables

1 influenced the levels of IR-induced DNA damage directly after the challenging dose of (2
 2 Gy) of X-ray, or the rate of DNA damage repair measured 10' and 15' post-X-ray.



3

4 **Figure 2. Levels of DNA damage measured by the comet assay.** *F₂* progeny grouped
 5 according to *F₀* variables (irradiation and genotype indicated at the bottom). Box plot of
 6 *ssb/als* (the upper panel), and oxidised DNA lesion (*ssb/als* not subtracted) (lower panel)
 7 measured in whole blood given 2 Gy of X-ray in vitro. The term “Baseline” indicates the levels
 8 of DNA damage before X-ray exposure, i.e. endogenous DNA damage levels. The group
 9 denoted 0 represent measurements immediately after X-ray, and 10 and 15 min after X-ray.

10

11

12 **Table 2. Multivariable regression model by outcome (*ssb/als*).** The significance of *F₀*
 13 experimental variables on *ssb* DNA-lesions at baseline, immediately after X-ray, and at the
 14 rate of repair in *F₂* progeny investigated using four regression models. Footnotes describe
 15 the interpretations of the independent variables upon the outcome, with statistically
 16 significant levels (*p*-value <0.05) given in bold.

SSB/als	Multivariable regression model by outcome							
Dependent variable	Baseline DNA-damage level		DNA-damage directly after X-ray		DNA-damage 10 min after X-ray		DNA-damage 15 min after X-ray	
	Coef. (95% CI)	P	Coef. (95% CI)	P	Coef. (95% CI)	P	Coef. (95% CI)	P
Baseline ^a			0.330 (-0.464 - 1.124)	.394	-1.256 (-2.278 - -0.233)	.019	0.730 (-0.124 - 1.585)	.089
F ₀ is irradiated ^b	1.117 (0.121 - 2.113)	.030	1.021 (-0.850 - 2.892)	.266	1.849 (-0.560 - 4.258)	.124	-0.509 (-2.521 - 1.504)	.602
F ₀ lack Ogg1 ^c	0.057 (-0.939 - 1.053)	.906	0.571 (-1.077 - 2.219)	.476	-0.382 (-2.504 - 1.740)	.710	0.085 (-1.688 - 1.858)	.921
Interaction between F ₀ irradiation and the lack of Ogg1 ^d	-0.528 (-1.913 - 0.857)	.435	-1.641 (-3.971 - 0.689)	.156	-1.376 (-4.375 - 1.624)	.348	-0.967 (-3.473 - 1.539)	.428

^a Is the baseline levels of DNA damage associated with the outcome? ^b Is F₀ irradiation associated with the outcome? ^c Is F₀ being *Ogg1*^{-/-} associated with the outcome? ^d Interaction between ^b and ^c? Are the variables ^b and/or ^c more extreme/weaker when they occur together?

1

2 The levels of oxidative DNA lesions (ssb levels not subtracted) (Fig. 2, Tab. 3) were not
3 affected by the F₀ experimental variables at any of the analysed time points, and when the
4 oxidative lesions were subtracted from the levels of ssb – only a slight increase in
5 oxidative lesions was seen (data not shown).

6

7

8

9

10

11 **Table 3. Multivariable regression model by outcome (Fpg-sensitive sites).** The
12 significance of F₀ experimental variables on ssb DNA-lesions at baseline, immediately after
13 X-ray, and the rate of repair were investigated by four regression models. Footnotes describe
14 the interpretations of the independent variables upon the outcome, with statistically
15 significant levels (p-value <0.05) in bold.

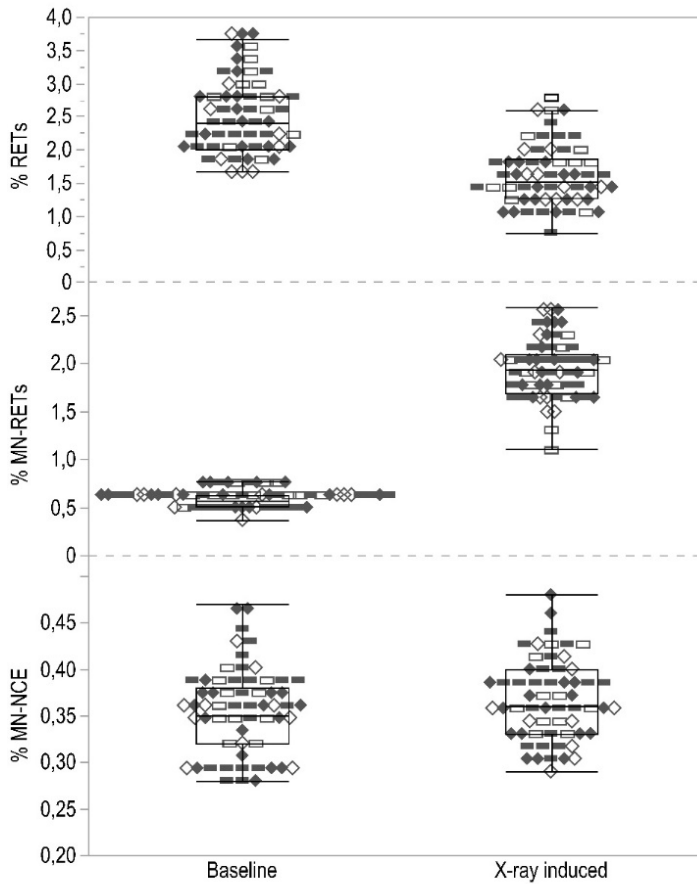
Oxidative lesions	Linear regression model by outcome							
Dependent variable	Baseline DNA-damage level		DNA-damage directly after X-ray		DNA-damage 10 min after X-ray		DNA-damage 15 min after X-ray	
Independent Variables	Coef. (95% CI)	P	Coef. (95% CI)	P	Coef. (95% CI)	P	Coef. (95% CI)	P
Baseline ^a			-1.173 (-2.965 - 0.619)	.177	-0.536 (-1.610 - 0.538)	.308	0.785 (-0.567 - 2.136)	.238
F ₀ is irradiated ^b	0.429 (-0.658 - 1.517)	.419	1.529 (-2.429 - 5.487)	.413	0.682 (-1.794 - 3.157)	.570	-0.250 (-3.367 - 2.865)	.868
F ₀ lack Ogg1 ^c	0.319 (-0.768 - 1.407)	.546	1.249 (-2.799 - 5.297)	.511	0.058 (-2.398 - 2.514)	.961	-0.704 (-3.795 - 2.387)	.638
Interaction between F ₀ irradiation and the lack of Ogg1 ^d	-1.123 (-2.635 - 0.390)	.137	-3.733 (-9.242 - 1.775)	.164	-1.070 (-4.661 - 2.521)	.539	-1.371 (-5.893 - 3.149)	.532

^a Is the baseline levels of DNA damage associated with the outcome*? ^b Is F₀ irradiation associated with the outcome? ^c Is F₀ being *Ogg1*^{-/-} associated with the outcome? ^d Interaction between ^b and ^c? Are the variables ^b and/or ^c more extreme/weaker when they occur together?

1

2 Micronuclei (MN) assay

3 An *in vivo* acute challenge dose of X-ray (0.5 Gy) caused a significant (p<0.000) reduction
4 in the population of circulatory RETs and a significant (p<0.000) increase in
5 micronucleated RETs (MN-RETs) (Fig. 3). The X-ray challenge did not impact the levels of
6 micronucleated normochromatic erythrocytes (MN-NCE), which were expected as this is
7 a marker of chronic exposure.



1

2 **Figure 3. MN assay.** Percentage of blood reticulocytes (%RET), micronucleated
 3 reticulocytes (%MN-RET) and micronucleated normochromatic erythrocytes (%MN-NCE)
 4 at baseline and after in vivo X-ray (0.5 Gy). All individual data point is visualised, including
 5 box plots. Markers represent the F_0 groups stratified in F_0 treatment (unexposed (Ctrl) and
 6 chronic low dose rate irradiation (IR)) and F_0 genotype ($Ogg1^{-/-}$ (KO) and $Ogg1^{+/-}$ (He)); \diamond =
 7 Ctrl He, \square = Ctrl KO, \blacklozenge = IR He, \blacksquare = IR KO

8 Radiation-induced damage was evident in the increased levels of %MN-RETs, and the
 9 reduction in %RETs after X-ray (Fig. 3). This X-ray induced response occurred
 10 irrespectively to the F_0 irradiation and genotype (Tab. 4). The levels of normochromatic
 11 erythrocytes (i.e., mature erythrocytes without RNA) (% MN-NCE) is not affected by the
 12 exposure (Fig. 3, lower panel), but this is due to the nature of MN-NCE formation which

1 requires at least two days after a hematopoietic response. Thus, MN-NCE is a marker for
 2 chronic exposure and is irrelevant after the acute exposure regime used in this study.

3 **Table 4. Multivariable regression model by outcome (MN assay).** The significance of F_0
 4 variables and F_2 weight on baseline levels and X-ray-induced effects in blood reticulocytes
 5 (%RET), micronucleated reticulocytes (%MN-RET) and micronucleated normochromatic
 6 erythrocytes (%MN-NCE) after an in vivo exposure to 0.5 Gy were tested in five linear
 7 regression models. Footnotes describe the interpretations of the independent variables upon
 8 the outcome, with statistically significant levels (p -value <0.5) in bold.

MicroFlow	MN at baseline						MN after X-ray			
	RETs		MN-RET		MN-NCE		RETs		MN-RET	
	Coef. (95% CI)	P	Coef. (95% CI)	P	Coef. (95% CI)	P	Coef. (95% CI)	P	Coef. (95% CI)	P
Baseline^a							0.137 (-0.083 - 0.356)	.218	1.309 (0.395 - 2.223)	.006
F_0 is irradiated^b	0.329 (-0.103 - 0.762)	.133	0.046 (-0.017 - 0.108)	.150	0.003 (-0.036 - 0.030)	.860	-0.142 (-0.498 - 0.214)	.428	-0.033 (-0.248 - 0.181)	.757
F_0 lack <i>Ogg1</i>^c	0.372827 (-0.106 - 0.852)	.124	0.054 (-0.016 - 0.123)	.127	0.018 (-0.019 - 0.055)	.337	0.164 (-0.231 - 0.558)	.409	-0.144 (-0.382 - 0.094)	.231
Interaction between F_0 irradiation and the lack of <i>Ogg1</i>^d	-0.642 (-1.236 - 0.049)	.034	-0.072 (-0.158 - 0.014)	.100	-0.004 (-0.050 - 0.041)	.855	0.009 (-0.490 - 0.507)	.972	0.162 (-0.134 - 0.457)	.278
Weight^e	-0.029 (-0.068 - 0.009)	.137	0.004 (-0.002 - 0.009)	.177	0.006 (0.003 - 0.009)	.000	-0.017 (-0.049 - 0.014)	.276	0.029 (0.010 - 0.048)	.004

^a Is the baseline level of RETs and MN-RETs relevant for outcome? ^b Is F_0 irradiation relevant for the outcome? ^c Is F_0 being *Ogg1*^{-/-} relevant for the outcome? ^d Are the variables ^b and/or ^c more extreme/weaker when they both occur together? ^e Is weight relevant for the outcome?

9

10 Evaluating the baseline levels of RETs, MN-RETs or MN-NCE in the unexposed F_2 mice,
 11 there were no evidence that F_0 -irradiation and genotype affected the measured endpoint
 12 (Tab. 4). The data also displayed a statistically significant effect in F_2 mice to have a
 13 disposition of lower levels of RETs when there is an interaction between F_0 irradiation
 14 and F_0 *Ogg1*^{-/-} (coef: -0.642, 95% CI: -1.236 to -0.049, p -value = 0.034). However, there
 15 was no evidence that F_0 irradiation and F_0 genotype alone affected the levels of baseline
 16 RETs (p -values 0.133 and 0.124, respectively).

1 After F₂ mice received the *in vivo* X-ray challenge dose (0.5 Gy), there was no evidence
2 that the F₀ experimental variables affected the reduction in numbers of RETs or the
3 formation of MN-RETs (Tab. 4). Although, as expected, the baseline levels of MN-RETs
4 impacted the level of MN-RETs after the challenging X-ray radiation dose (coef. 1.309,
5 95% CI: 0.395 - 2.223, p-value = 0.006, Tab. 4). We also found that the body weight at
6 irradiation significantly affected the MN-RETs outcome (coef. 0.029, 95% CI: 0.01 - 0.048,
7 p-value = 0.004, Tab. 4), however not at baseline.

8 **DISCUSSION**

9 In the present study, our objective was to investigate if paternal F₀ irradiation impacted
10 genomic instability in the F₂ offspring following a challenging dose of X-ray. DNA damage,
11 pre-mutagenic lesions (comet assay) and chromosomal aberrations (MN assay) were
12 used as markers for genomic instability.

13 It is well known that X-ray causes cytogenic damage (Hlatky et al., 2002), *in vitro*
14 (Brunborg et al., 2023; Gutzkow et al., 2013; Sioen et al., 2020) and *in vivo* (Graupner et
15 al., 2017; Odagiri et al., 1994; Risom et al., 2003). As expected, we observed an increase in
16 micronuclei formation and pre-mutagenic comet assay DNA lesions in F₂ males after the
17 acute challenging dose of X-ray. However, induction of damage after the challenge was not
18 affected by irradiation status or the genotype of the F₀ males. We did, however, observe
19 an increase in the basal levels of DNA lesions in the F₂ mice originating from irradiated F₀
20 males, regardless of *Ogg1*-status, in nucleated blood cells (Tab. 2). The increased
21 spontaneous formation in DNA lesions in nucleated blood cells, were not corroborated by
22 a similar increase in the spontaneous formation of micronuclei in erythrocytes (Tab. 3).
23 The observed increase in the effect size (level of %tail-DNA) in F₂ mice from irradiated F₀
24 was very small and could be ascribed to methodological variation in the comet assay.

25 To the best of our knowledge, this study is the first to address paternal induced genomic
26 instability in F₂ after chronic low dose rate gamma radiation. Though, Barber et al. (2006)
27 showed similar comet assay results in F₁ progeny of X-ray irradiated F₀ mice. They
28 demonstrated increased endogenous levels of double- and single-strand breaks (ssb) in
29 bone marrow cells from F₁ mice (8 weeks old) of irradiated fathers (1 Gy (BALB/c) and 2
30 Gy (CBA/Ca)), mated to F₁ 6 weeks after X-ray. In the same study, mutation rates
31 (expanded simple tandem repeat, ESTR) were also elevated in sperm, spleen, and bone

1 marrow cells in all F₁ mice originating from irradiated F₀ males for both strains (Barber
2 et al., 2006). In contrast, a study by Paris et al. (2015), also addressing the F₁ generation
3 after paternal irradiation (1 Gy X-ray, mating 6 weeks after) status did not impact the
4 endogenous DNA damage levels in bone marrow and spleen cells in 3-month-old F₁
5 offspring (Paris et al., 2015).

6 In our study, the exposure status of F₀ males did not affect the efficiency of DNA repair
7 measured by the comet assay following the 2 Gy *in vitro* irradiation of F₂ whole blood. A
8 similar result was also observed in Barber et al. 2006, in F₁, where the repair capacity of
9 *in vitro* irradiated bone marrow cells (using a much higher dose, 10 Gy X-ray) was not
10 affected by the irradiation exposure status of irradiated fathers (Barber et al., 2006).

11 Only a slight increase in net Fpg-sensitive sites was detected in the comet assay. This is in
12 line with two other studies performed in our lab investigating Fpg-sensitive lesions after
13 acute (Graupner et al., 2017) and chronic X-ray exposure (Graupner et al., 2017; Graupner
14 et al., 2016). Others have reported net increase in Fpg-sensitive sites both *in vitro*
15 (Purschke et al., 2004) and *in vivo* (Risom et al., 2003) comet assay. One obvious reason
16 for our slight increase in net Fpg-sensitive sites could be related to that we routinely we
17 routinely calibrate the Fpg-concentration in cells treated with an agent that induce a
18 different spectrum of DNA lesions (mostly base oxidations) compared to ionising
19 radiation, which also induce significant levels of complex and clustered DNA lesions. It is
20 conceivable that the high affinity and resulting sequestering of Fpg related to such lesions
21 may inadvertently have led to an underestimation of oxidative lesions. Our Fpg-enzyme
22 is regularly calibrated using cells exposed to the phototoxic Ro-compound (Ro-12-9786).
23 Thus, future studies could address this by including an assay control (pre-exposed cells)
24 or another positive control in the setup exposed to a different oxidation agent than X-ray
25 (Møller et al., 2017).

26 It is challenging to assess the relevance of transmitted RIGI comparing human and animal
27 studies, as human studies are hampered with several potentially confounding effects and
28 often address effects in either the F₁ generation or measure changes in the irradiated
29 parental germline. Also, the exposure regimes, dose, dose rate, and exposure duration
30 differ. Arguments exists for an increased tendency for transgenerational genomic
31 instability in mice offspring originating from the paternal line given acute doses >1 Gy, as
32 low/medium doses < 1 Gy, including chronic LDR, dose not destabilise the F₁ genome

1 (Dubrova and Sarapultseva, 2020; Mughal et al., 2012). We assume that the timing of
2 exposure relative to the time of conception play a role, as it is assumed that the exposed
3 spermatozoa contain higher levels of DNA damage compared to spermatozoa originating
4 from exposed stem cell spermatogonia (as in this study). Spermatogonia may undergo cell
5 death or restore the damaged DNA, as has been showed following exposure to other
6 stressors (Olsen et al., 2010). It could be speculated that the abovementioned aspects may
7 protect from radiation-induced transgenerational effects. However, many questions
8 remain concerning this topic (Fukunaga et al., 2022), emphasising the need to pursue,
9 potential mechanisms for radiation-induced transgenerational effects.

10 To conclude, the results show indications of stem cell derived radiation-induced
11 transgenerational genomic instability due to the increased endogenously occurring DNA
12 damage level. However, due to the low effect size we consider the difference to be of low
13 or no biological relevance. There was no evidence that the F₀ genotype or that the
14 radiation status affected radiation-induces cytogenic damage, or DNA damage
15 immediately after given a challenging dose of X-ray or the ability to repair the induced
16 ssb/als damage.

17 **ACKNOWLEDGEMENTS**

18 Funding was received from the Research Council of Norway through its Centers of
19 Excellence funding scheme, project number 223268/F50 CERAD.

20 The authors wish to thank Victor Ong for animal care at NIPH, and Jill Andersen for
21 technical assistance.

22 **DECLARATION OF INTEREST**

23 The authors report no conflict of interest.

24 **REFERENCES**

- 25 Asare N, Duale N, Slagsvold HH, Lindeman B, Olsen AK, Gromadzka-Ostrowska J, et al.
26 Genotoxicity and gene expression modulation of silver and titanium dioxide
27 nanoparticles in mice. *Nanotoxicology* 2016; 10: 312-21,
28 doi:10.3109/17435390.2015.1071443
- 29 Barber R, Plumb MA, Boulton E, Roux I, Dubrova YE. Elevated mutation rates in the germ line of
30 first- and second-generation offspring of irradiated male mice. *Proc Natl Acad Sci U S A*
31 2002; 99: 6877-82, doi:10.1073/pnas.102015399

- 1 Barber RC, Hickenbotham P, Hatch T, Kelly D, Topchiy N, Almeida GM, et al. Radiation-induced
2 transgenerational alterations in genome stability and DNA damage. *Oncogene* 2006; 25:
3 7336-42, doi:10.1038/sj.onc.1209723
- 4 Bjerke HH, P. O. . The gamma irradiation facility FIGARO – Report on the measurements of dose
5 rate in the cobolt-60 irradiation field. NRPA Technical document no. 2, Norwegian
6 Radiation Protection Authority, Østerås, 2014,
- 7 Bohacek J, Mansuy IM. Molecular insights into transgenerational non-genetic inheritance of
8 acquired behaviours. *Nat Rev Genet* 2015; 16: 641-52, doi:10.1038/nrg3964
- 9 Boiteux S, Huisman O. Isolation of a formamidopyrimidine-DNA glycosylase (fpg) mutant of
10 *Escherichia coli* K12. *Mol Gen Genet* 1989; 215: 300-5,
- 11 Brunborg G, Eide DM, Graupner A, Gutzkow K, Shaposhnikov S, Kruszewski M, et al. Calibration
12 of the comet assay using ionising radiation. *Mutation Research/Genetic Toxicology and
13 Environmental Mutagenesis* 2023; 885: 503560,
14 doi:<https://doi.org/10.1016/j.mrgentox.2022.503560>
- 15 Collins AR, Oscoz AA, Brunborg G, Gaivao I, Giovannelli L, Kruszewski M, et al. The comet assay:
16 topical issues. *Mutagenesis* 2008; 23: 143-51, doi:10.1093/mutage/gem051
- 17 Dertinger SD, Torous DK, Hayashi M, MacGregor JT. Flow cytometric scoring of micronucleated
18 erythrocytes: an efficient platform for assessing in vivo cytogenetic damage. *Mutagenesis*
19 2011; 26: 139-45, doi:10.1093/mutage/geq055
- 20 Duale N, Olsen AK, Christensen T, Butt ST, Brunborg G. Octyl methoxycinnamate modulates gene
21 expression and prevents cyclobutane pyrimidine dimer formation but not oxidative DNA
22 damage in UV-exposed human cell lines. *Toxicol Sci* 2010; 114: 272-84,
23 doi:10.1093/toxsci/kfq005
- 24 Dubrova YE, Sarapultseva EI. Radiation-induced transgenerational effects in animals. *Int J Radiat
25 Biol* 2020: 1-7, doi:10.1080/09553002.2020.1793027
- 26 Fukunaga H, Yokoya A, Prise KM. A Brief Overview of Radiation-Induced Effects on
27 Spermatogenesis and Oncofertility. *Cancers (Basel)* 2022; 14,
28 doi:10.3390/cancers14030805
- 29 Gapp K, Bohacek J. Epigenetic germline inheritance in mammals: looking to the past to
30 understand the future. *Genes Brain Behav* 2018; 17: e12407, doi:10.1111/gbb.12407
- 31 Gomes AM, Barber RC, Dubrova YE. Paternal irradiation perturbs the expression of circadian
32 genes in offspring. *Mutat Res* 2015; 775: 33-37, doi:10.1016/j.mrfmmm.2015.03.007
- 33 Graupner A, Eide DM, Brede DA, Ellender M, Lindbo Hansen E, Oughton DH, et al. Genotoxic
34 effects of high dose rate X-ray and low dose rate gamma radiation in *Apc(Min/+)* mice.
35 *Environ Mol Mutagen* 2017; 58: 560-569, doi:10.1002/em.22121
- 36 Graupner A, Eide DM, Instanes C, Andersen JM, Brede DA, Dertinger SD, et al. Gamma radiation at
37 a human relevant low dose rate is genotoxic in mice. *Sci Rep* 2016; 6: 32977,
38 doi:10.1038/srep32977
- 39 Graupner A, Instanes C, Andersen JM, Brandt-Kjelsen A, Dertinger SD, Salbu B, et al. Genotoxic
40 effects of two-generational selenium deficiency in mouse somatic and testicular cells.
41 *Mutagenesis* 2015; 30: 217-25, doi:10.1093/mutage/geu059

- 1 Gutzkow KB, Duale N, Danielsen T, von Stedingk H, Shahzadi S, Instanes C, et al. Enhanced
2 susceptibility of obese mice to glycidamide-induced sperm chromatin damage without
3 increased oxidative stress. *Andrology* 2016; 4: 1102-1114, doi:10.1111/andr.12233
- 4 Gutzkow KB, Langleite TM, Meier S, Graupner A, Collins AR, Brunborg G. High-throughput comet
5 assay using 96 minigels. *Mutagenesis* 2013; 28: 333-40, doi:10.1093/mutage/get012
- 6 Hanahan D, Weinberg RA. Hallmarks of cancer: the next generation. *Cell* 2011; 144: 646-74,
7 doi:10.1016/j.cell.2011.02.013
- 8 Hansen EL RHI, Hetland PO, Bjerke H. Absorbed doses to water for x-ray dosimetry on a PXI X-
9 RAD 225, Part I - Measurements. NRPA Technical Document Series 7. NRPA, 2015,
- 10 Hansen SH, Olsen AK, Sørderlund EJ, Brunborg G. In vitro investigations of glycidamide-induced
11 DNA lesions in mouse male germ cells and in mouse and human lymphocytes. *Mutat Res*
12 2010; 696: 55-61, doi:10.1016/j.mrgentox.2009.12.012
- 13 Hlatky L, Sachs RK, Vazquez M, Cornforth MN. Radiation-induced chromosome aberrations:
14 insights gained from biophysical modeling. *Bioessays* 2002; 24: 714-23,
15 doi:10.1002/bies.10126
- 16 Huang L, Snyder AR, Morgan WF. Radiation-induced genomic instability and its implications for
17 radiation carcinogenesis. *Oncogene* 2003; 22: 5848-54, doi:10.1038/sj.onc.1206697
- 18 Izumi S, Koyama K, Soda M, Suyama A. Cancer incidence in children and young adults did not
19 increase relative to parental exposure to atomic bombs. *Br J Cancer* 2003; 89: 1709-13,
20 doi:10.1038/sj.bjc.6601322
- 21 Kamiya K, Ozasa K, Akiba S, Niwa O, Kodama K, Takamura N, et al. Long-term effects of radiation
22 exposure on health. *Lancet* 2015; 386: 469-78, doi:10.1016/s0140-6736(15)61167-9
- 23 Klungland A, Rosewell I, Hollenbach S, Larsen E, Daly G, Epe B, et al. Accumulation of
24 premutagenic DNA lesions in mice defective in removal of oxidative base damage. *Proc*
25 *Natl Acad Sci U S A* 1999; 96: 13300-5,
- 26 Kodaira M, Ryo H, Kamada N, Furukawa K, Takahashi N, Nakajima H, et al. No evidence of
27 increased mutation rates at microsatellite loci in offspring of A-bomb survivors. *Radiat*
28 *Res* 2010; 173: 205-13, doi:10.1667/rr1991.1
- 29 Kodaira M, Satoh C, Hiyama K, Toyama K. Lack of effects of atomic bomb radiation on genetic
30 instability of tandem-repetitive elements in human germ cells. *Am J Hum Genet* 1995;
31 57: 1275-83,
- 32 Koturbash I, Baker M, Loree J, Kutanzi K, Hudson D, Pogribny I, et al. Epigenetic dysregulation
33 underlies radiation-induced transgenerational genome instability in vivo. *Int J Radiat*
34 *Oncol Biol Phys* 2006; 66: 327-30, doi:10.1016/j.ijrobp.2006.06.012
- 35 Legoff L, D'Cruz SC, Tevosian S, Primig M, Smagulova F. Transgenerational Inheritance of
36 Environmentally Induced Epigenetic Alterations during Mammalian Development. *Cells*
37 2019; 8, doi:10.3390/cells8121559
- 38 Lind OC, Helen Oughton D, Salbu B. The NMBU FIGARO low dose irradiation facility. *Int J Radiat*
39 *Biol* 2018: 1-6, doi:10.1080/09553002.2018.1516906
- 40 Marcho C, Oluwayiose OA, Pilsner JR. The preconception environment and sperm epigenetics.
41 *Andrology* 2020, doi:10.1111/andr.12753

- 1 Merrifield M, Kovalchuk O. Epigenetics in radiation biology: a new research frontier. *Front Genet*
2 2013; 4: 40, doi:10.3389/fgene.2013.00040
- 3 Moorhouse AJ, Scholze M, Sylvius N, Gillham C, Rake C, Peto J, et al. No evidence of increased
4 mutations in the germline of a group of British nuclear test veterans. *Scientific Reports*
5 2022; 12: 10830, doi:10.1038/s41598-022-14999-w
- 6 Mughal SK, Myazin AE, Zhavoronkov LP, Rubanovich AV, Dubrova YE. The dose and dose-rate
7 effects of paternal irradiation on transgenerational instability in mice: a radiotherapy
8 connection. *PLoS One* 2012; 7: e41300, doi:10.1371/journal.pone.0041300
- 9 Møller P, Jantzen K, Løhr M, Andersen MH, Jensen DM, Roursgaard M, et al. Searching for assay
10 controls for the Fpg- and hOGG1-modified comet assay. *Mutagenesis* 2017; 33: 9-19,
11 doi:10.1093/mutage/gex015
- 12 Odagiri Y, Takemoto K, Fenech M. Micronucleus induction in cytokinesis-blocked mouse bone
13 marrow cells in vitro following in vivo exposure to X-irradiation and cyclophosphamide.
14 *Environ Mol Mutagen* 1994; 24: 61-7,
- 15 OECD. Test No. 474: Mammalian Erythrocyte Micronucleus Test, 2016.
- 16 Olsen AK, Andreassen A, Singh R, Wiger R, Duale N, Farmer PB, et al. Environmental exposure of
17 the mouse germ line: DNA adducts in spermatozoa and formation of de novo mutations
18 during spermatogenesis. *PLoS One* 2010; 5: e11349, doi:10.1371/journal.pone.0011349
- 19 Olsen AK, Duale N, Bjaras M, Larsen CT, Wiger R, Holme JA, et al. Limited repair of 8-hydroxy-
20 7,8-dihydroguanine residues in human testicular cells. *Nucleic Acids Res* 2003; 31: 1351-
21 63,
- 22 Olsen AK, Lindeman B, Wiger R, Duale N, Brunborg G. How do male germ cells handle DNA
23 damage? *Toxicol Appl Pharmacol* 2005; 207: 521-31, doi:10.1016/j.taap.2005.01.060
- 24 Paris L, Giardullo P, Leonardi S, Tanno B, Meschini R, Cordelli E, et al. Transgenerational
25 inheritance of enhanced susceptibility to radiation-induced medulloblastoma in
26 newborn Ptch1(+)/(-) mice after paternal irradiation. *Oncotarget* 2015; 6: 36098-112,
27 doi:10.18632/oncotarget.5553
- 28 Purschke M, Kasten-Pisula U, Brammer I, Dikomey E. Human and rodent cell lines showing no
29 differences in the induction but differing in the repair kinetics of radiation-induced DNA
30 base damage. *Int J Radiat Biol* 2004; 80: 29-38, doi:10.1080/09553000310001642885
- 31 Risom L, Møller P, Vogel U, Kristjansen PE, Loft S. X-ray-induced oxidative stress: DNA damage
32 and gene expression of HO-1, ERCC1 and OGG1 in mouse lung. *Free Radic Res* 2003; 37:
33 957-66, doi:10.1080/1071576031000150788
- 34 Russo A, Pacchierotti F, Cimini D, Ganem NJ, Genesca A, Natarajan AT, et al. Genomic instability:
35 Crossing pathways at the origin of structural and numerical chromosome changes.
36 *Environ Mol Mutagen* 2015; 56: 563-80, doi:10.1002/em.21945
- 37 Shen Z. Genomic instability and cancer: an introduction. *J Mol Cell Biol* 2011; 3: 1-3,
38 doi:10.1093/jmcb/mjq057
- 39 Sioen S, Cloet K, Vral A, Baeyens A. The Cytokinesis-Block Micronucleus Assay on Human
40 Isolated Fresh and Cryopreserved Peripheral Blood Mononuclear Cells. *Journal of*
41 *Personalized Medicine* 2020; 10: 125,

1 Taft KRPaRA. Reproductive Biology of the Laboratory Mouse. The Mouse in Biomedical
2 Research: Normative Biology, Husbandry, and Models. 3 av Elsevier Inc., American College
3 of Laboratory Animal Medicine, 2007, pp. 91-97.

4 Torous DK, Hall NE, Murante FG, Gleason SE, Tometsko CR, Dertinger SD. Comparative scoring of
5 micronucleated reticulocytes in rat peripheral blood by flow cytometry and microscopy.
6 Toxicol Sci 2003; 74: 309-14, doi:10.1093/toxsci/kfg143

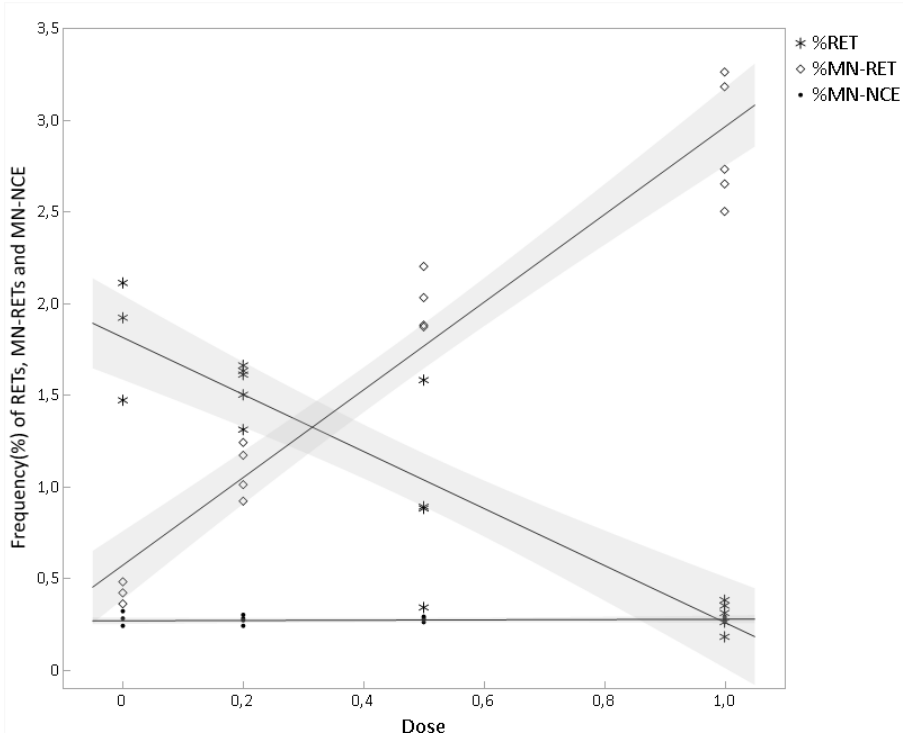
7 UNSCEAR. UNSCEAR 2006, "Effects of Ionizing radiation" Volume II, Annex C "Non-targeted and
8 delayed effects of exposure to ionizing radiation" UN, New York, 2006,

9 Yeager M, Machiela MJ, Kothiyal P, Dean M, Bodelon C, Suman S, et al. Lack of transgenerational
10 effects of ionizing radiation exposure from the Chernobyl accident. Science 2021; 372:
11 725-729, doi:10.1126/science.abg2365

12 Yoshimoto Y, Neel JV, Schull WJ, Kato H, Soda M, Eto R, et al. Malignant tumors during the first 2
13 decades of life in the offspring of atomic bomb survivors. Am J Hum Genet 1990; 46:
14 1041-52,

15
16
17
18
19
20
21
22
23
24
25

1 SUPPLEMENTARY



2

3 **Figure S1. Pilot study of the dose response of MN.** Naïve B6-mice is used, blood samples
4 is drawn 45 hours after 0.2, 0.5 and 1 Gy of acute whole body X-ray. Fitted lines is displayed
5 with 95% CI.

6

7

8

9

10

11

12

1 Multivariable regression models

2 Thirteen multivariable regression models performed using STATA corresponding to one
3 model per outcome:

- 4 • ssb/als: baseline, directly after X-ray, 10 min post-X-ray, 15 min post-X-ray;
- 5 • oxidative lesions: baseline, directly after X-ray, 10 min post-X-ray, 15 min post-X-
- 6 ray;
- 7 • MN-assay: Baseline (RETs, MN-RETs, MN-NCEs), post-X-ray (RETs, MN-RETs)).

8 One-by-one independent variable were added to the model to illustrate the robustness
9 of the model.

10 Ssb/als

11 Baseline

SSB/ALS Variable	Model 1		Model 2		Model 3	
	Coef. (95% CI)	P value	Coef. (95% CI)	P value	Coef. (95% CI)	P value
F ₀ is irradiated ^b	0.816 (0.149 - 1.483)	0.019	0.844 (0.160 - 1.527)	0.018	1.117 (0.121 - 2.113)	0.030
F ₀ lack Ogg1 ^c			-0.216 (-0.900 - 0.467)	0.517	0.057 (-0.939 - 1.053)	0.906
Interaction between F ₀ irradiation and the lack of Ogg1 ^d					-0.528 (-1.913 - 0.857)	0.435
_intercept	5.109 (4.627 - 5.591)	0.000	5.207 (4.627 - 5.787)	0.000	5.083 (4.412 - 5.755)	0.000

12

13

14 Ctrl vs directly after

SSB/ALS Controll vs XR Variable	Model 1		Model 2		Model 3		Model 4	
	Coef. (95% CI)	P value	Coef. (95% CI)	P value	Coef. (95% CI)	P value	Coef. (95% CI)	P value
Baseline	0.466 (-0.193 - 1.125)	0.156	0.456 (-0.319 - 1.231)	0.234	0.431 (-0.372 - 1.233)	0.275	0.330 (-0.464 - 1.124)	0.394
F ₀ is irradiated ^b			0.034 (-1.268 - 0.338)	0.956	0.088 (-1.269 - 1.445)	0.893	1.021 (-0.850 - 2.892)	0.266
F ₀ lack Ogg1 ^c					-0.255 (-1.444 - 0.934)	0.658	0.571 (-1.077 - 2.219)	0.476
Interaction between F ₀ irradiation and the lack of Ogg1 ^d							-1.641 (-3.971 - 0.689)	0.156
_intercept	10.151 (6.460 - 13.842)	0.000	10.188 (6.144 - 14.233)	0.000	10.433 (6.137 - 14.728)	0.000	10.572 (6.384 - 14.759)	0.000

15

1 Ctrl vs 10 min after X-ray:

SSB/ALS Controll vs XR Variable	Model 1		Model 2		Model 3		Model 4	
	Coef. (95% CI)	P value	Coef. (95% CI)	P value	Coef. (95% CI)	P value	Coef. (95% CI)	P value
Baseline	-0.822 (-1.710 - 0.066)	0.068	-1.065 (-2.083 - 0.048)	0.041	-1.171 (-2.171 - -0.171)	0.024	-1.256 (-2.278 - -0.233)	0.019
F ₀ is irradiated ^b			0.842 (-0.868 - 2.553)	0.317	1.067 (-0.625 - 2.758)	0.203	1.849 (-0.560 - 4.258)	0.124
F ₀ lack Ogg1 ^c					-1.075 (-2.556 - 0.407)	0.145	-0.382 (-2.504 - 1.740)	0.710
Interaction between F ₀ irradiation and the lack of Ogg1 ^d							-1.376 (-4.375 - 1.624)	0.348
_intercept	14.264 (9.292 - 19.236)	0.000	15.171 (9.860 - 20.482)	0.000	16.200 (10.846 - 21.555)	0.000	16.317 (10.925 - 21.708)	0.000

2

3 Ctrl to 15 min after:

SSB/ALS Controll vs XR Variable	Model 1		Model 2		Model 3		Model 4	
	Coef. (95% CI)	P value	Coef. (95% CI)	P value	Coef. (95% CI)	P value	Coef. (95% CI)	P value
Baseline	0.499 (-0.238 - 1.237)	0.174	0.829 (0.022 - 1.636)	0.045	0.790 (-0.040 - 1.619)	0.061	0.730 (-0.124 - 1.585)	0.089
F ₀ is irradiated ^b			-1.142 (-2.499 - 0.214)	0.094	-1.058 (-2.462 - 0.345)	0.131	-0.509 (-2.521 - 1.504)	0.602
F ₀ lack Ogg1 ^c					-0.401 (-1.631 - 0.828)	0.502	0.085 (-1.688 - 1.858)	0.921
Interaction between F ₀ irradiation and the lack of Ogg1 ^d							-0.967 (-3.473 - 1.539)	0.428
_intercept	5.185 (1.057 - 9.314)	0.016	3.955 (-0.256 - 8.166)	0.064	4.340 (-0.102 - 8.781)	0.055	4.422 (-0.083 - 8.926)	0.054

4

5 Oxidative lesions

6 Baseline

FPG Controll vs XR Variable	Model 1		Model 2		Model 3		Model 4	
	Coef. (95% CI)	P value	Coef. (95% CI)	P value	Coef. (95% CI)	P value	Coef. (95% CI)	P value
F ₀ is irradiated ^b			-0.185 (-0.946 - 0.577)	0.619	-0.151 (-0.931 - 0.628)	0.690	0.429 (-0.658 - 1.517)	0.419
F ₀ lack Ogg1 ^c					-0.261 (-1.041 - 0.518)	0.493	.319 (-0.768 - 1.407)	0.546
Interaction between F ₀ irradiation and the lack of Ogg1 ^d							-1.123 (-2.635 - 0.390)	0.137
_intercept			7.691 (7.141 - 8.241)	0.000	7.810 (7.148 - 8.471)	0.000	7.546 (6.813 - 8.279)	0.000

7

1 Ctrl vs directly after (n=16 immediately after X-ray)

FPG Control vs XR Variable	Model 1		Model 2		Model 3		Model 4	
	Coef. (95% CI)	P value	Coef. (95% CI)	P value	Coef. (95% CI)	P value	Coef. (95% CI)	P value
Baseline	-0.889 (-2.545 - 0.767)	0.269	-0.973 (-2.730 - 0.784)	0.253	-0.926 (-2.749 - 0.897)	0.290	-1.173 (-2.965 - 0.619)	0.177
F ₀ is irradiated ^b			-0.597 (-3.285 - 2.092)	0.640	-0.392 (-3.263 - 2.479)	0.771	1.529 (-2.429 - 5.487)	0.413
F ₀ lack Ogg1 ^c					-0.795 (-3.601 - 2.010)	0.548	1.249 (-2.799 - 5.297)	0.511
Interaction between F ₀ irradiation and the lack of Ogg1 ^d							-3.733 (-9.242 - 1.775)	0.164
_intercept	22.044 (9.816 - 34.272)	0.002	22.995 (9.620 - 36.370)	0.003	22.985 (9.163 - 36.807)	0.003	23.968 (10.589 - 37.346)	0.002

2

3 Ctrl vs 10 min after X-ray:

FPG Control vs XR Variable	Model 1		Model 2		Model 3		Model 4	
	Coef. (95% CI)	P value	Coef. (95% CI)	P value	Coef. (95% CI)	P value	Coef. (95% CI)	P value
Baseline	-0.392 (-1.321 - 0.537)	0.390	-0.386 (-1.346 - 0.574)	0.412	-0.429 (-1.420 - 0.563)	0.377	-0.536 (-1.610 - 0.538)	0.308
F ₀ is irradiated ^b			0.093 (-1.527 - 1.713)	0.906	0.145 (-1.519 - 1.809)	0.857	0.682 (-1.794 - 3.157)	0.570
F ₀ lack Ogg1 ^c					-0.467 (-2.144 - 1.210)	0.567	0.058 (-2.398 - 2.514)	0.961
Interaction between F ₀ irradiation and the lack of Ogg1 ^d							-1.070 (-4.661 - 2.521)	0.539
_intercept	15.370 (8.273 - 22.467)	0.000	15.27593 (7.801 - 22.751)	0.000	15.816 (7.946 - 23.686)	0.000	16.404 (8.136 - 24.671)	0.001

4

5 Ctrl vs 15 min after X-ray:

FPG Control vs XR Variable	Model 1		Model 2		Model 3		Model 4	
	Coef. (95% CI)	P value	Coef. (95% CI)	P value	Coef. (95% CI)	P value	Coef. (95% CI)	P value
Baseline	1.119 (-0.130 - 2.368)	0.077	1.048 (-0.208 - 2.303)	0.097	0.922 (-0.326 - 2.171)	0.139	0.785 (-0.567 - 2.136)	0.238
F ₀ is irradiated ^b			-1.092 (-3.211 - 1.027)	0.295	-0.938 (-3.033 - 1.157)	0.360	-0.250 (-3.367 - 2.865)	0.868
F ₀ lack Ogg1 ^c					-1.377 (-3.488 - 0.735)	0.188	-0.704 (-3.795 - 2.387)	0.638
Interaction between F ₀ irradiation and the lack of Ogg1 ^d							-1.371 (-5.893 - 3.149)	0.532
_intercept	2.260 (-7.282 - 11.802)	0.627	3.368 (-6.407 - 13.143)	0.481	4.959 (-4.950 - 14.868)	0.308	5.712 (-4.694 - 16.118)	0.264

6

7

1 MN analysis

2 RET

Controll vs XR	Model 1		Model 2		Model 3		Model 4		Model 5	
	Coef. [95% CI]	P value	Coef. (95% CI)	P value	Coef. (95% CI)	P value	Coef. (95% CI)	P value	Coef. (95% CI)	P value
Baseline	0.163 (-0.047 - 0.373)	0.126	0.158 (-0.051 - 0.367)	0.136	0.157 (-0.048 - 0.363)	0.130	.161 (-0.055 - 0.376)	0.141	0.136 (-0.083 - 0.356)	0.218
F ₀ is irradiated ^b			-.157 (-0.397 - 0.084)	0.199	-0.157 (-0.394 - 0.080)	0.190	-0.172 (-0.524 - 0.181)	0.333	-0.142 (-0.498 - 0.214)	0.428
F ₀ lack Ogg1 ^c					0.195 (-0.032 - 0.422)	0.090	.1771998 -2169992 .5713988	0.371	.164 (-0.231 - 0.558)	0.409
Interaction between F ₀ irradiation and the lack of Ogg1 ^d							.028 -4697983 .5258771	0.911	.009 (-0.490 - 0.507)	0.972
Weight									-0.017 (-0.049 - 0.014)	0.276
_intercept	1.205 (0.677 - 1.733)	0.000	1.318 (0.765 - 1.871)	0.000	1.217 (0.660 - 1.773)	0.000	1.218 .6557277 1.779792	0.000	1.880 (0.549 - 3.210)	0.007

3

4 MN-RET

Controll vs XR	Model 1		Model 2		Model 3		Model 4		Model 5	
	Coef. (95% CI)	P value	Coef. (95% CI)	P value	Coef. (95% CI)	P value	Coef. (95% CI)	P value	Coef. (95% CI)	P value
Baseline	1.479 (0.537 - 2.421)	0.003	1.440 (0.496 - 2.384)	0.003	1.446 (0.504 - 2.388)	0.003	1.563 (0.598 - 2.527)	0.002	1.306 (0.395 - 2.223)	0.006
F ₀ is irradiated ^b			0.084 (-0.071 - 0.240)	0.283	0.084 (-0.071 - 0.240)	0.281	-.008 (-0.238 - 0.221)	0.943	-0.033 (-0.248 - .181)	0.757
F ₀ lack Ogg1 ^c					-0.083 (-.232 - 0.065)	0.265	-0.195 (-0.448 - 0.057)	0.127	-0.144 (-0.382 - 0.094)	0.231
Interaction between F ₀ irradiation and the lack of Ogg1 ^d							0.174 (-0.144 - 0.491)	0.278	0.162 (-0.134 - 0.457)	0.278
Weight									0.029 (0.010 - 0.048)	0.004
_intercept	1.085 (0.543 - 1.627)	0.000	1.053 (0.509 - 1.597)	0.000	1.093 (0.545 - 1.641)	0.000	1.086 (0.539 - 1.634)	0.000	0.213 (-0.556 - 0.981)	0.581

5

Paper III:

The authors` contributions are in compliance with the Vancouver agreement, and were as follows:

The authors` contributions follows the Vancouver agreement, and each contribution were: The irradiation of F0 were part of an animal experiment planned by AKO, DE, CI, DAB and GB, HD participated in termination in harvest of biological samples. HD, CI and AKO participated in the conceptualisation of the transgenerational sub-project. HD performed all the experimental planning, coordinated the irradiation and termination of F2 generations, and did all the laboratory work, supervised by CI and GB. HD performed all data processing and statistical analysis, advised by RW and ED. HD made the visualizations and result tables in the manuscript. HD wrote the first draft of the manuscript, and all authors have contributed by reading and commenting. The manuscript is finalized by HD, approved by all authors.

ISBN: 978-82-575-2068-7

ISSN: 1894-6402



Norwegian University
of Life Sciences

Postboks 5003
NO-1432 Ås, Norway
+47 67 23 00 00
www.nmbu.no